การสร้างเส้นใยไคโตซานขนาดนาโนโดยเทคนิคการปั่นด้วยไฟฟ้าสถิตย์เพื่อใช้ในการตรึงเซลล์

นางสาว ปริศฎาวรรณ ชูมณี

วิทยานิพนธ์นี้เป็นส่วนหนึ่งของการศึกษาตามหลักสูตรปริญญาวิศวกรรมศาสตมหาบัณฑิต
สาขาวิชาวิศวกรรมเคมี ภาควิชาวิศวกรรมเคมี
คณะวิศวกรรมศาสตร์ จุฬาลงกรณ์มหาวิทยาลัย
ปีการศึกษา 2553

FABRICATION OF CHITOSAN NANOFIBERS BY ELECTROSPINNING TECHNIQUE FOR CELL IMMOBILIZATION

Miss Prissadawan Chumanee

A Thesis Submitted in Partial Fulfillment of the Requirements
for the Degree of Master of Engineering Program in Chemical Engineering
Department of Chemical Engineering
Faculty of Engineering
Chulalongkorn University
Academic Year 2010

Thesis Title	FABRICATION OF CHITOSAN NANOFIBERS BY ELECTROSPINNING TECHNIQUE FOR CELL IMMOBILIZATION
By	Miss Prissadawan Chumanee
Field of Study	Chemical Engineering
Thesis Advisor	Assistant Professor Varong Pavarajarn, Ph.D.

Accepted by the Faculty of Engineering, Chulalongkorn University in Partial Fulfillment of the Requirements for the Master's Degree

..... Dean of the Faculty of Engineering
(Associate Professor Boonsom Lerdhirunwong, Dr.Ing.)

THESIS COMMITTEE

..... Chairman
(Apinan Soottitantawat, D.Eng.)

..... Thesis Advisor
(Assistant Professor Varong Pavarajarn, Ph.D.)

..... Examiner
(Associate Professor Chirakarn Muangnapoh, Dr. Ing.)

..... External Examiner
(Nawin Viriya-empikul, D.Eng.)

ปริศฎาวรรณ ชูมณี: การสร้างเส้นใยไคโตซานขนาดนาโนโดยเทคนิคการปั่นด้วยไฟฟ้าสถิตย์เพื่อใช้ในการตรึงเซลล์ (FABRICATION OF CHITOSAN NANOFIBERS BY ELECTROSPINNING TECHNIQUE FOR CELL IMMOBILIZATION).
อ. ที่ปรึกษาวิทยานิพนธ์หลัก : ผศ. ดร.วรงค์ ปวราจารย์, 160 หน้า

งานวิจัยนี้ได้ทำการศึกษาการสร้างเส้นใยไคโตซานขนาดนาโนด้วยเทคนิคการปั่นด้วยไฟฟ้าสถิตย์โดย ซึ่งมีวัตถุประสงค์ในการศึกษาถึงความเป็นไปได้ของการสร้างเส้นใยไคโตซานบริสุทธิ์ขนาดนาโนด้วยเทคนิคการปั่นด้วยไฟฟ้าสถิตย์รวมถึงการยึดติดและการมีชีวิตของเซลล์แบคทีเรียทั้งแบคทีเรียแกรมบวกและแบคทีเรียแกรมลบบนเส้นใยนาโนที่สร้างขึ้น โดยในส่วนของความสามารถในการขึ้นรูปพบว่าสารละลายไคโตซานที่มีน้ำหนักโมเลกุล 100, 400, 760 kDa เพียงอย่างเดียวไม่สามารถปั่นเป็นเส้นใยได้แต่จะถูกฉีดออกมาเป็นหยดเท่านั้น ไคโตซานจะสามารถปั่นเป็นเส้นใยได้ก็ต่อเมื่อเติมพอลิไวนิลแอลกอฮอล์เป็นสารช่วยการปั่นเส้นใยหรือการทำปฏิกิริยาไฮโดรไลซิสของไคโตซาน ในส่วนของการตรึงเซลล์แบคทีเรียและความสามารถในการมีชีวิตอยู่นั้นพบว่าแบคทีเรียแกรมลบสามารถยึดติดและมีการรอดชีวิตของเซลล์บนเส้นใยไคโตซานขนาดนาโนได้มากกว่าแบคทีเรียแกรมบวก จากการศึกษาการมีชีวิตของเซลล์แบคทีเรียด้วยเครื่องฟลูออเรสเซนต์ไมโครสโคปีแสดงให้เห็นว่าการบ่มเชื้อเป็นเวลา 12 ชั่วโมงมีความเหมาะสมให้เซลล์แบคทีเรียรอดชีวิตบนพื้นผิวของไคโตซาน นอกจากนั้นการเพิ่มเวลาของปฏิกิริยาไฮโดรไลซิสของไคโตซานจะเพิ่มการยึดติดและความสามารถในการมีชีวิตของแบคทีเรียบนพื้นผิวไคโตซานด้วยบทบาทของปฏิกิริยาการกำจัดหมู่อะซีติลและน้ำหนักโมเลกุลของไคโตซานที่ลดลงในขณะเกิดปฏิกิริยาไฮโดรไลซิส นอกจากนั้นเมื่อเปรียบการยึดติดและการรอดชีวิตของเซลล์แบคทีเรียบนไคโตซานในรูปแบบเส้นใยและฟิล์มไคโตซานพบว่าเส้นใยไคโตซานขนาดนาโนให้ผลการทดลองที่ดีมากกว่าฟิล์มไคโตซาน

ภาควิชา วิศวกรรมเคมี ลายมือชื่อ ปริศฎาวรรณ ชูมณี
สาขาวิชา วิศวกรรมเคมี ลายมือชื่ออ.ที่ปรึกษา
ปีการศึกษา 2553

5070342521 : MAJOR CHEMICAL ENGINEERING
KEYWORDS: CHITOSAN/ NANOFIBERS/ CELL IMMOBILIZATION

PRISSADAWAN CHUMANEE: FABRICATION OF CHITOSAN NANOFIBERS BY ELECTROSPINNING TECHNIQUE FOR CELL IMMOBILIZATION. THESIS ADVISOR: ASSISTANT PROFESSOR VARONG PAVARAJARN, Ph.D., 160 pp.

In this study, chitosan nanofibers were fabricated by electrospinning technique. It is an objective of this research to investing the feasibility of pure chitosan nanofibers fabrication via the electrospinning technique and to investigate bacterial attachment and cells viability of Gram-positive *Brevibacillus agri* strain 13 and Gram-negative *Acinetobacter baylyi* strain GFJ2 on the electrospun nanofibers. The fabrication of pure chitosan nanofibers was found to be unsuccessful. Only sprayed droplets were obtained. In order to obtain nanofibers, either the addition of polyvinyl alcohol (PVA) as a spinning aid or the hydrolysis of chitosan is needed. Formability, morphology and size distribution of the electrospun nanofibers using various preparation conditions are reported. For the results of bacterial attachment and viability, it has been proven that attachment of Gram-negative bacteria on chitosan is more effective than Gram-positive bacteria. Fluorescence microscopy results showed the optimal of incubation time of bacteria to be 12 h to get the highest fraction of live cells on the chitosan surface. Increasing hydrolysis time results in increased cell attachment and viability on the surface by the role of deacetylation and molecular weight reduced by hydrolysis reaction. Moreover, the chitosan in nanofibers form shows better cell attachment than chitosan in the form of films.

Department: Chemical Engineering Student's Signature ปริศดาวรรณ ชูมณี
Field of Study: Chemical Engineering Advisor's Signature
Academic Year: 2010

ACKNOWLEDGEMENTS

The author would like to express their highest gratitude to Assistant Professor Varong Pavarajarn for his invaluable guidance, excellent, kind supervision, support and encouragement thoughout this research.

Highly appreciation is also given to Assistant Professor. Alisa Vangnai, Department of Biochemistry, Chulalongkorn University for kind attention, recommendations allowing me to do the experimental and also would like to thank Doctor Apinan Sootitantawat, as a chairman, Associate Professor Chirakan Muangnapoh, and Doctor Nawin Viriya-empikul, as the members of thesis committee.

Furthermore, I would like to thank all teachers who educated and gave valuable suggestions.

Many thanks for kind suggestion and useful help to Associate Professor Tawatchai Charinpanitkul, Miss Pusanisa Patharachotesawate and many friends in the Center of Excellent in Particle Technology (CEPT) from Chulalongkorn University who always provided encouragement, suggestions and friendship along the thesis study.

Moreover, I would like to thanks Department of Biochemistry and Department of Botany, Chulalongkorn University for support me to do the experiment and use the equipments during ten months research in the cell immobilization parts.

Finally, I would like to express my greatest gratitude to my family and Kavin Nitasnajarukul for their love, support, encouragement and understanding thoughout my study.

CONTENTS

Page

Page

LIST OF TABLES

Page

LIST OF FIGURES

Page

Page

Page

Page

Page

Page

Page

Page

Page

Page

CHAPTER I

INTRODUCTION

Chitosan is a high-molecular-weight polysaccharide, which is obtained by deactylation of naturally occurring chitin derived from skeletal of arthrpods and mollusks. It is generally prepared by partial deacetylation of chitin in a hot alkali solution. Because of several unique and interesting biological properties such as bio-compatibility, bio-degradability, toxicity, chitosan has been considered for the development of membranes, gel, beads and fibers for fiber industries [1, 2].

Electrospinning technique has been investigated extensively to easily and inexpensively produce nanoscaled fibers. The electrospun nanofibers have been investigated for many applications, such as templates, reinforcement, filtration, catalysis, biomedical and pharmaceutical applications, and electronic and optical devices [3-5]. Especially in the area of filtration, electrospun nanofibers have shown distinctive characteristics and superiority. In recent years, filtration process has received increasing interest in industries. Immobilization of bacterial cells onto the filtration media has also been developed for the application in biofiltration. Some researchers have studied and developed support materials, particularly with regard to porosity and the shape of the material including fibers. Thus, the chitosan nanofibers fabricated by electrospinning techniques could result in higher efficiency of cells immobilization and can be used as support materials in the future. Nevertheless, it has been known that it is difficult to produce chitosan nanofibers via electrospinning technique because of the repulsion of cations. Many polymers such as PVA or PEO have been mixed with chitosan, as the spinning aid, to shield this repulsion and the composite fibers could be spun. However, durability and compatibility of these spinning aids toward the use as biofiltration might not be as good as chitosan [6, 7].

Interaction between chitosan and bacterial cell is due to its cationic nature to bind with sialic acid in phospholipids. Nevertheless, some researchers have suggested that the mechanism of the chitosan-bacteria interaction depends on whether the bacteria are Gram-positive or Gram-negative [8, 9]. Furthermore, the selection of the appropriate support materials has been largely fortuitous and has relied upon the organism's own ability to attach to the surface. Cells have been enclosed in a polymer matrix which is porous enough to allow the diffusion of substrate to the cells. Because of these limited attention has been paid to the efficiency and control of the immobilization of live cells on support materials or to the physiological activity of individually immobilized bacteria.

In this research, chitosan nanofibers, as well as nanofibers of chitosan blended with PVA, were fabricated by electrospinning. Effects of various factors, including chitosan molecular weight and blending ratio, on formability and morphology of the fibers as well as the application in cell immobilization were investigated.

Objective of this thesis are as follows:

1.1.1 To study the feasibility of pure chitosan nanofibers fabrication and to compare the formation of electrospun nanofibers using pure chitosan to that with the addition of poly (vinyl alcohol) (PVA) and to that using hydrolyzed chitosan.

1.1.2 To study the feasibility of cell immobilization on chitosan nanofubes.

1.1.3 To compare the capability of cells attachment on chitosan nanofibers fabricated by electrospinng with that on chitosan films.

This thesis is divided into five chapters as follows:

Chapter I provides an overview of this thesis.

Chapter II explains the basic theory about this work such as introduction of chitosan, electrospinning process, cell immobilization methods and the general bacteria characteristics. Literature reviews of the previous works related to this research are also presented.

Chapter III shows the chemical reagents and experimental procedures.

Chapter V shows the experimental results and discussion.

Chapter VI, the last chapter, shows overall conclusions and recommendations for future research.

CHAPTER II

BACKGROUND AND LITERATURE REVIEW

2.1 Chitosan

Chitosan is a cationic polymer comprising of copolymers of β-(1-4)-linked D-glucosamine (deacetylated unit) and N-acetyl-D-glucosamine as shown in Figure 2.1. Chitosan is obtained from chitin, which is a natural polysaccharide found particularly in the shell of crustacean, cuticles of insects and cell walls of fungi. Chitin is the second most abundant polymerized carbon found in nature.

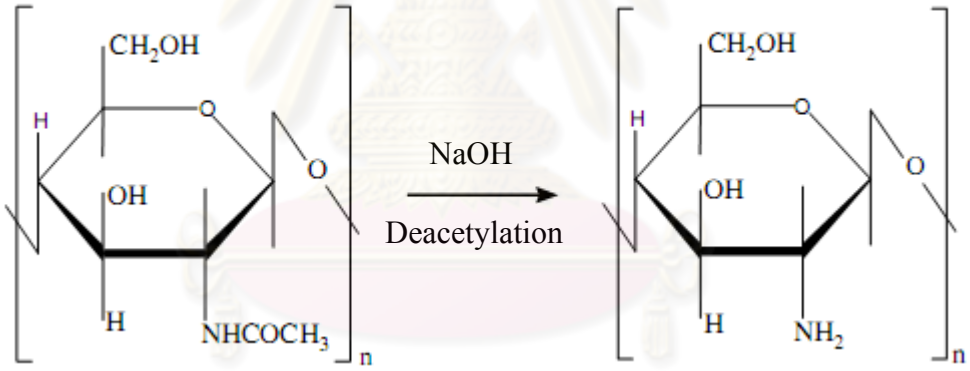

Chitin Chitosan

Figure 2.1 Chemical structure of chitin and chitosan.

Hirano (1996) presented about the production and consumption of chitin and chitosan, as well as their practical applications in biotechnology. The applications include the use as: 1) cationic agents for polluted waste-water treatment, 2) agricultural materials, 3) food and feed additives, 4) hypocholesteolemic agents, 5) biomedical and pharmaceutical materials, 6) wound-healing materials, 7) blood anticoagulant, antithrombogenic and hemostatic materials, 8) cosmetic ingredients, 9) textile, paper, film and sponge sheet materials, 10) chromatographic and immobilizing media, and

11) analytical reagents. It has been proved to be biologically renewable, biodegradable, biocompatible, non-antigenic, non-toxic and biofunctional. The term chitosan has been used to describe a series of polymers of different degrees of deacetylation defined in terms of the percentage of primary amino groups in the polymer backbone. The degree of deacetylation of typical commercial chitosan is usually between 70% and 95%, with molecular weight between 10 and 1000 kDa. The properties, biodegradability and biological role of chitosan are dependent on the relative proportion between of N-acetyl-amine and D-glucos amine residues. In preparing chitosan, ground shells are deproteinated and demineralized by sequential treatments with alkali and acid, after which the extracted chitin is deacetylated to chitosan by alkaline hydrolysis at high temperature. Production of chitosan via this process is inexpensive, easy and can provide additional control over chitosan final properties. In addition, chitosan molecule has amino and hydroxyl groups which can be modified chemically providing high chemical versatility. Morever, it can be metabolized by certain human enzymes, especially lysozyme. Therefore, it is considered biodegradable. Chitosan is also a bioadhesive material. The adhesive property of chitosan in a swollen state has shown to persist well during repeated contact between chitosan and the substrate, impling that, in addition to the adhesion by hydration, many other mechanisms, such as hydrogen bonding and ionic interactions might also have involved.

Khor et al. (2003) reviewed the extraction of chitin from shellfish sources. More than 40 years have lapsed since this biopolymer had aroused the interest of the scientific community around the world for its potential biomedical applications. Chitin, together with its variants, especially its deacetylated counterpart chitosan, has been shown to be useful as a wound dressing material, drug delivery vehicle and a candidate for tissue engineering. The promise for this biomaterial is vast and will continue to increase as the chemistry to extend its capabilities and new biomedical applications are investigated. It is interesting to note that a majority of these works has come from Asia. Japan has been the undisputed leader, but other Asian nations, namely Korea, Singapore, Taiwan and Thailand have also made notable contributions.

Dutta et al. (2008) summarized all the known methods of formation of chitosan based films with antimicrobial properties and discussed their subsequent applicability in the area of food preservation. Active biomolecules such as chitosan and its derivatives have a significant role in food application area. Chitosan-based films have proven to be very effective in food preservation. The presence of amino group in C2 position of chitosan provides major functionality towards biotechnological needs, particularly, in food applications. Chitosan-based polymeric materials can be formed into fibers, films, gels, sponges, beads or even nanoparticles. Chitosan films have shown potential to be used as a packaging material for the quality preservation of a variety of food. Chitosan has exhibited microbial activity in a wide variety of pathogenic and spoilage microorganisms, including fungi, and Gram-positive and Gram-negative bacteria.

2.2 Electrospinning Process

2.2.1 General description of electrospinning process

The process of electrospinning, namely utilizing electrostatic forces to generate polymer fibers, can be traced back to the process of electrospraying, in which solid polymer droplets are formed rather than fibers. In fact, a number of processing parameters must be optimized in order to generate fibers as opposed to droplets. A typical electrospinning apparatus can be used to form fibers, droplets, or a beaded structure depending on the various processing parameters, such as distance between source and collector or applied potential. In recent works, a greater understanding of processing parameters has led to the formation of fibers with diameters in the range of 100-500 nm, typically referred to as nanofibers. A typical electrospinning set up is consisted of a capillary through which the liquid to be electrospun is forced; a high voltage source with positive or negative polarity, which provides electrical charges to the liquid; and a grounded collector (Figure 2.2). A syringe pump, gravitational force, or pressurized gas are typically employed as a mean to force the liquid through a small-diameter capillary forming a pendant drop at

the tip of the capillary. An electrode from the high-voltage source is then immersed in the liquid or can be directly attached to the capillary if a metal needle is used.

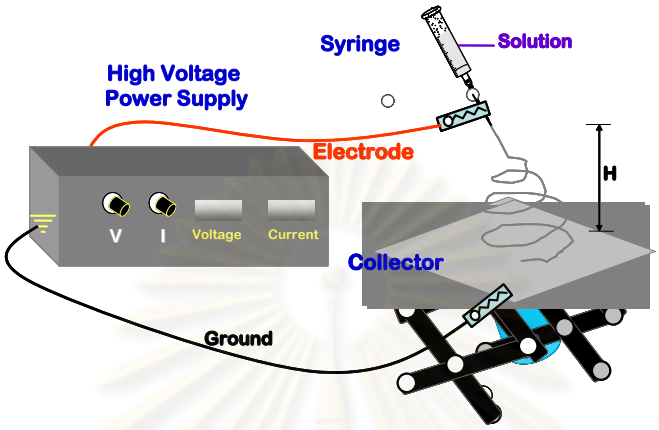

Figure 2.2 Schematic of a typical electrospinning system.

Upon the application of the potential from the high-voltage source, charges are injected into the liquid. Increasing the electric field strength causes the repulsive interactions between like charges in the liquid and causes the attractive forces between the oppositely charged liquid and at the collector to begin to exert tensile forces on the liquid, elongating the pendant drop at the tip of the capillary. As the electric field strength is increased further, a point will be reached at which the electrostatic forces balance out the surface tension of the liquid. If the applied voltage is increased beyond this point a fiber jet will be ejected from the apex of the cone and accelerates toward the grounded collector. Huang et al. (2003) recognized an electrospinning technique for the fabrication of polymer nanofibers. Various polymers have been successfully electrospun into ultrafine fibers in recent years, mostly from polymer solution in solvent and some in melt form. Potential applications based on such fibers, including their uses as reinforcement in nanocomposite, have been realized. Comprehensive reviews have been presented on researches and developments related to electrospun polymer nanofibers including processing, structure and property characterization, applications, and modeling and simulations.

Nowadays, the development of the nanofibers has led to resurgence in interest regarding the electrospinning process due to potential applications in filtration, protective clothing, and biological applications such as tissue engineering scaffolds and drug delivery devices as schematically shown in Figure 2.3.

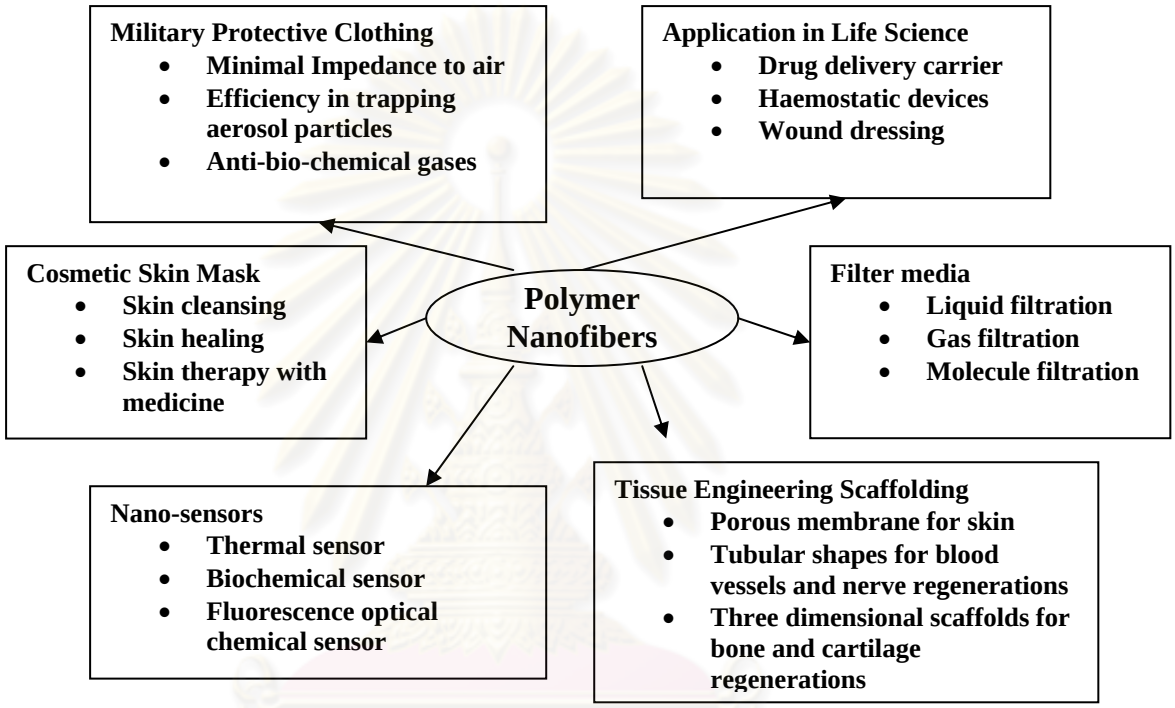

Figure 2.3 Potential applications of electrospun polymer nanofibers (Huang et al., 2003).

Ma et al. (2005) prepared cellulose nanofibers membrane by electrospinning as affinity membrane. Cellulose acetate (CA) solution (0.16 g/ml) in a mixed solvent of acetone/DMF/trifluoroethylene (3:1:1) was electrospun into nonwoven fiber mesh with the fiber diameter ranging from 200 nm to 1 μm. The CA nanofiber mesh was heat-treated at 208 °C for 1 h to improve structural integrity and mechanical strength, and then treated in 0.1 M NaOH solution in H_2O/ethanol (4:1) for 24 h to obtain regenerated cellulose (RC) nanofiber mesh, which was used as a novel filtration membrane.

2.2.2 Electrospinning of chitosan

Geng et al. (2005) produced electrospun chitosan nanofibers from aqueous chitosan solution using concentrated acetic acid solution as a solvent. A uniform nanofibrous mat with average fiber diameter of 130 nm was obtained. The concentration of the aqueous acetic acid higher than 30% was prerequisite for chitosan nanofiber formation, because more concentrated acetic acid in water progressively decreased surface tension of the chitosan solution and concomitantly increased charge density of jet without significant effect on solution viscosity. However, acetic acid solution higher than 90% did not dissolve enough chitosan to make spinnable viscous concentration. Only chitosan of a molecular weight of 106,000 g/mol produced bead-free chitosan nanofibers, while low- or high-molecular-weight chitosans of 30,000 and 398,000 g/mol did not. Average fiber diameters and size distribution decreased with increasing electric field and more bead defects appeared at 5 kV/cm or more.

Bhattarai et al. (2005) presented controllable chitosan/PEO nanofibers with an average diameter from a few microns down to 40 nm that were fabricated by electrospinning. The nanofibers can be deposited as a nonwoven membrane or as a highly aligned bundle. Rheological study combined with SEM characterization revealed that the spinnability of chitosan solution was substantially improved when the solution viscosity was reduced. Introducton of Triton X-100™ as a surfactant and DMSO as a cosolvent into chitosan solution allowed the solution to be spinnable at high chitosan/PEO ratios, and substantially improved the spinnability of the solution and the fibrous structure of as-spun nanofibers. The nanofibrous membrane of chitosan/PEO with a ratio of 9 to 1 retained good structural integrity in water and exhibited better adhesion of chondrocytes than its cast film counterpart. SEM images further confirmed that chitosan/PEO nanofibers promoted the adhesion of chondrocyte (HTB-94) and osteoblast (MG-63) cells
and maintained characteristic cell morphology and thus cell phenotype, and may serve as a potential candidate for bone tissue engineering.

Lei et al. (2006) prepared nanofibers with average diameters between 20 and 100 nm by electrospinning of 82.5% deacetylated chitosan (M_v = 1600 kDa) mixed with poly(vinyl alcohol) (PVA, M_w = 124–186 kDa) in 2% (v/v) aqueous acetic acid. The formation of bicomponent fibers was feasible with 3% (v/v) acetic acid containing up to an equal mass of chitosan. Finer fibers, fewer beaded structures and more efficient fiber formation were observed with increasing PVA content. Nanoporous fibers could be generated by removing the PVA component in the 17/83 chitosan/PVA bicomponent fibers with 1 M NaOH (12 h). Fiber formation efficiency and composition uniformity improved significantly when the molecular weight of chitosan was halved by alkaline hydrolysis (50 wt % aqueous NaOH, 95 °C, 48 h). The improved uniform distribution of chitosan and PVA in the bicomponent fibers was attributed to better mixing mostly due to the reduced molecular weight and to the increased deacetylation of the chitosan.

Homayoni et al. (2009) studied the problem of chitosan with the electrospinning technique. Because of chitosan high viscosity, which limits its spinability, the problem could be resolved through the application of an alkali treatment which hydrolyzes chitosan chains and so decreased its molecular weight. Solution of the treated chitosan in 70–90% acetic acid aqueous solution produced nanofibers with appropriate quality and processing stability. Decreasing the concentration of acetic acid in the solvent increased the mean diameter of the nanofibers. Optimum nanofibers are achieved with chitosan which was hydrolyzed for 48 h. The diameter of these nanofibers (140 nm) was strongly affected by the electrospinning conditions as well as by the concentration of the solvent. FTIR investigations proved that neither the alkali treatment nor the electrospinning process change the chemical nature of the polymer.

2.3 Cell Immobilization

Attachment of cells onto a solid surface is probably the mildest among cell immobilization techniques. In its simplest form, it is also one of the processes that does not result in a high-value added product. The success of the technique depends,

in the first instance, upon the properties of the cells themselves. The natural evolution of species has produced many organisms that are capable of adhering to surface. Some techniques in waste water treatment, e.g. the trickling filter system, have made use of this property for decades. In adsorption, there is generally an initial weak attachment of the cells, which can be easily reversed. This is followed by development of stronger (multiple attachment) binding. Extracellular material produced by the cells is often an important factor in fixing the cells to the adsorption substrate. This step may be followed by a natural entrapment of the cells in a biopolymer matrix.

For industrial processes, the selection of the appropriate support material has been largely fortuitous and has relied mainly upon the organism's own ability to attach to the surface. The more recent active interest in the adsorption process has led to study and development of all kinds of support materials, ranging from simple crude mineral substances to complex ion-exchange derivatives of organic polymers. In addition, the physical form of the support has received considerable attention, particularly with regard to porosity and shape of the material. Techniques for the immobilization of cells can be classified into two methods, i.e., attachment and entrapment.

2.3.1 Entrapment method

Entrapment method employs a variety of matrices that have been used for cell immobilization such as natural polymeric gels (e.g. agar, carrageenan, alginate, chitosan and cellulose derivatives) and synthetic polymers (e.g. polyacrylamide, polyurethane, polyvinyl) Entrapment in natural polymeric gels has become a preferred technique for cell immobilization because of the toxicity problems associated with synthetic polymeric materials. The use of natural gels is, however, limited by their mechanical strength and the lack of open spaces to accommodate active cell growth resulting in their rupture and the release of cells into the growth medium. The advantages accruable from such bio-structures are reusability, non-toxicity,

mechanical strength for necessary support and open spaces within the matrix for growing cells, thus, avoiding rupture and diffusion problems.

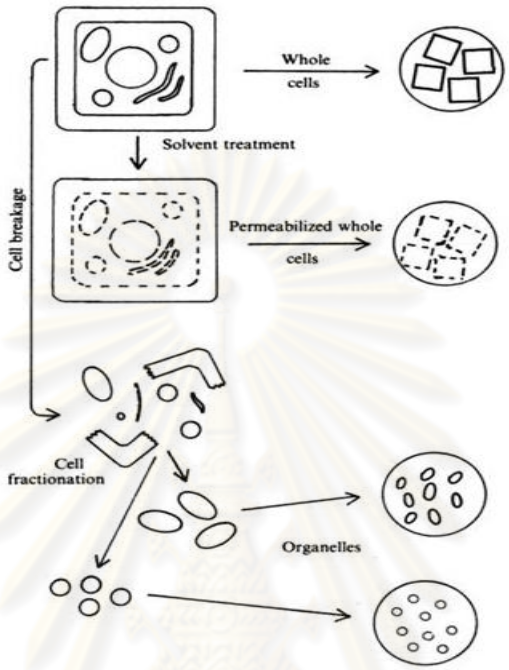

Figure 2.4 The immobilization of the biocatlytic activity of cells by entrapment.

2.3.2 Attachment method

Attachment method has utilized synthetic foams such as polyurethane foams and nylon sponge as a substrate for immobilization. Recently, stainless steel sponges have also been described as a suitable synthetic material for fungi immobilization (Ignacio et al., 2006). One of the advantages found for the use of stainless steel sponges is that dyes do not adsorb onto it. Also, natural supports (i.e., organic materials) can be used to immobilize fungi by the attachment method. Neverthless, the use of natural supports can cause problems in a bioreactor. For example, degradation and loss of the supporting material may lead to blockages in the waste stream and a constant flow of wastewater may lead to permanent losses of enzymes from the fungal extracellular matrix.

2.4 Background for Bacteria Used in This Research

For individual bacterial cell, Gram was a scientist who invented a technique called Gram staining by which bacteria can be divided into two groups based on the chemical and physical properties of their cell walls. The difference in Gram-reaction of these two groups of bacteria is thought to be due to a difference in the structure of their cell walls. Gram-positive cell walls consist of many layers or peptidoglycan and do not posses a lipid outer membrane. Gram-negative cell walls on the other hand have only one or a few layers of peptidoglycan but posses an outer membrane consisting of various lipid complexes. The term Gram-negative or Gram-positive refers to the staining procedure used to determine the cell wall composition of unknown bacteria, which helps determining the appropriate antimicrobial treatment by physicians. It does not refer to the electrical charge of the bacteria. Both Gram-negative and Gram-positive bacteria are negatively charged. The characteristics listed in Table 2.1 are generally presented for the between differences of Gram-positive and Gram-negative bacterial. Schematic cross sections of these structures are shown in Figure 2.5.

Table 2.1 Characteristics of Gram-positive and Gram-negative bacteria.

Components	**Gram- positive**	**Gram- negative**
Peptidoglycan	60-100%	5-20%
Lipid content	0.2%	10-20%
Polysaccharide	35-60%	15-20%
Thickness	20-80 nm.	10 nm.
Teichoic acid	Accessory polymers covalently linked to Peptidoglycan	No
Cell wall	1 membrane layer	2 layers

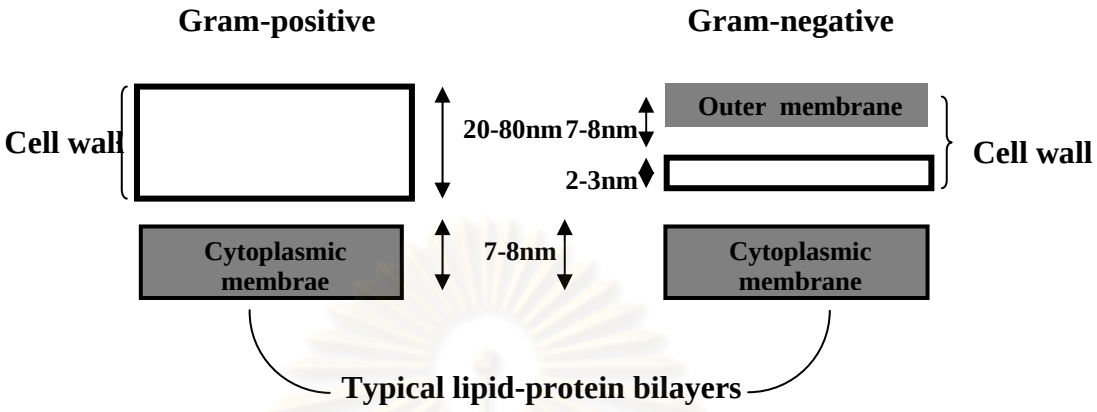

Figure 2.5 Schematic cross sections of cell structure.

2.4.1 Acinetobacter baylyi

Acinetobacter is a Gram-negative bacterium that is readily found throughout the environment including drinking and surface water, soil, sewage and various types of foods. *Acinetobacter* is also commonly found as a harmless coloniser on the skin of healthy people and usually poses very few risks. In this study, *Acinetobacter baylyi* strain GFJ2 was isolated from fruit peel. *Acinetobacter* cells are short, measuring 1.0-1.5 by 1.5-2.5 microns elliptoid during growth. They often become more coccoid during the stationary phase. Cells are found in pairs or small clusters. The groups form smooth, pale colonies on solid media. *Acinetobacter* is strictly aerobic, catalase positive, and oxidase negative. It is the last properly that can be used to distinguish *Acinetobacter* from other infective bacteria. These bacteria can use various selection of organic materials as source for carbon.

2.4.2 Brevibacillus agri

Brevibacillus is a Gram-positive bacteria related to *Bacillus*. *Bacillus* is a genus of rod-shaped bacteria and a member of the division *Firmicutes*. *Bacillus* species are obligate aerobes, and test positive for the enzyme catalase. *Bacillus*

includes both free-living and pathogenic species. Under stressful environmental conditions, the cells produce oval endospores that can stay dormant for extended period. The cell wall of *Bacillus* is a structure on the outside of the cell that forms the second barrier between the bacterium and the environment, and at the same time maintains triangle shape and withstands the pressure generated by the cell's turgor. The cell wall is composed of teichoic and teichuronic acids. The role of the cytoskeleton in shape generation and maintenance is important.

Kongpol et al. (2009) presented about a *Brevibacillus agri* strain 13, which was isolated and characterized as a Gram-positive organic-solvent-tolerant bacterium able to grow at 45 °C. It can tolerate high concentration (5% and 20%, v/v) of various organic solvents with a broad range of log P_{ow} when the organic solvent was provided as a nonaqueous layer. Although it can tolerate a number of aromatic solvents, it cannot utilize them as a sole carbon source. The surface characteristics of cells exposed to organic solvent were investigated using the bacterial adhesion to hydrocarbon test, a contact angle measurement, ζ potential determination, and fluorescence microscopy analysis and compared with that of non-exposed cells. The results showed that although it has a hydrophilic cell surface, it has a unique indigenous cell surface characteristic in which the cells can stabilize solvent-in-water emulsion by adhering to the solvent—water interface of the solvent droplets. The tolerance and predilection of *B. agri* strain 13 toward organic solvents may suggest its potential application as a whole-cell biocatalyst for the biotransformation process of water-immiscible substrate(s).

2.5 Interaction between Cell and Chitosan

Hong et al. (2001) presented the bacterial activities of six chitosans and six chitosan oligomers with different molecular weights (Mws) against four Gram-negative (*Escherichia coli, Pseudomonas fluorescens, Salmonella typhimurium, and Vibrio parahaemolyticus*) and seven Gram-positive bacteria (*Listeria monocytogenes, Bacillus megaterium, B. cereus, Staphylococcus aureus, Lactobacillus plantarum, L. brevis, and L. bulgaricus*). Chitosan generally showed stronger bactericidal effects

with gram-positive bacteria than gram-negative bacteria. The minimum inhibitory concentration (MIC) of chitosan ranged from 0.05% to > 0.1% depending on the bacteria and Mws of chitosan.

Fierro et al. (2007) showed the effect of chitosan immobilization of *Scenedesmus* spp. cells on its viability, growth and nitrate and phosphate uptake. *Scenedesmus* sp. (strains 1 and 2) and *Scenedesmus obliquus* immobilized in chitosan beads showed high viability after the immobilization process. Immobilized *Scenedesmus* sp. strain 1 had higher growth rate than its free living counterpart. The immobilized cells accomplished 70% nitrate and 94% phosphate removal within 12 h of incubation while the free-living cells removed 20% nitrate and 30% phosphate within 36 h of treatment. Blank chitosan beads were responsible for up to 20% nitrate and 60% phosphate uptake at the end of the experiment. Chitosan is a suitable matrix for immobilization of microalgae, particularly *Scenedesmus* sp., but this system should be improved before being need for water quality control.

Hui et al. (2004) studied about the bactericidal activity of chitosan acetate solution against *Escherichia coli* and *Staphylococcus aureus* was by evaluating the enumeration of viable organisms at different incubation times. Morphologies of bacteria treated with chitosan were observed by transmission electron microscopy (TEM). The interaction of chitosan with synthetic phospholipid membranes was studied. Results showed that chitosan increased the permeability of the outer membrane, inner membrane and ultimately disrupted bacterial cell membranes, with the release of cellular contents. This damage was likely caused by the electrostatic interaction between NH_3^+ groups of chitosan acetate and phosphoryl groups of phospholipid components of cell membranes.

Chung and Chen (2007) investigated the bacterial activity of chitosan by assessing the mortality rates of *Escherichia coli* and *Staphylococcus aureus* based on the extent of damaged or missing cell walls and the degree of leakage of enzymes and nucleotides from different cellular locations. Chitosan was found to react with both the cell wall and the cell membrane, but not simultaneously, indicating that the

inactivation of *E. coli* by chitosan occurs via a two-step sequential mechanism: an initial separation of the cell wall from its cell membrane, followed by destruction of the cell membrane. The similarity between the bacterial profiles and patterns of chitosan and those of two control substances verified this mechanism. The bacterial activity of chitosan could be altered by blocking the amino functionality through coupling of the chitosan to active agarose derivatives. These results verify the status of chitosan as a natural bactericide.

Desai et al. (2009) fabricated nanofibrous filter media by electrospinning of chitosan/PEO blend solutions onto a spunbonded non-woven polypropylenesubstrate. They demonstrated the usage of chitosan-based nanofibrous filter media to effectively filter out heavy metal ions, pathogenic microorganisms, and contaminant particulate media from both air and water media. Heavy metal binding, anti-microbial and physical filtrations efficiencies of these chitosan-based filter media were studied and correlated with the surface chemistry and physical characteristics of these nanofibrous filter media. Filtration efficiency of the nanofiber mats was strongly related to the size of the fibers and its surface chitosan content. Hexavalent chromium binding capacity up to 35 mg chromium/g chitosan was exhibited by chitosan-based nanofibrous filter media along with a 2–3 log reduction in *E. coli* bacteria. After 6 h of contact time, the chitosan blend fibers did show 2–3 log reduction in *E. coli*. Air and water filtration efficiencies of the nanofibrous filter media were measured using aerosol and PS beads suspended in water respectively. It was shown that the nano fibrous filter had high efficiencies which correlated with the fibrous media size and shape. These results indicated the advantage of chitosan nanofibers in filters and its commercial applicability.

CHAPTER III

EXPERIMENTAL

This section involves the equipment and chemical reagents used in the research. The main experimental procedures will be explained in 4 parts: 1) preparation of solution for electrospinning, 2) chitosan nanofibers fabrication by electrospinning technique, 3) characterization of the obtained chitosan nanofibers, 4) characterization of nanofibers and cell attachment on chitosan nanofibers.

3.1 Chemical Reagents

1. Chitosan (Biolife, Thailand; Mw~100 kDa, 400 kDa and 760 kDa)
2. Poly(vinyl alcohol) (Ajax Finechem, Australia; Mw~ 80 kDa)
3. Glacial acetic acid (Analytical grade; BDH, England)
4. Sodium hydroxide (Analytical grade; Merck Ltd., Thailand)
5. Sodium chloride (Analytical grade; Merck Ltd., Thailand)
6. Potassium dihydrogen phosphate (Analytical grade; Merck Ltd., Thailand)
7. Potassium hydrogen phosphate (Analytical grade; Merck Ltd., Thailand)
8. LIVE/DEAD® *Bac*Light™ Bacterial viability kit (Model L7012, Molecular Probes, Invitrogen Corporation, USA.)

3.2 Preparation of Electrospinning Solution

3.2.1 Hydrolyzed chitosan

For a set of experiments to verify the effect of chitosan hydrolysis on the formation of nanofibers, chitosan with molecular weight of 760,000 g/mol was used. Hydrolysis was done by using 50% NaOH solution. The mixture of 1:25 (w/v) chitosan/NaOH solution was heated at 95°C for various period of time, in the range of 0-48 h. Each sample was strained and rinsed with distilled water before being dried at 60°C for 6 h. The electrospinning solution was then prepare by redissolving the

hydrolyzed chitosan in 90% wt. acetic acid solution under magnetic stirrer until the solution became clear and homogeneous.

3.2.2 Preparation of chitosan/PVA blend

For the fabrication of chitosan/PVA composite fibers, predetermined amount of chitosan was firstly dissolved in 90% wt. acetic acid solution under magnetic stirring overnight at room temperature. At the same time, an aqueous solution of 10% wt. PVA was prepared at 80°C. Then, chitosan solution and PVA solution were blended together at predetermined blending ratio, under constant stirring by a magnetic stirrer, until homogeneous solution of Chitosan/PVA was obtained. The blending chitosan to PVA solution is shown in Table 3.1.

Table 3.1 The blending chitosan to PVA solution

Chitosan 100kDa		Chitosan 400kDa		Chitosan 760kDa	
CS content (%w/v)	PVA content (%w/v)	CS content (%w/v)	PVA content (%w/v)	CS content (%w/v)	PVA content (%w/v)
0	0.10	0	0.10	0	0.10
0.004	0.08	0.003	0.08	0.002	0.08
0.008	0.06	0.006	0.06	0.004	0.06
0.012	0.04	0.009	0.04	0.006	0.04
0.016	0.02	0.012	0.02	0.008	0.02
0.020	0	0.015	0	0.010	0

3.3 Electrospinning of the Prepared Solution

A typical electrospinning set up was consisted of a capillary through which the solution to be electrospun was forced; a high voltage source with positive polarity, which injects charge in to the solution; and a grounded collector (see Figure 2.2). Electrospinning of the prepared solution was done according to the procedure described in literatures. Briefly, the solution was placed into a 10 ml syringe with a

stainless steel needle (diameter of 25mm). Then, the electrical field with a potential of 25 kV across the distance of 10 cm between the tip of the needle and the collector plate was supplied to the solution, which consequently produced ultrathin fibers travelling from the needle to the collector.

3.4 Characterizations

3.4.1 Characterization of electrospinning solution

Two main factors have been reported to affect electrospinability of the solution, i.e, viscosity and conductivity of the solution. The viscosity of the electrospinning solution was measured by a Brookfield Viscometer (model DV-II+ Programmable) at the condition of shear rate equal to 1.00 rpm and the spinning time of 1 minute. On the other hand, the electrical conductivity of the solution was measured by conductivity meter (model LC116, Mettler Toledo Instruments, China).

3.4.2 Characterization of electrospun fibers

The morphology of the electrospun fibers was observed under a scanning electron microscope (JEOL model JSM-6301F and HITACHI model S3400). The diameter of the electrospun nanofibers was measured with SemAfore image analyzing program. For each experiment, average fiber diameter and size distribution were determined from the data of about 100 measurements of the randomly selected fibers.

3.5 Cell Attachment

3.5.1 Mineral medium

The mineral medium was used for screening, isolation and cultivation of bacterial cells. The mineral medium was comprised of media and trace element.

I. Media

The media was prepared from:

Na_2HPO_4	1.4196 g
KH_2PO_4	1.3609 g
$MgSO_4.7H_2O$	0.0985 g
$CaCl.H_2O$	0.0059 g

All components were dissolved in 1 liter of distilled water and adjusted pH to 7 by 1N NaOH. The mineral medium was autoclaved at 121°C for 15 minutes.

II. Trace element

H_3BO_3	0.116 g
$FeSO_4.7H_2O$	0.278 g
$ZnSO_4.7H_2O$	0.115 g
$MnSO_4H_2O$	0.169 g
$CuSO_4H_2O$	0.038 g
$CoCl_2.6H_2O$	0.024 g
MoO_3	0.010 g

Trace element solution was separately prepared from the media as a stock solution. All components were dissolved in 100 ml of distilled water. The solution was autoclaved at 121°C for 15 minutes. The sterile trace element was supplemented in mineral medium at the condition of 0.15(v/v).

III MMSAY

Stock I	4 ml
Distilled water	96 ml
Trace element(0.1%)	0.1 ml
Yeast(0.1%)	0.1 g
AmS(1mM)	0.1 ml
Sucinate(4mM)	0.1 ml

MMSAY medium was dissolved in 100 ml of distilled water and its was autoclaved at 121°C for 15 minutes.

IV. Luria Bertani medium (LB)

Trypton	10 g
Yeast Extract	5 g
NaCl	10 g

LB medium was dissolved in 1 liter of distilled water and adjusted to pH 7.0. Then it was autoclaved at 121°C for 15 minutes.

3.5.2 Starter preparation and inoculation

The streak plate method is a rapid and simple technique of mechanically diluting a relatively large concentration of microorganisms to a small, scattered population of cells. It isused to obtain isolated colonies on a large part of the agar surface, so that desired species can then be brought into pure culture. Proper streaking of plates is an indispensable tool in microbiology. In most cases, a closed inoculating loop is used for streaking plates. Streak plates are made from a broth culture, an agar slant or from an agar plate. A loopful of inoculum is transferred from the source and put on the agar surface. A small spot is spreaded during the initial transfer. The first phase of the streaking pattern is begun. Several basic pattern are shown in Figure 3.1. The three-phase streaking pattern is recommended for beginners because it is most likely to give satisfactory results with suspensions having a wide range of microbial density. Single drop from the loop as it was rubbed along the agar surface can be developed into separate colonies in the inocubator for 20 hours. *Acinetobacter baylyi* strain GFJ2 was incubated at room temperature while *Brevibacillus agri* strain 13 was incubated at 45°C.

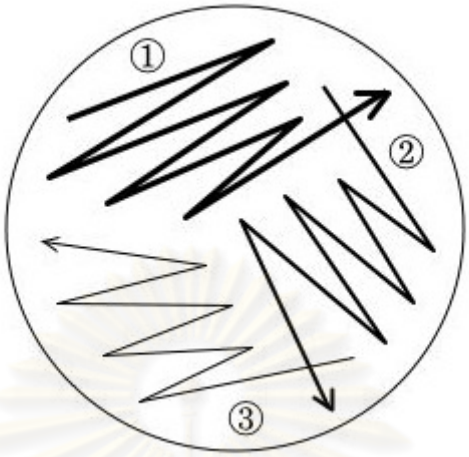

Figure 3.1 Streak plate pattern.

To inoculate a single colony onto broth medium, the sterilized inoculated loop was used to pick a single colony in the streak plate and place into the broth medium. The incubated medium was placed into an incubator shaker with 250 rpm operated at room temperature for 20 hours for *Acinetobacter baylyi* strain GFJ2 while *Brevibacillus agri* strain 13 was shaken at 45°C, 250 rpm for 20 hours. After that, bacteria grew in saturated manner in the broth medium. This is called a starter which was used as a bacterial stock.

3.5.3 Bacterial immobilization

Cell immobilization onto the electrospun chitosan nanofibers was tested by the following procedure. A blank aluminum foil was used as a control reference. All samples were sterilized under UV radiation prior to test with bacteria.

In this research, two strains of bacteria, i.e., *Brevibacillus agri* strain 13 and *Acinetobacter baylyi* strain GFJ2, were used to test the cell immobilization onto the electrospun chitosan nanofibers. In order to prepared the bacterial cells, 5 ml from broth medium were used for the cell proliferation in a 100 ml of medium (1% inoculum). The incubation was done for 20 h, under constant shaking at 250 rpm at 45°C for *Brevibacillus agri* strain 13 and at room temperature for *Acinetobacter*

baylyi strain GFJ2. After that, the medium was centrifuge at 5000 rpm for 15 minutes. The high density cells were placed into 20 ml of medium solution.

For the test of bacterial attachment, 100 µl of the bacterial cells solution was dropped onto 1.5x1.5 cm^2 piece of the testing sample in the agar plate. The agar plate was then taken into an incubator. The incubating temperature was 45°C for *Brevibacillus agri* strain 13 and room temperature for *Acinetobacter baylyi* strain GFJ2. After the predetermined incubation period, in the range of 0-48 h, the sample was taken out and rinsed with 0.5 ml (0.1 M, pH=7.04) phosphate buffer to remove unattached cells, twice. In order to determine the bacterial cells attached on chitosan nanofibers, the optical density of the initial bacterial cell solution and that of the washed solution was measured by spectrophotometer at 600 nm (OD_{600}). The Colony Forming Unit (CFU) was calculated from a standard calibration curve for *Acinetobacter baylyi* strain GFJ2 and *Brevibacillus agri* strain 13. Finally the sample was dried before subjected to the observation via SEM.

3.5.4 Bacterial viability

Conventional methods for examining cell viability and morphology utilize different fluorescent dyes to preferentially stain viable or dead cell. The LIVE/DEAD *Bac*Light Bacterial viability kit provides a novel two color fluorescence assay of bacterial viability by utilize mixtures SYTO9 green fluorescent nucleic acid stain and the red fluorescent nucleic acid stain , propidium iodide to differentiate between cells with intact (viable) and compromised (dead or injured) membranes. The LIVE/DEAD *Bac*Light kit has been investigated extensively to easily, reliably and quantitatively distinguish live and dead bacteria analysis with a fluorescence microscopy [10]. It not only helps to monitoringcell viability and morphology but also proves reliable for both gram-positive and gram-negative bacteria.

Viability testing of cells attached onto the electrospun chitosan nanofibers tested by Live/Dead® *Baclight*™ *Bac*terial Viability Kit (model L7012). This kit is well suited for microscopic and quantitative analyses.

The *Bac*terial Viability kit consists of two nucleic acid stain, i.e., the green-fluorescence 3.34 mM SYTO9 dye solution in DMSO (Component A) and the red-fluorescence 20 mM Propidium iodide dye solution in DMSO (Component B). For preparation of the dye stock solution, two dye components were combined at the ratio between Component A and Component B of 1:1 in a microfuge tube. The dye mixture was added with 3µL for each mL of 1M NaCl, and mixed thoroughly.

For the test of bacterial viability, 50 µL of the dye solution was dropped onto 1.5x1.5 cm^2 piece of the testing sample in the LB plate. The sample was then incubated for 15 minutes. The incubating condition was room temperature in the dark for both *Brevibacillus agri* strain 13 and *Acinetobacter baylyi* strain GFJ2. After incubation period, the sample was taken out and observed in a fluorescence microscope (Olympus model BX-51). The fluorescence from both live (green fluorescence) and dead (red fluorescence) cells were detected using excitation wavelength of 470 nm. The emission for the green and red channel was detected at the wave length of 510-540 nm and 620-650 nm, respectively. For each experiment, the populations of both live bacteria and dead bacteria were determined from the data of about 3 points from the randomly selected area.

CHAPTER IV

RESULTS AND DISCUSSION

This chapter is divided into 5 parts: 1) electrospinning of pure chitosan, 2) the effects of chitosan hydrolysis and PVA addition on electrospinability, 3) morphology of chitosan nanofibers fabricated by electrospinning technique, 4) bacterial cell attachment on chitosan nanofibers, 5) viability of bacterial on chitosan nanofibers.

4.1 Electrospinning of Pure Chitosan

For the electrospinning of pure chitosan, usings of chitosan solution with the concentration of 2%, 1.5% and 1% for the chitosan molecular weight of 100, 400 and 760 kDa, respectively, the results are shown in Figure 4.1. It should be noted that the concentration of chitosan in the solution investigated was the highest concentration that allowed to be electrospun. The solutions with the concentration higher than these values were too viscous to be spinnable. The SEM images in Figure 4.1 reveal that only sprayed droplets were obtained in all conditions. No fiber was found. Generally, the formation of droplets or fibers is controlled by viscosity of the solution [11, 12]. However, for chitosan, which is a cationic polysaccharide with amino groups at the C2 position, the repulsive interaction among the polycations on the chitosan chains has been thought to prevent sufficient chain entanglement requires for the formation of fibers via electrospinning [13]. It was presumed that the jet of chitosan solution was stable for a short period after being ejected from the tip of the needle. After that, the jet broke up, while the solvent evaporation took place, resulting in the formation of particles. All attempts to produce pure chitosan nanofibers from the raw chitosan failed. Therefore, other approachs, i.e., the use of hydrolyzed chitosan or the use of PVA as the spinning aid, were further investigated.

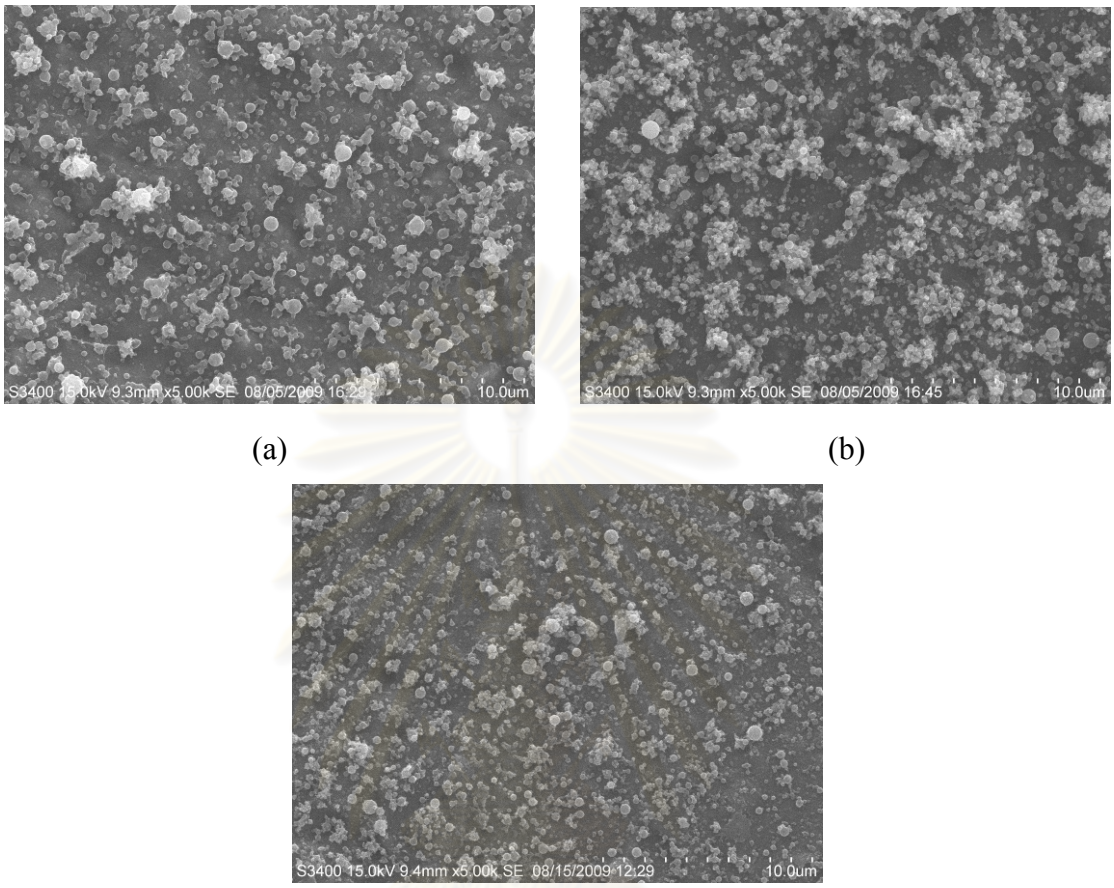

(a) (b)

(c)

Figure 4.1 SEM micrographs of products from the electrospinning of pure chitosan solution prepared by using chitosan with molecular weight of 100 (a), 400 (b) and 760 kDa (c), respectively.

4.2 The Effect of Chitosan Hydrolysis and PVA Addition on Electrospinability

The processing parameters, as well as solution parameters play important role in the formation of the fibers by electrospinning. In relative order of their impact on the electrospinning process, viscosity and conductivity of the solution are considered to be important factors. Very different results can be obtained using the same kind of the solution and the same electrospinning set up if the viscosity and conductivity of the solution are changed. Therefore, the effects of chitosan hydrolysis and PVA addition, on viscosity and conductivity of the solution were firstly investigated. The discussion of each effect is provided in the following subsections.

4.2.1 Viscosity of hydrolyzed chitosan and chitosan/PVA solutions

In preliminary experiments, solutions of pure chitosan with molecular weight of 100, 400 and 760 kDa was found to have viscosity of 65, 164.27 and 210.73 cP, respectively. As mentioned in the previous section, these solutions could be not electrospun into fibers. Only collections of spherical beads were found on the collector. After being hydrolyzed, chitosan could form a solution with increased viscosity, as shown in Figure 4.2. The viscosity of the solutions of chitosan hydrolyzed for 6 to 48 h were increased to 229.63 and 1951.10 cP, respectively. However, for the chitosan being hydrolyzed for 6 and 12 h, the electric force could not initiate the formation of fibers, in the similar manner as that for pure chitosan. This might also be the result of low viscosity as seen in Figure 4.2.

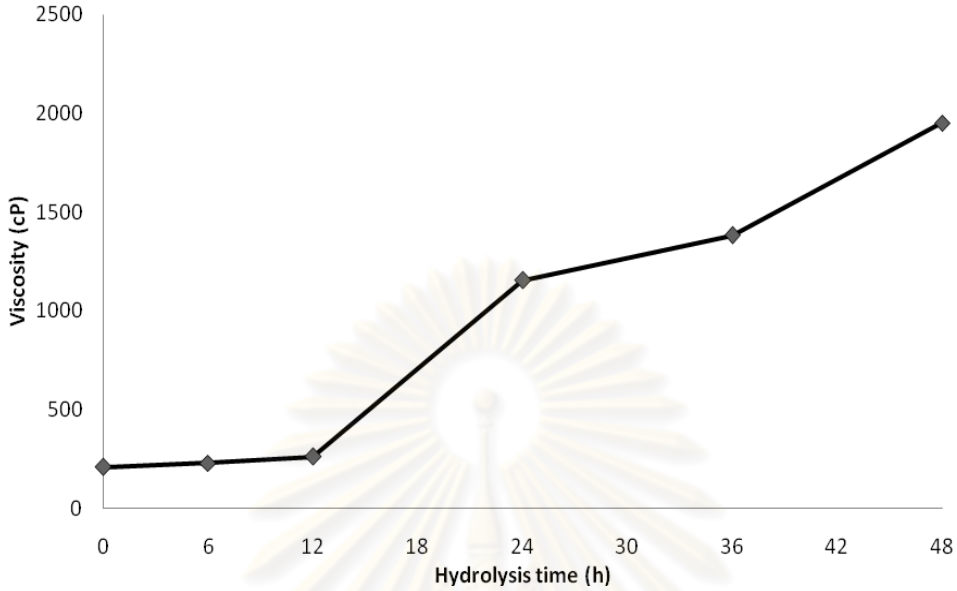

Figure 4.2 Viscosity of the solution of hydrolyzed chitosan in 90% (v/v) acetic acid, as a function of hydrolysis time for chitosan. The molecular weight of chitosan was 760 kDa.

For addition of PVA to chitosan solution, similar trend was observed. The increased amount of PVA resulted in the increase in the viscosity of the solution. The viscosity of chitosan solution was also increased with increasing of chitosan molecular weight. The result was shown in Figure 4.3 as well as in Table 4.1.

Table 4.1 Viscosity of chitosan/PVA solution

PVA Content (%w/v)	100 kDa chitosan		400 kDa chitosan		760 kDa chitosan	
	Chitosan Content (%w/v)	Viscosity (cP)	Chitosan Content (%w/v)	Viscosity (cP)	Chitosan Content (%w/v)	Viscosity (cP)
0.10	0	825.00±1.00	0	825.00±1.00	0	825.00±1.00
0.08	0.004	1079.00±8.93	0.003	1161.00±6.00	0.002	1204.83±2.67
0.06	0.008	664.00±9.54	0.006	847.33±1.53	0.004	1015.67±2.52
0.04	0.012	428.00±4.00	0.009	536.30±2.31	0.006	685.50±8.81
0.02	0.016	290.00±5.57	0.012	314.50±0.96	0.008	463.10±4.43
0	0.020	65.00±2.65	0.015	164.27±2.51	0.010	210.73±1.46

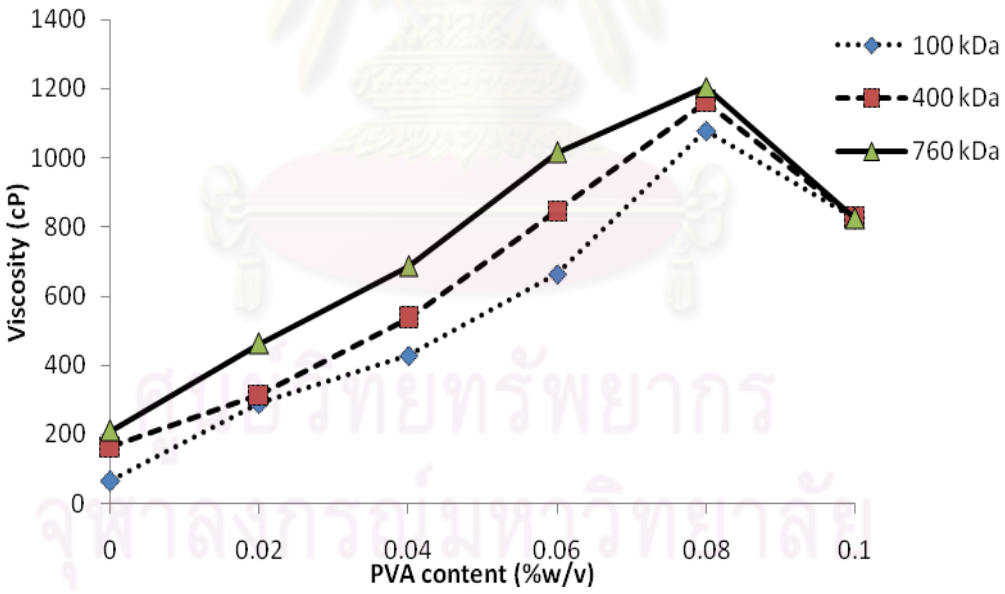

Figure 4.3 Viscosity of the solution of chitosan/PVA at different of chitosan molecular weight.

4.2.2 Conductivity of hydrolyzed chitosan and chitosan/PVA solution

The conductivity of the hydrolyzed chitosan solution was affect by hydrolysis time, while that of the chitosan/PVA solution was affected by both PVA content and the molecular weight of chitosan. The conductivity of the hydrolyzed chitosan solution is shown in Figure 4.4. For short period of hydrolysis, the conductivity of the solution was not significantly changed. However, after 24 h of hydrolysis with NaOH, the conductivity greatly increased. When the hydrolysis time was increased, the resistance of groups imposed by the arrangement of the C2 and C3 substituent in the sugar ring that affected the deacetylation of the polymer chain was increased, in addition to the increase in the positive charge of polymer chain [14]. Consequently, the conductivity of the hydrolyzed chitosan solution was greatly increased.

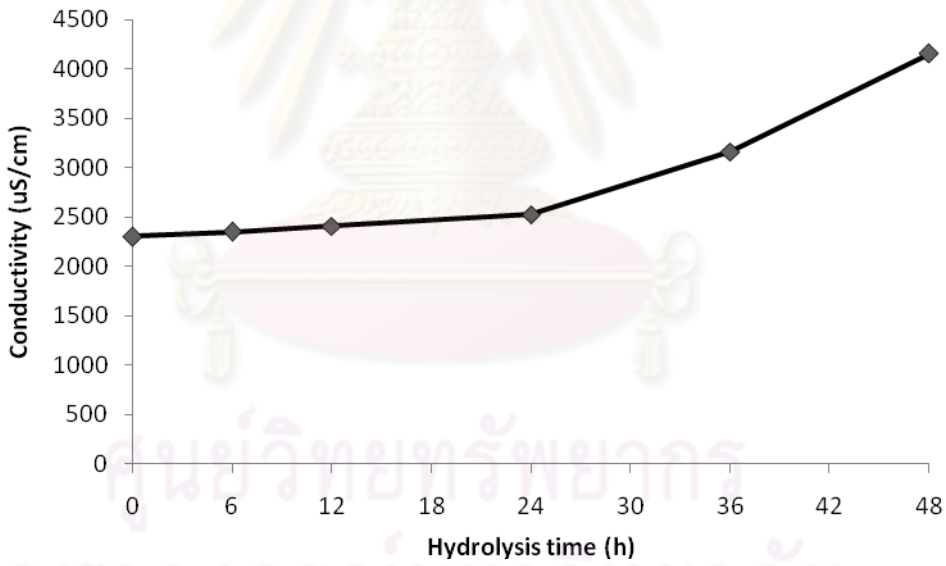

Figure 4.4 The conductivity of hydrolyzed chitosan solution.

For the addition of PVA as the spinning aid, it was found that the conductivity of blended solution was decreased by the content of PVA. This might be due to the strong interaction of hydrogen bond occurred between chitosan and PVA molecule in the blended solution tesulting in decreased amount of free ions in the solution. Thus the conductivity of the solution with the addition of PVA was decreased. On the other hand, increasing the molecular weight of chitosan would result in the decrease in the

conductivity. It would be explained by the role of the intermolecular interactions. Increasing in molecular weight, chitosan could have block arrangement of acetylated and deacetylated units and might reduce available sites of amino groups on the chitosan molecule [15], resulting in the decreased in conductivity. The results are shown in Table 4.2 and Figure 4.5.

The addition of cationic would increase the conductivity of polymer solution and resulted in higher number of charges in the solution so that charge repulsion may obstruct the entanglement of polymer chains. Thus the fiber jet of higher conductivity solution could be subjected to higher tensile force in the presence of an electric field than a fiber jet from a solution with low conductivity.

Table 4.2 The conductivity of chitosan/PVA solution.

PVA content (%w/v)	Conductivity (μS/cm)		
	100 kDa chitosan	400 kDa chitosan	760 kDa chitosan
0.10	747	747	747
0.08	1389	1138	1034
0.06	1451	1313	1103
0.04	2020	1824	1391
0.02	3421	2610	2250
0	4850	3280	2300

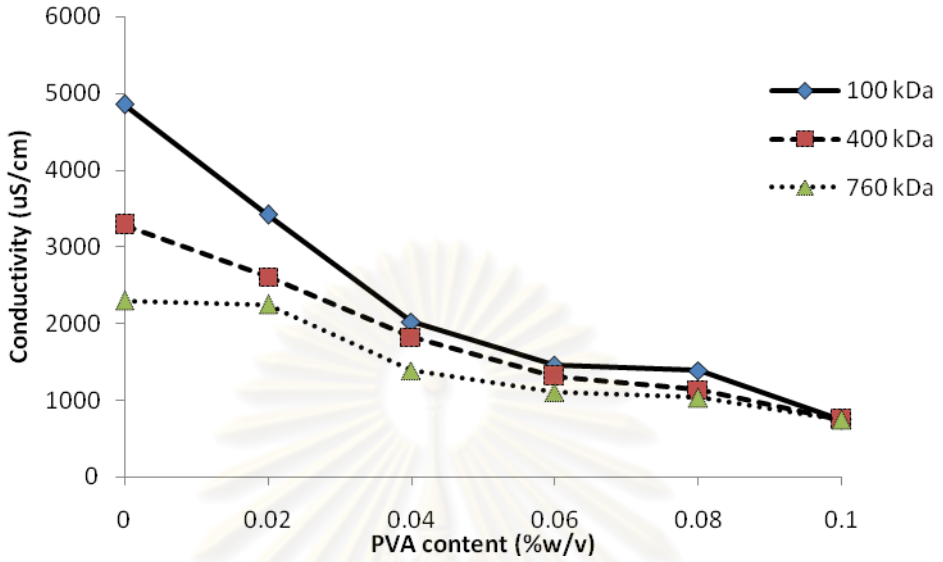

Figure 4.5 The conductivity of chitosan/PVA solution.

4.3 Morphology of Chitosan Nanofibers Fabricated by Electrospinning Technique

4.3.1 Morphology of electrospun hydrolyzed chitosan

Electrospinning of hydrolyzed chitosan solution was conducted using 10 cm tip-to-collector distance and 25 kV of applied electric field. The solutions were prepared using the highest amount of the hydrolyzed chitosan dissolvable into 90 % acetic acid, which depended on the duration of the hydrolysis period that chitosan had experienced. As shown in Figure 4.6, for a hydrolysis period in the range of 0 - 48 h, the maximum soluble amount of hydrolyzed chitosan increased with the hydrolysis time.

Nevertheless, it was found that the solution prepared from chitosan that had been hydrolyzed for 0, 6 and 12 h could not be spun into fibers. Only spherical droplets were found on the collector. By increasing the hydrolysis time up to 24 h, nanofibers with average diameter of 117.4 nm could be generated. The prolonged period of hydrolysis time to 36 and 48 h resulted in the decreased fiber diameter of

39.2 and 25.2 nm, respectively, as shown in Figure 4.7. These behaviors can be explained by the role of NaOH in the further deacetylation of chitosan polymeric chains. When the hydrolysis time was increased, in addition to the increase in the positive charge of the polymers chain, the molecular weight of chitosan was also decreased, which enabled chitosan molecules to align more effectively in the electrical field during the electrospinning process [16, 17]. It was also suggested that the average length of the polymeric chain of chitosan after hydrolysis may be below the required length for entanglement coupling formation. Regarding electrospinning parameters, the chitosan concentration affected spinability of the solution by affecting on the viscosity of the solution, which was directly related to chitosan chain entanglement. On the other hand, the conductivity of the solution influenced the fiber size and fiber morphology. Increasing conductivity was resulted in decreased fiber diameter and nonuniform fiber morphology, which leaded to a dramatic bending instability as well as a broad diameter distribution.

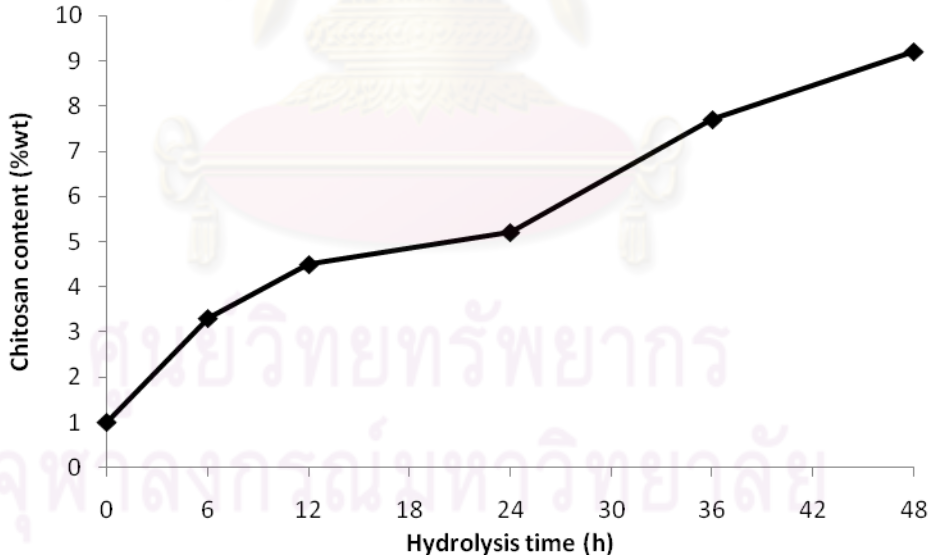

Figure 4.6 Maximum solubility of chitosan hydrolyzed for various period of hydrolysis.

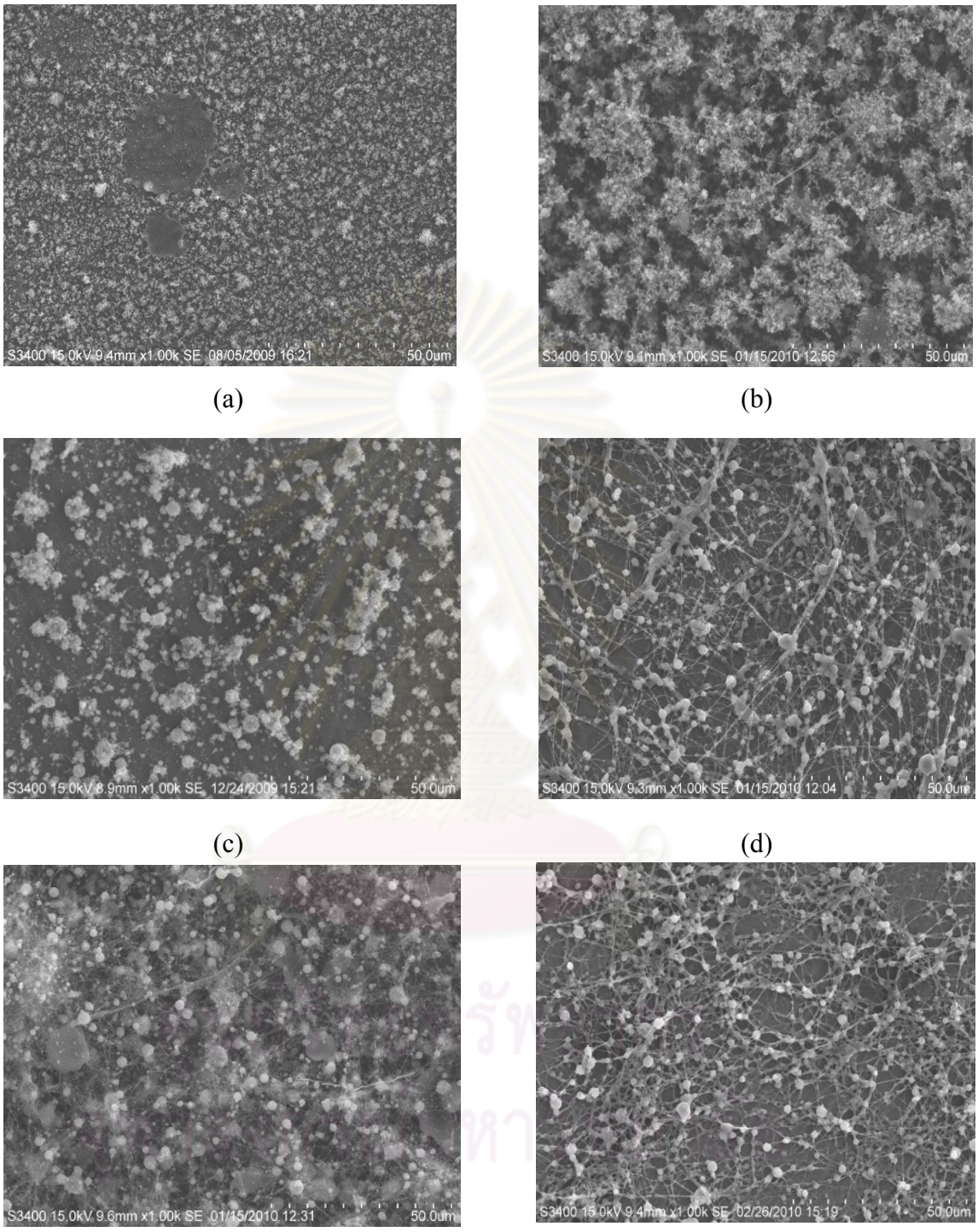

Figure 4.7 SEM micrographs of nanofibers formed from electrospinning of hydrolyzed chitosan dissolved in 90% (w/v) acetic acid. The hydrolysis time was varied from 0 h (a), 6 h (b), 12 h (c), 24 h (d), 36 h (e) and 48 h (f), respectively.

4.3.2 Morphology of electrospun chitosan/PVA composite

The electrospinning of chitosan/PVA composite was done using the condition of 10 cm tip-to-collector distance and 25 kV of applied electric field. SEM micrographs of nanofibers formed from the solution with various chitosan/PVA blending ratio spun under the same condition are shown in Figure 4.8-4.10. It was found that, for the solution with low PVA content, the electric force could not initiate the formation of fibers, in the similar manner as that for pure chitosan. The fibers could be seen at moderated or high content of PVA. The fact that the spinning solution with high chitosan content could not be electrospun into nanofibers may be the result from the interaction between polycationic group of chitosan that prevented molecular entanglement of polymer chains needed in the formation of continuous fibers. Nevertheless, as the charge density was increased, a higher elongation forces were imposed to the jet of the solution formed by the electrical field. Since the overall tension in the fibers depended upon self repulsion of excess charges on the jet, excessive charges leaded to small fibers [17, 18]. Thus, the average diameter of the fibers tended to be small with large number of bead formed when the chitosan content was increased. However, size of the beads decreased in compensation with the increased in non-uniformity of fiber diameter. The results for average fiber diameter and fraction of the product that was formed into fibers are shown in Table 4.3. For the addition of PVA as the spinning aid, the hydroxyl functional groups was also give the strong interaction of hydrogen bond between chitosan and PVA molecule in the blended solution. These behaviors were closely related to the result of viscosity and conductivity.

Table 4.3 The effect of chitosan content and molecular weight of chitosan on electrospun fiber morphology.

100 kDa chitosan			400 kDa chitosan			760 kDa chitosan		
Chtiosan content (%w/v)	Average diameter (nm)	Fiber percentage (%)	Chitosan content (%w/v)	Average diameter (nm)	Fiber percentage (%)	Chitosan content (%w/v)	Average diameter (nm)	Fiber percentage (%)
0.004	81.7	91.6	0.003	118.3	98.0	0.002	88.5	98.4
0.008	62	82.0	0.006	101.1	87.6	0.004	82.2	90.0
0.012	49.5	46.0	0.009	53.4	72.8	0.006	58.0	82.4
0.016	39.5	12.5	0.012	41.1	30.8	0.008	42.8	45.2

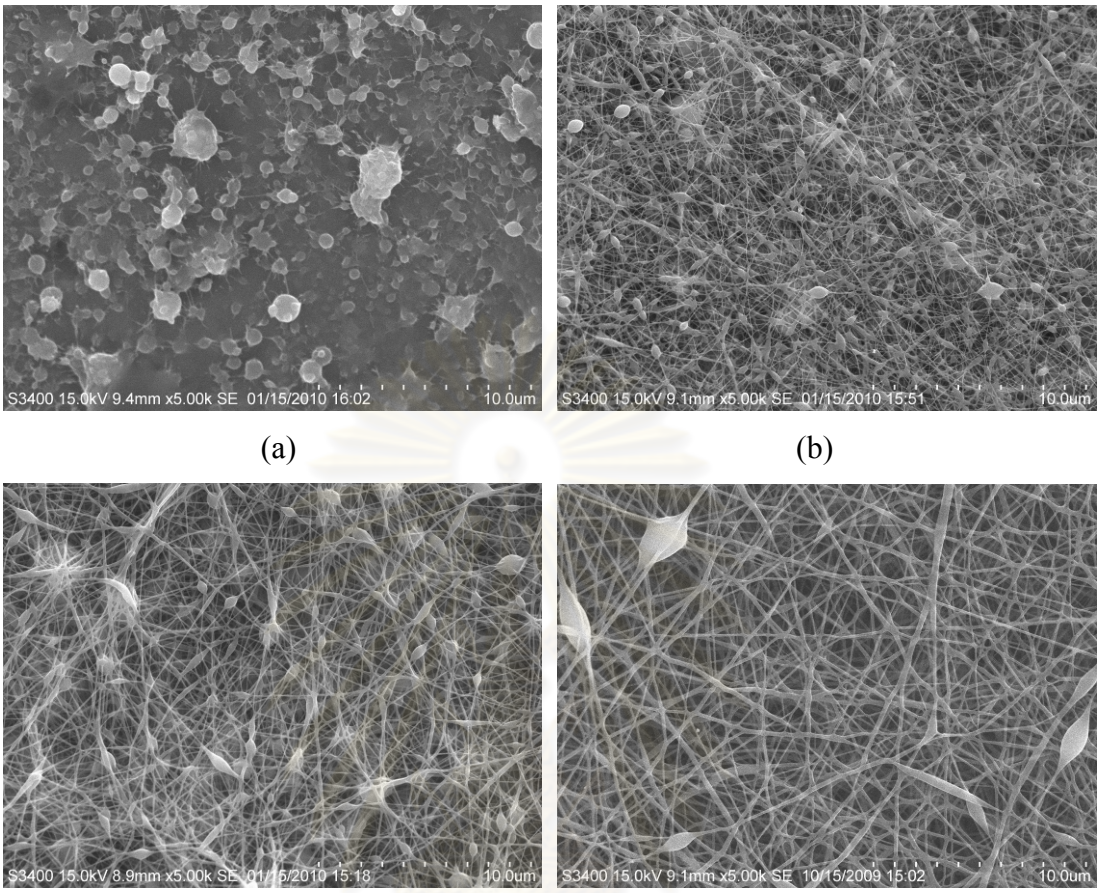

Figure 4.8 SEM micrographs of nanofibers electrospun from chitosan/PVA solution containing various contents of PVA: (a) 0.02, (b) 0.04, (c) 0.06 and (d) 0.08 wt%. The molecular weight of chitosan was 100 kDa.

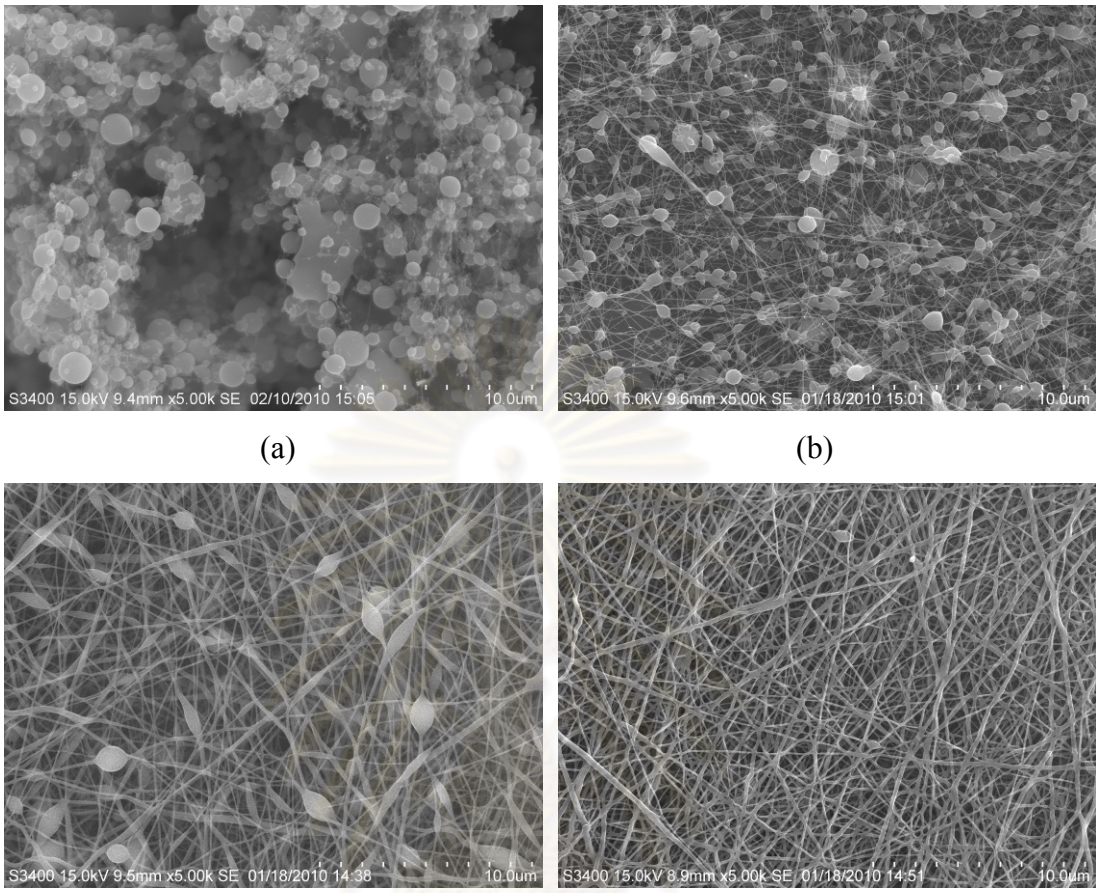

(a) (b)

(c) (d)

Figure 4.9 SEM micrographs of nanofibers electrospun from chitosan/PVA solution containing various contents of PVA: (a) 0.02, (b) 0.04, (c) 0.06 and (d) 0.08 wt%. The molecular weight of chitosan was 400 kDa.

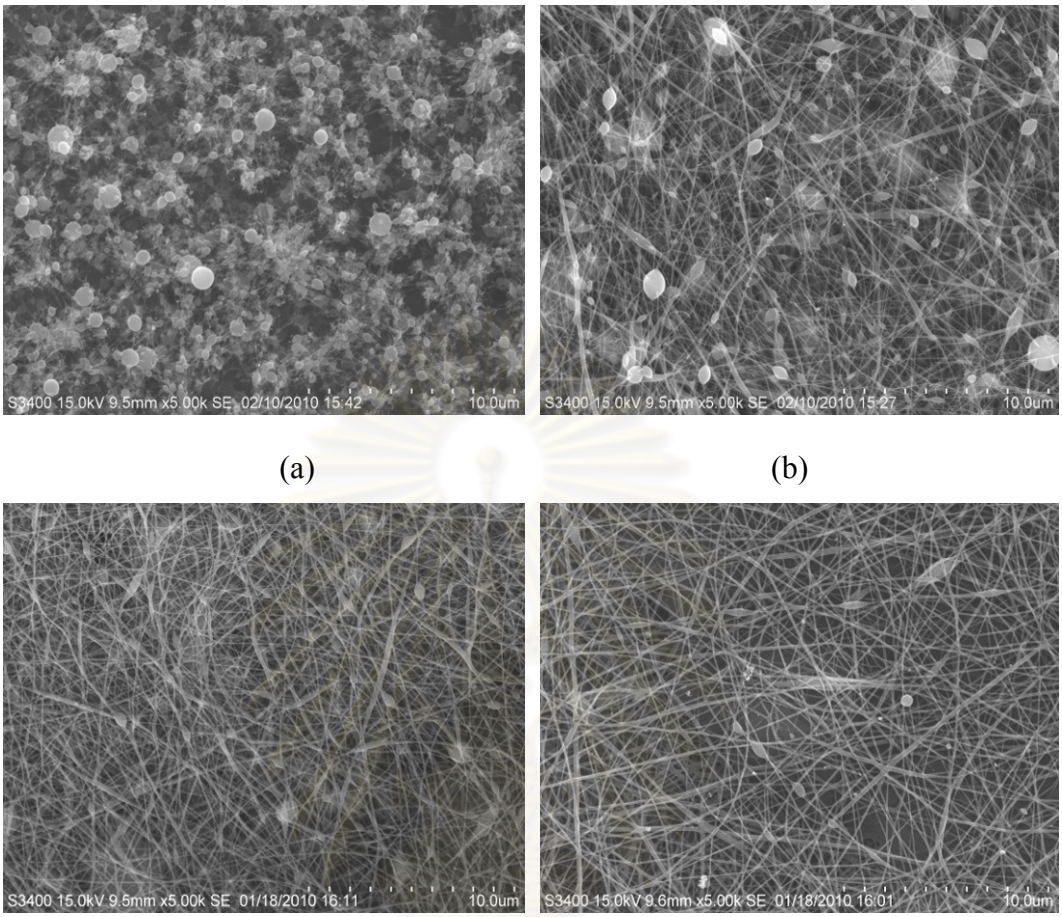

Figure 4.10 SEM micrographs of nanofibers electrospun from chitosan/PVA solution containing various contents of PVA: (a) 0.02, (b) 0.04, (c) 0.06 and (d) 0.08 wt%. The molecular weight of chitosan was 760 kDa.

In the electrospinning of nanofibers, molecular weight is also one of the most effective variables to control morphology and diameter of the fibers. It has been reported that low molecular weight polymer tends to form beads more than fibers, while high molecular weight polymer generate fibers with larger average diameter and less beads. In this study, the morphology of the fibers formed using different chitosan molecular weight were compared. In generally using 100 kDa chitosan, thin nanofibers were generated with large beads. When the molecular weight was increased to 400 kDa and 760 kDa, respectively, the average diameter of the fibers was increased. Size of the beads was decreasing in compensation with the increased and non-uniform fiber diameter. These behaviors were closely related to viscosity and spinnability of the solution.

4.4 Cell Attachment on Chitosan Nanofibers

4.4.1 Cell attachment on hydrolyzed chitosan nanofibers

4.4.1.1 Effect of incubation time

In order to investigate the effect of incubation time on the attachment of bacterial cells, chitosan hydrolyzed for 6 and 48 h were chosen. The Colony Forming Unit (CFU) was calculated from a standard curve of either *Acinetobacter baylyi* strain GFJ2 or *Brevibacillus agri* strain 13. The initial optical density (OD_{600}) of the bacterial cells solution for *Acinetobacter baylyi* strain GFJ2 and for *Brevibacillus agri* strain 13 was about 0.85 and 1.0, which was corresponding to 1.8981×10^{13} and 1.4760×10^{9} CFU, respectively. The total number of bacterial cells attached on hydrolyzed chitosan nanofibers are shown in Figure 4.11 and 4.12 for *A. baylyi* GFJ2 and *B. Agri* 13, respectively.

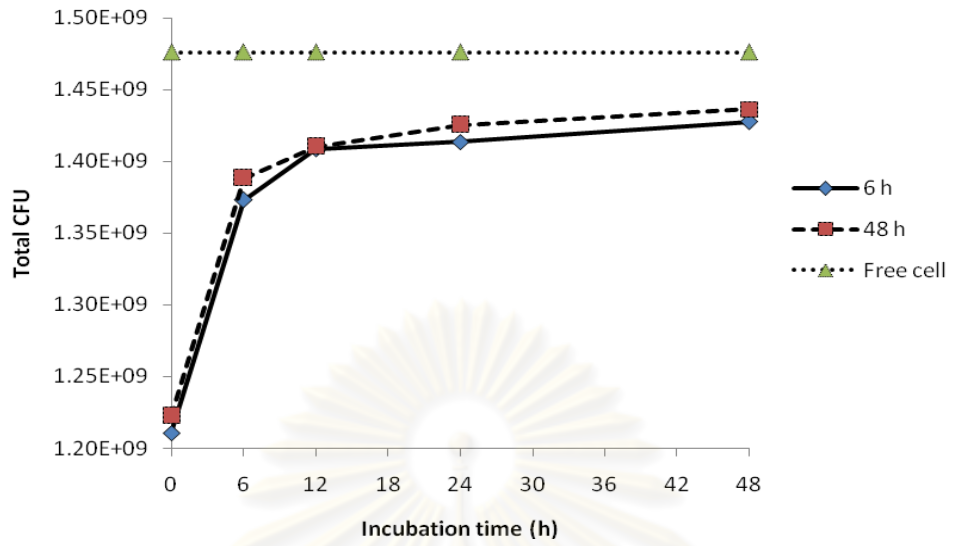

Figure 4.11 Total CFU of Gram-positive *Brevibacillus agri* strain13 attached onto electrospun chitosan fibers, formed from chitosan hydrolyzed for 6 (____) and 48 h (…..), after various incubation time. The dotted line represents the CFU value of the free cells.

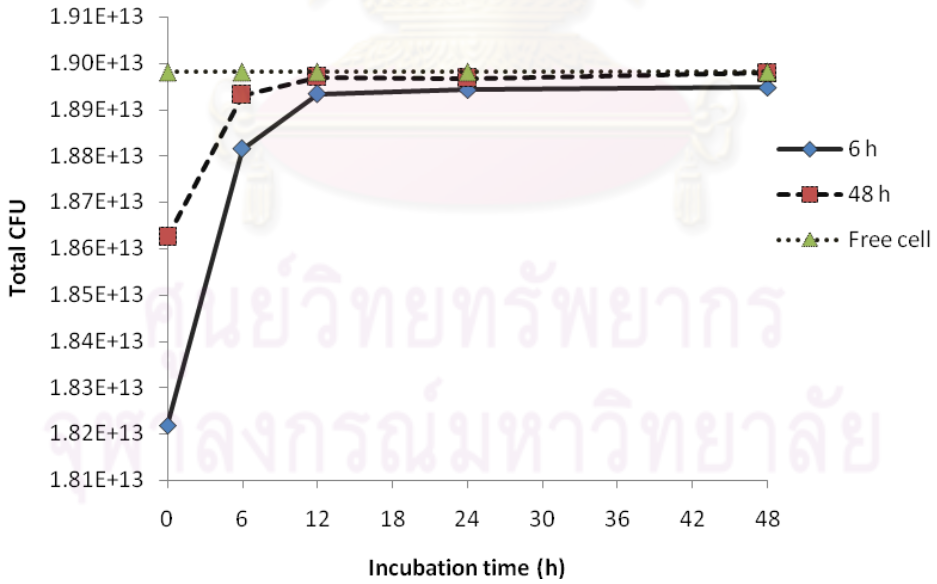

Figure 4.12 Total CFU of Gram-negative *Acinetobacter baylyi* strain GFJ2 attached onto electrospun chitosan fibers, formed from chitosan hydrolyzed for 6 (___) and 48 h(….) after various incubation time. The dotted line represents the CFU value of the free cells.

Similar trend was found for both of Gram-negative and Gram-positive bacteria. The amount of bacterial cell attachment was increased when the incubation time was increased. At incubation time of 0 h, (i.e., right after when cells were exposed to chitosan samples) most of both bacterial cells was easily washed away. Nevertheless, some of the cells could adhere to chitosan sample even right after their explosure to chitosan. At 6 and12 h of incubation, increased bacterial cells attachment on the surface was obsearved. When the contact time between chitosan fibers and the bacteria was prolonged to 24 and 48 h, the attachment of gram-negative *Acinetobacter baylyi* strain GFJ2 bacteria on the chitosan sample had reached the stable stage, which was very closely to the CFU of the free cells. On the other hand, gram-positive *Brevibacillus agri* strain 13 bacteria continued to increase toward the value of free cells. It is possible that the microorganism may be induced to attach to chitosan by altering the physical and chemical properties by ionic attraction of bacterial cells and the chitosan surface. Chitosan is a cationic polysaccharide that acts as a glue to initiate bacterial-surface interactions. Increasing the contact time between chitosan fibers and the bacterial cells tends to increase the interaction rate.

4.4.1.2 Effect of hydrolysis time of chitosan

To compare the bacterial attachment on hydrolyzed chitosan nanofibers at various hydrolysis times, the incubation time of 12 and 24 h were chosen. The results showed that the number of both types of bacterial cells attached on the surface increased when the hydrolysis time of chitosan was increased. The results are shown in Figure 4.13-4.16. These results could be due to a significant role of a surface area-to-volume ratio. As previously mentioned, the hydrolysis time of 0, 6 and 12 h could produce chitosan nanofibers, but spherical particles were generated. On the other hand, the hydrolysis time of 24, 36 and 48 h could be resulted in nanofibers. The fiber diameter decreased as the hydrolysis time was increased. The results showed that amount of bacterial cells that were able to attach on the fiber mats was greater than on particles. This was the result from high surface area-to-volume ratio of fiber mats available for the bacterial cells to attach. Moreover, hydrophilicity of chitosan was

increased after chitosan was hydrolyzed. The hydrophilicity is one factor influencing the bacterial cells response to a substrate [19, 20].

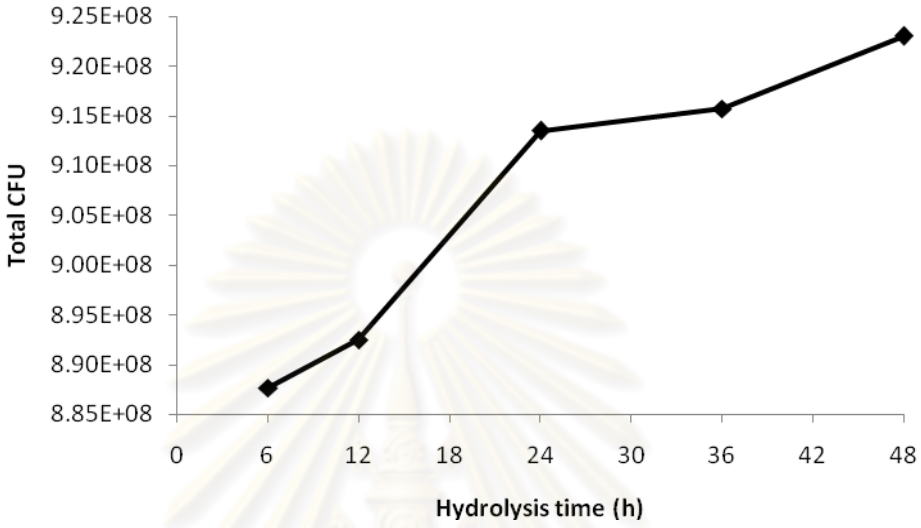

Figure 4.13 Total CFU of Gram-positive *Brevibacillus agri* strain 13 attached onto electrospun chitosan fibers, formed from chitosan being hydrolyzed for various period of time. The incubation time of the cells was 12 h.

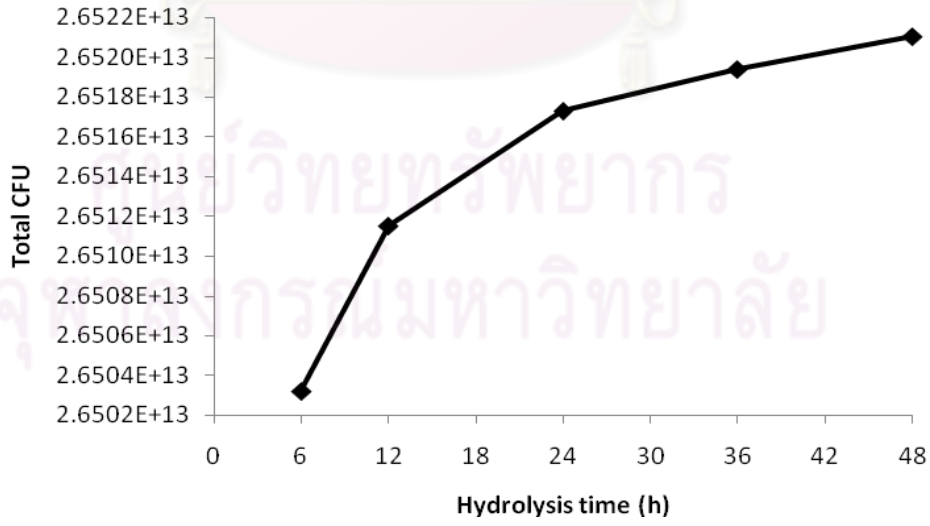

Figure 4.14 Total CFU of Gram-negative *Acinetobacter baylyi* strain GFJ2 attached onto electrospun chitosan fibers, formed from chitosan being hydrolyzed for various period of time. The incubation time of the cells was 12 h.

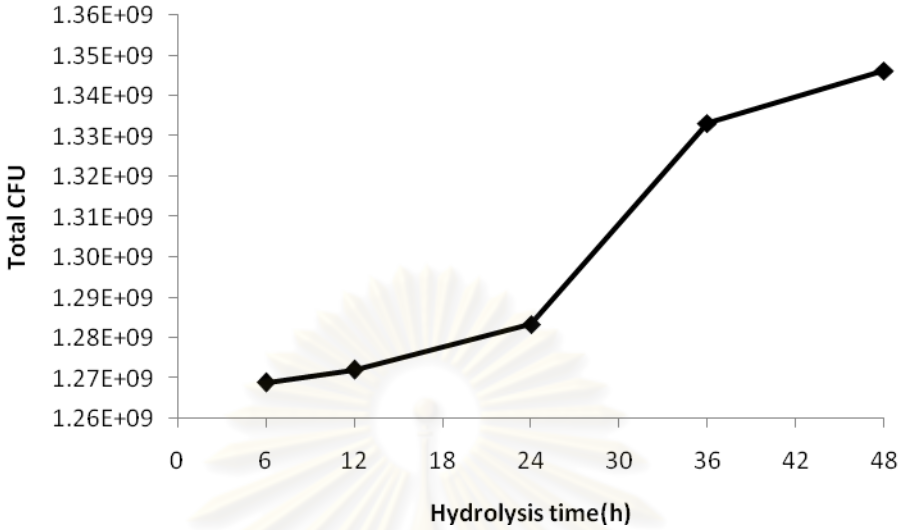

Figure 4.15 Total CFU of Gram-positive *Brevibacillus agri* strain No.13 attached onto electrospun chitosan fibers, formed from chitosan being hydrolyzed for various period of time. The incubation time of the cells was 24 h.

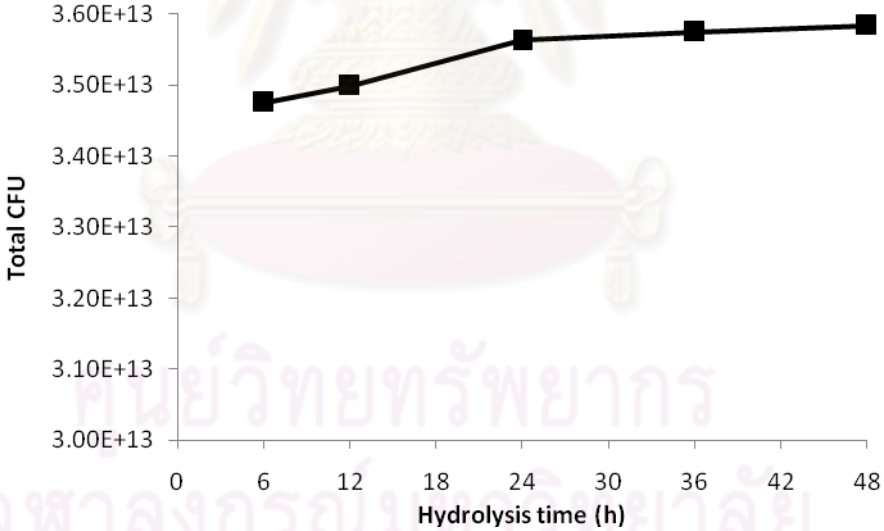

Figure 4.16 Total CFU of gram-negative *Acinetobacter baylyi* strain GFJ2 attached onto electrospun chitosan fibers, formed from chitosan being hydrolyzed for various period of time. The incubation time of the cells was 24 h.

To further confirm the attachment of bacterial cells onto the prepared chitosan nanofibers, the scanning electron microscopy was employed. SEM micrographs of the

samples, after certain period of incubation time, are shown in Figure 4.17-4.24. At 0 and 6 h of incubation time, most cells were formed as individual cell on the fibers. Only two to three cell colonies were appeared on the SEM image. When the contacting time between chitosan fibers and the bacteria was prolonged to 12 h, the number of Gram-negative *A. baylyi* strain GFJ2 bacteria observed on the sample increased exponentially, in much greater extent than that of Gram-positive *B. agri* strain 13 bacteria. After the incubation time of 24 and 48 h, both types of bacteria were found fully covering the chitosan. These results suggested that the interaction between bacteria cells and chitosan was related to the chemical and physical properties of cell wall. It has been known that chitosan easily carries more positive-charged amino groups in more acidic solution or when the degree deacetylation of chitosan is high [21]. The hydrolysis process could significantly increase the degree of deacetylation of chitosan, which probably lead to increased positive charge (NH_3^+) of polymer chains. Increasing of NH_3^+ group of chitosan resulted in increased free amino group to interact with cell wall via negatively charge of phospholipid components of cell membranes [22]. However, Gram-positive cell wall does not posses a lipid outer membrane but Gram-negative cell wall posses an outer membrane consisting of various lipid complexes [23]. This difference is responsible to different attaching behavior of Gram-positive and Gram-negative cells to chitosan.

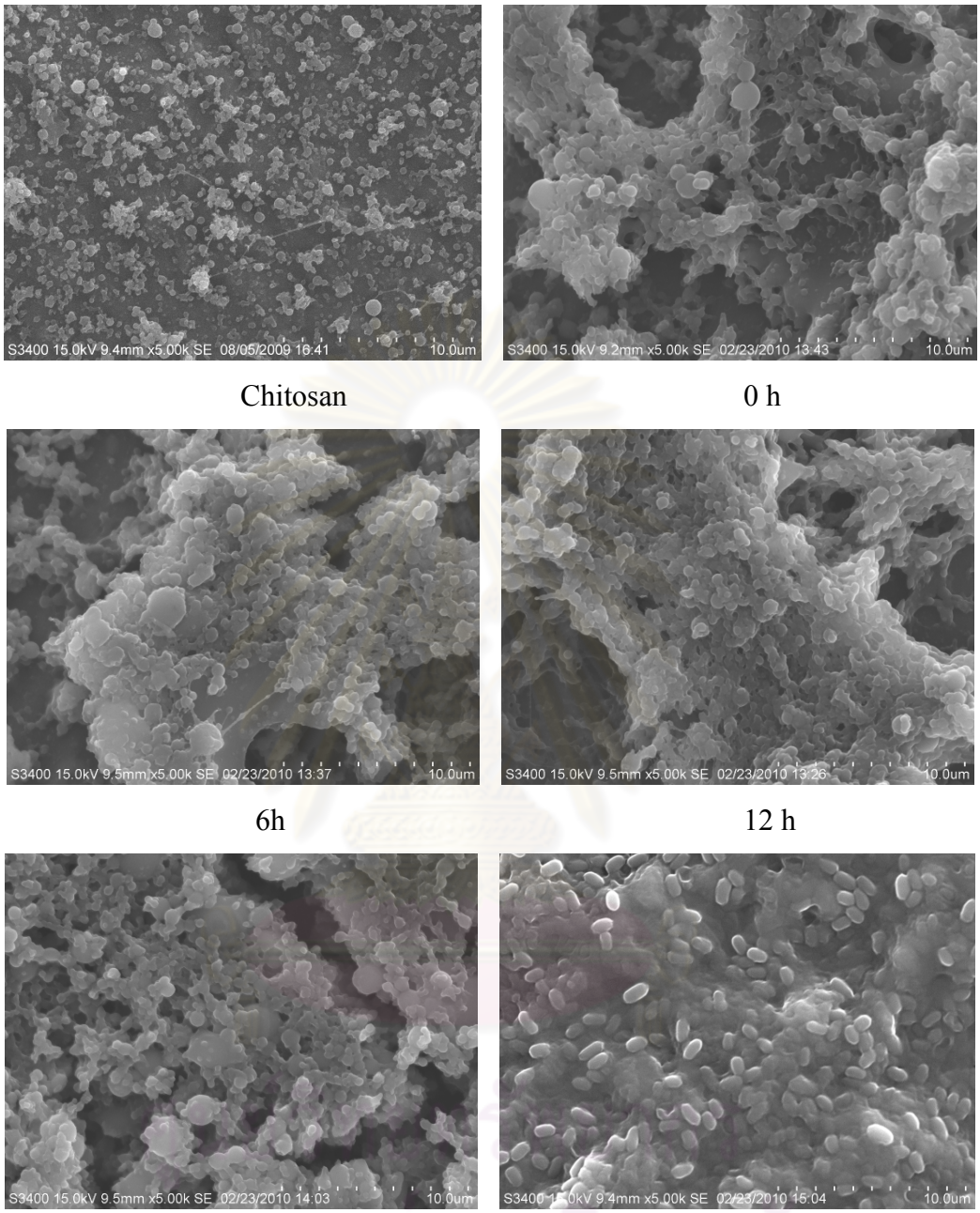

Figure 4.17 SEM micrographs of Gram-positive *Brevibacillus agri* strain 13 attached onto electrospun chitosan fibers, formed from chitosan hydrolyzed for 6 h, after various incubation times.

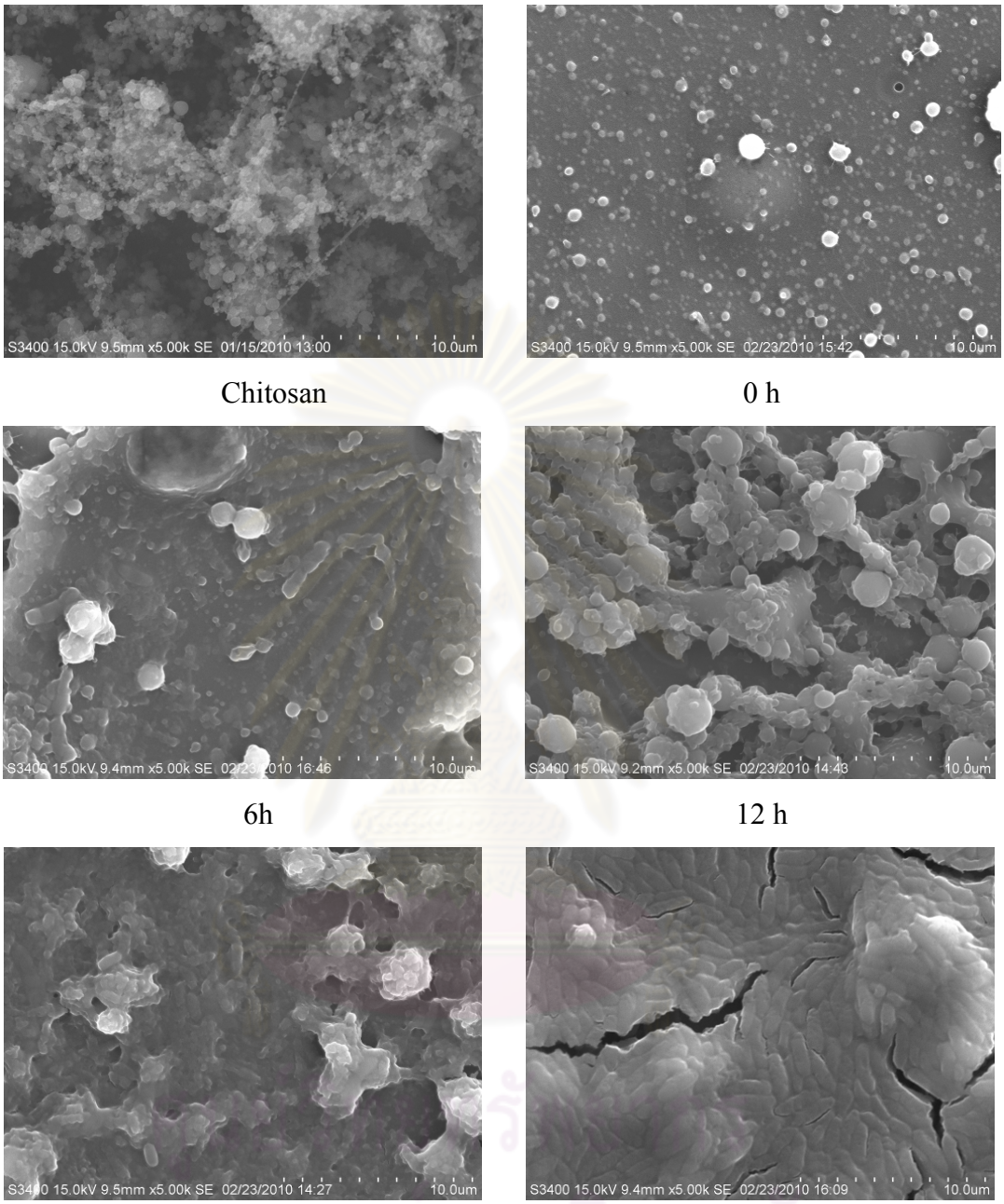

Figure 4.18 SEM micrographs of Gram-positive *Brevibacillus agri* strain 13 attached onto electrospun chitosan fibers, formed from chitosan hydrolyzed for 12 h, after various incubation times.

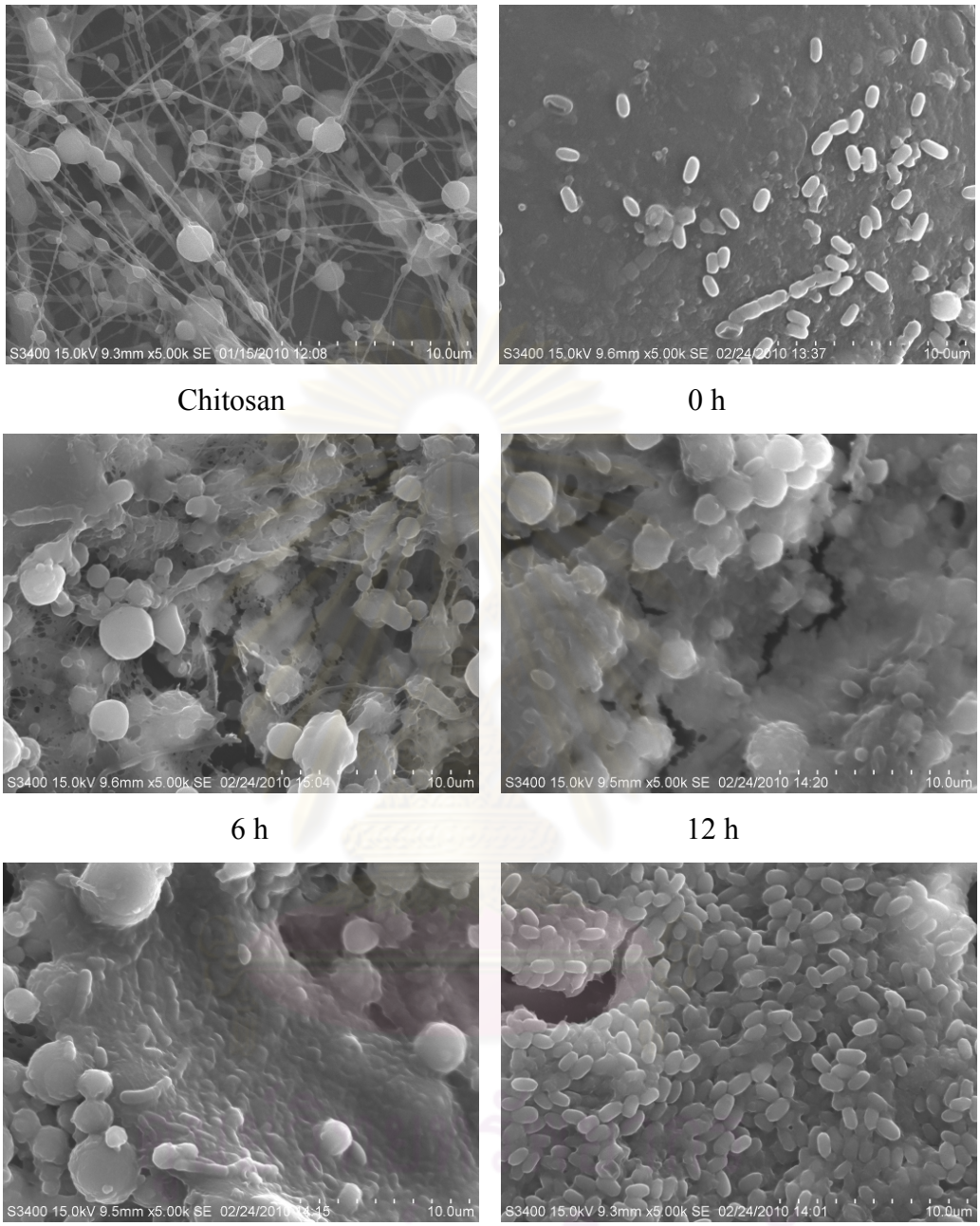

Figure 4.19 SEM micrographs of Gram-positive *Brevibacillus agri* strain 13 attached onto electrospun chitosan fibers, formed from chitosan hydrolyzed for 24 h, after various incubation times.

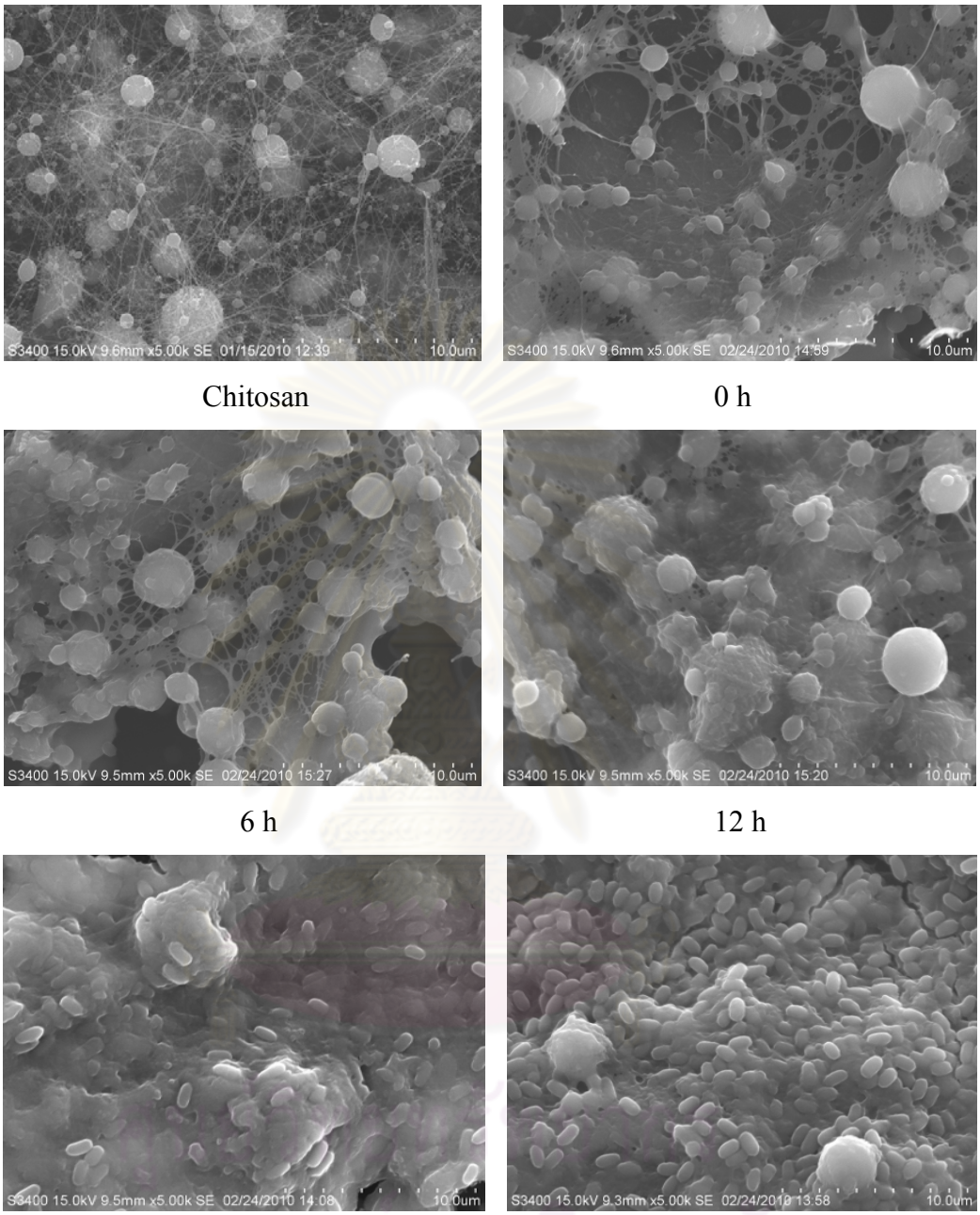

Figure 4.20 SEM micrographs of Gram-positive *Brevibacillus agri* strain 13 attached onto electrospun chitosan fibers, formed from chitosan hydrolyzed for 36 h, after various incubation times.

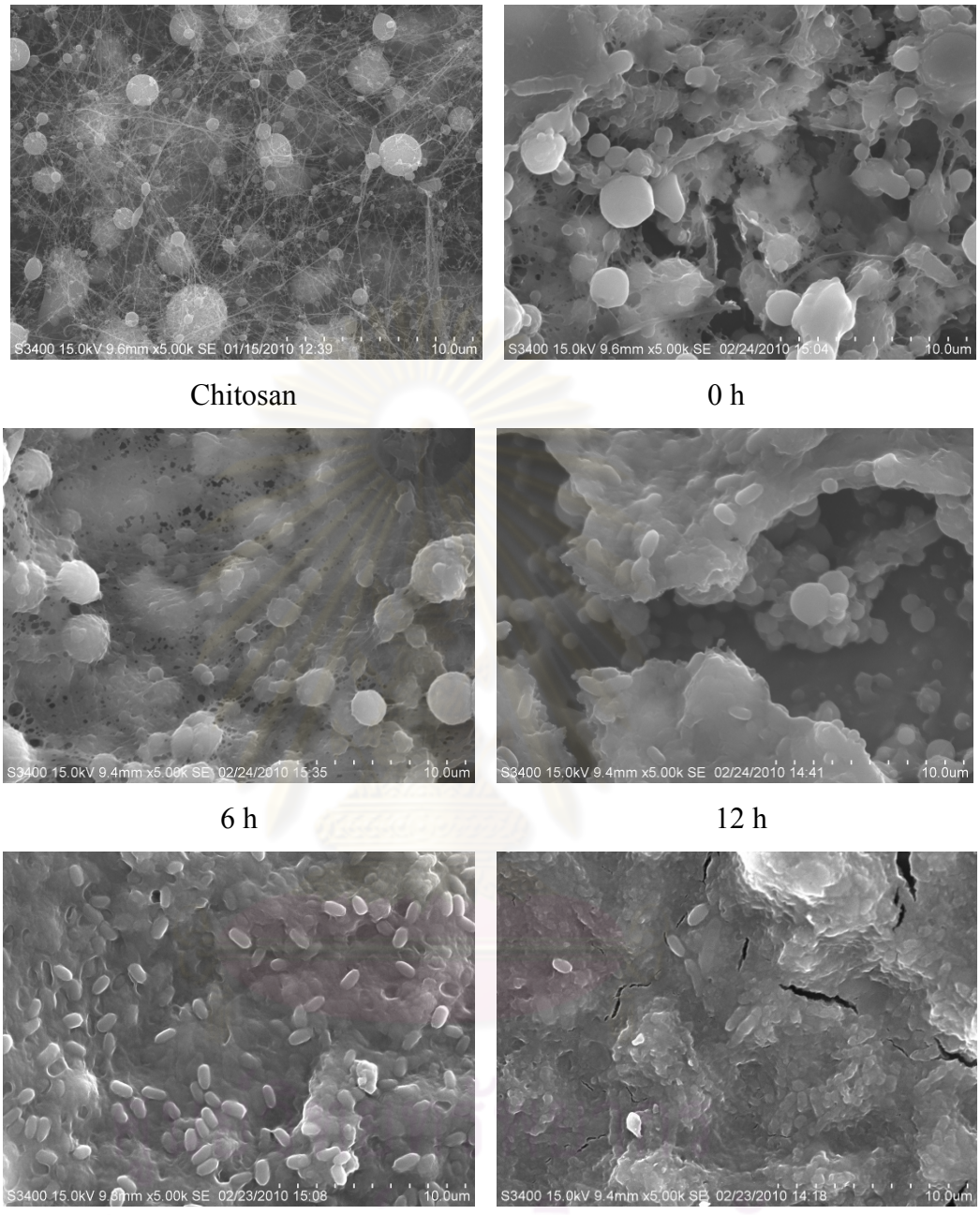

Figure 4.21 SEM micrographs of Gram-positive *Brevibacillus agri* strain 13 attached onto electrospun chitosan fibers, formed from chitosan hydrolyzed for 48 h, after various incubation times.

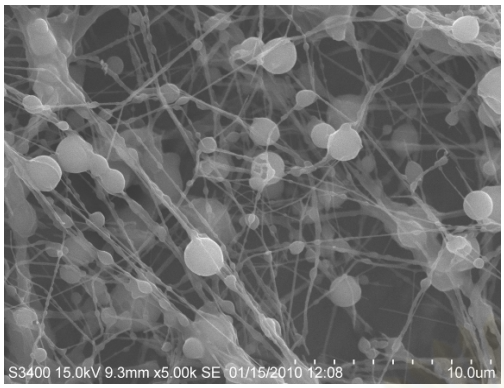

Chitosan

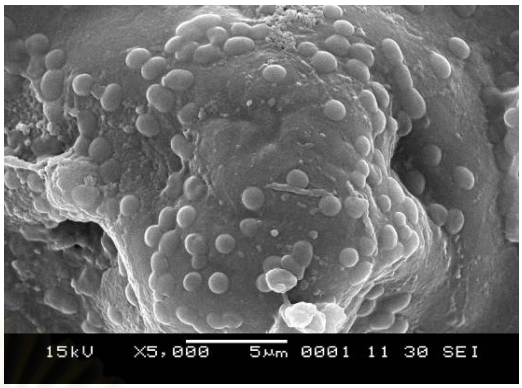

12 h

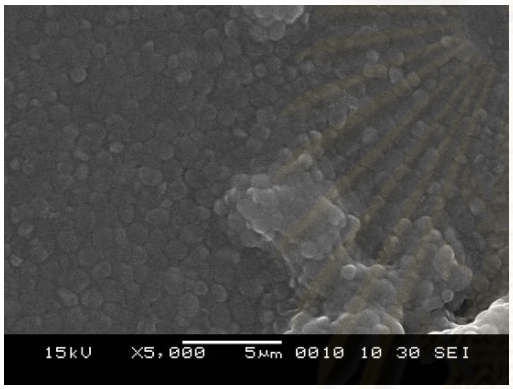

24 h

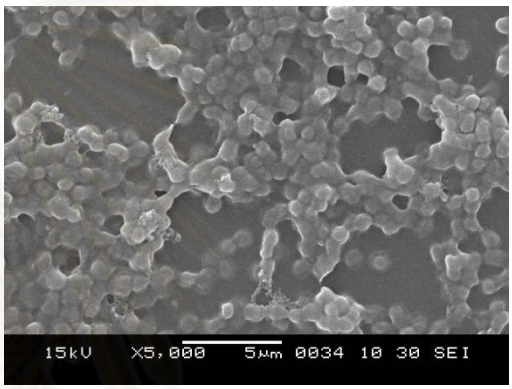

48 h

Figure 4.22 SEM micrographs of Gram-negative *Acinetobacter baylyi* strain GFJ2 attached onto electrospun chitosan fibers, formed from chitosan hydrolyzed for 24 h, after various incubation times.

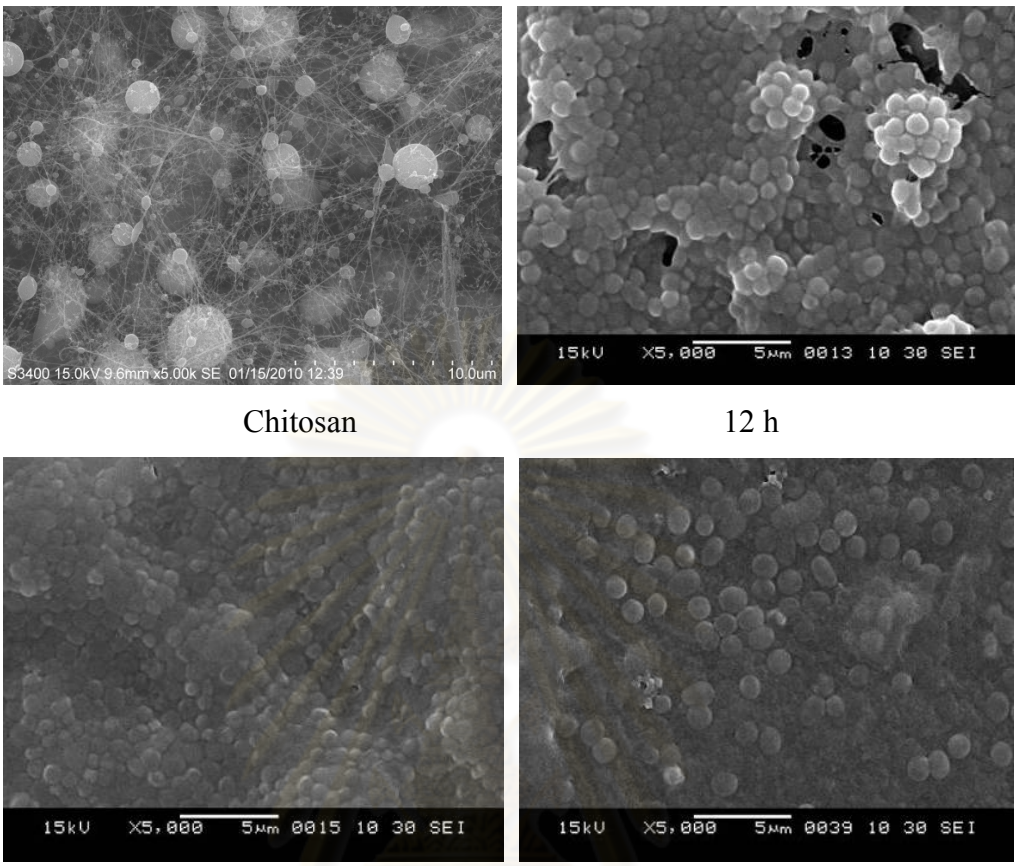

Chitosan 12 h

24 h 48 h

Figure 4.23 SEM micrographs of Gram-negative *Acinetobacter baylyi* strain GFJ2 attached onto electrospun chitosan fibers, formed from chitosan hydrolyzed for 36 h, after various incubation times.

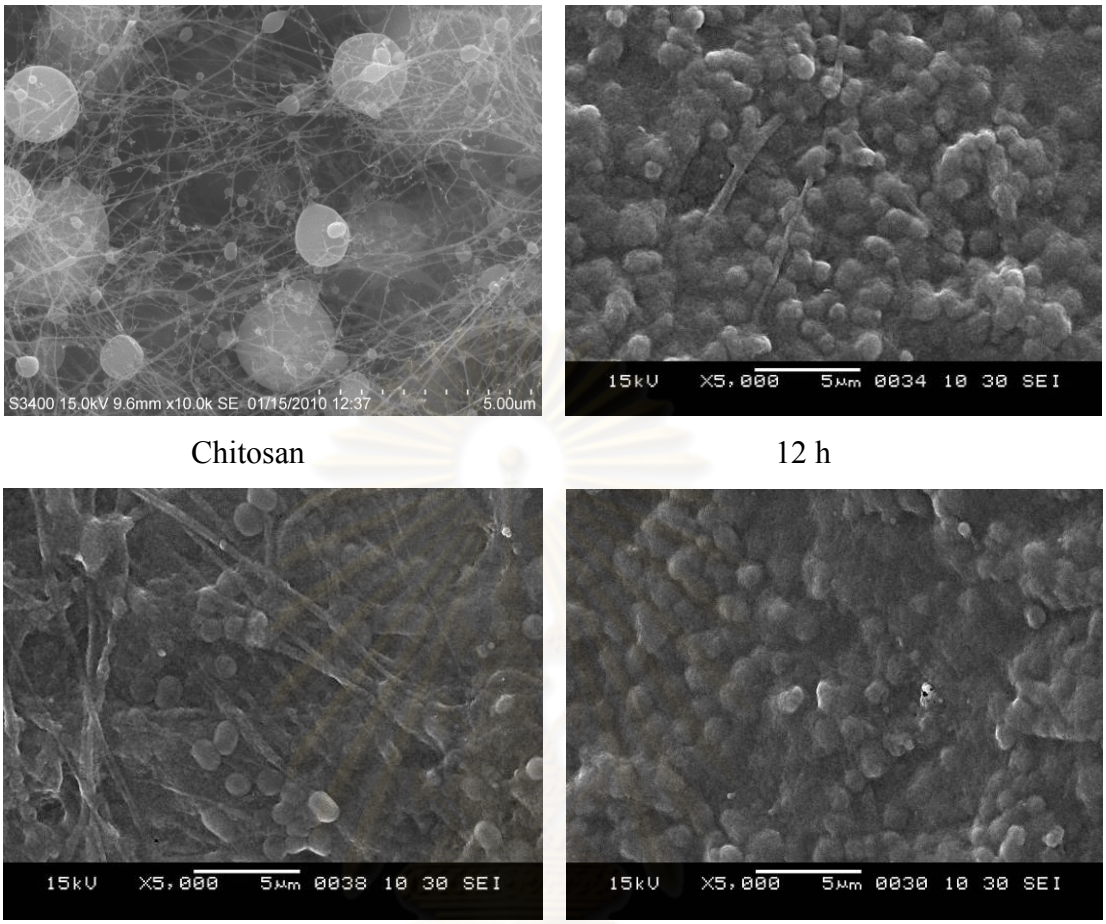

Chitosan 12 h

24 h 48 h

Figure 4.24 SEM micrographs of Gram-negative *Acinetobacter baylyi* strain GFJ2 attached onto electrospun chitosan fibers, formed from chitosan hydrolyzed for 48h, after various incubation times.

4.4.2 Cell attachment on hydrolyzed chitosan film

To verify the advantage of chitosan in form of nanofibers, it was compared, in term of cell attachment, with the hydrolyzed chitosan film. Both Gram-negative and Gram-positive bacteria were investigated. At 0 and 6 h of incubation time, most cells were loss with the washing, which indicated poor attachment to the films. Only two to three cell colonies were appeared on the surface. When the contact time between chitosan films and the bacteria was prolonged to 12 h, increased number of Gram-negative *A. baylyi* strain GFJ2 bacteria and Gram-positive *B. agri* strain 13 were found attached on the sample, but not yet fully covered the surface. After the incubation time of 24 and 48 h, the number of both types of bacteria cells were increased to the point that the whole chitosan films were covered with cells. SEM micrograph of *A. baylyi* strain GFJ2 and *B. agri* strain 13 attached on chitosan films that were prepared from chitosan hydrolyzed for various period of time are shown in Figure 4.25-4.30.

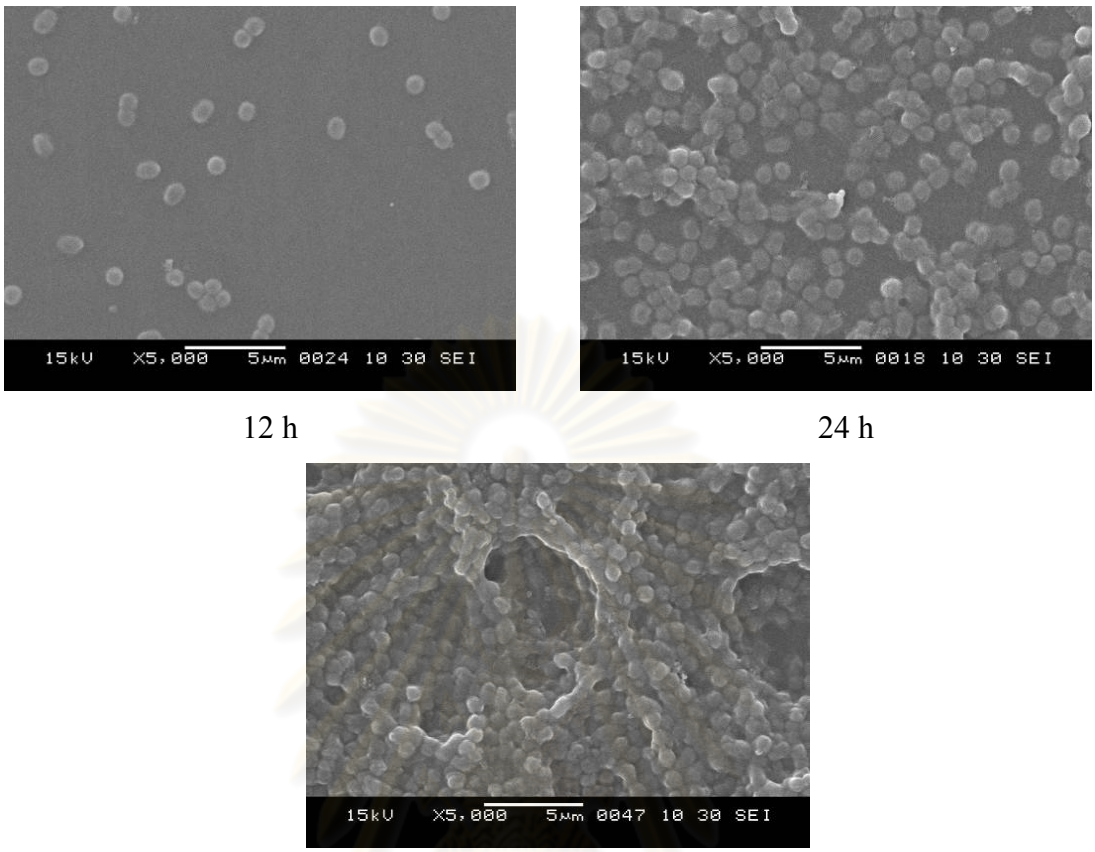

12 h 24 h

48 h

Figure 4.25 SEM micrographs of Gram-negative *Acinetobacter baylyi* strain GFJ2 attached onto chitosan film, formed from chitosan hydrolyzed for 24 h, after various incubation times.

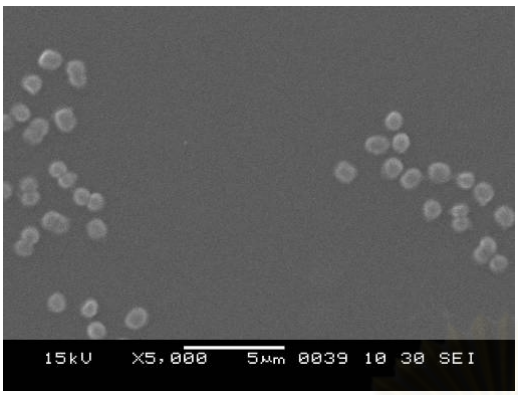

12 h

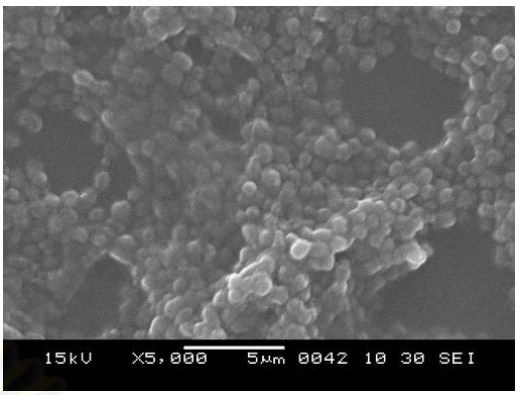

24 h

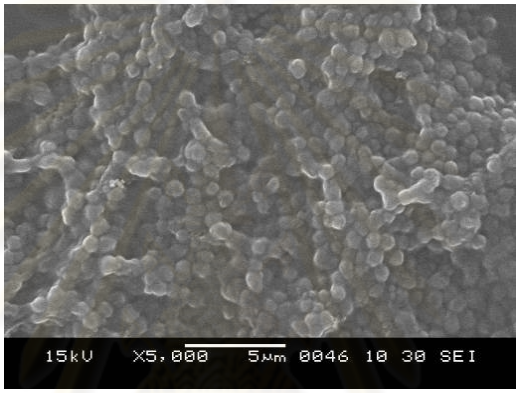

48 h

Figure 4.26 SEM micrographs of Gram-negative *Acinetobacter baylyi* strain GFJ2 attached onto chitosan film, formed from chitosan hydrolyzed for 36 h, after various incubation times.

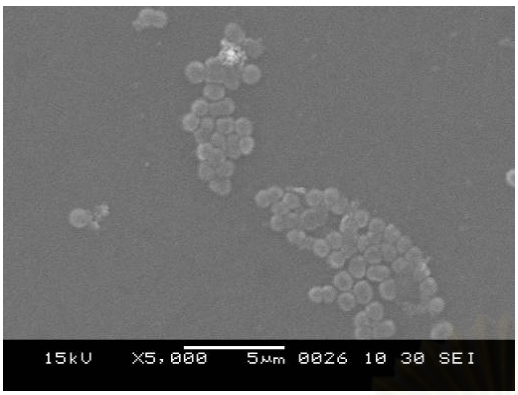

12 h

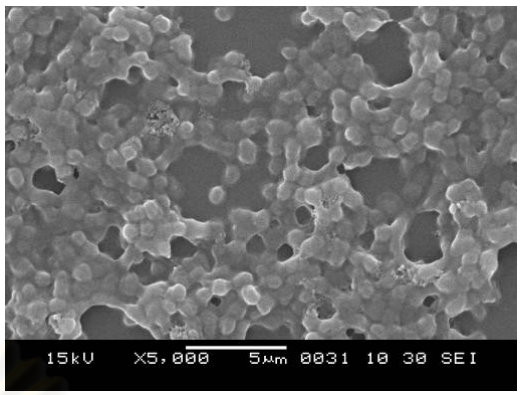

24 h

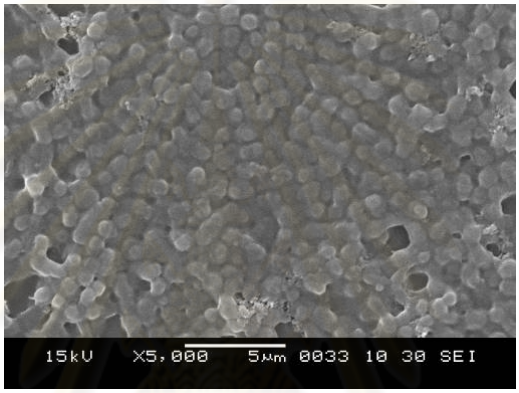

48 h

Figure 4.27 SEM micrographs of Gram-negative *Acinetobacter baylyi* strain GFJ2 attached onto chitosan film, formed from chitosan hydrolyzed for 48 h, after various incubation times.

12 h

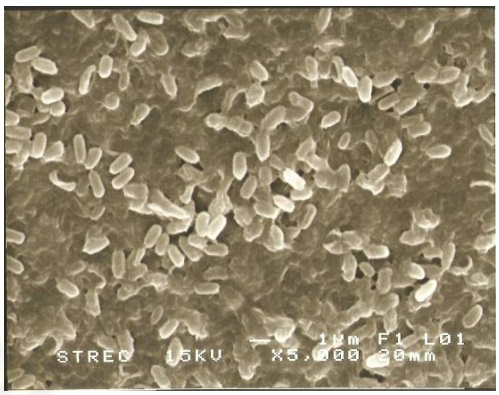

24 h

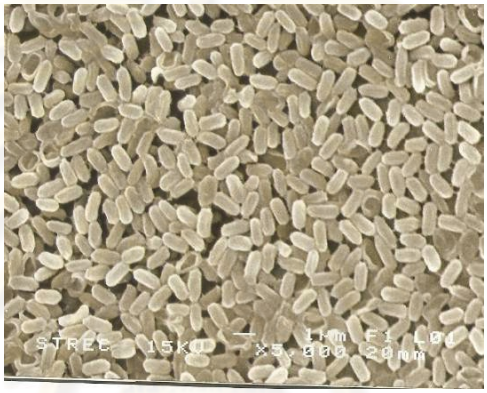

48 h

Figure 4.28 SEM micrographs of Gram-possitive *Brevibacillus agri* strain 13 attached onto chitosan film, formed from chitosan hydrolyzed for 24 h, after various incubation times.

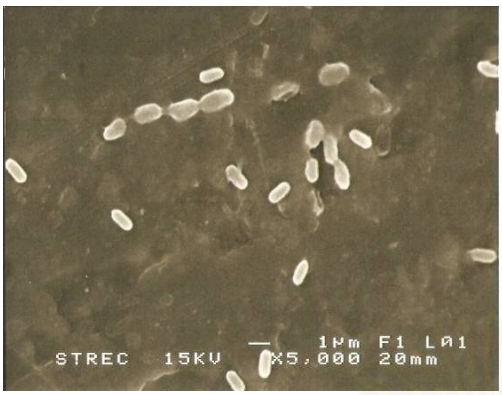

12 h

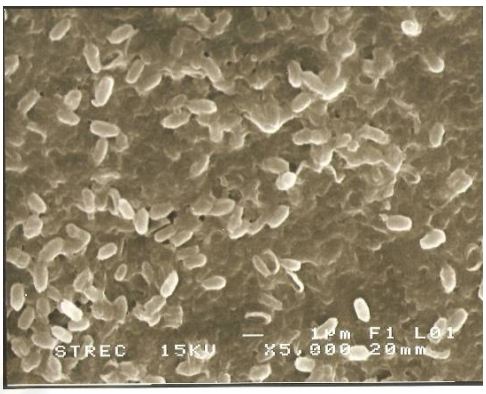

24 h

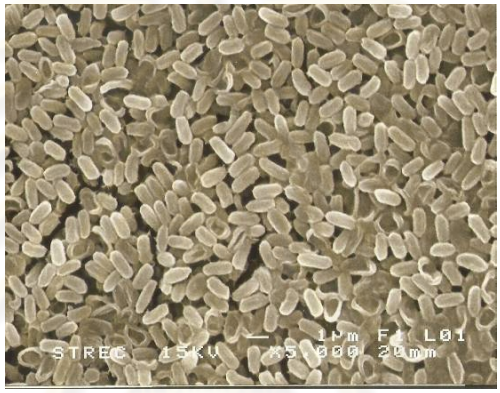

48 h

Figure 4.29 SEM micrographs of Gram-possitive *Brevibacillus agri* strain 13 attached onto chitosan film, formed from chitosan hydrolyzed for 36 h, after various incubation times.

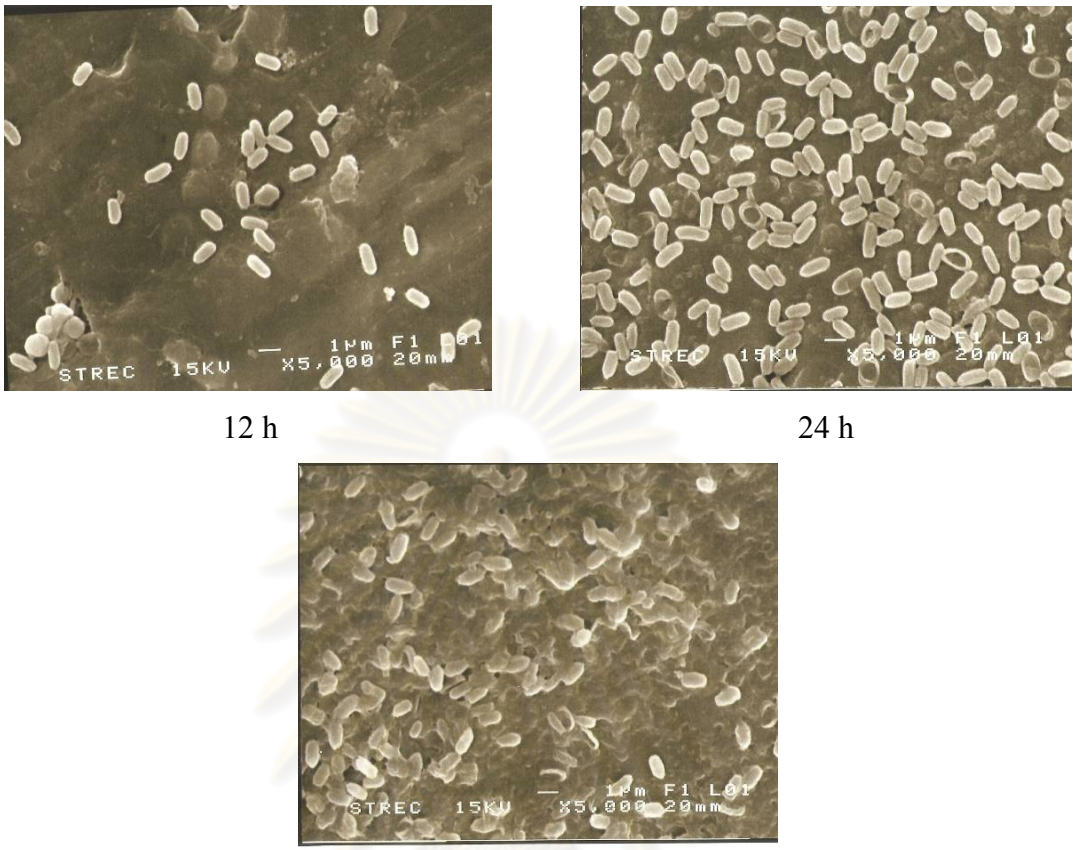

12 h 24 h

48 h

Figure 4.30 SEM micrographs of Gram-possitive *Brevibacillus agri* strain 13 attached onto chitosan film, formed from chitosan hydrolyzed for 48 h, after various incubation times.

In order to compare the amount of bacterial cell attached on chitosan films and nanofibers, the incubation time of 12 and 24 h were chosen. The comparison results are shown in Figure 4.31-4.34. Similar trend for both of Gram-negative and Gram-positive was found that the chitosan nanofibers provided more cell attachment than chitosan film. These results could be explained by the role of surface area-to-volume ratio for cell attachment. The structure of chitosan nanofibers has higher surface area-to-volume ratio than chitosan film.

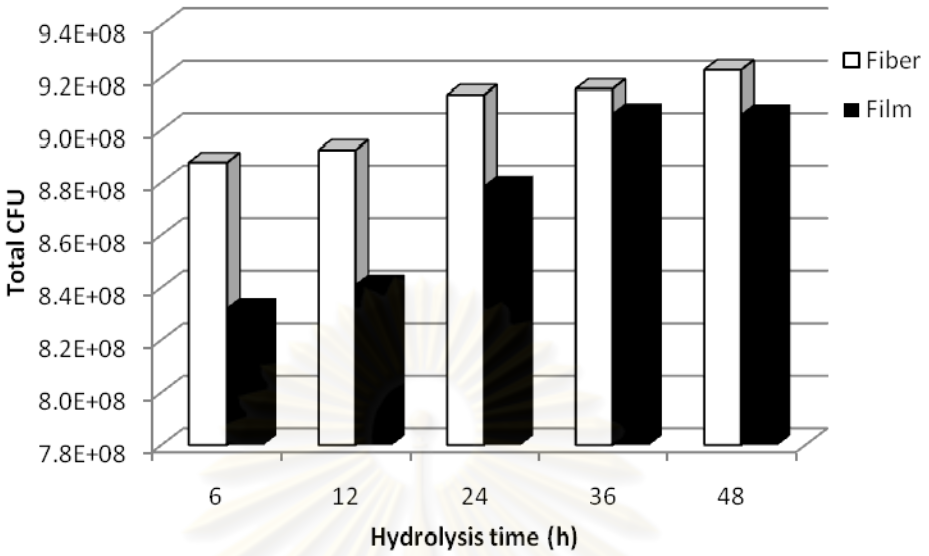

Figure 4.31 Total CFU of Gram-positive *Brevibacillus agri* strain 13 attached onto electrospun chitosan fibers and chitosan films, at 12 h of incubation time, formed from chitosan hydrolyzed for various periods of time.

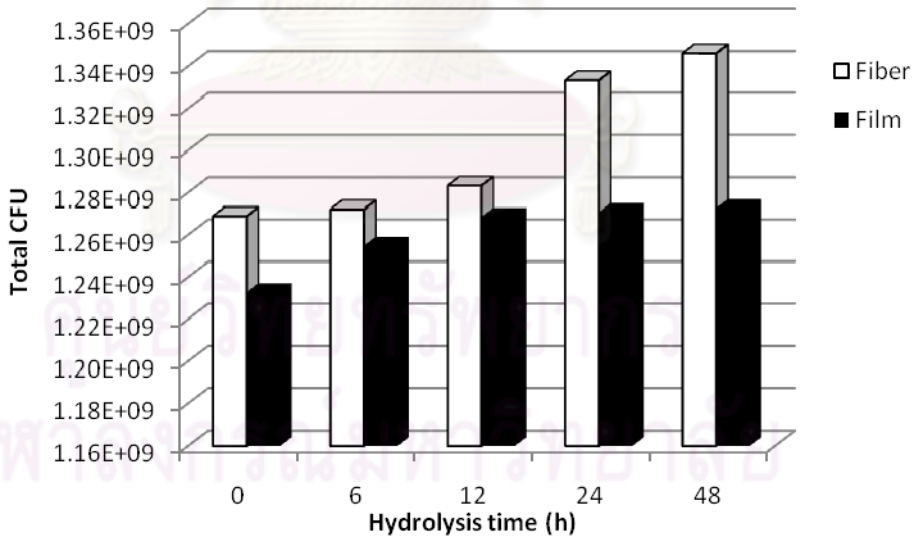

Figure 4.32 Total CFU of Gram-positive *Brevibacillus agri* strain 13 attached onto electrospun chitosan fibers and chitosan films, at 24 h of incubation time, formed from various chitosan hydrolyzed for various periods of time.

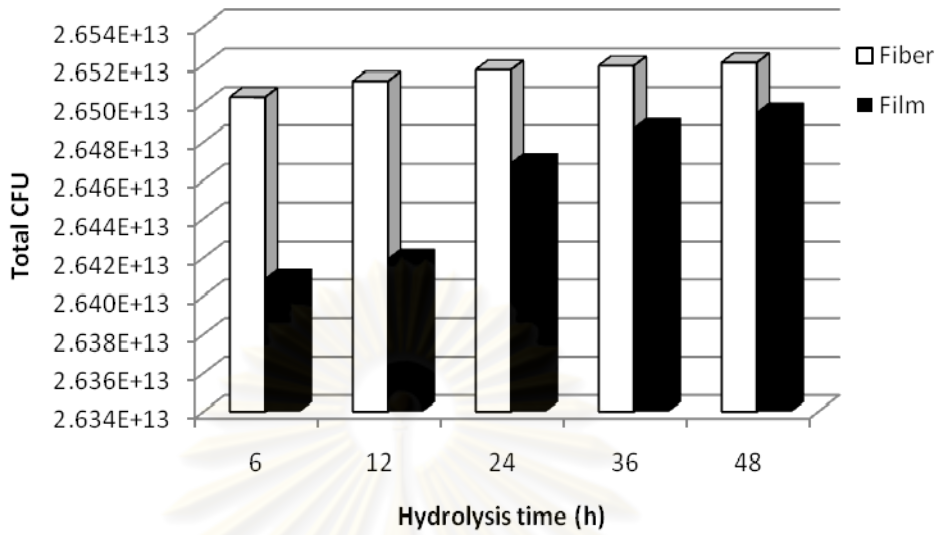

Figure 4.33 Total CFU of Gram-negative *Acinetobacter baylyi* strain GFJ2 attached onto electrospun chitosan fibers and chitosan films, at 12 h of incubation time, formed from chitosan hydrolyzed for various periods of time.

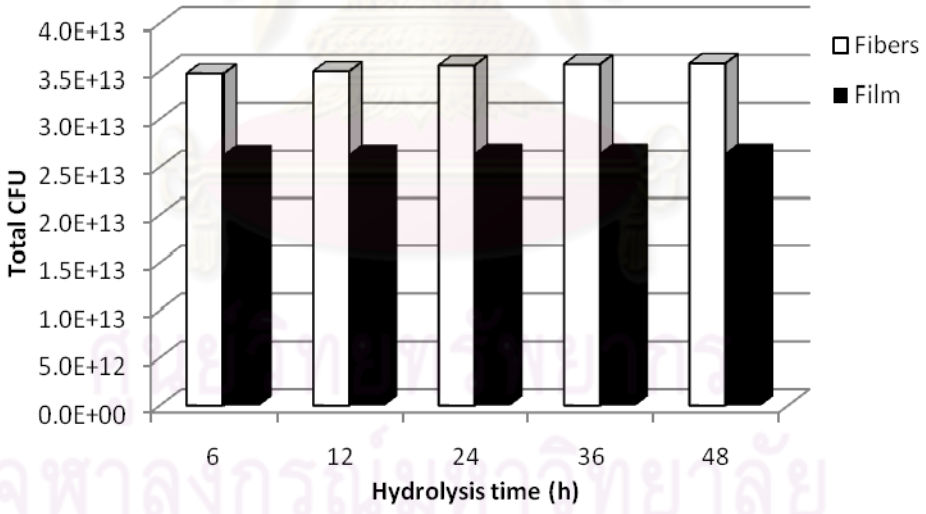

Figure 4.34 Total CFU of Gram-negative *Acinetobacter baylyi* strain GFJ2 attached onto electrospun chitosan fibers and chitosan films, at 24 h of incubation time, formed from various chitosan hydrolyzed for various periods of time.

4.4.3 Cell attachment on chitosan/PVA nanofibers

The capability of cells attachment on chitosan/PVA nanofibers, as a function of chitosan content, was investigated by using molecular weight of chitosan of 760 kDa. The incubation time of 12 and 24 h were chosen for investigation of cell attachment for both Gram-negative and Gram-positive bacteria. The results, regarding the number of cells attached to the nanofibers, are shown in Figure 4.35-4.38.

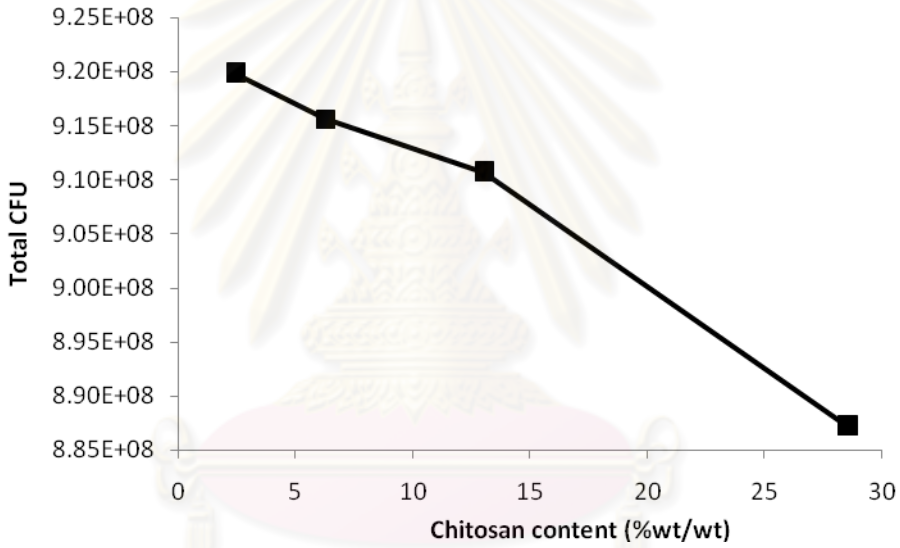

Figure 4.35 Total CFU of Gram-positive *Brevibacillus agri* strain 13 attached onto chitosan/PVA nanofibers with various chitosan contents, at 12 h of incubation time.

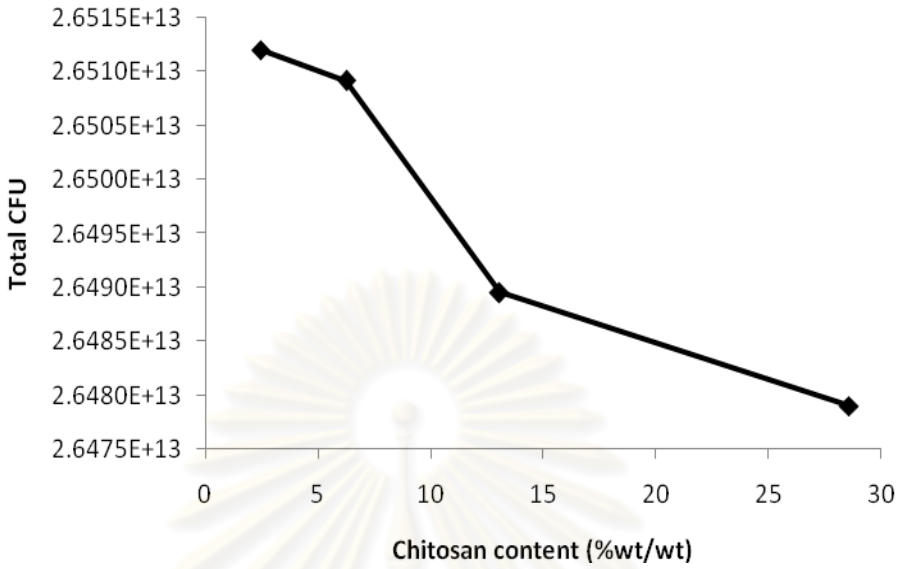

Figure 4.36 Total CFU of Gram-negative *Acinetobacter baylyi* strain GFJ2 attached onto chitosan/PVA nanofibers with various chitosan contents, at 12 h of incubation time.

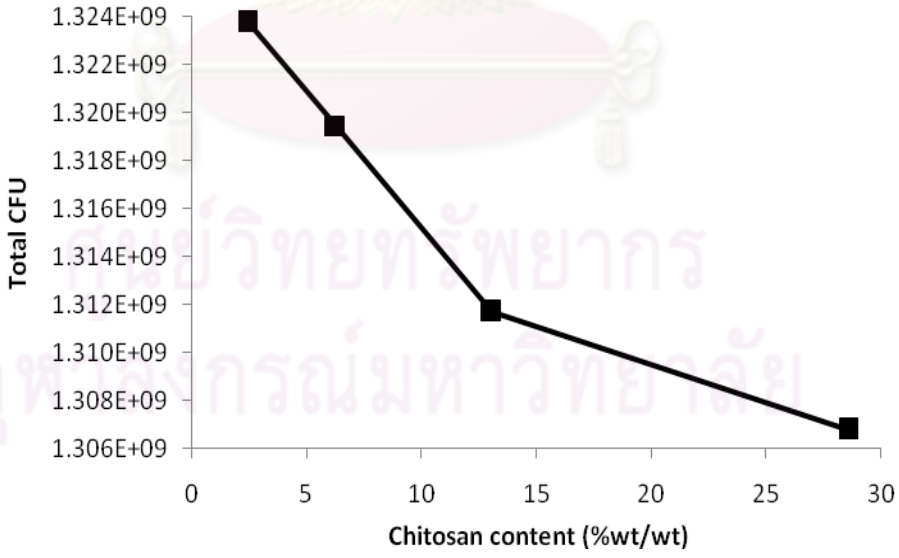

Figure 4.37 Total CFU of Gram-positive *Brevibacillus agri* strain 13 attached onto chitosan/PVA nanofibers with various chitosan contents, at 24 h of incubation time.

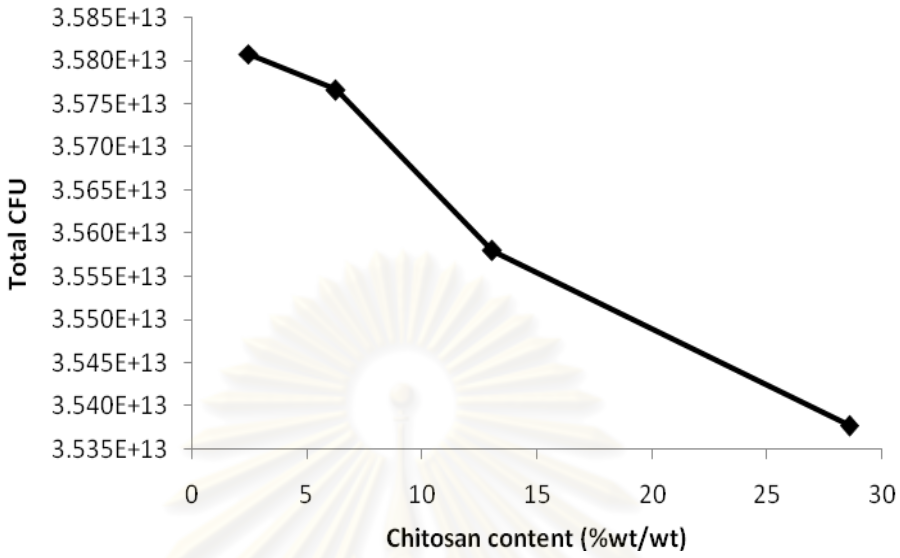

Figure 4.38 Total CFU of Gram-negative *Acinetobacter baylyi* strain GFJ2 attached onto chitosan/PVA nanofibers with various chitosan contents, at 24 h of incubation time.

At 2.44 %wt/wt of chitosan content in the fibers, it was found that most of bacterial cells, for both types of bacteria, were attached on surface. When the chitosan contents was increased to 6.25, 13.04 and 28.57 %wt/wt, the number of bacterial cell attached on the surface was decreased. These results could be explained by the role of chitosan content and molecular weight of chitosan. As previously discussed, at high chitosan contents, the electrospinning yielded not only fibers but also beads. Decreasing chitosan contents in the electrospinning solutions could generate more fibers and less beads, resulting in increased surface area-to-volume ratio. High surface area-to-volume ratio of the fiber mats made it available for the bacterial cells to attach. Moreover, as it has been known that the positively charged chitosan interacts with negatively charged cell surface, the amino groups (NH_3^+) as the active functional group was found to be essential factor affecting the bacterial cells attachment [22-24]. Chitosan is a cationic polysaccharide with amino group at the C2 position. The addition of chitosan contents would also increase the number of NH_3^+ groups leading to the free amino group that could alter cell permeability. Due to outer membrane

damage, it involves changes in the hydrophilicity and charge density of the cell surface.

To prove the effect of molecular weight on chitosan/PVA nanofibers, the chitosan with molecular weight 100 kDa, 400 kDa and 760 kDa were investigated, using 24 h for incubation time and Gram-negative *Acinetobacter baylyi* strain GFJ2 bacteria. The results are shown in Figure 4.39.

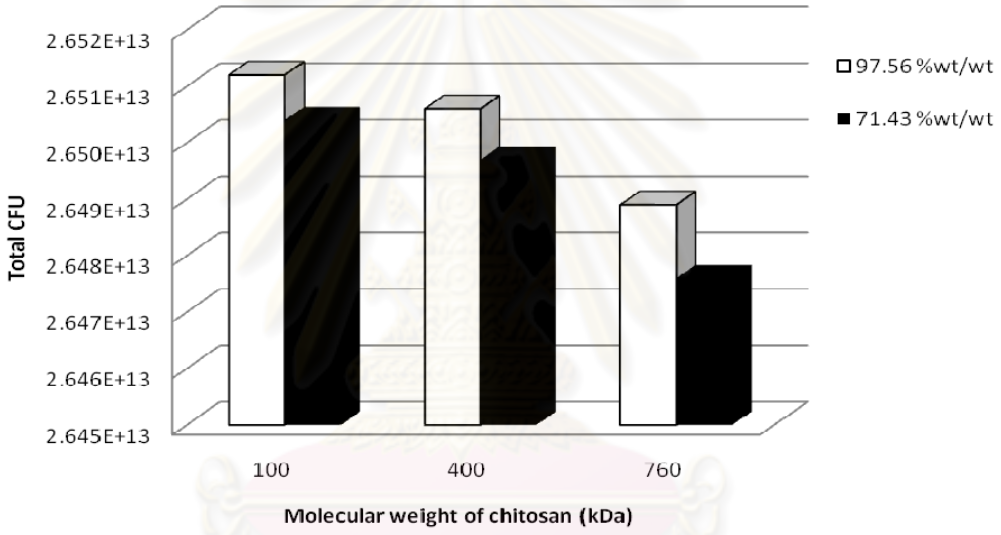

Figure 4.39 Total CFU of Gram-negative *Acinetobacter baylyi* strain GFJ2 attached onto chitosan/PVA nanofibers, at 24 h incubation time, formed from various PVA contents (%wt/wt) and molecular weight of chitosan.

These results could be confirmed that molecular weight of chitosan affected bacterial cells attachment. Closely relating to viscosity and spinability, molecular weight of chitosan affected the behavior of chitosan such as chain conformation, solubility and degree of substitution. High molecular weight chitosan could have block arrangement of acetylated and deacetylated units. Intermolecular interactions may reduce available sites on the chitosan molecule. The number of amino groups (NH_3^+) as the active functional group was low and resulted in reduced available sites for the bacterial cells to attach on the chitosan surfaces.

4.5 Viability of Bacterial Cells Attaching on Chitosan Nanofibers

In the immobilization by attachment, the bacterial cells were bounded to the carrier material via reversible surface interactions. The forces involved are ionic and H-bonding interaction as well as hydrophobic forces. Due to low amount of free amino groups on its surface, chitosan could be considered as neutral and there is a low possibility of interaction through H-bonding or ionic forces. As the amount of free amino groups were increased, the ionic and H-bonding forces becomes more relevant. These behaviors are closely related to cells viability on chitosan. In this sections, the viability of attaching on chitosan prepared by various is presented.

4.5.1 Viability of bacterial cells attaching on hydrolyzed chitosan nanofibers

4.5.1.1 Effect of incubation time

In order to determine the bacterial viability on hydrolyzed chitosan nanofibers at various incubation times, the hydrolysis time of 6 and 48 h were chosen. The initial optical densities (OD_{600}) of bacterial cells solution (i.e., free cells) for *A. baylyi* strain GFJ2 and *B. agri* strain 13 were 0.85 and 1.0, which were corresponding to the colony forming unit of 1.8981×10^{13} and 1.4760×10^{9} CFU, respectively. The percentage of live cells attaching on hydrolyzed chitosan nanofibers is shown in Figure 4.40-4.41. The florescence images of dyed live cells (green) and dead cells (red) on hydrolyzed chitosan are shown in Figure 4.42-4.45.

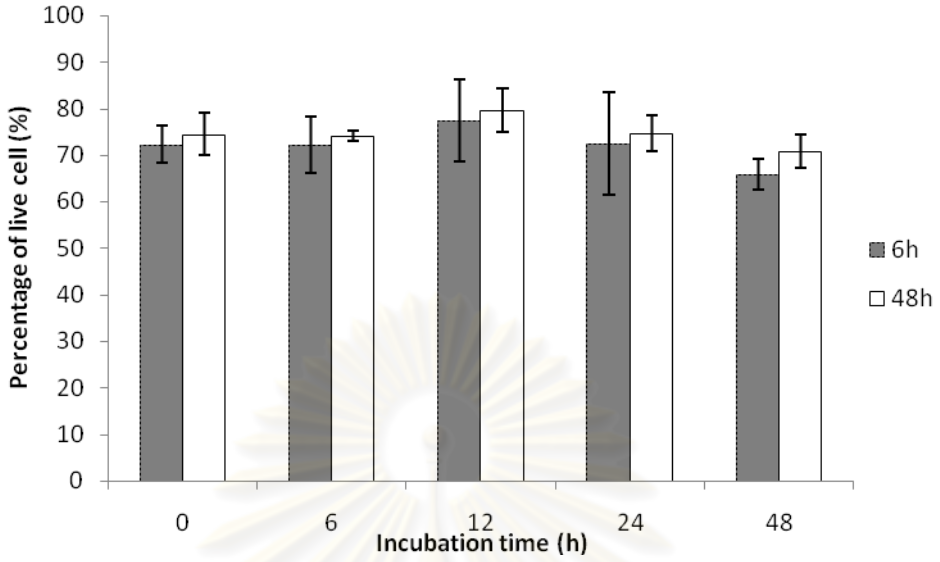

Figure 4.40 Percentage of live cells for Gram-positive *Brevibacillus agri* strain No.13 attached onto electrospun chitosan fibers, formed from chitosan hydrolyzed for 6 and 48 h, after various incubation times.

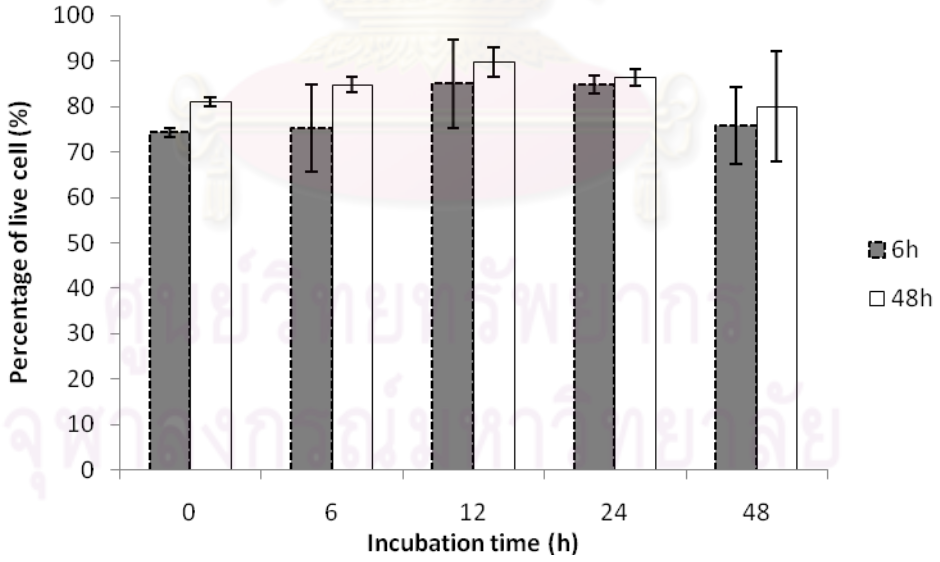

Figure 4.41 Percentage of live cells for Gram-negative *Acinetobacter baylyi* strain GFJ2 attached onto electrospun chitosan fibers, formed from chitosan hydrolyzed for 6 and 48h, after various incubation times.

Similar trend for both of Gram-negative and Gram-positive was found. The percentage of live cells attaching on the hydrolyzed chitosan was slightly increased when the incubation time was increased to 12 h. When the incubation time between chitosan fibers and the bacteria cells was prolonged to 24 h, the percentage of live cells attaching on the sample was slightly decreased. Nevertheless, the fraction of live cells was relatively high. It is possible that the microorganism may be induced to attach by altering the physical and chemical properties according to ionic attraction of bacterial cells and the chitosan surface. Chitosan is a cationic polysaccharide that acts as a glue to initiate bacterial-surface interactions. Increasing the contact time between chitosan fibers and the bacterial cells tends to increase the interaction rate. However, the carbon sources could be presumed to limit in this study. When the incubation time was prolonged to 12 h, much of the carbon sources was still available for cells. After the incubation time up to 24 h, the carbon source for bacterial cells was decreased. In addition to the comparison of the percentage of viable cells for both Gram-positive and Gram-negative, it was found that the survival of Gram-positive bacteria on chitosan was less than Gram-negative. This result could be explained by the difference in chemical properties of their cell walls. Gram-positive cell walls do not posses a lipid outer membrane while Gram-negative cell walls posses an outer membrane consisting of various lipid complexes [25, 26]. When the positive charges on amino groups of chitosan interacted with negatively charged bacterial cells wall, it leaded to the leakage of intracellular constituents.

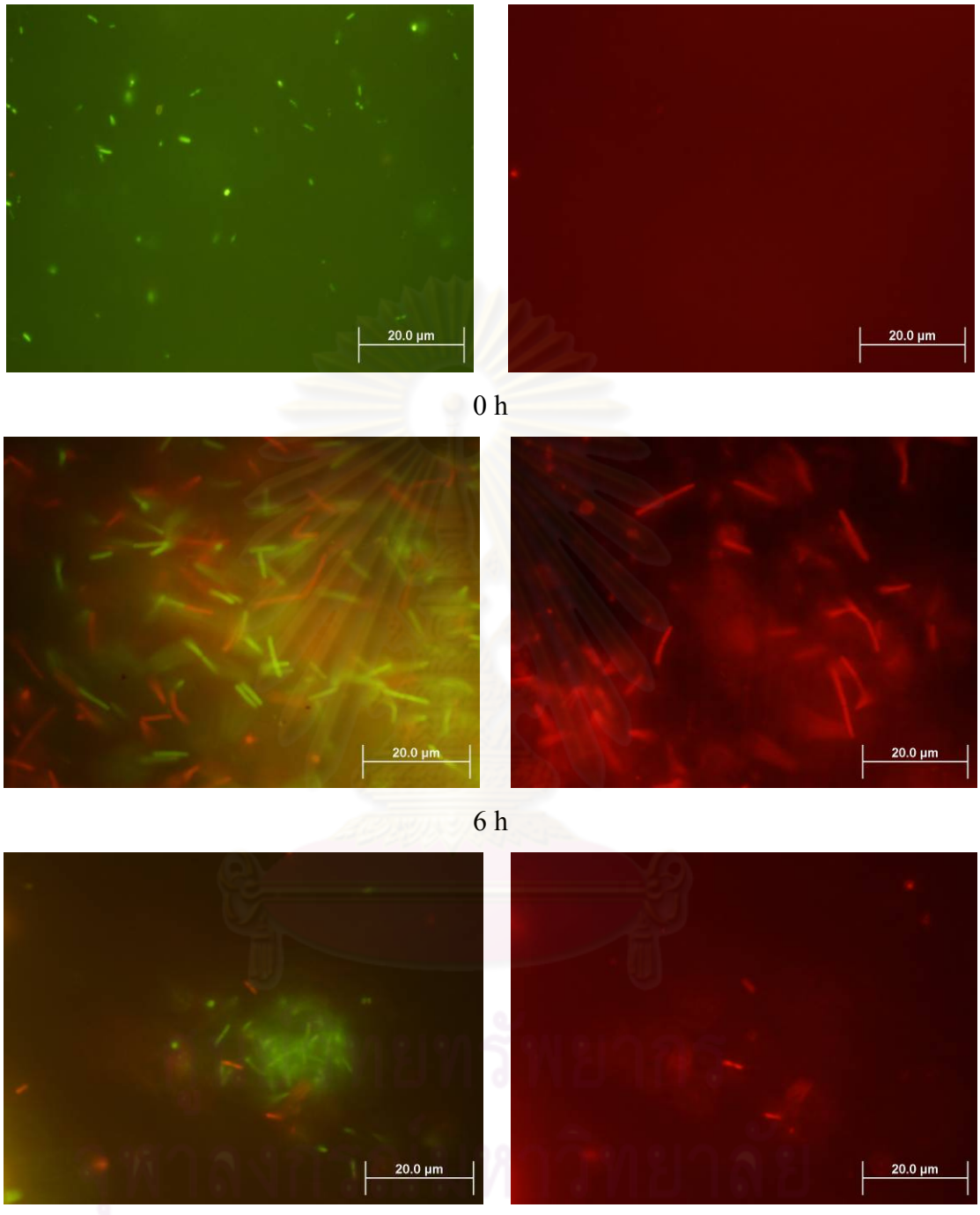

Figure 4.42 Fluorescence micrograph of Gram- positive *B. agri* strain 13 attaching on the electrospun chitosan nanofibers, that were prepared from chitosan hydrolyzed for 6 h, after various incubation time. The green fluorescence indicated live cells, while the red fluorescence indicated dead cells.

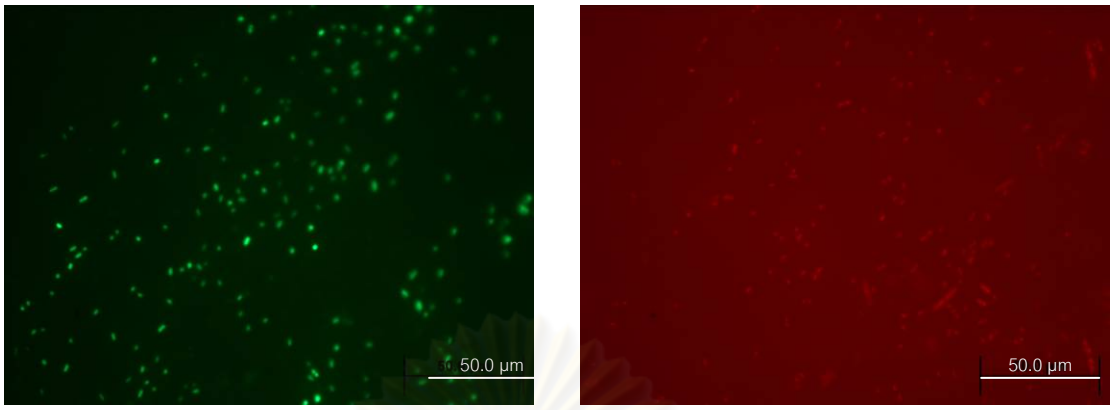

24 h

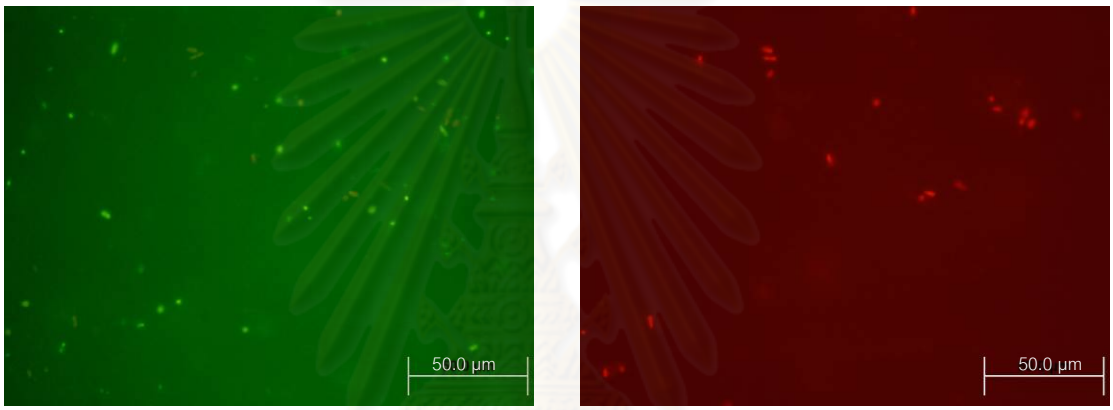

48 h

Figure 4.42 (continued).

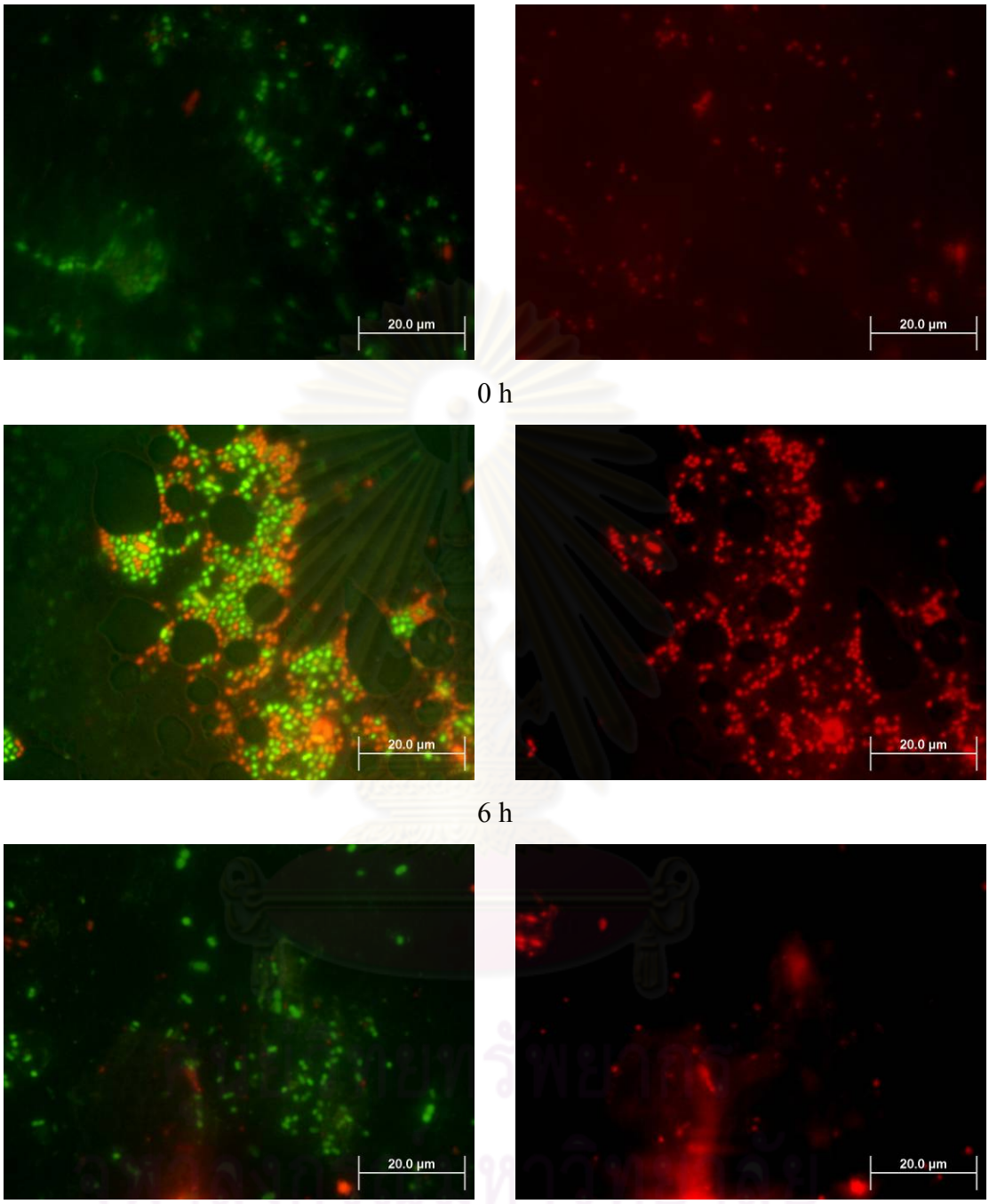

Figure 4.43 Fluorescence micrograph of Gram- negative *A. baylyi* strain GFJ2 attaching on the electrospun chitosan nanofibers, that were prepared from chitosan hydrolyzed for 6 h, after various incubation time. The green fluorescence indicated live cells, while the red fluorescence indicated dead cells.

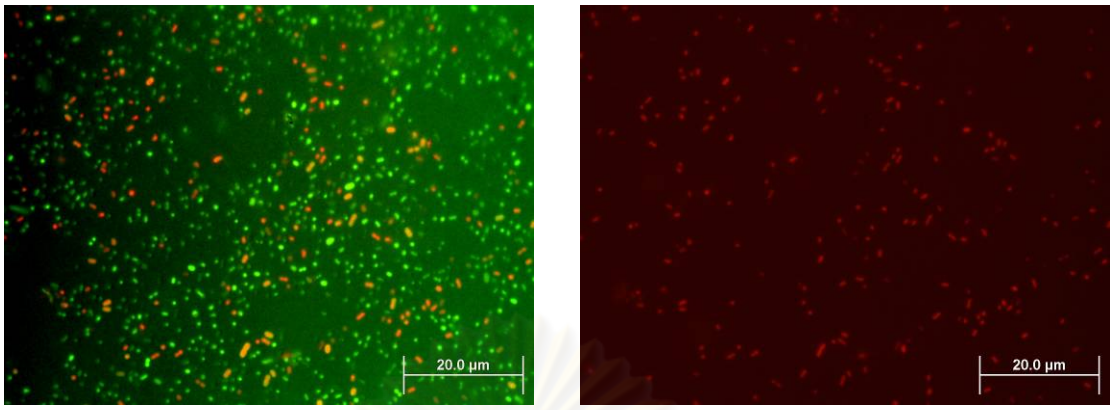

24 h

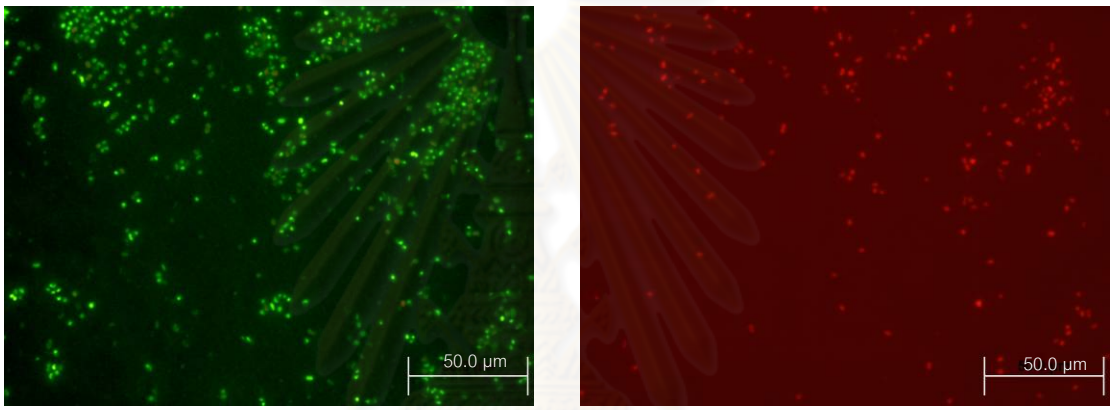

48 h

Figure 4.43 (continued).

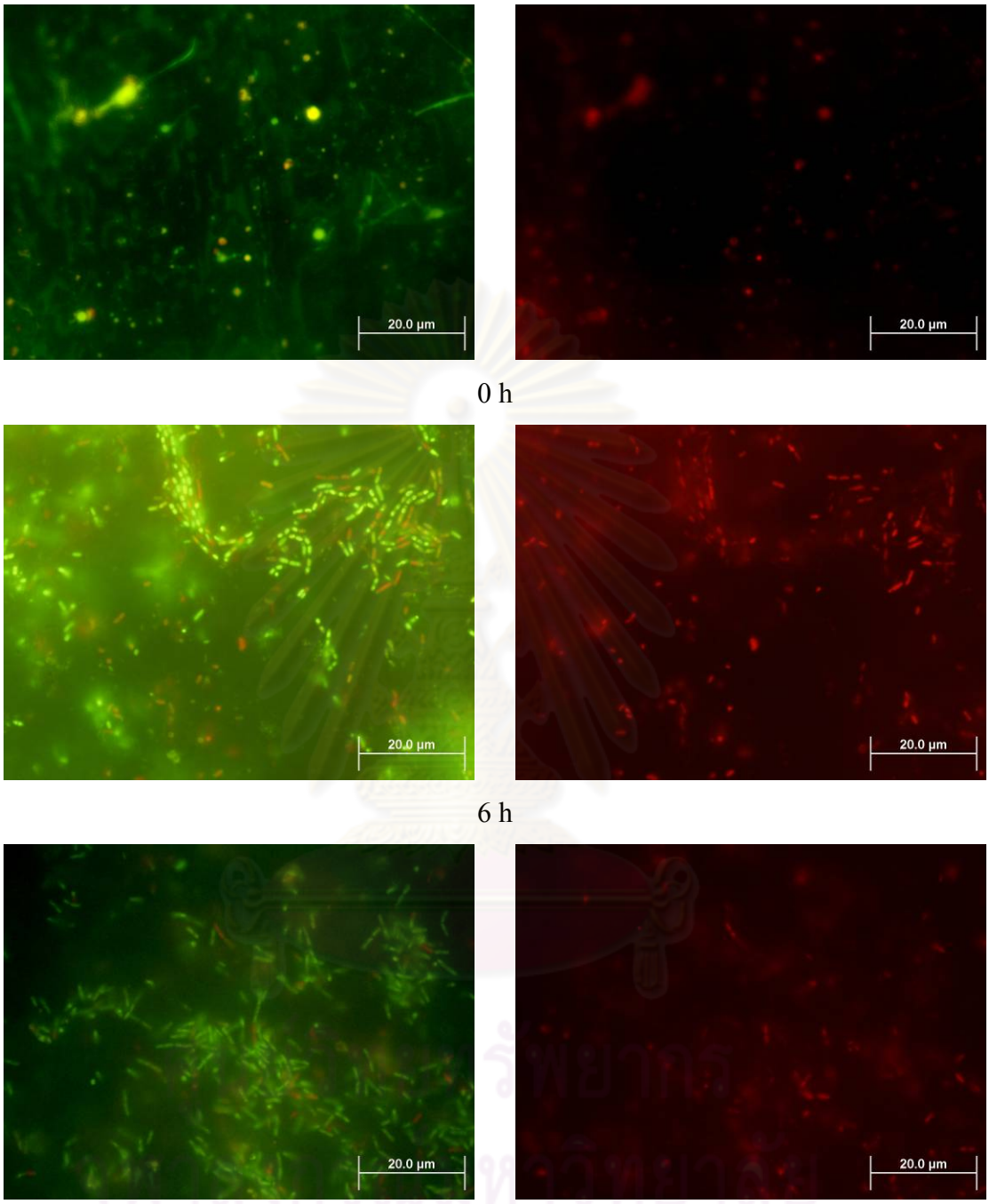

Figure 4.44 Fluorescence micrograph of Gram- positive *B. agri* strain 13 attaching on the electrospun chitosan nanofibers, that were prepared from chitosan hydrolyzed for 48 h, after various incubation time. The green fluorescence indicated live cells, while the red fluorescence indicated dead cells.

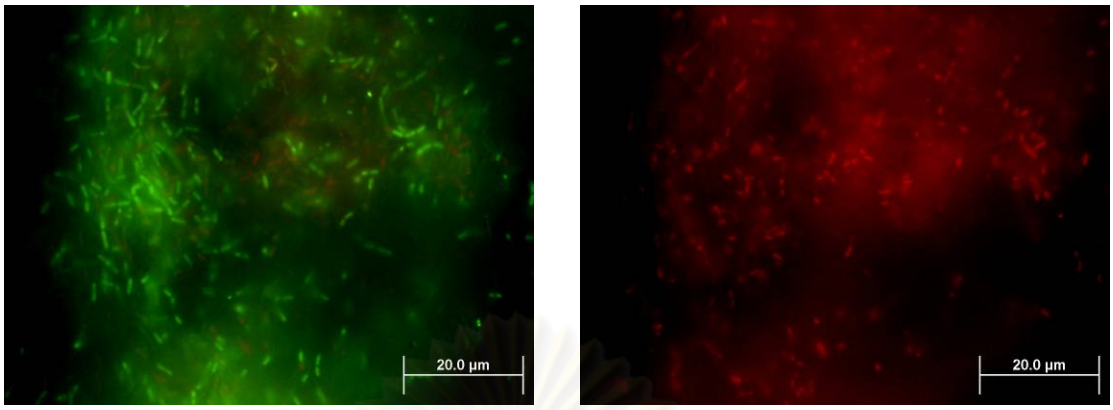

24 h

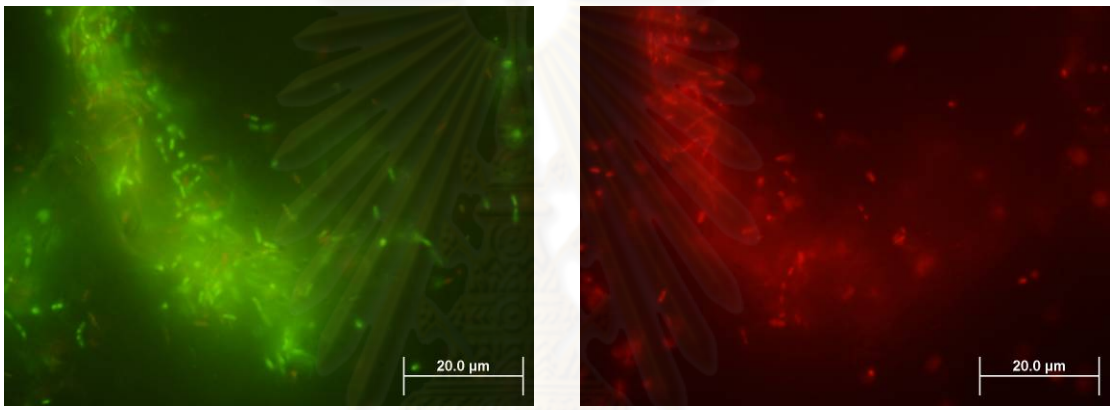

48 h

Figure 4.44 (continued).

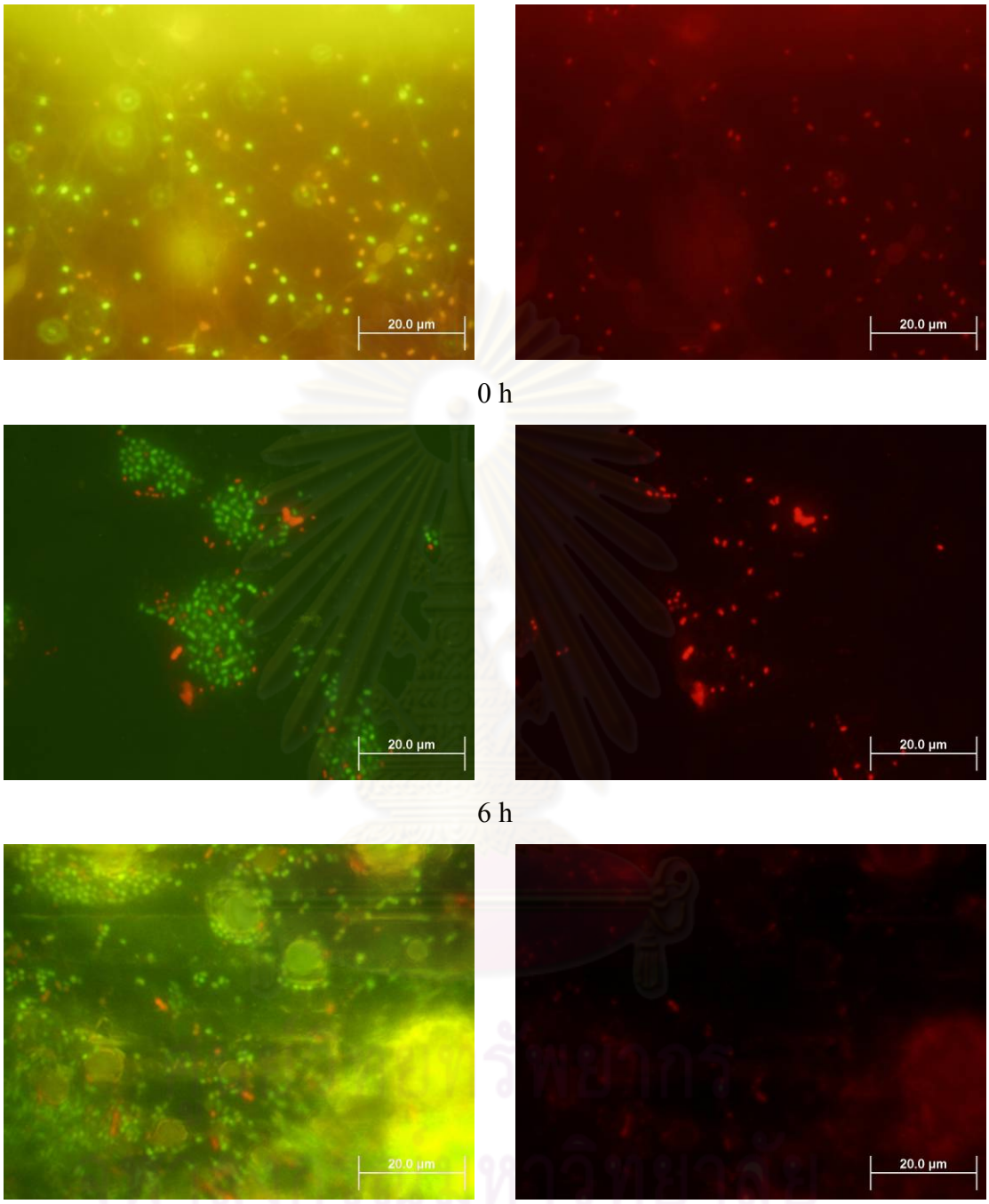

Figure 4.45 Fluorescence micrograph of Gram- negative *A. baylyi* strain GFJ2 attaching on the electrospun chitosan nanofibers, that were prepared from chitosan hydrolyzed for 48 h, after various incubation time. The green fluorescence indicated live cells, while the red fluorescence indicated dead cells.

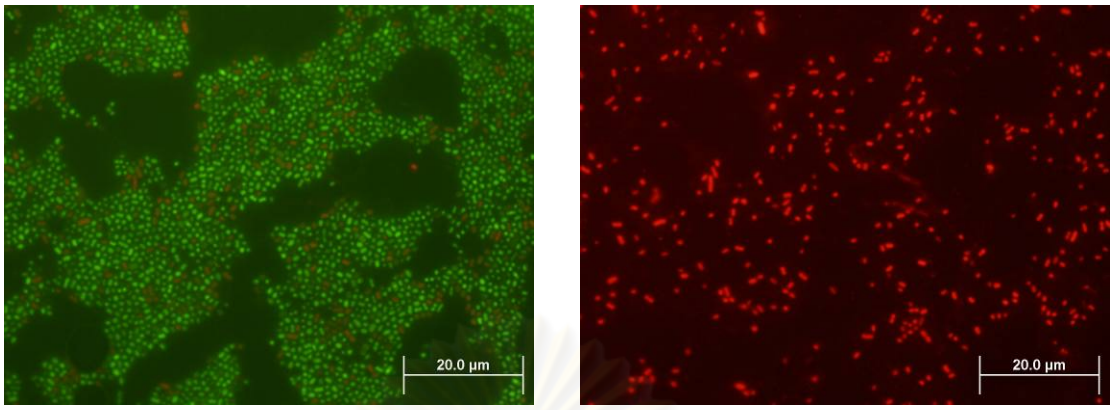

24 h

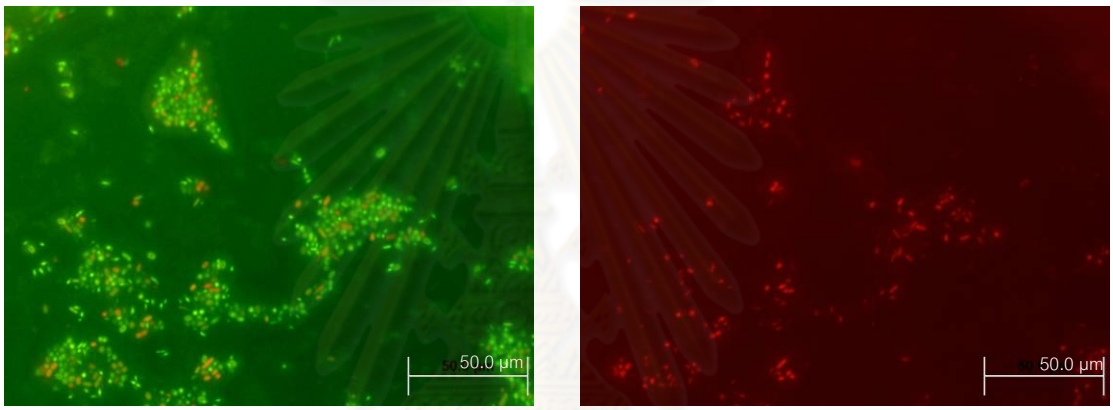

48 h

Figure 4.45 (continued).

4.5.1.2 Effect of hydrolysis time of chitosan

To compare the effect of hydrolysis time of chitosan on cells viability, the incubation time of 12 and 24 h were chosen. It was found that the percentage of live cells for both types of bacteria attaching on the surface increased when the hydrolysis time of chitosan was increased. The results are shown in Figure 4.46-4.47. The trend of percentage of live cells with respect to the hydrolysis time was similar for both incubation times. Increasing of hydrolysis time of chitosan resulted in increased cells viability. The results are shown in Figure 4.48-4.49.

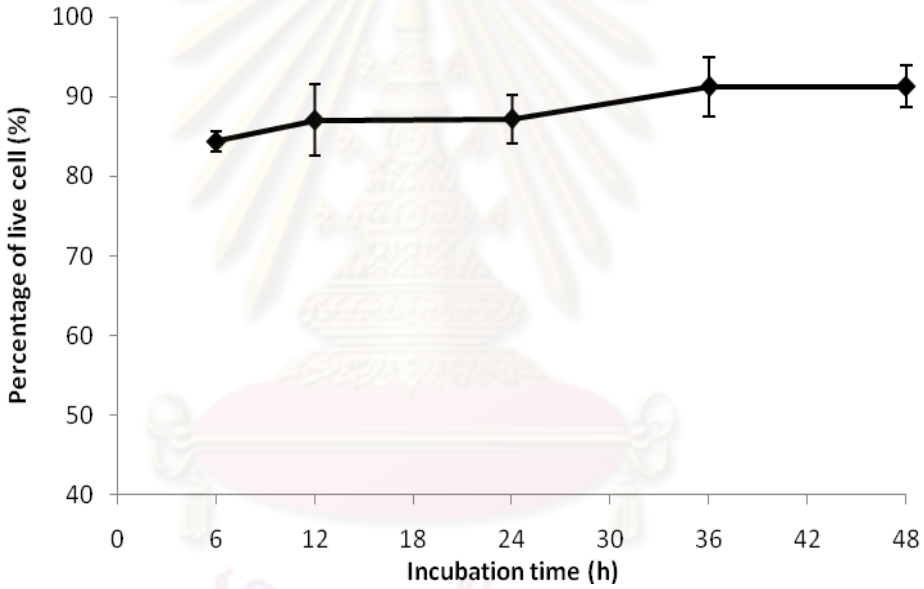

Figure 4.46 Percentage of live cells for Gram-positive *Brevibacillus agri* strain No.13 attaching on electrospun chitosan fibers, prepared from chitosan being hydrolyzed for period time, after the incubation time of 12 h.

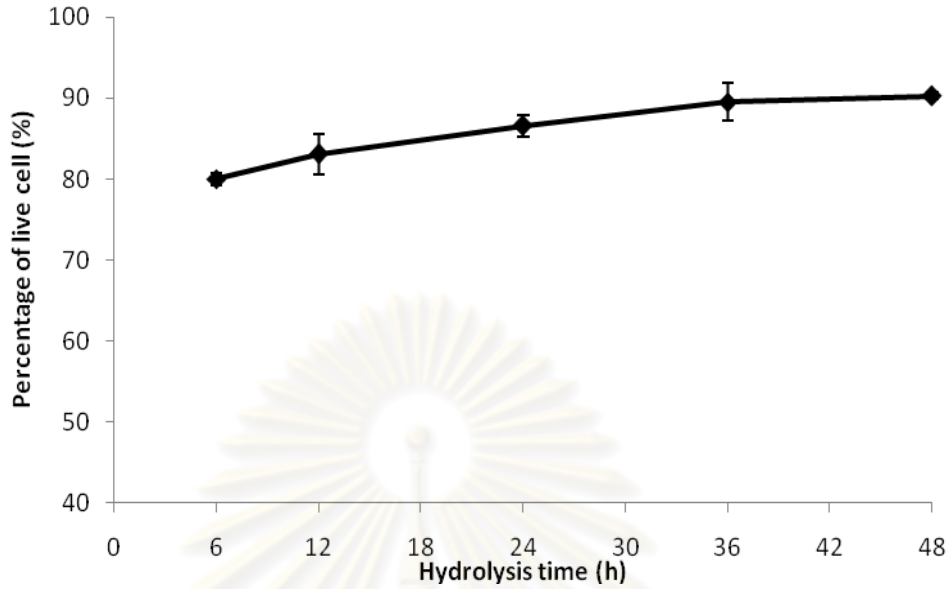

Figure 4.47 Percentage of live cell for Gram-positive Brevibacillus agri strain No.13 attaching on electrospun chitosan fibers, prepared from chitosan being hydrolyzed for period time, after the incubation time of 24 h.

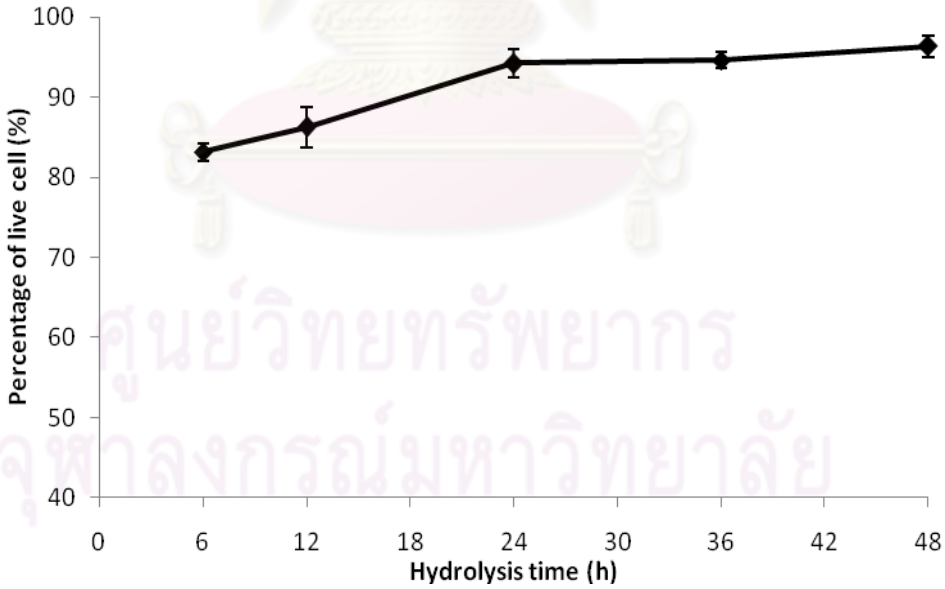

Figure 4.48 Percentage of live cell for Gram-negative *Acinetobacter baylyi* strain GFJ2 attaching on electrospun chitosan fibers, prepared from chitosan being hydrolyzed for period time, after the incubation time of 12 h.

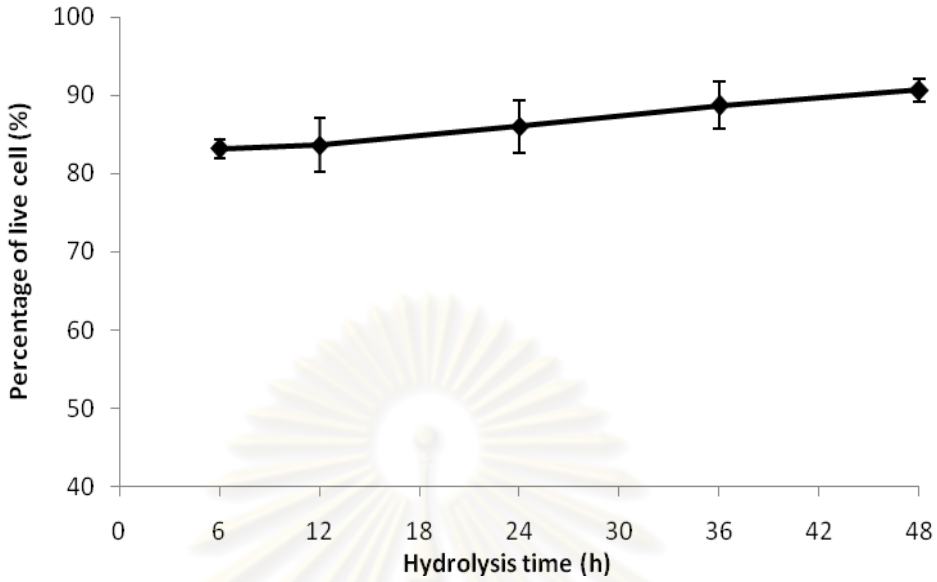

Figure 4.49 Percentage of live cell for Gram-negative *Acinetobacter baylyi* strain GFJ2 attaching on electrospun chitosan fibers, prepared from chitosan being hydrolyzed for period time, after the incubation time of 12 h.

The results were not only explained by the surface area-to-volume ratio available for cells attachment on the surface but also due to a significant role of the cationic behavior of chitosan. Although the degree of deacetylation is the one of the most important chemical characteristics of chitosan, the influence of molecular weight on the viscosity of chitosan solution also played a significant role.

To clearly explain the hydrolysis of chitosan, the FT-IR spectrum of chitosan after being hydrolyzed for various period of time shown in Figure 4.50. Chitosan shows a broad O-H stretching at wave number between 2800-2900 cm^{-1} and the absorbtion corresponding to polysaccharide structure at wave number between 1155-850 cm^{-1}. Another major absorption band at 1600 cm^{-1} represents the free amino group ($-NH_2$) at C2 position of glucosamine. The peak at 1641 cm^{-1} and 1324 cm^{-1} corresponds to a CO-NH of amide I and amide II deformation to CH_2 group [27-30]. Noted that, for chitosan, the peak at 1600 cm^{-1} has larger intensity than at 1641 cm^{-1} and 1324 cm^{-1} which suggests effective deactylation. Decreasing of the peak at 1641 cm^{-1} and 1324 cm^{-1} corresponding to higher deactylation. From the results, at 6, 12 , 24, 36 and 48 h of hydrolysis, it was indicated that there was an intensification of the

peak at 1600 cm^{-1} while the peak at 1641 cm^{-1} of CO-NH appeared only after 48 h for hydrolysis time. However, the difference was shown at the peak of 1324cm^{-1} which indicated that when the hydrolysis time was prolonged to 48 h, it resulted in the increased deacetylation. It is possible due to the propagation of the hydrolysis reaction. Nevertheless, all of hydrolyzed chitosan is not fully deacetylated. The interaction between chitosan and anionic surface active species of phospholipids from cell wall depended on the amino group at C2 position. The presence of free amino groups along the chitosan chain allows this macromolecule to dissolve in diluted acidic solution. Increasing free amino groups, which also related to the increased chitosan solubility, leaded to the increase in positive charge of the polymer chains for cell to attach on the surface.

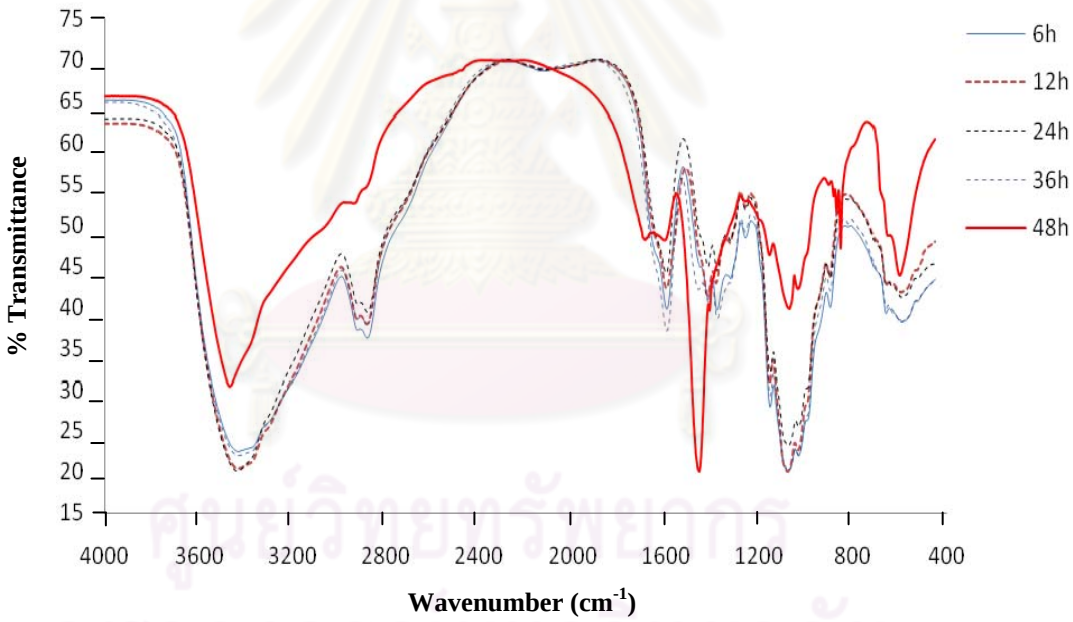

Figure 4.50 FT-IR spectra of chitosan being hydrolyzed for various period of time.

In fact, the highest of cells viability was found on chitosan hydrolyzed for 48 h. It is possible to presume in regard of biocompatibility that decreasing the molecular weight of chitosan was able to decrease a toxicity toward bacteria. To confirm the effect of chitosan molecular weight on cell viability, the FT-IR spectrum of chitosan obtained at different hydrolysis times were analyzed. The peak of polysaccharide

structure at wave number between 896-1155 cm^{-1} was found. It was found that when the hydrolysis time was increased, the intensity of the polysaccharide group was decreased and the peak corresponding to ring breathing at 849-901 cm^{-1} appeared. This result indicated that the saccharide structure of the molecule was opened by dehydration of saccharide rings and cut into the polymer chain by hydroxyl groups of NaOH. It is attributed to a complex process including dehydration of sacharide rings, depolymerization and decomposition of the acetylated and deacetylated units of polymers that could reduce the polymer chain length and the molecular weight of chitosan [31]. In addition, the solubility of the hydrolyzed chitosan was increased due to the decreased molecular weight [32]. The live cells and dead cells are shown in Figure 4.51-4.54.

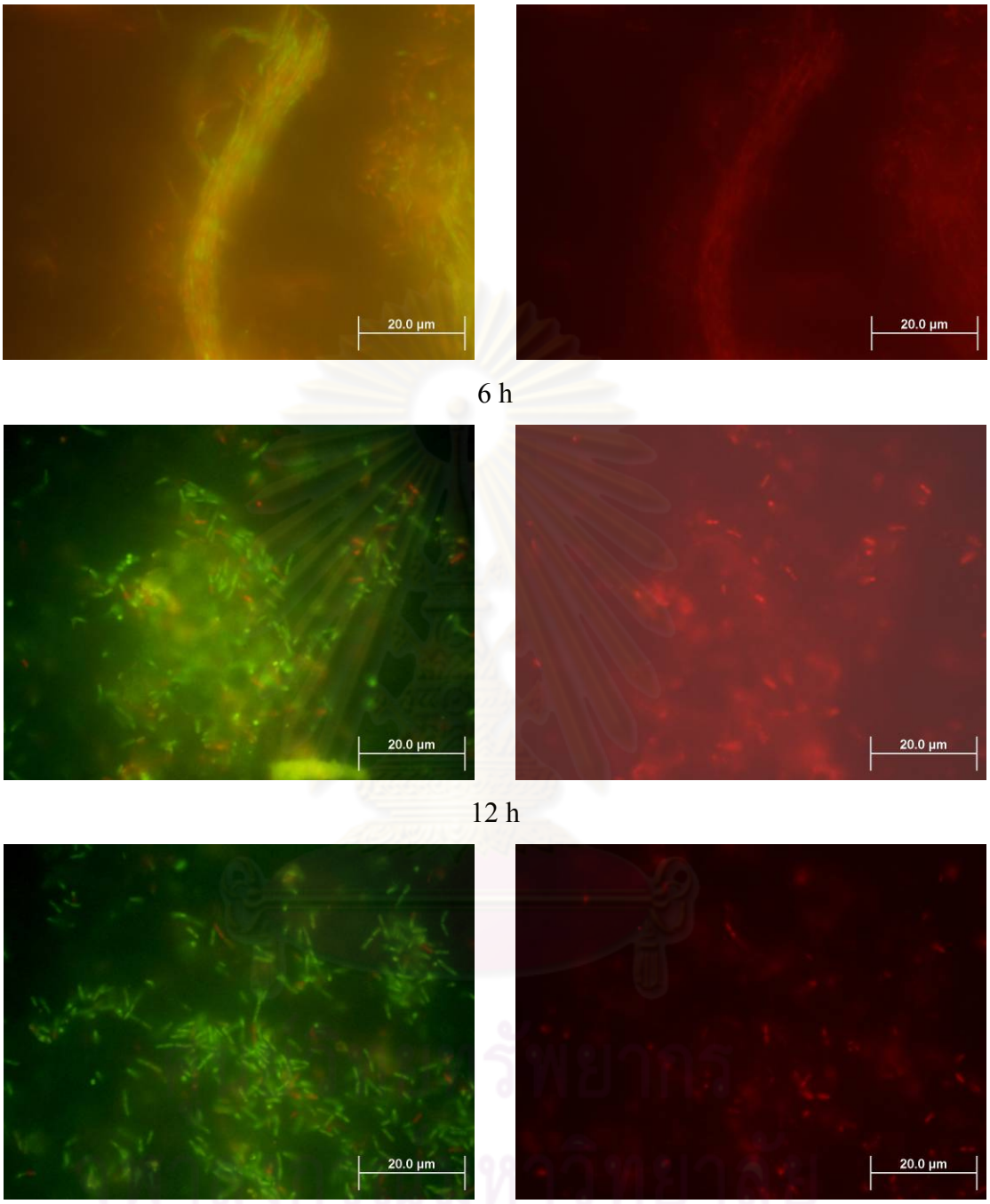

Figure 4.51 Fluorescence micrographs of Gram-positive *B. agri* No.13 attached on electrospun chitosan nanofibers that were prepared from chitosan hydrolyzed for various period of time, after the incubation time of 12 h.

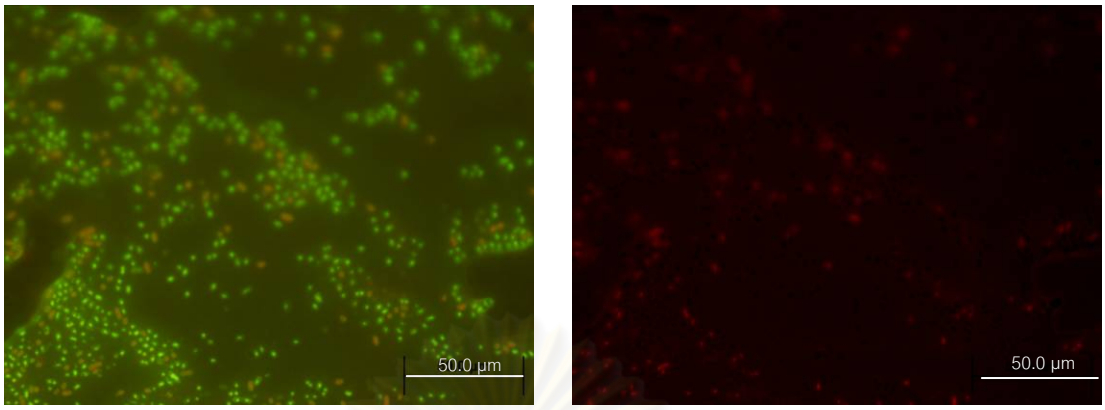

36 h

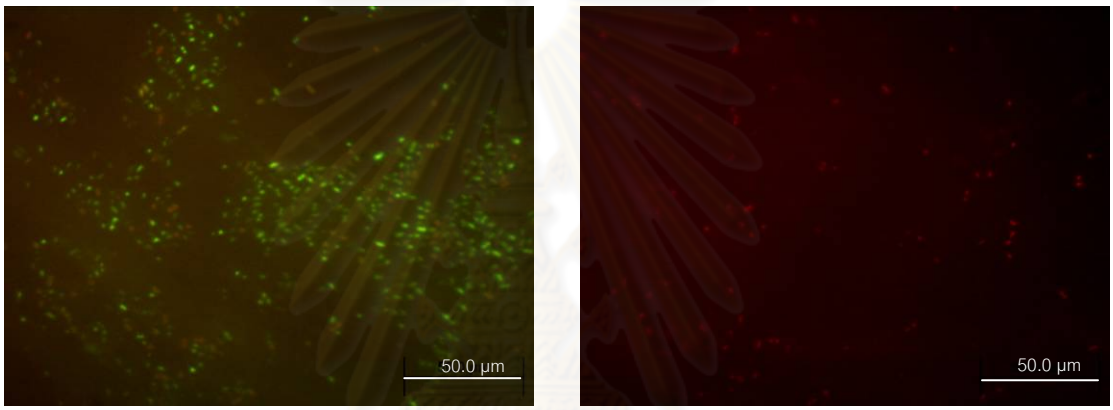

48 h

Figure 4.51 (continued)

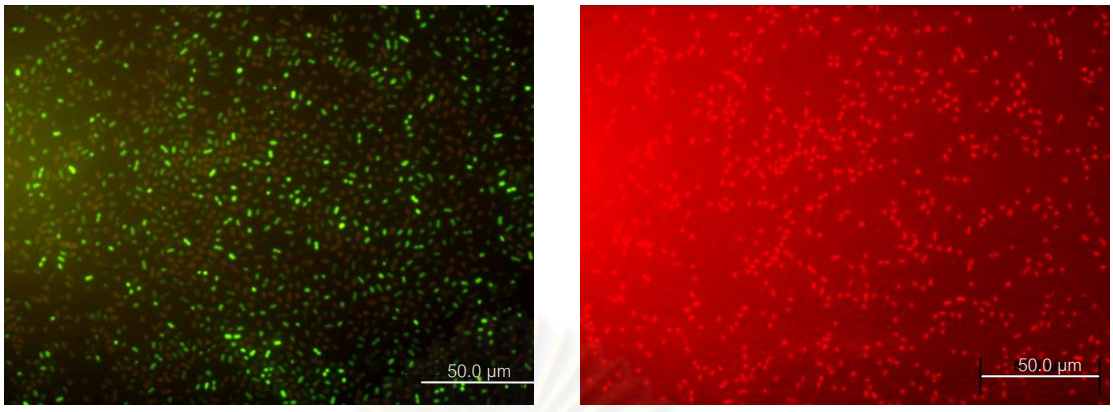

6 h

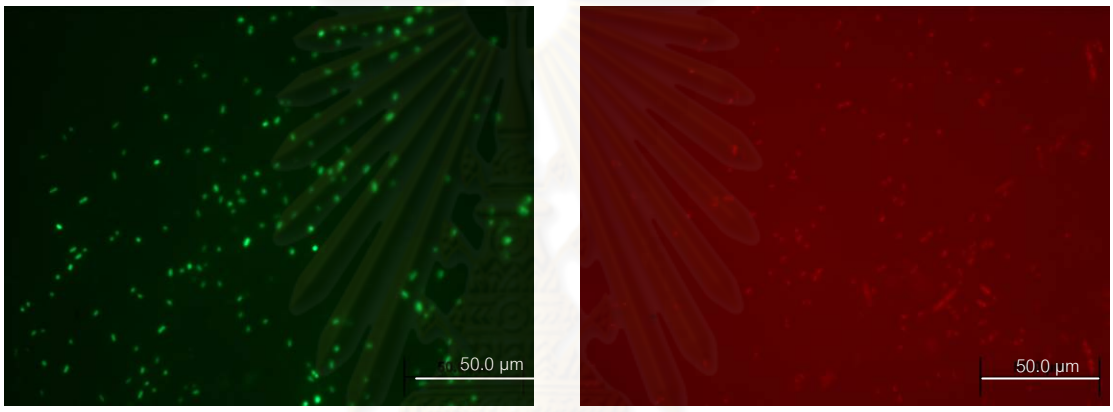

12 h

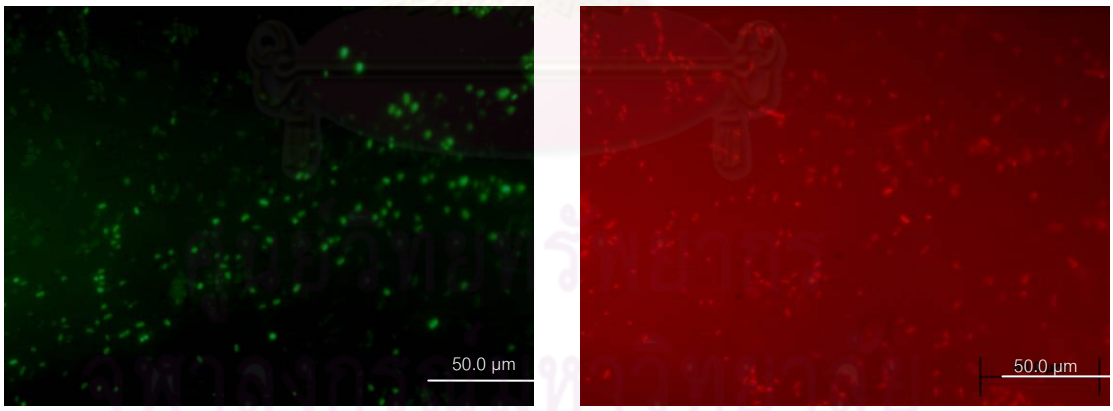

24 h

Figure 4.52 Fluorescence micrographs of Gram-negative *A. baylyi* strain GFJ2 attached on electrospun chitosan nanofibers that were prepared from chitosan hydrolyzed for various period of time, after the incubation time of 12 h.

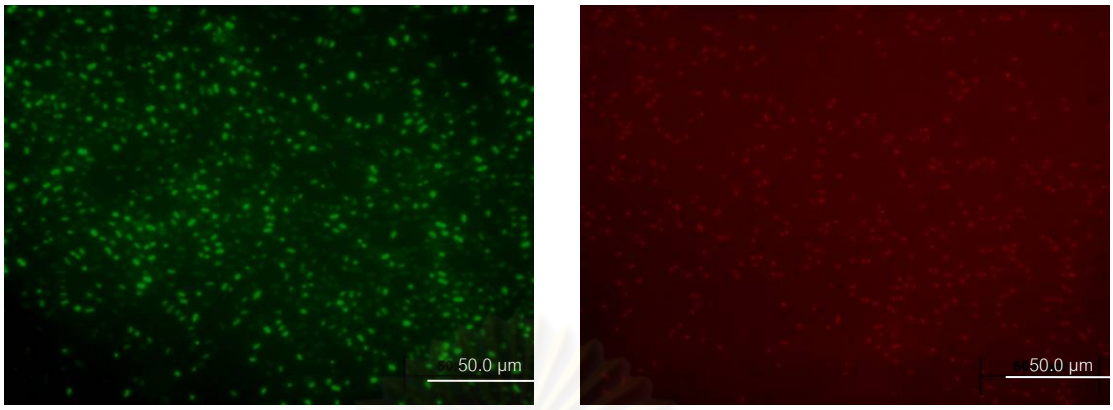

36 h

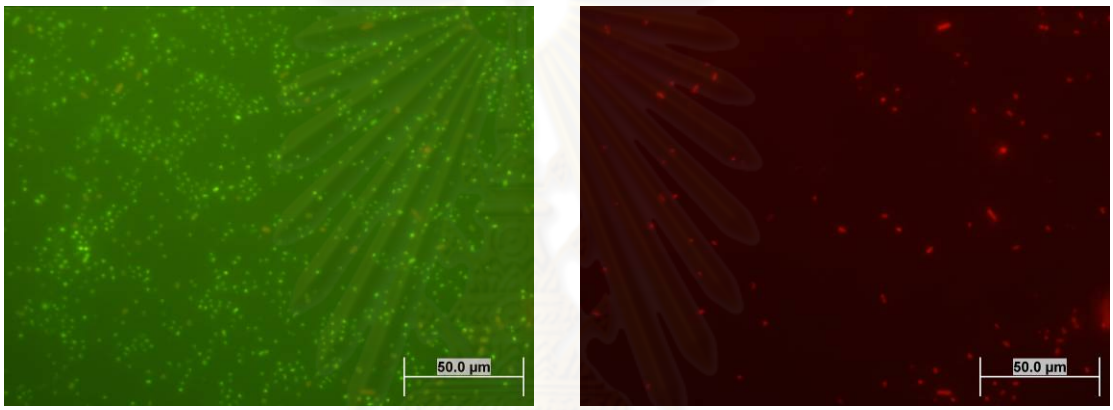

48 h

Figure 4.52 (continued)

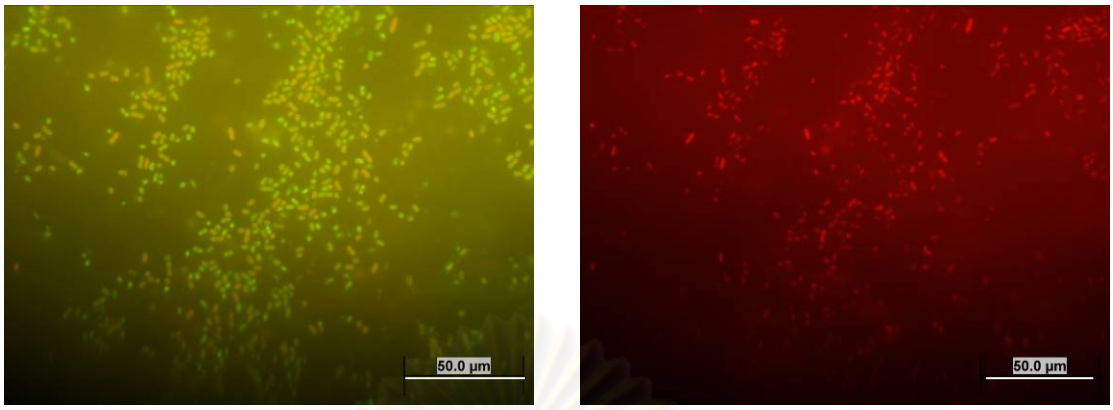

6 h

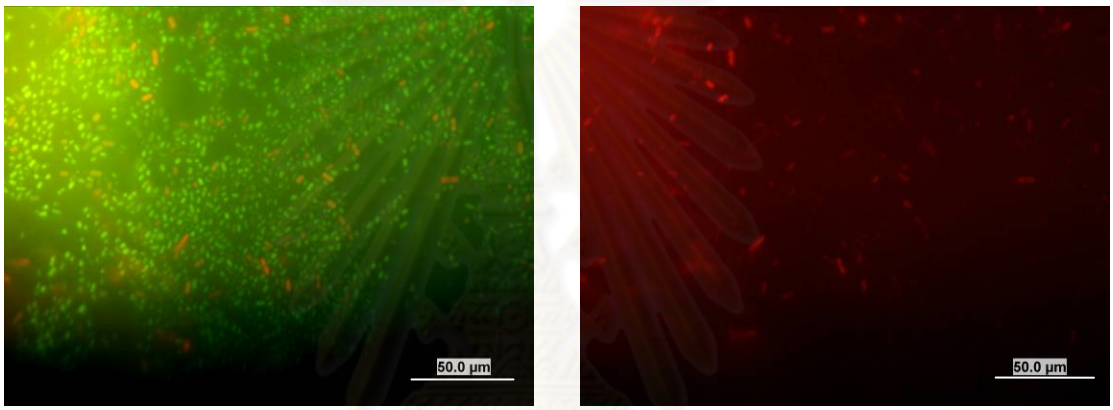

12 h

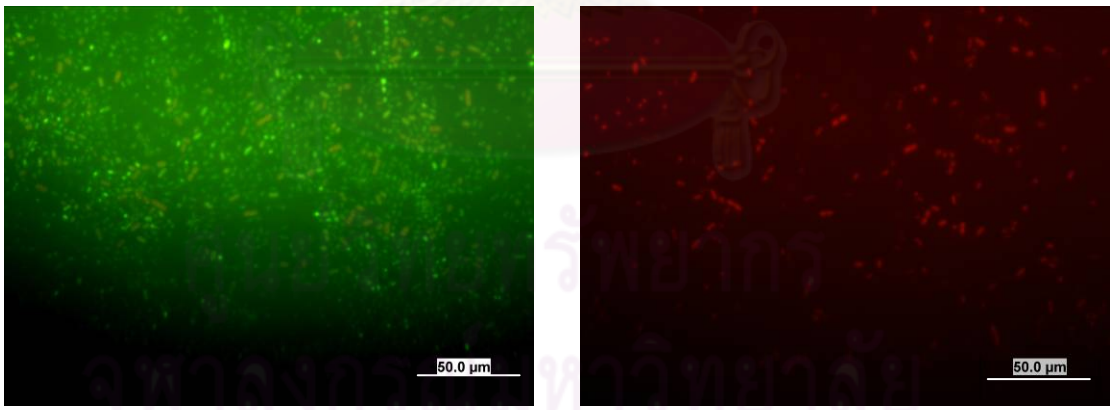

24 h

Figure 4.53 Fluorescence micrographs of Gram-positive *B. agri* No.13 attached on electrospun chitosan nanofibers that were prepared from chitosan hydrolyzed for various period of time, after the incubation time of 24 h.

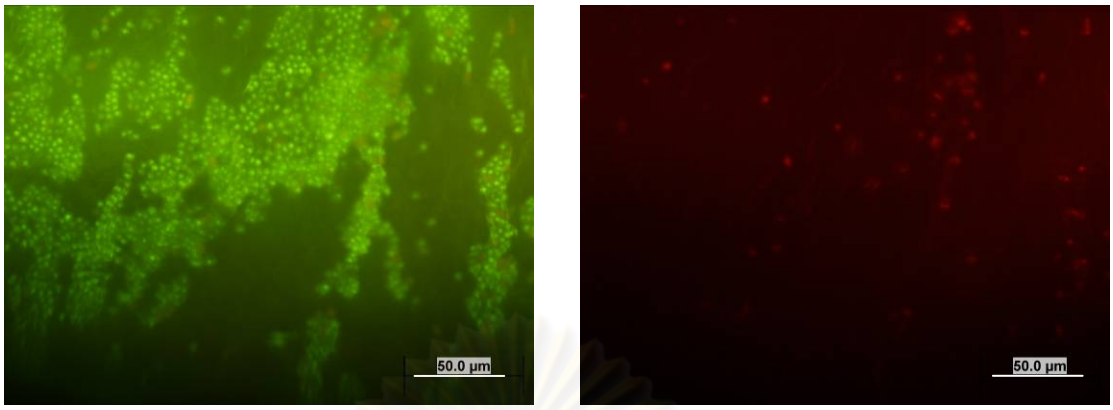

36 h

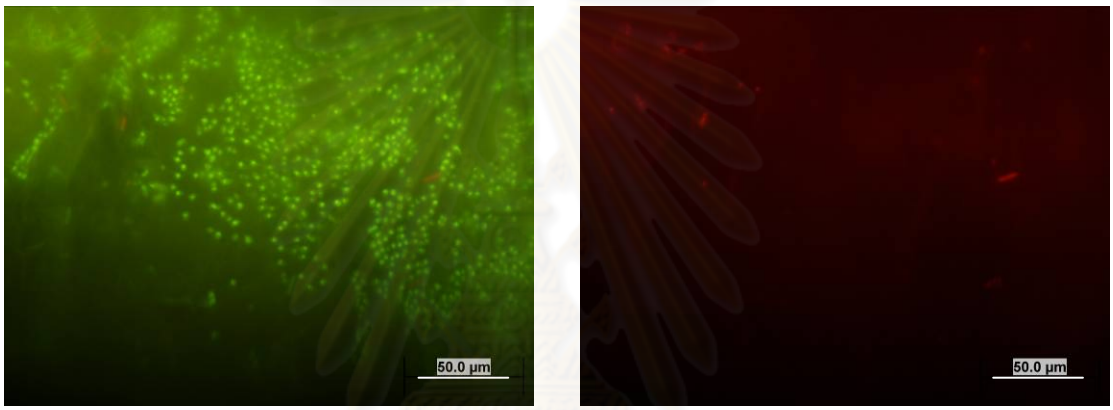

48 h

Figure 4.53 (continued)

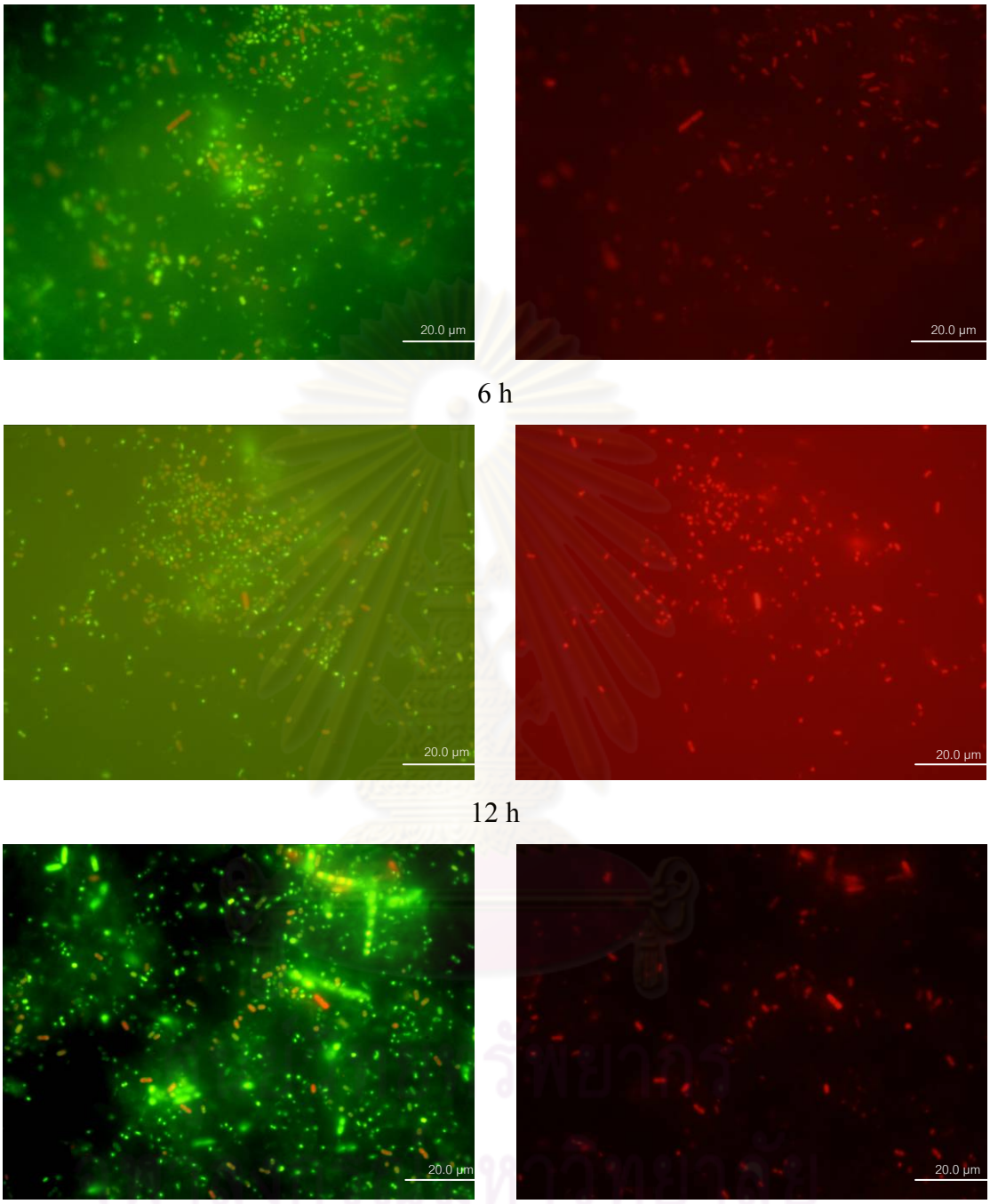

Figure 4.54 Fluorescence micrographs of Gram-negative *A. baylyi* strain GFJ2 attached on electrospun chitosan nanofibers that were prepared from chitosan hydrolyzed for various period of time, after the incubation time of 24 h.

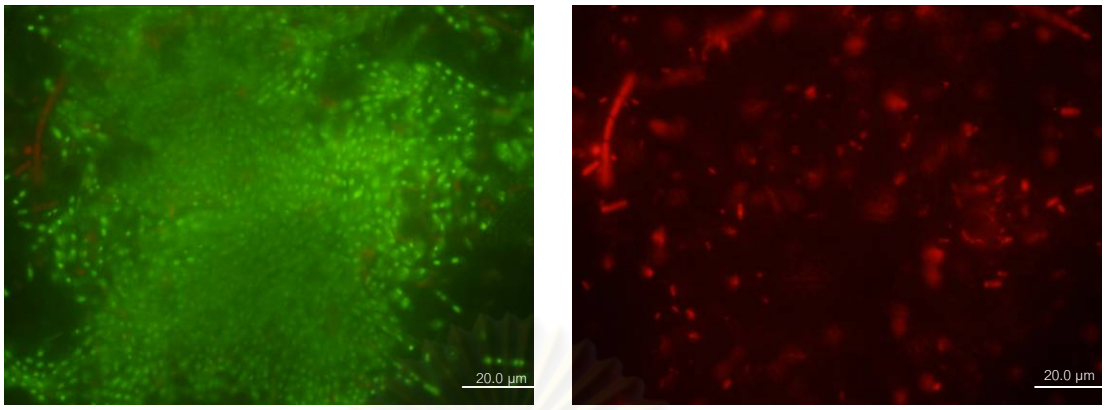

36 h

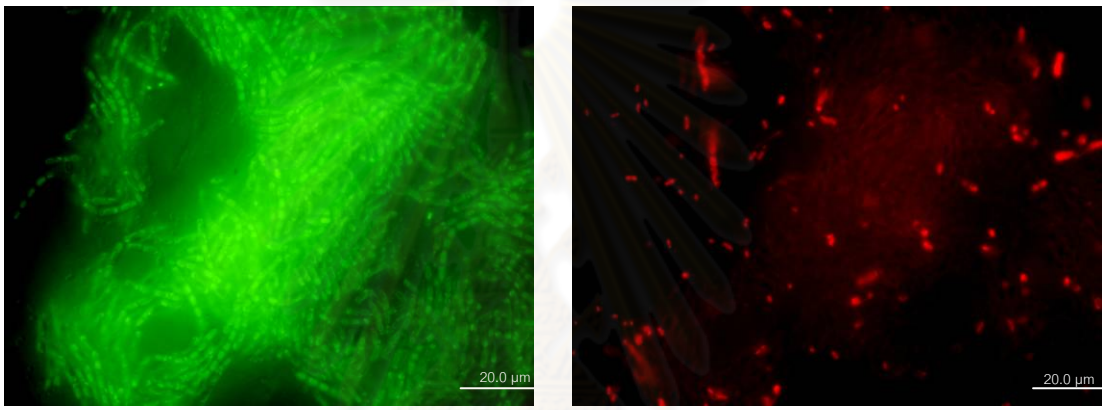

48 h

Figure 4.54 (continued)

4.5.2 Viability of bacterial cells attaching on hydrolyzed chitosan film

For the comparative study of the percentage of live cells attaching on chitosan films and nanofibers, the incubation time of 12 and 24 h were chosen. Similar trend for both of Gram-negative and Gram-positive bacteria were found. Higher percentage of viable cells were attaching on chitosan fibers than those on chitosan films. Moreover, both types of bacterial cells showed the increase in the percentage of live cells attaching on the surface of chitosan being hydrolyzed for prolonged period of time. The results are shown in Figure 4.55-4.56 for Gram-negative *Acinetobacter Baylyi* strain GFJ2 and in Figure 4.57 -4.58 for Gram-positive *Brevibacillus agri* strain 13.

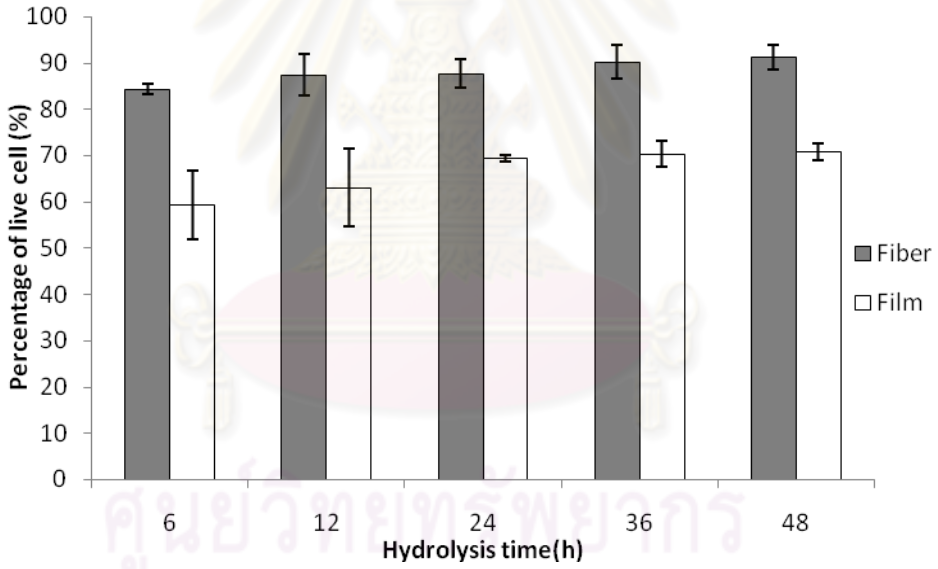

Figure 4.55 Percentage of live cells for Gram-positive *Brevibacillus agri* strain 13 attaching on electrospun chitosan fibers and chitosan films, prepared from chitosan being hydrolyzed for various periods of time, after the incubation time of 12 h.

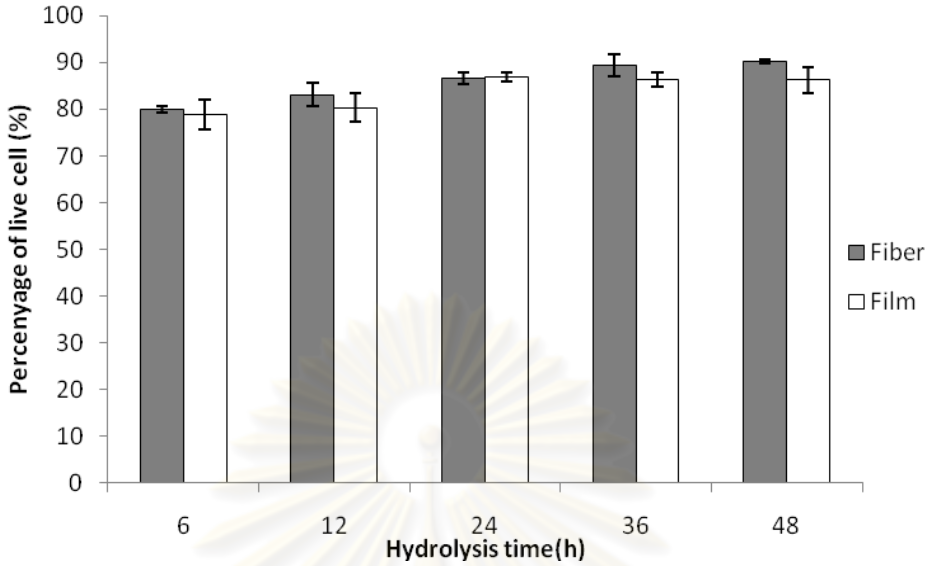

Figure 4.56 Percentage of live cells for Gram-positive *Brevibacillus agri* strain 13 attaching on electrospun chitosan fibers and chitosan films, prepared from chitosan being hydrolyzed for various periods of time, after the incubation time of 24 h.

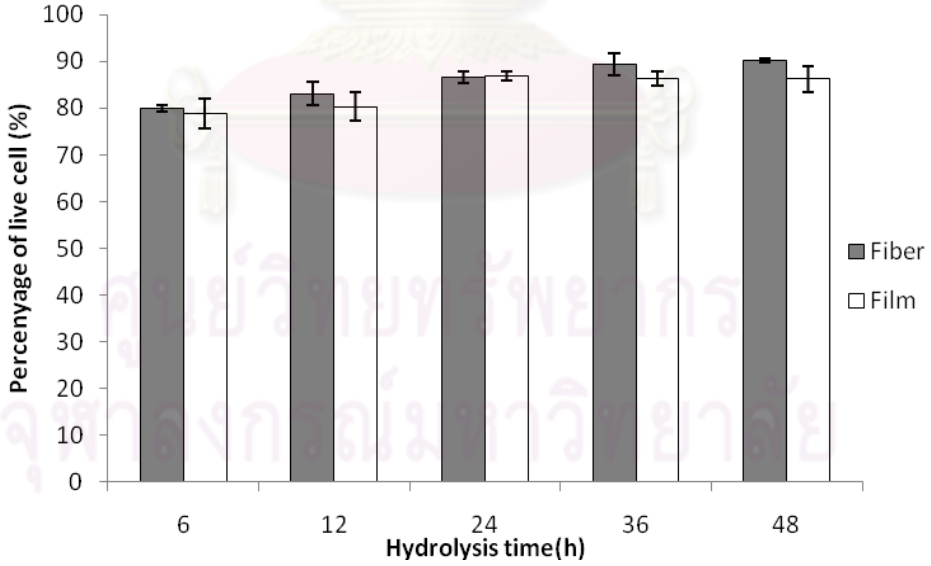

Figure 4.57 Percentage of live cells for Gram-negative *Acinetobacter baylyi* strain GFJ2 attaching on electrospun chitosan fibers and chitosan films, prepared from chitosan being hydrolyzed for various periods of time, after the incubation time of 12 h.

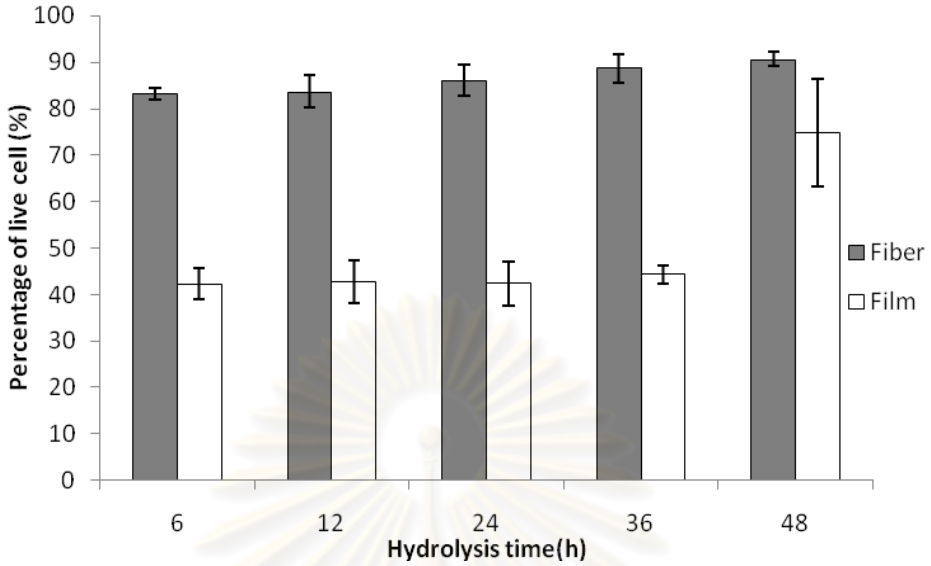

Figure 4.58 Percentage of live cell for Gram-negative *Acinetobacter baylyi* strain GFJ2 attaching on electrospun chitosan fibers and chitosan films, prepared from chitosan being hydrolyzed for various periods of time, after the incubation time of 24 h.

Although hydrolyzed chitosan nanofibers and films were prepared from the same solution, it was found that the chitosan in form of nanofibers resulted in higher cells viability than chitosan films. These results could be due to a significant role of a surface area-to-volume ratio. A sheet of randomly aligned fibers showed the surface morphology with grooves, ridges and highly porousity formed between the nanofibers that assisted cell attachment. The high porousity of the nanofibers also allowed cell migration, nutrient flow and oxygen transfer to immobilized microorganisms thus enhancing cell supporting capacity and consequently thier viability. Availability of oxygen is one of the most important parameters. The nanofibers which was more porous than the films allowed oxygen diffusion from the bottom of the sheet though the nanofibers sheet to the bacterial cells attaching on top of the sheet, in addition to the direct diffusion to the cells. Oxygen has transferred into chitosan support via diffusion due to difference in oxygen concentration in direction perpendicular to the chitosan sheet. It should be noted that the observation by the fluorescence microscope revealed multi-layers of cells on top of the chitosan sheet. For the cell attachment on chitosan films, most of the dead cells were observed in the bottom layer close to

chitosan. It is possible that low oxygen concentration of the cells stack caused cells to die. Furthermore, negative charges of cells wall interacted with amino groups from chitosan such that it resulted in damages in outer membrane of the cells, which changed the hydrophilicity and charge density of the cell surface. The fluorescence micrographs of live cells and dead cells on chitosan fibers and chitosan films prepared at various conditions are shown in Figure 4.59-4.78.

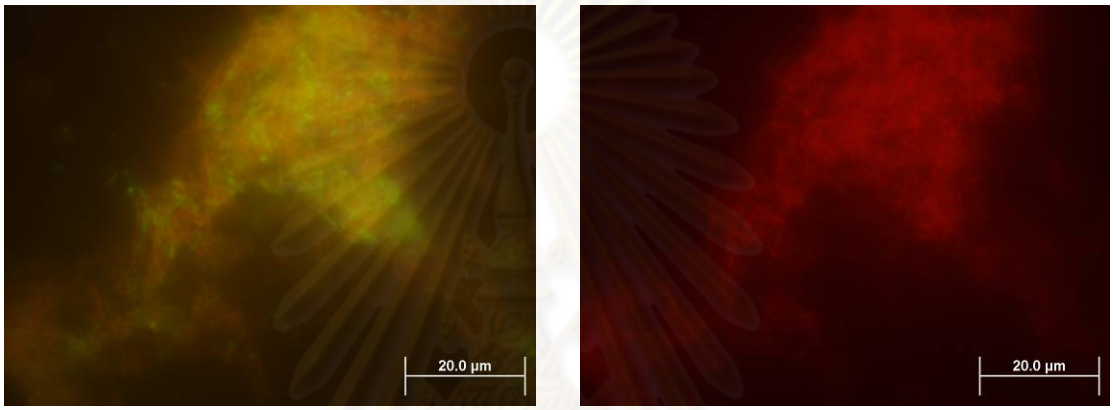

Film

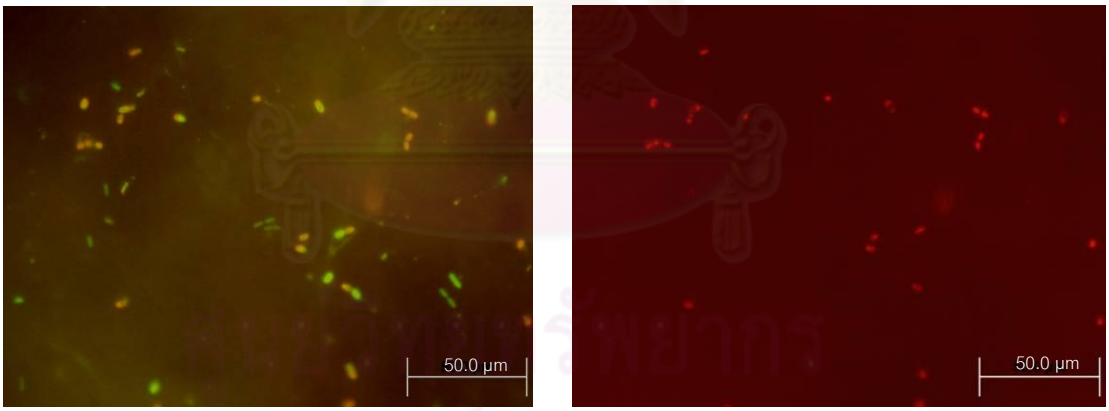

Fiber

Figure 4.59 Fluorescence micrographs of Gram-positive *B. agri* No.13 attaching on electrospun chitosan fibers and chitosan films that were prepared from chitosan hydrolyzed for 6 h, after 12 h of incubation.

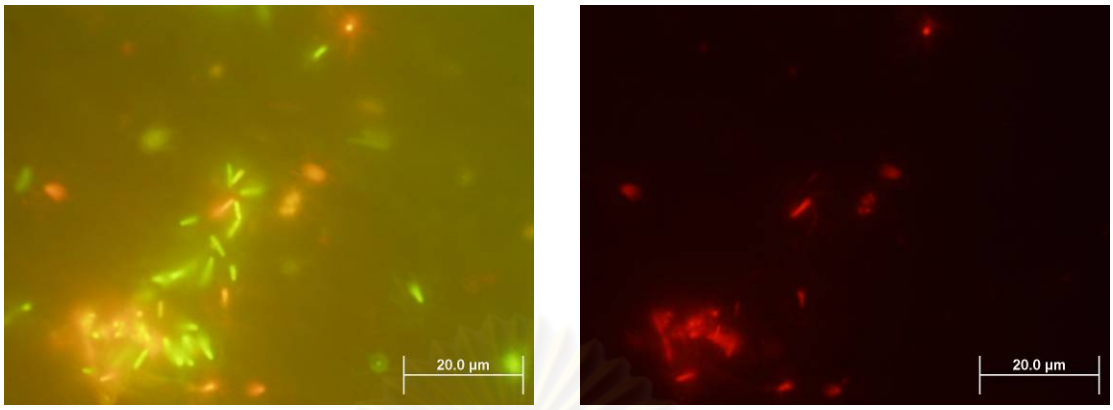

Film

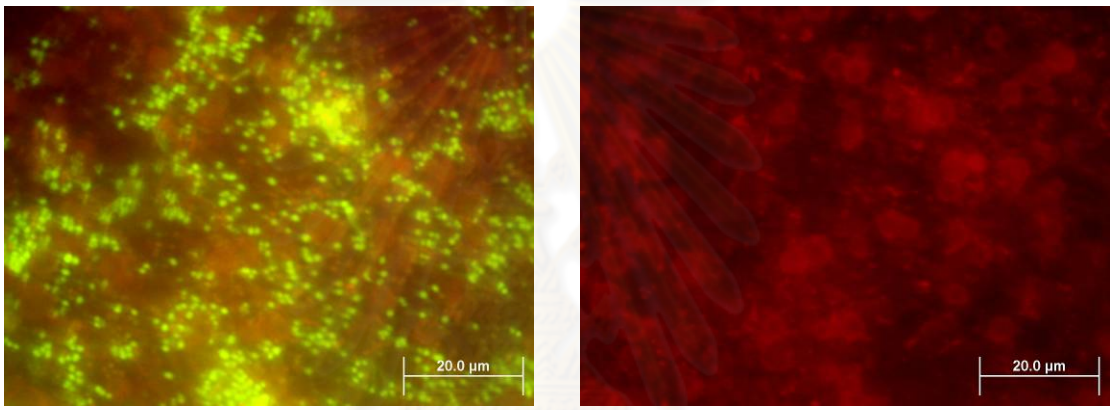

Fiber

Figure 4.60 Fluorescence micrographs of Gram-positive *B. agri* No.13 attaching on electrospun chitosan fibers and chitosan films that were prepared from chitosan hydrolyzed for 12 h, after 12 h of incubation.

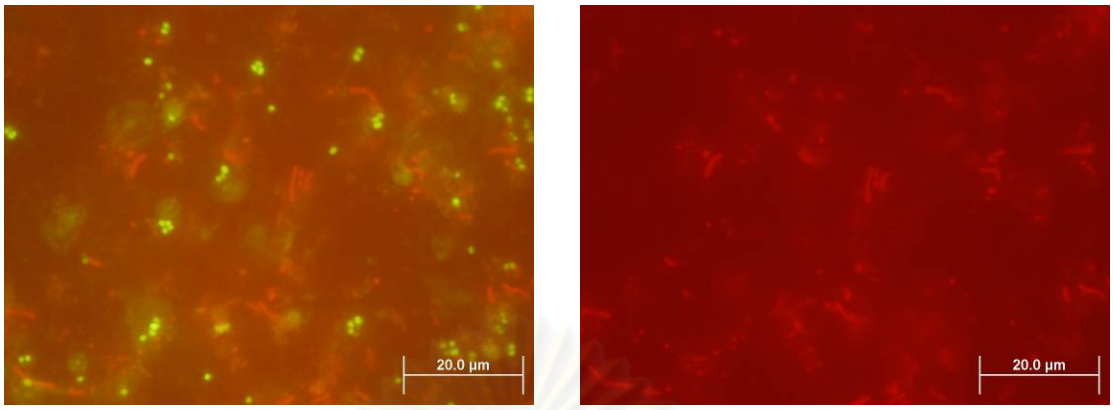

Film

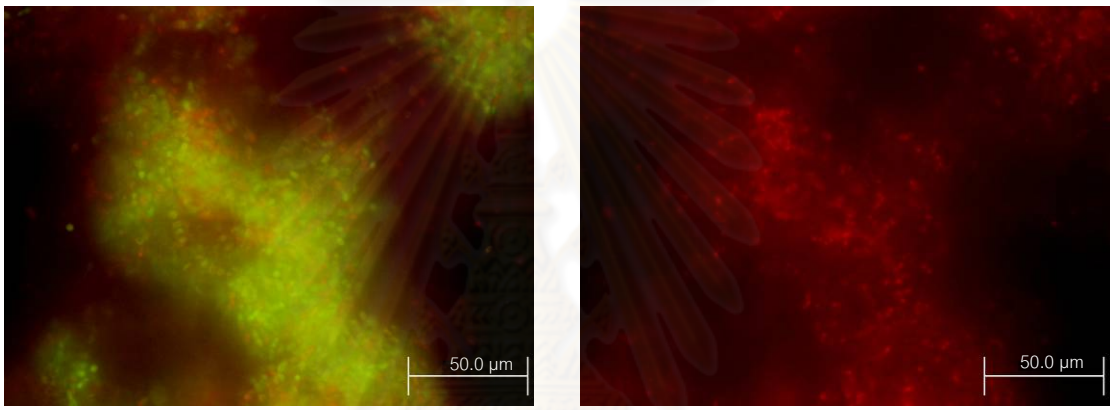

Fiber

Figure 4.61 Fluorescence micrographs of Gram-positive *B. agri* No.13 attaching on electrospun chitosan fibers and chitosan films that were prepared from chitosan hydrolyzed for 24 h, after 12 h of incubation.

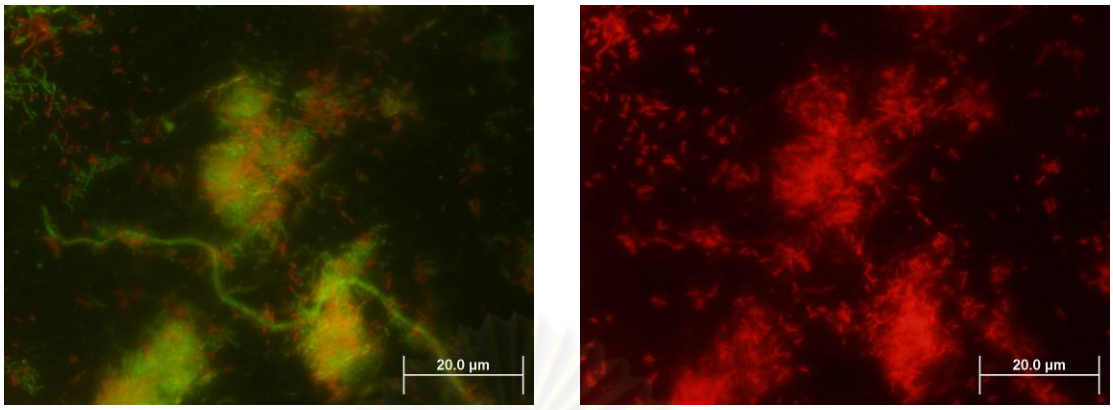

Film

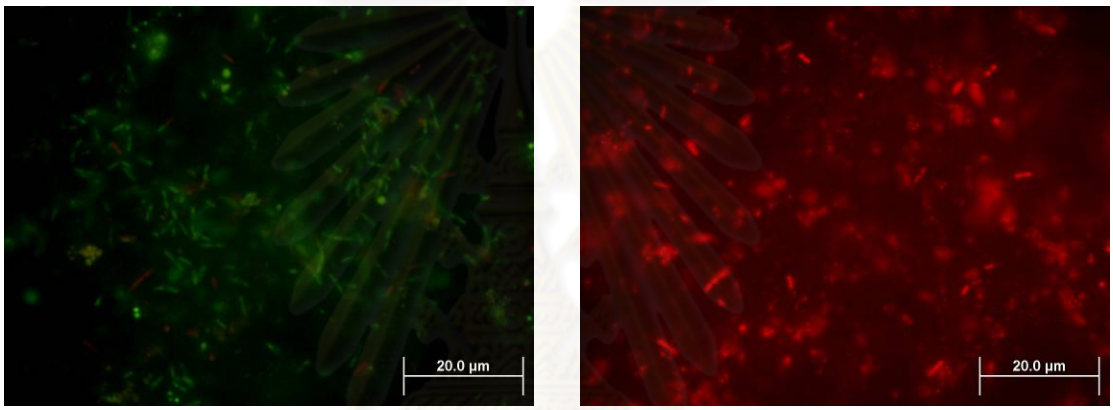

Fiber

Figure 4.62 Fluorescence micrographs of Gram-positive *B. agri* No.13 attaching on electrospun chitosan fibers and chitosan films that were prepared from chitosan hydrolyzed for 36 h, after 12 h of incubation.

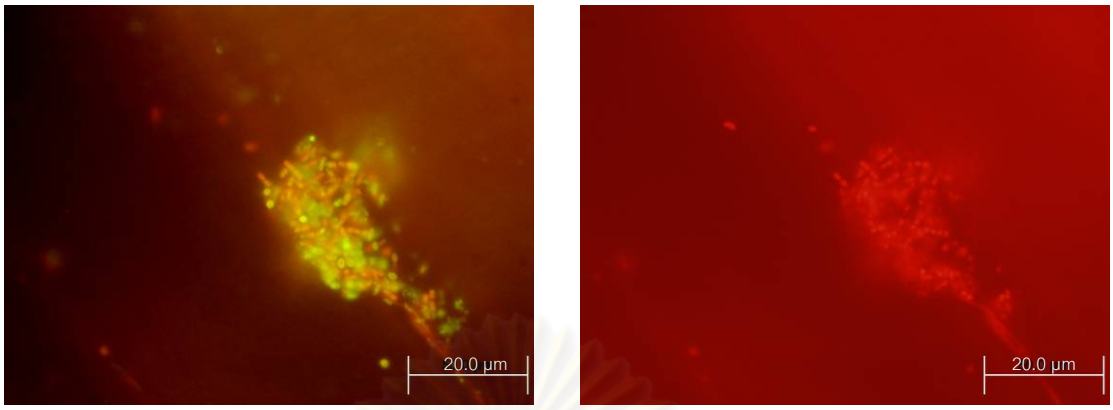

Film

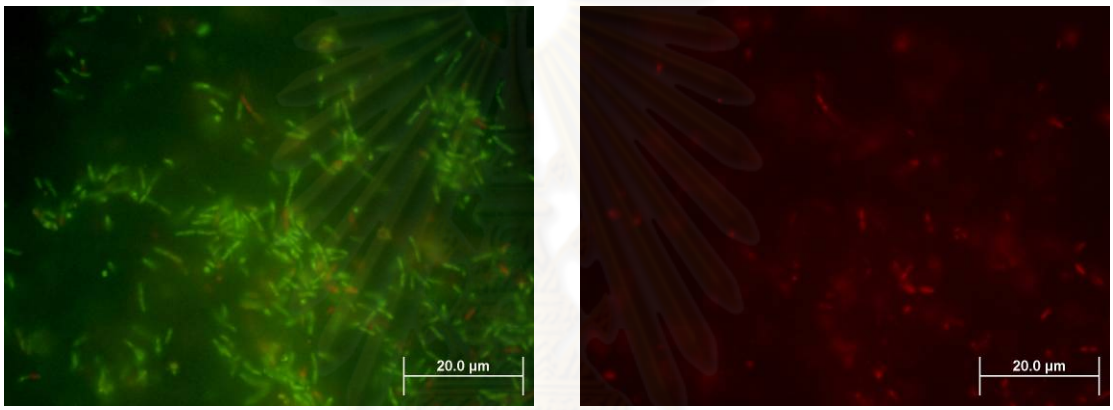

Fiber

Figure 4.63 Fluorescence micrographs of Gram-positive *B. agri* No.13 attaching on electrospun chitosan fibers and chitosan films that were prepared from chitosan hydrolyzed for 48 h, after 12 h of incubation.

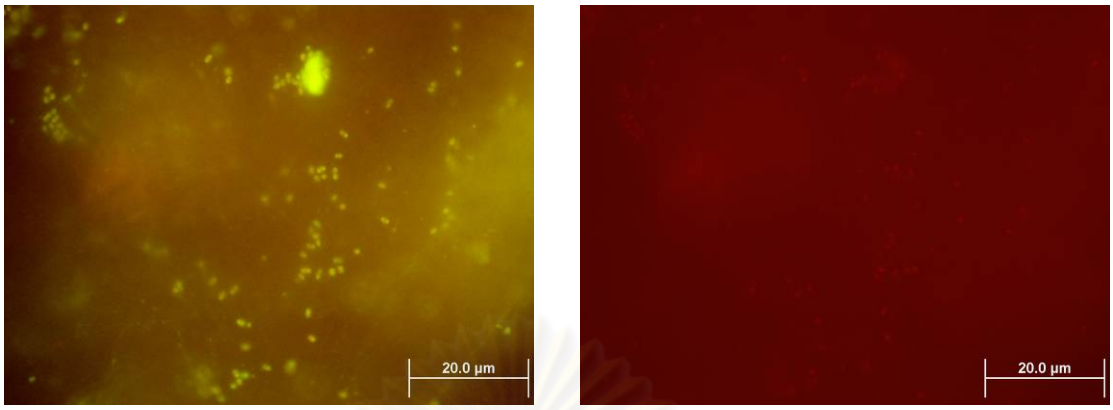

Film

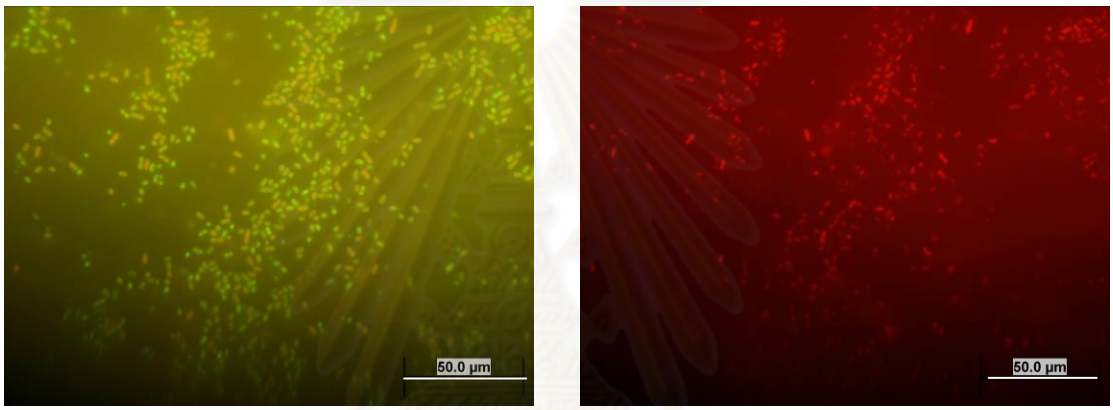

Fiber

Figure 4.64 Fluorescence micrographs of Gram-negative *A. baylyi* strain GFJ2 attaching on electrospun chitosan fibers and chitosan films that were prepared from chitosan hydrolyzed for 6 h, after 12 h of incubation.

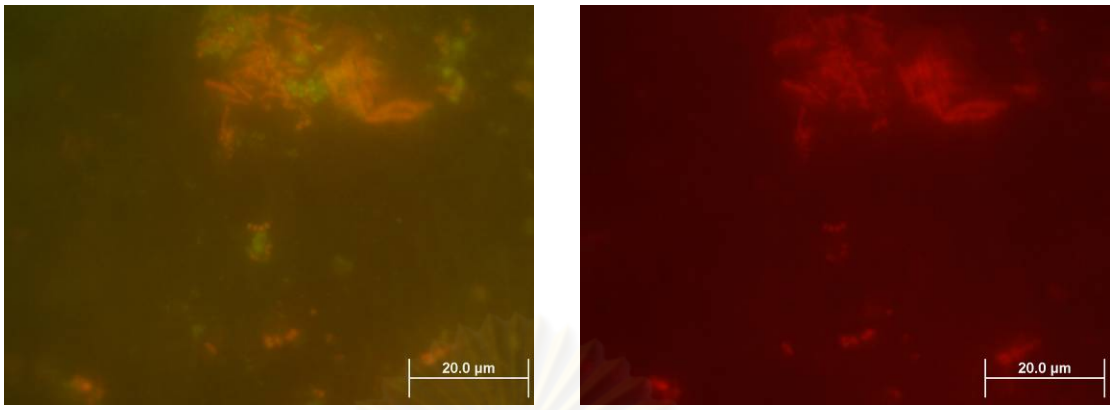

Film

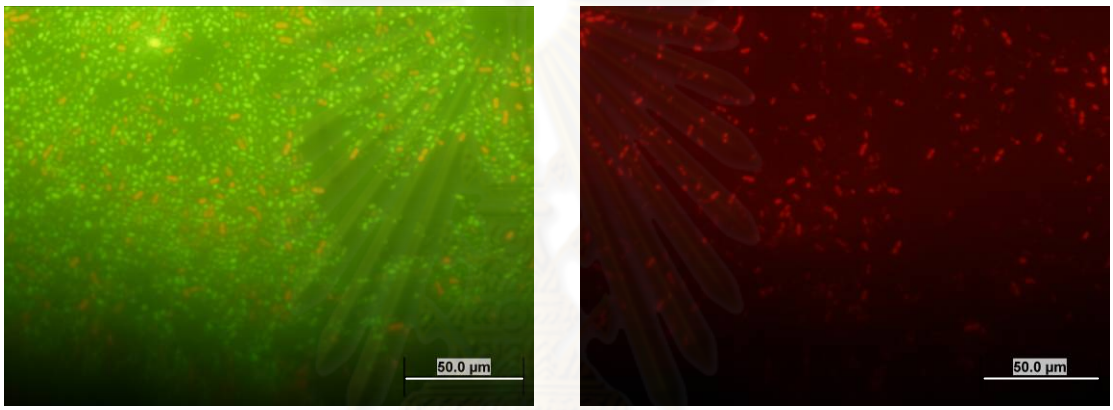

Fiber

Figure 4.65 Fluorescence micrographs of Gram-negative *A. baylyi* strain GFJ2 attaching on electrospun chitosan fibers and chitosan films that were prepared from chitosan hydrolyzed for 12 h, after 12 h of incubation.

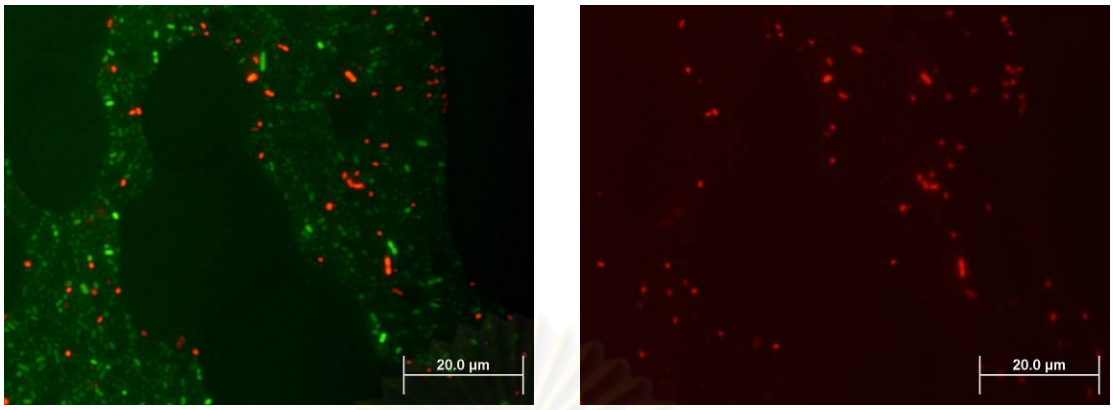

Film

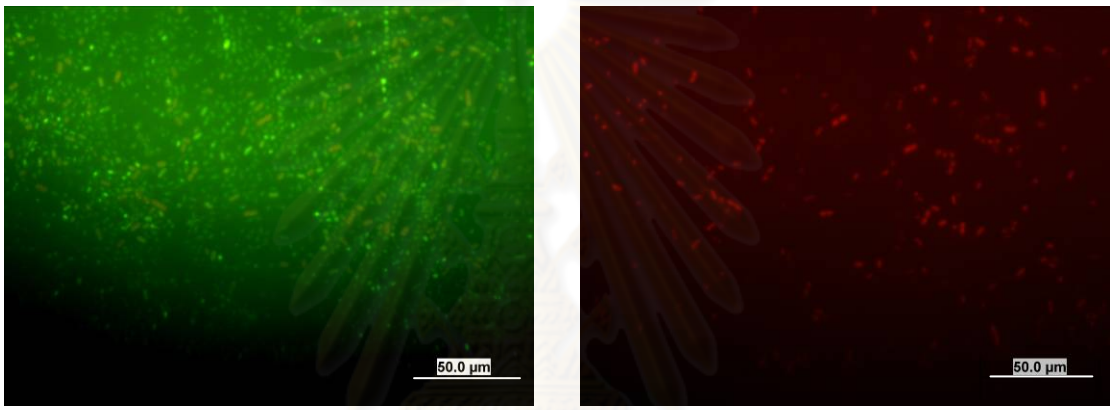

Fiber

Figure 4.66 Fluorescence micrographs of Gram-negative *A. baylyi* strain GFJ2 attaching on electrospun chitosan fibers and chitosan films that were prepared from chitosan hydrolyzed for 24 h, after 12 h of incubation.

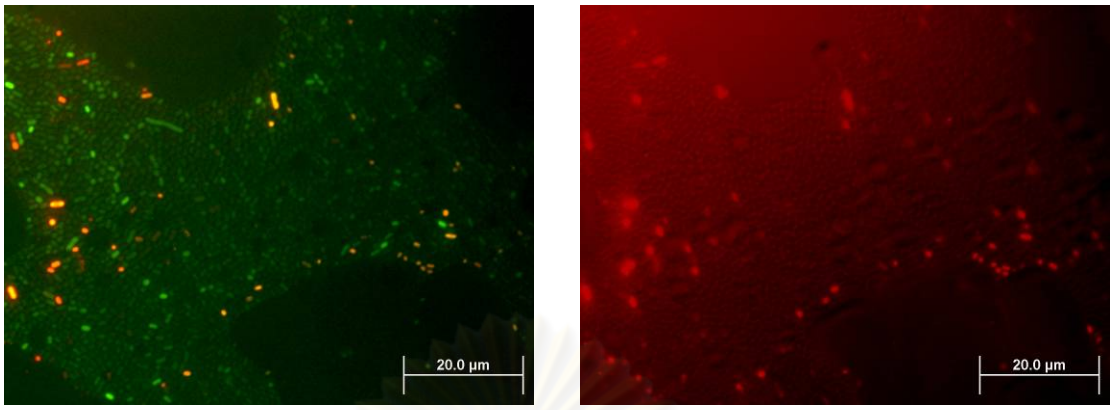

Film

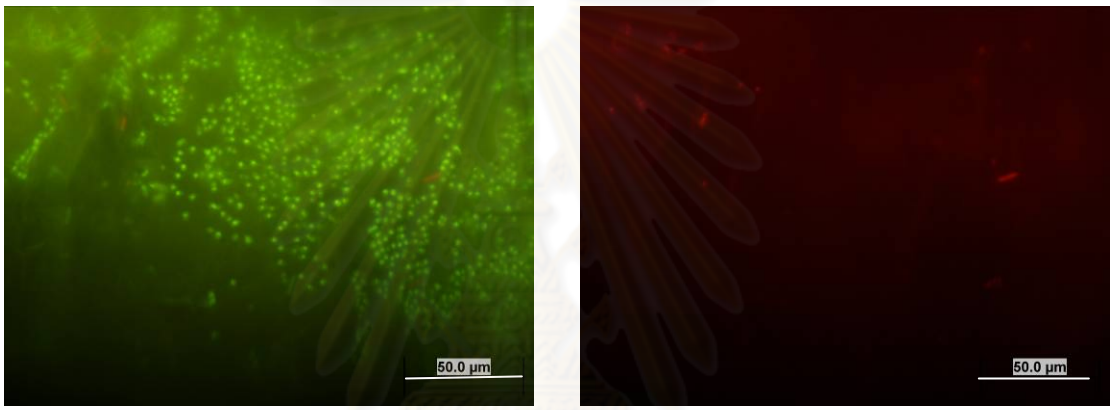

Fiber

Figure 4.67 Fluorescence micrographs of Gram-negative *A. baylyi* strain GFJ2 attaching on electrospun chitosan fibers and chitosan films that were prepared from chitosan hydrolyzed for 36 h, after 12 h of incubation.

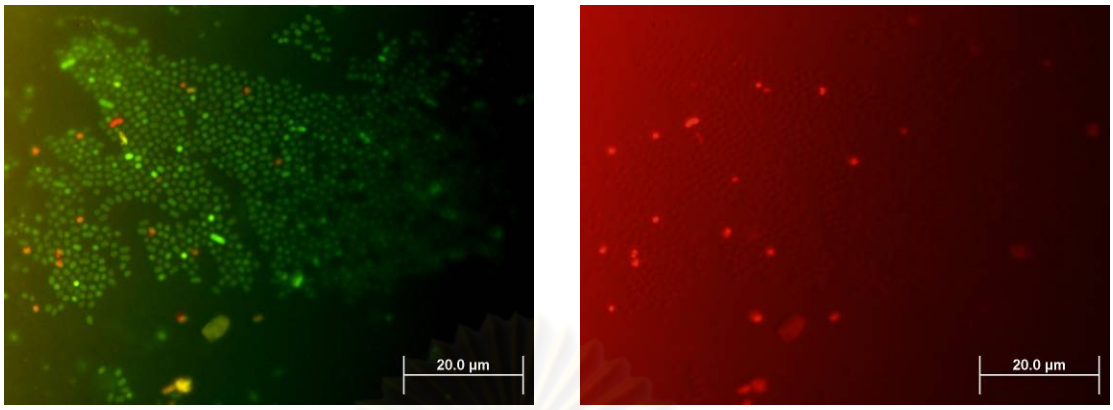

Film

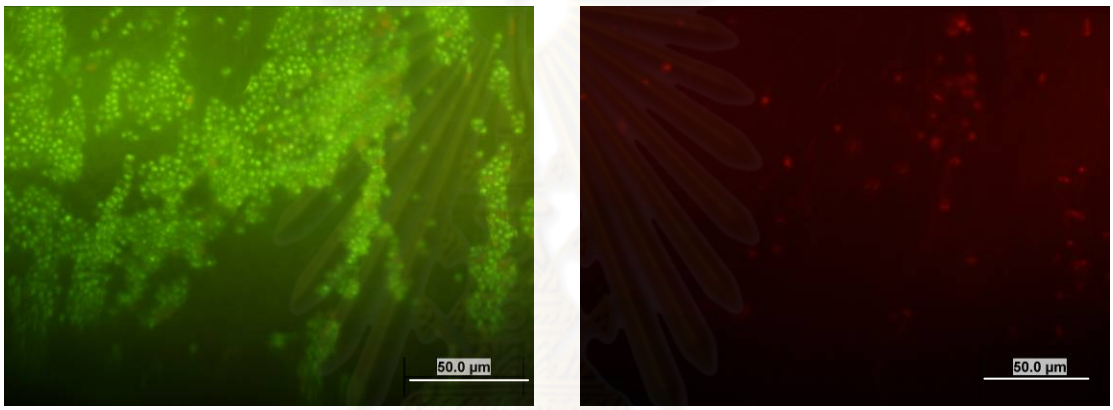

Fiber

Figure 4.68 Fluorescence micrographs of Gram-negative *A. baylyi* strain GFJ2 attaching on electrospun chitosan fibers and chitosan films that were prepared from chitosan hydrolyzed for 48 h, after 12 h of incubation.

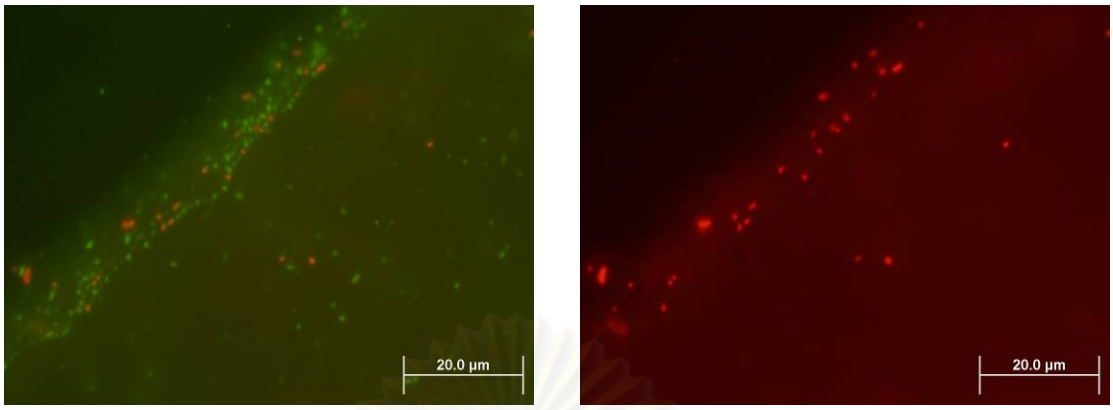

Film

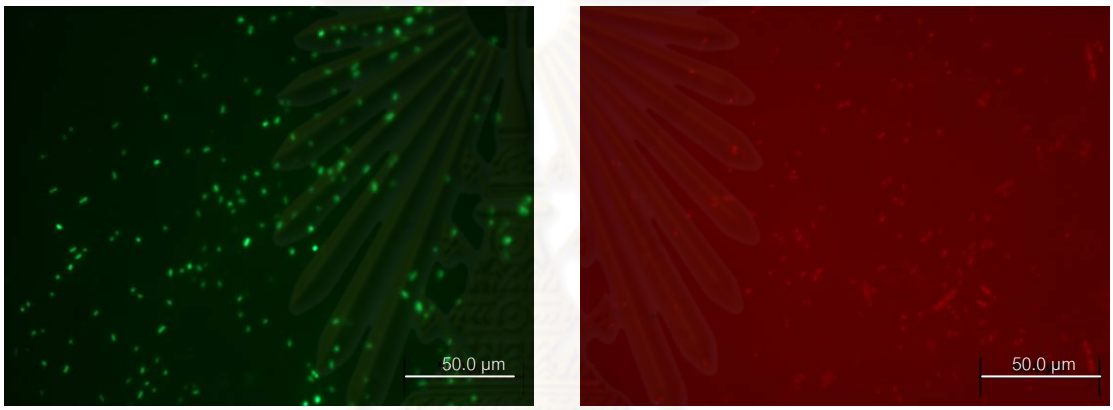

Fiber

Figure 4.69 Fluorescence micrographs of Gram-positive *B. agri* No.13 attaching on electrospun chitosan fibers and chitosan films that were prepared from chitosan hydrolyzed for 6 h, after 24 h of incubation.

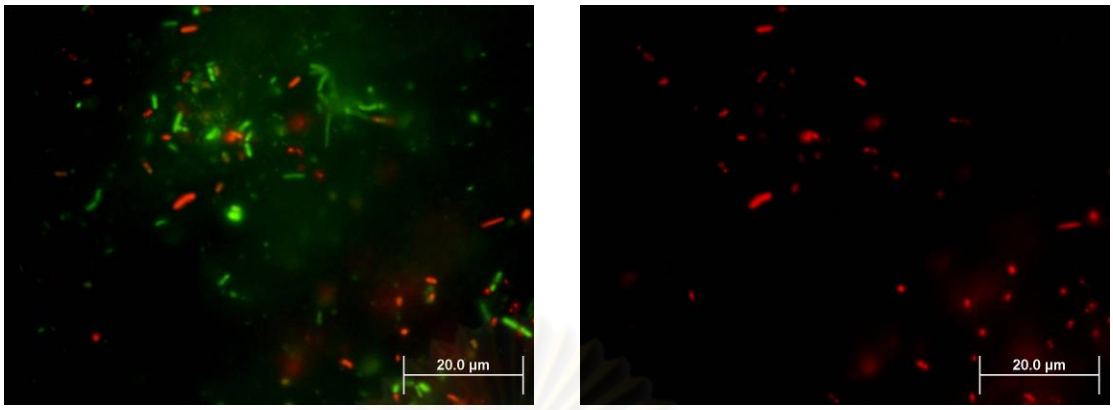

Film

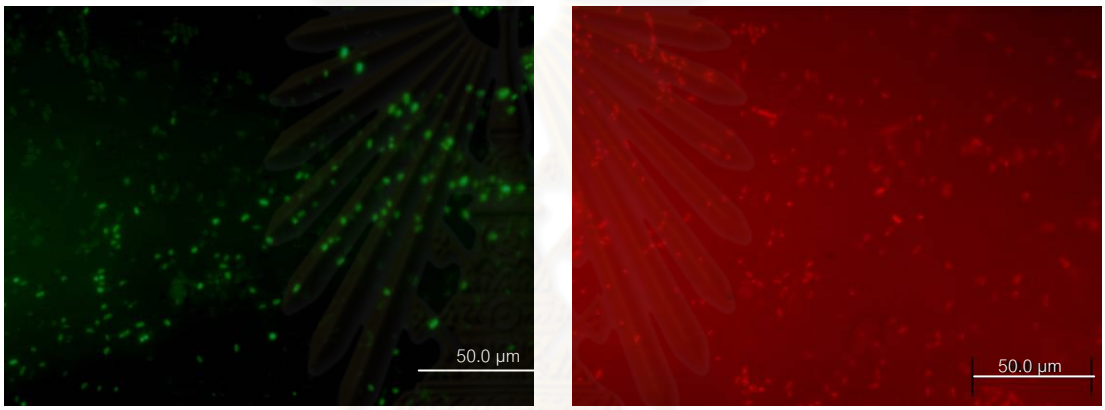

Fiber

Figure 4.70 Fluorescence micrographs of Gram-positive *B. agri* No.13 attaching on electrospun chitosan fibers and chitosan films that were prepared from chitosan hydrolyzed for 12 h, after 24 h of incubation.

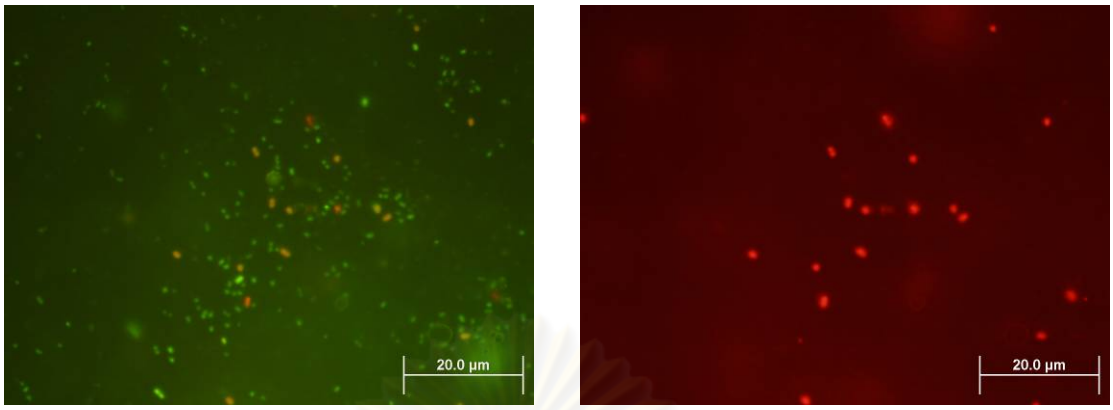

Film

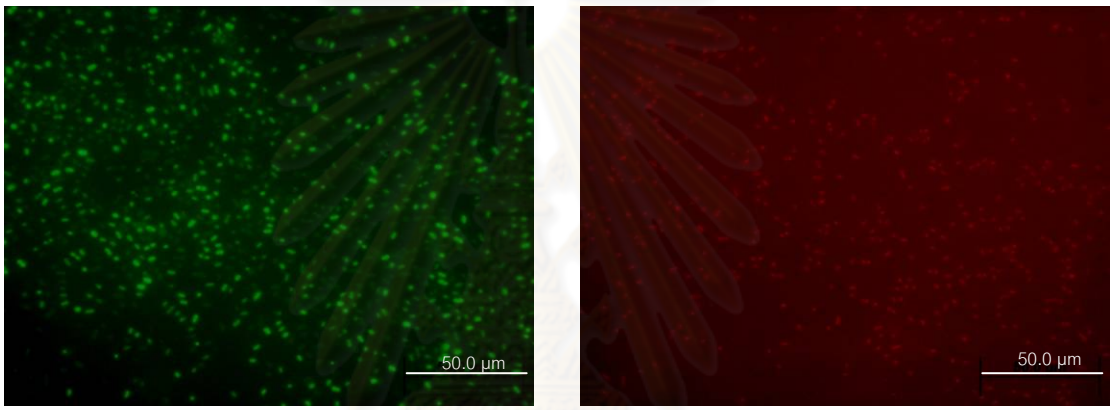

Fiber

Figure 4.71 Fluorescence micrographs of Gram-positive *B. agri* No.13 attaching on electrospun chitosan fibers and chitosan films that were prepared from chitosan hydrolyzed for 24 h, after 24 h of incubation.

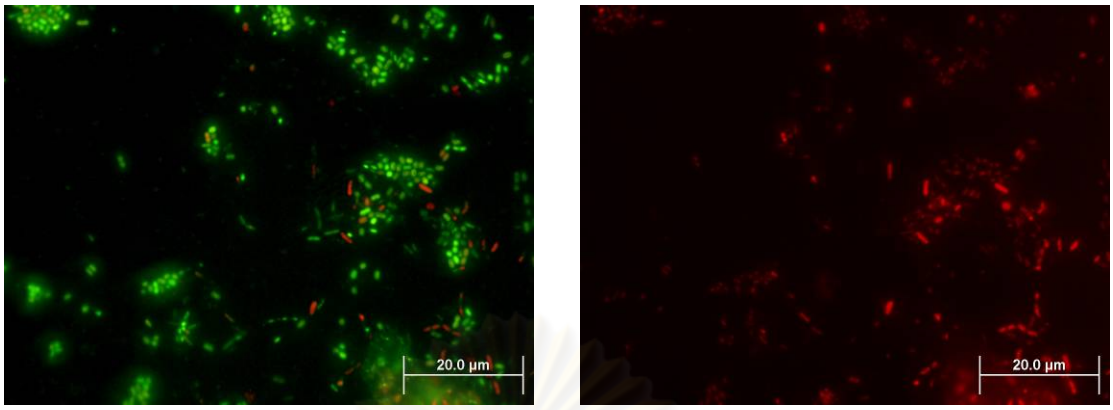

Film

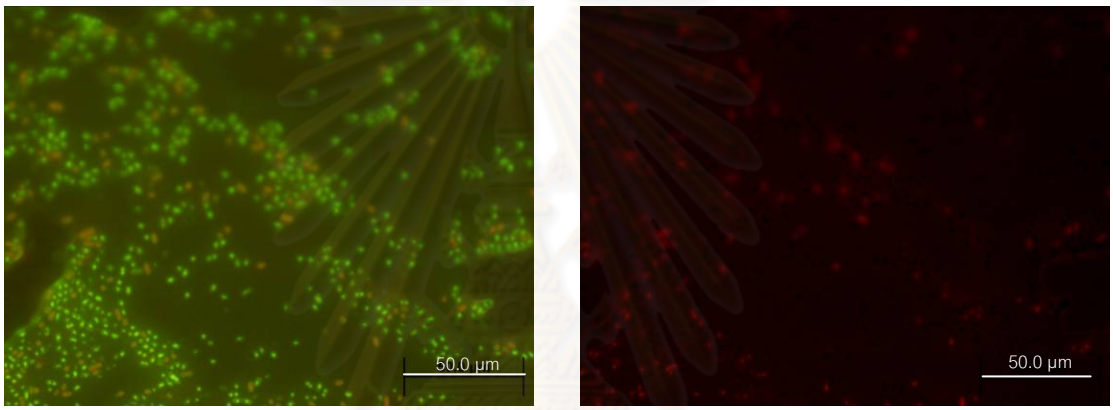

Fiber

Figure 4.72 Fluorescence micrographs of Gram-positive *B. agri* No.13 attaching on electrospun chitosan fibers and chitosan films that were prepared from chitosan hydrolyzed for 36 h, after 24 h of incubation.

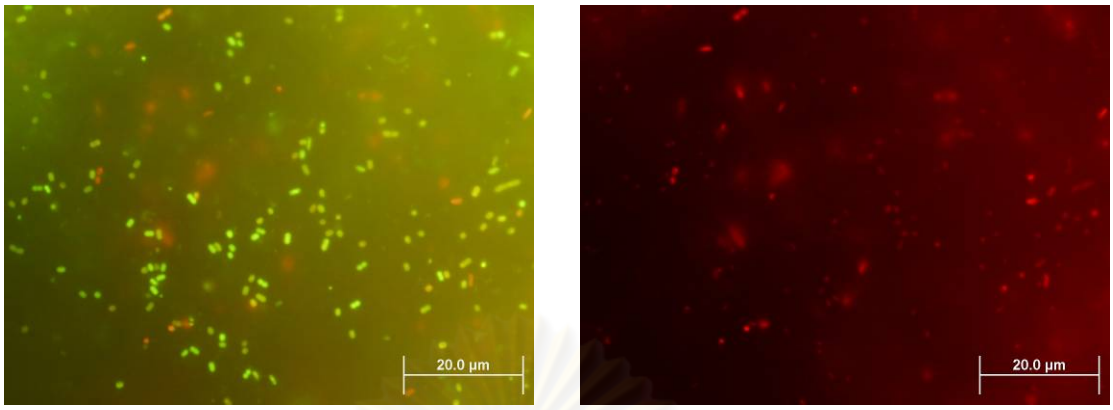

Film

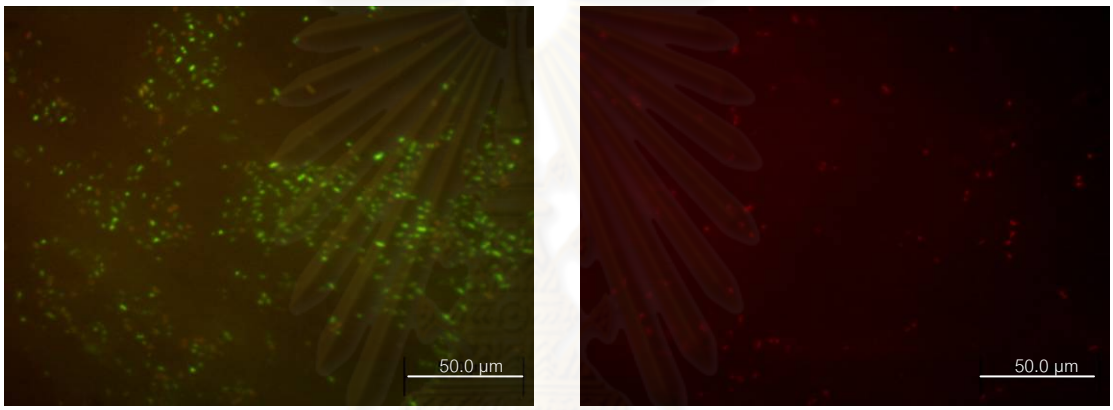

Fiber

Figure 4.73 Fluorescence micrographs of Gram-positive *B. agri* No.13 attaching on electrospun chitosan fibers and chitosan films that were prepared from chitosan hydrolyzed for 48 h, after 24 h of incubation.

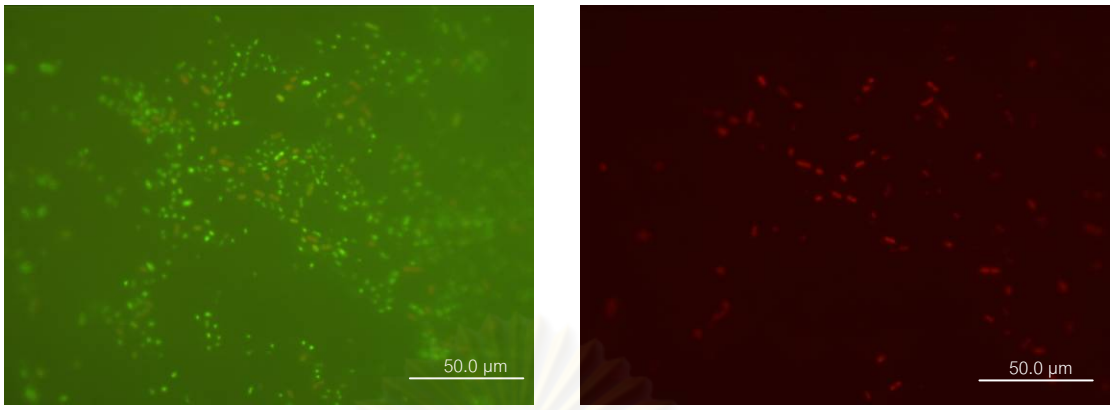

Film

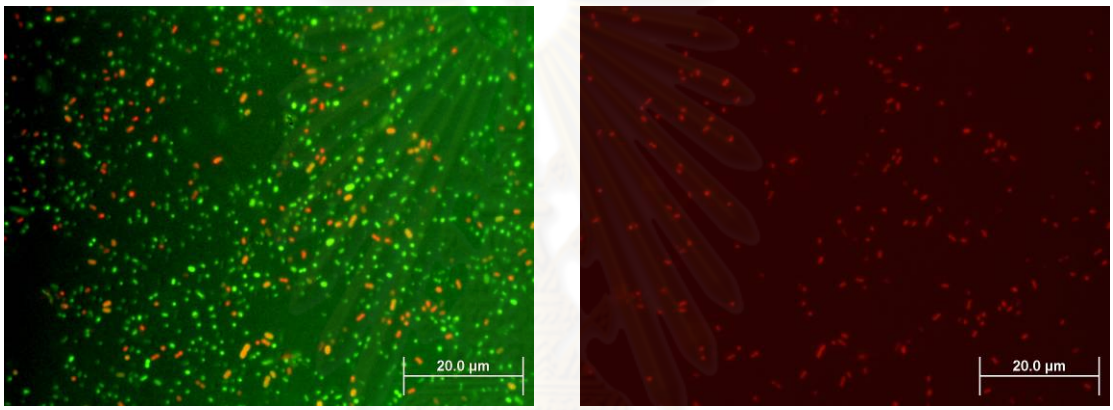

Fiber

Figure 4.74 Fluorescence micrographs of Gram-negative *A. baylyi* strain GFJ2 attaching on electrospun chitosan fibers and chitosan films that were prepared from chitosan hydrolyzed for 6 h, after 24 h of incubation.

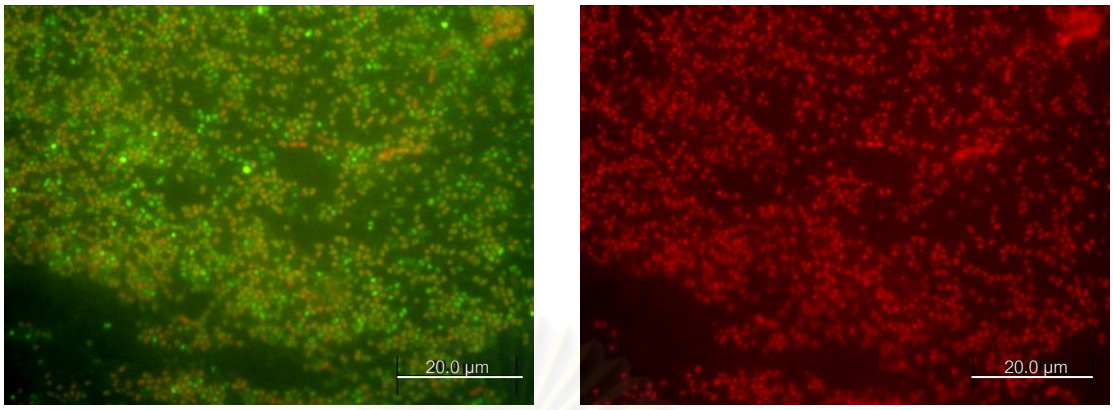

Film

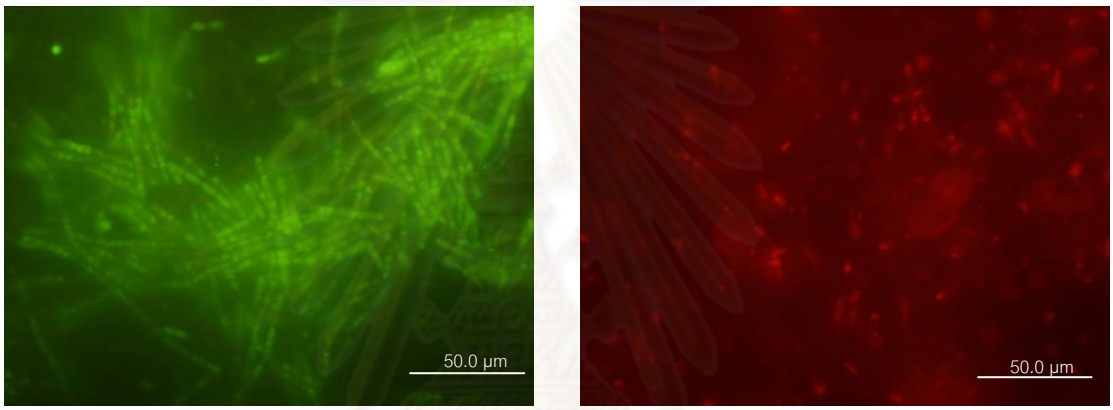

Fiber

Figure 4.75 Fluorescence micrographs of Gram-negative *A. baylyi* strain GFJ2 attaching on electrospun chitosan fibers and chitosan films that were prepared from chitosan hydrolyzed for 12 h, after 24 h of incubation.

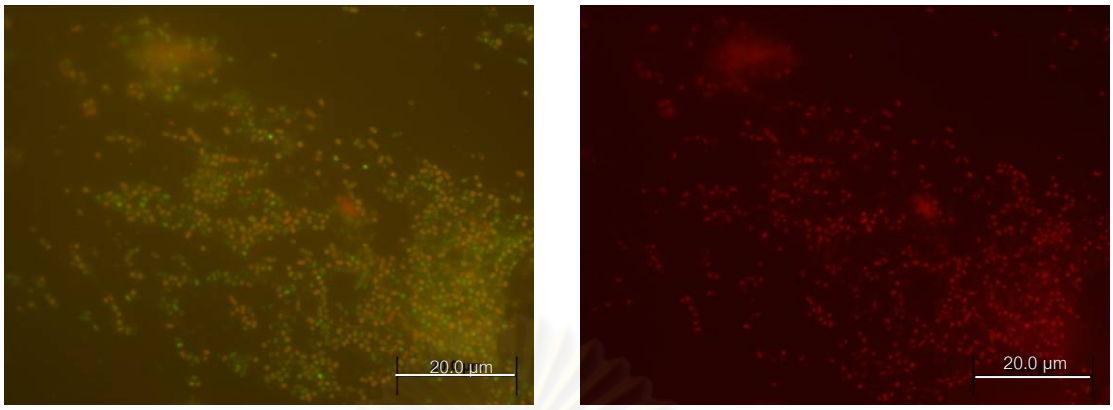

Film

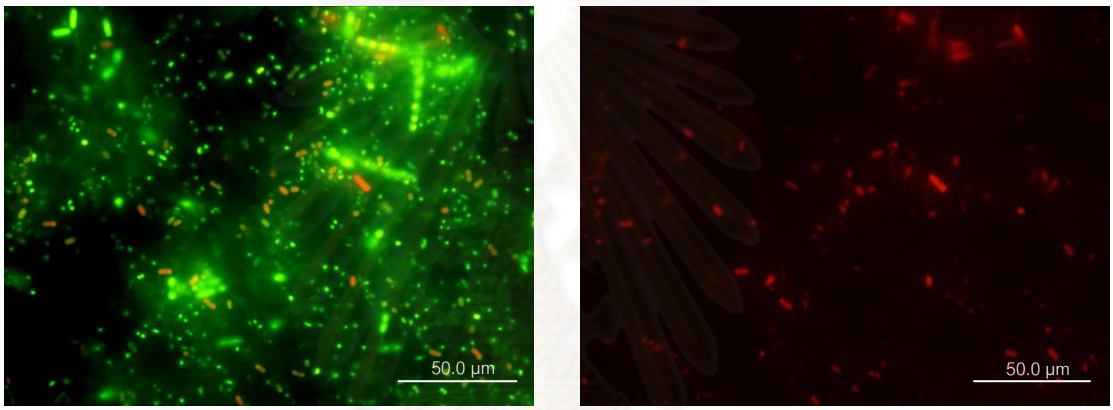

Fiber

Figure 4.76 Fluorescence micrographs of Gram-negative *A. baylyi* strain GFJ2 attaching on electrospun chitosan fibers and chitosan films that were prepared from chitosan hydrolyzed for 24 h, after 24 h of incubation.

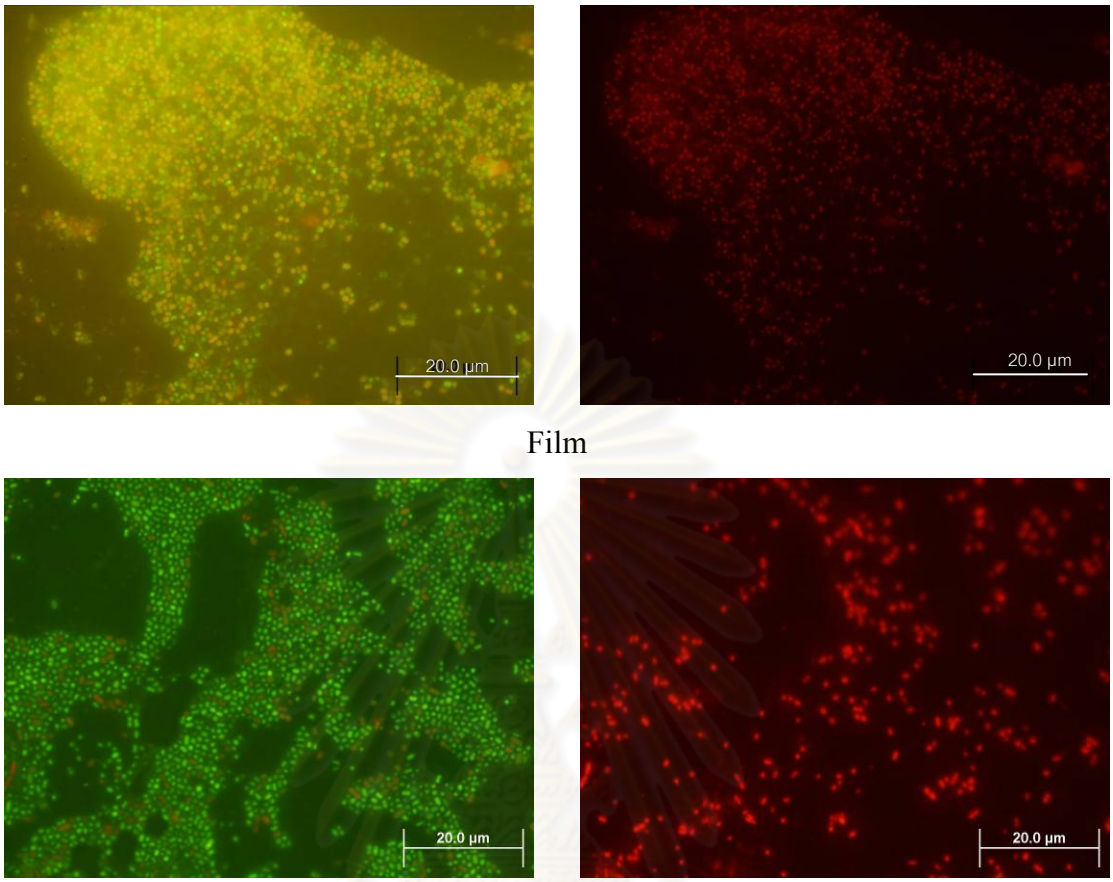

Figure 4.77 Fluorescence micrographs of Gram-negative *A. baylyi* strain GFJ2 attaching on electrospun chitosan fibers and chitosan films that were prepared from chitosan hydrolyzed for 36 h, after 24 h of incubation.

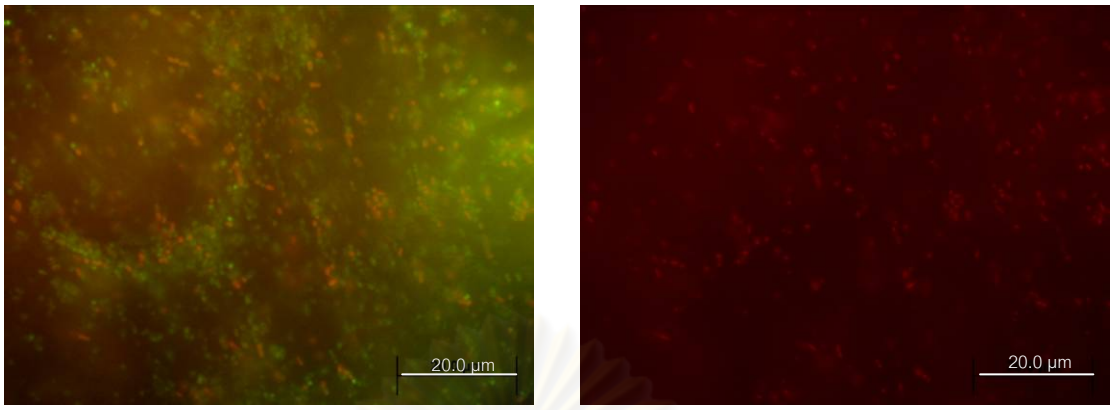

Film

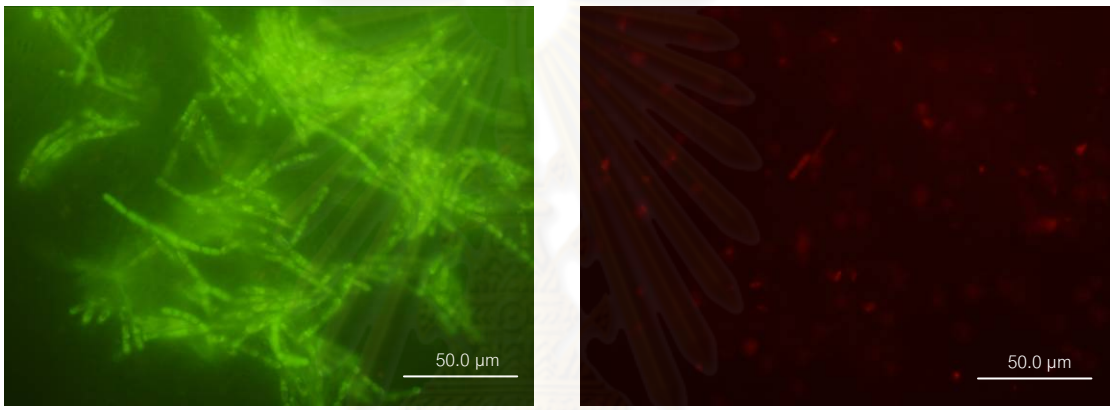

Fiber

Figure 4.78 Fluorescence micrographs of Gram-negative *A. baylyi* strain GFJ2 attaching on electrospun chitosan fibers and chitosan films that were prepared from chitosan hydrolyzed for 48 h, after 24 h of incubation.

4.5.3 Viability of bacterial cells attaching on chitosan/PVA nanofibers

In the study of cells viability on chitosan/PVA nanofibers fabricated by electrospinning, the chitosan with molecular weight 760 kDa were chosen. The cell attachment was investigated after 12 and 24 h of incubation for both Gram-negative and Gram-positive bacteria. The similar trend for both Gram-negative *Acinetobacter baylyi* strain GFJ2 and Gram-positive *Brevibacillus agri* strain 13 was observe, as shown in Figure 4.79 -4.82.

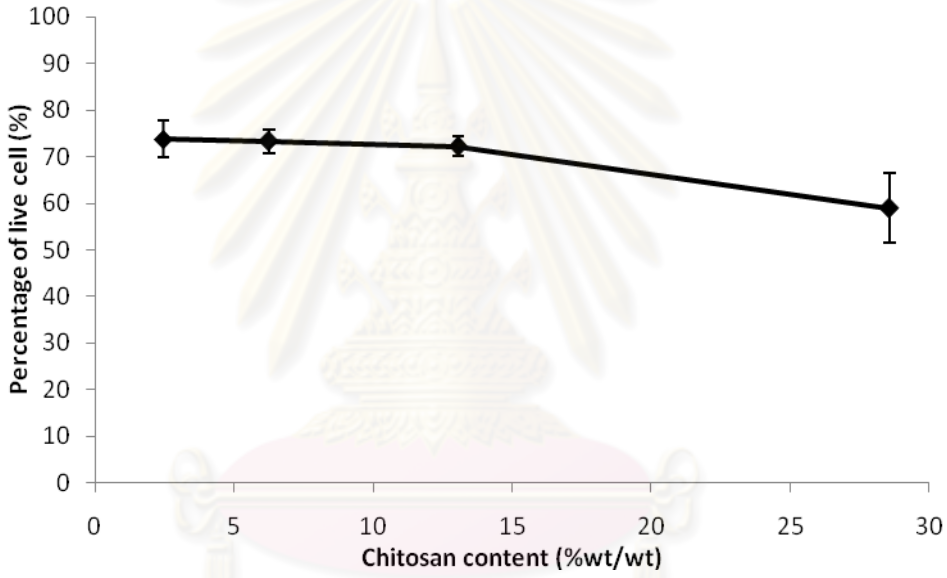

Figure 4.79 Percentage of live cells for Gram-positive *Brevibacillus agri* strain 13 attaching on chitosan/PVA nanofibers with various chitosan contents, after the incubation time of 12 h.

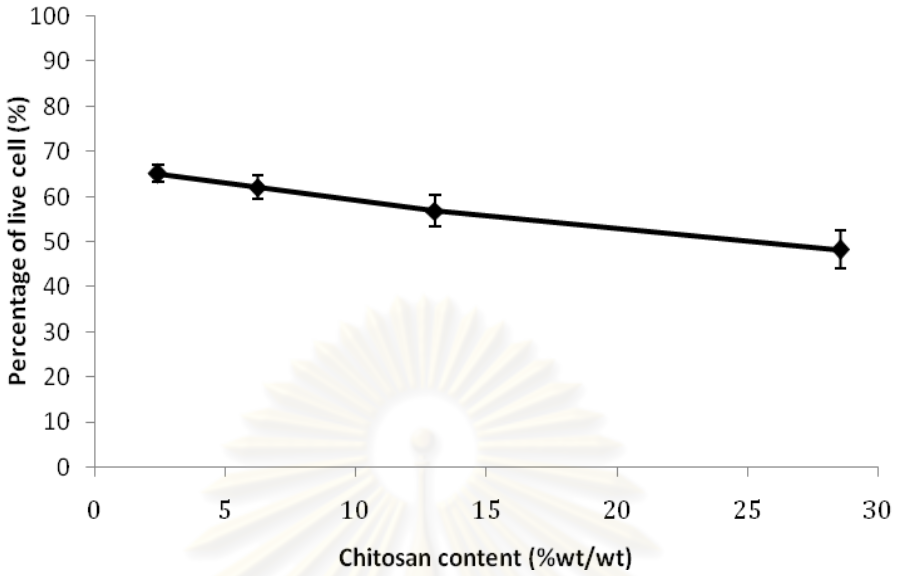

Figure 4.80 Percentage of live cells for Gram-positive *Brevibacillus agri* strain 13 attaching on chitosan/PVA nanofibers with various chitosan contents, after the incubation time of 24 h.

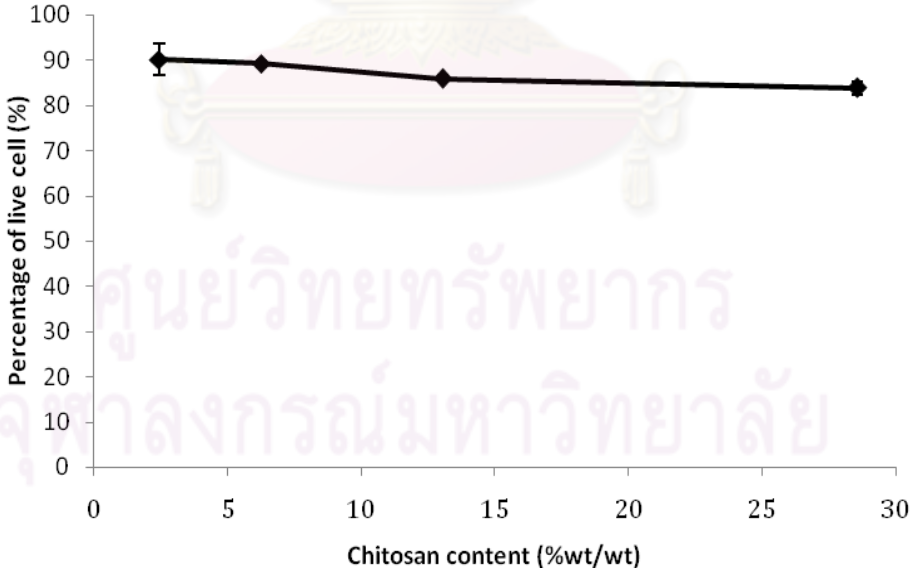

Figure 4.81 Percentage of live cells for Gram-negative *Acinetobacter baylyi* strain GFJ2 attaching on chitosan/PVA nanofibers with various chitosan contents, after the incubation time of 12 h.

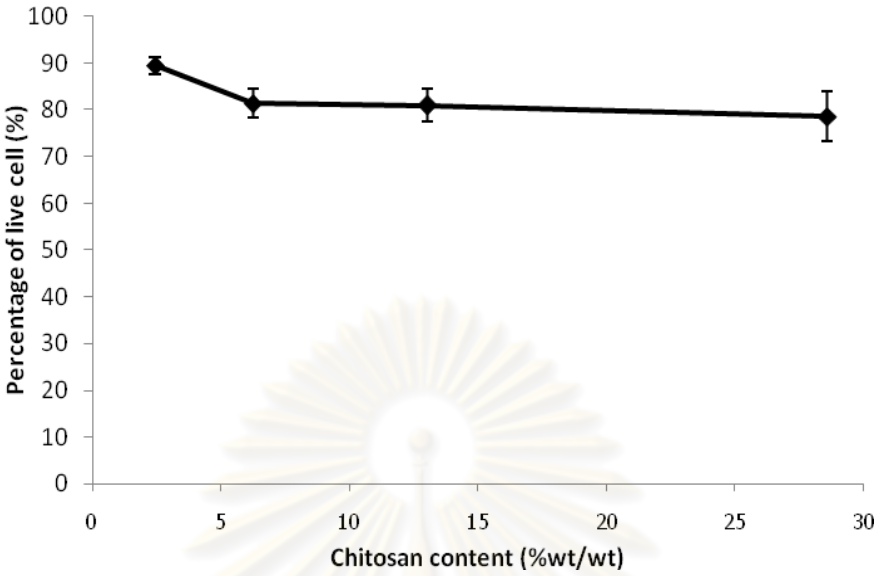

Figure 4.82 Percentage of live cells for Gram-negative *Acinetobacter baylyi* strain GFJ2 attaching on chitosan/PVA nanofibers with various chitosan contents, after the incubation time of 24 h.

At the lowest of chitosan content investigated (i.e., 2.44 %wt), all experiments for both types of bacterial cells indicated that the percentage of live cells attaching on surface was the highest. When the chitosan content was increased, it resulted in the decrease in the viability of cells on the surface. The results could be explained in the similar manner as what have been described in previous sections. The positive charges chitosan interacts with negative charges on the surface of the cells. The amino groups (NH_3^+) as the active functional group was found to be effective in obstructing the bacterial cells attachment [33]. The increase of chitosan content would increase the number of NH_3^+ groups leading to the free amino group that could be alter cell permeability. Due to the damage of the outer cell membrane, the hydrophilicity and charge density of the cell surface may be changed. The fluorescence micrographs of live cells and dead cells on chitosan/PVA fibers fabricated with various chitosan contents are shown in Figure 4.83-4.86.

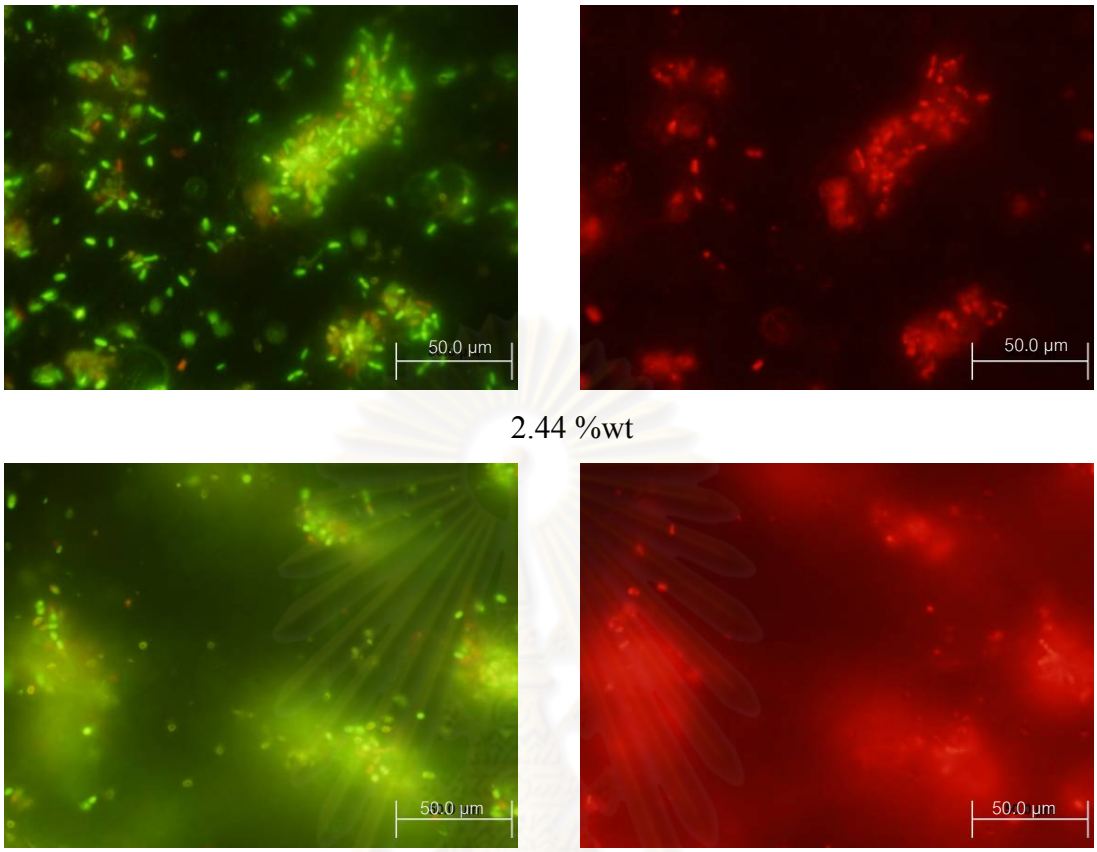

Figure 4.83 Florescence micrograph of Gram-positive *B. agri* strain 13 attaching on electrospun chitosan/PVA fibers that were prepared with various chitosan contents, after 12 h of incubation time.

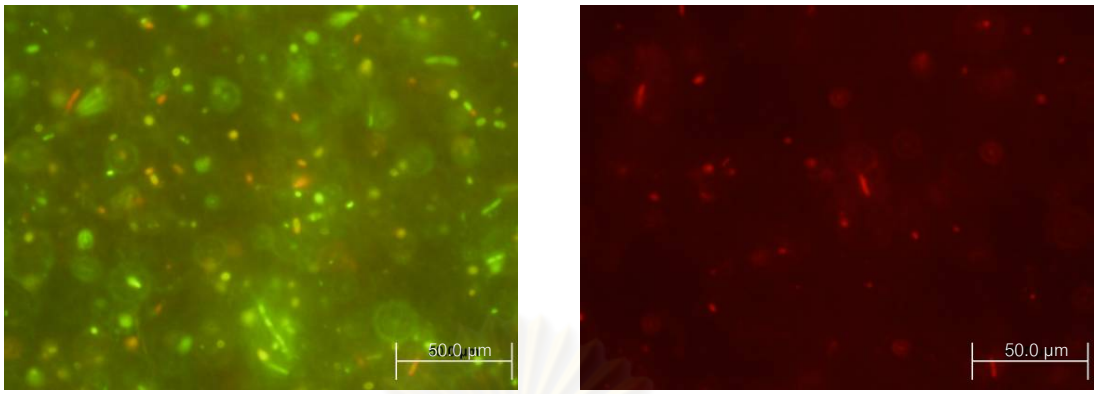

13.04 %wt

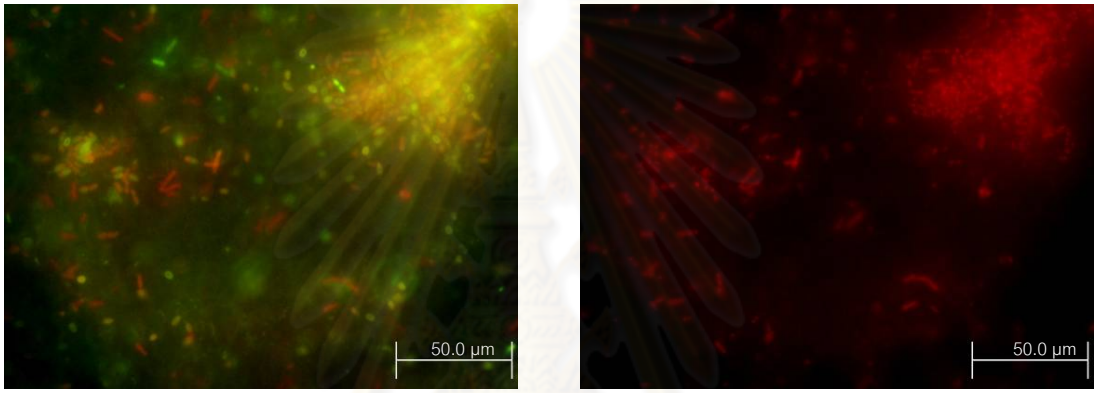

28.57 %wt

Figure 4.83 (continued).

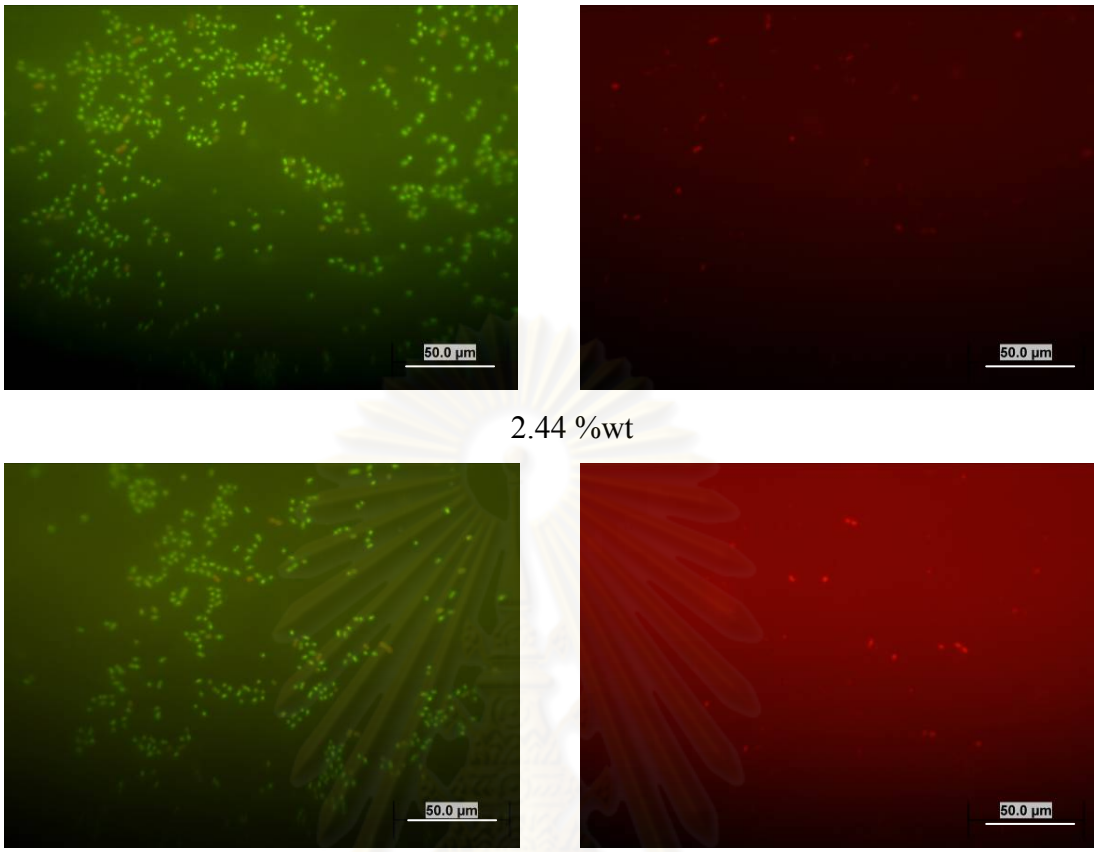

Figure 4.84 Florescence micrograph of Gram-negative *A. Baylyi* strain GFJ2 attaching on electrospun chitosan/PVA fibers that were prepared with various chitosan contents, after 12 h of incubation time.

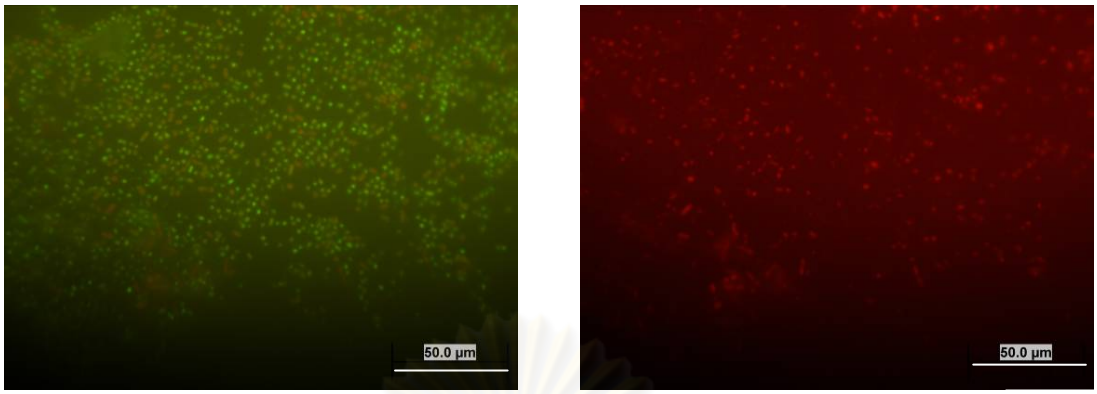

13.04 %wt

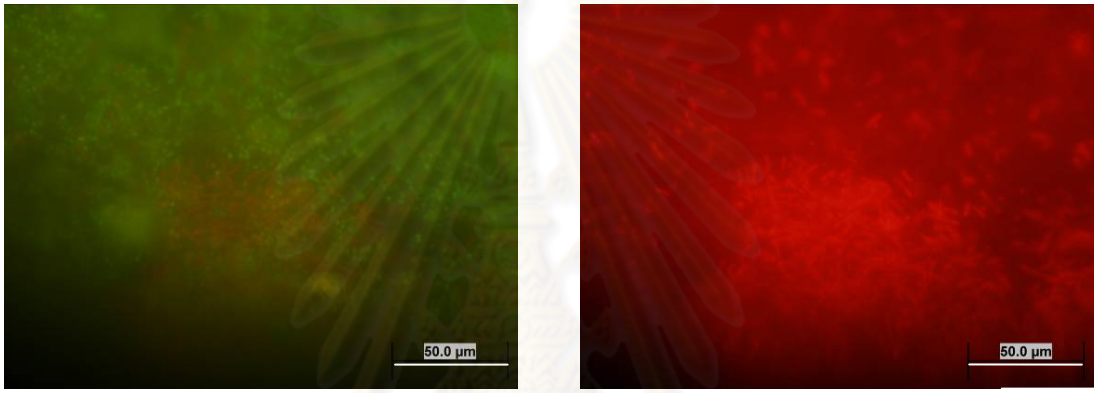

28.57 %wt

Figure 4.84 (continued).

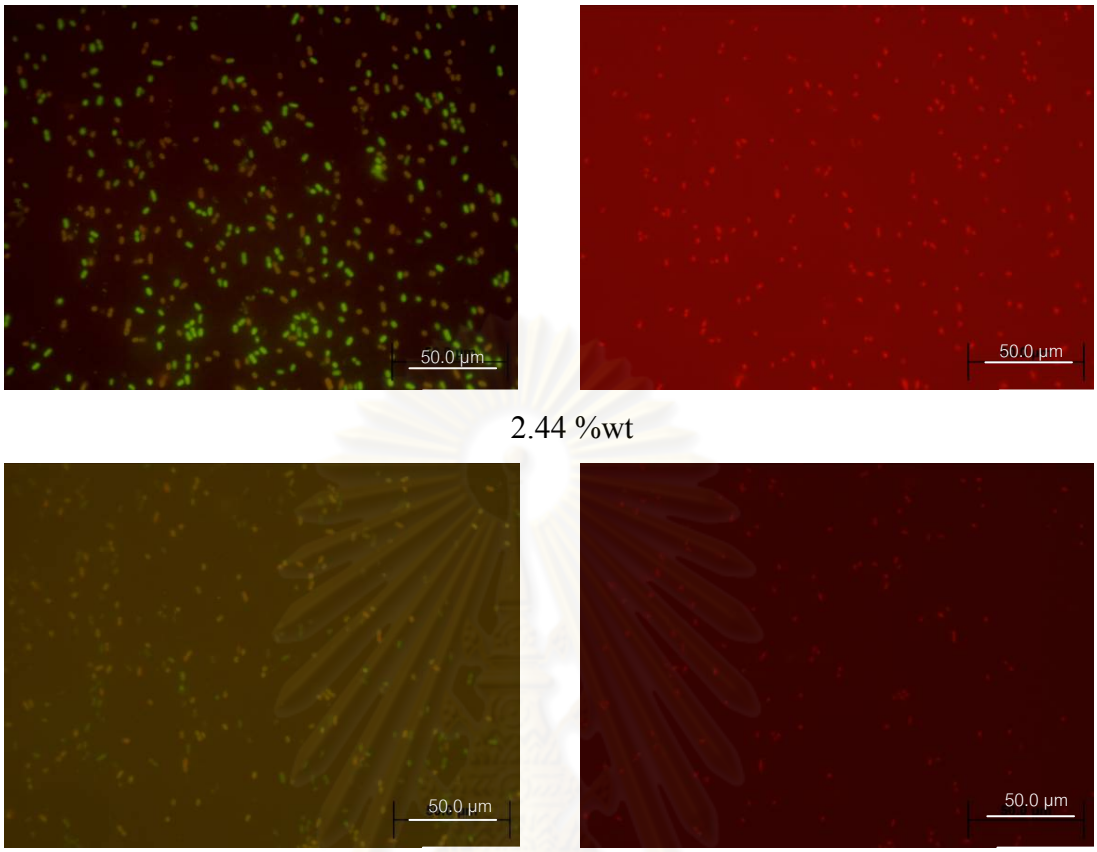

Figure 4.85 Florescence micrograph of Gram-positive *B. agri* strain 13 attaching on electrospun chitosan/PVA fibers that were prepared with various chitosan contents, after 24 h of incubation time.

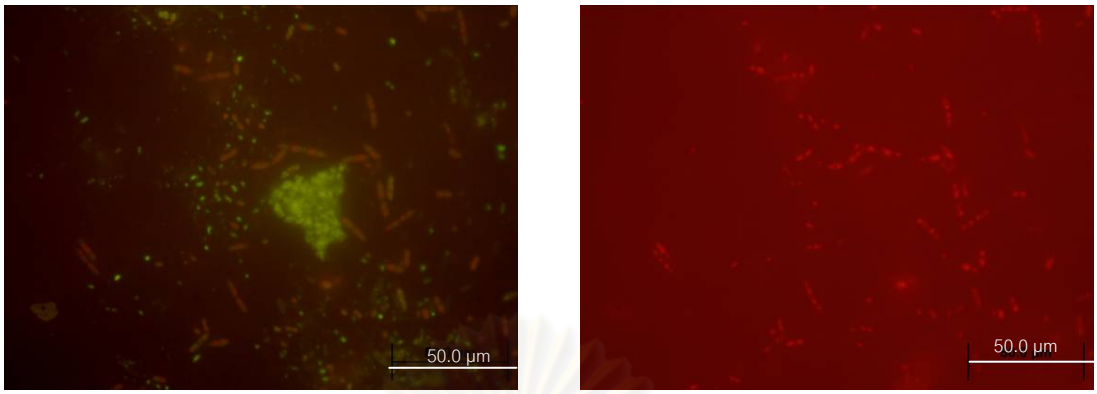

13.04 %wt

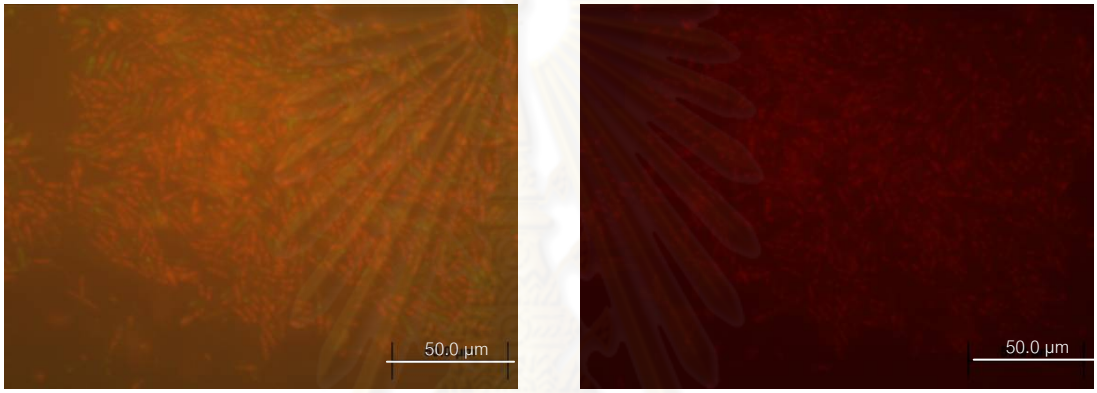

28.57 %wt

Figure 4.85 (continued).

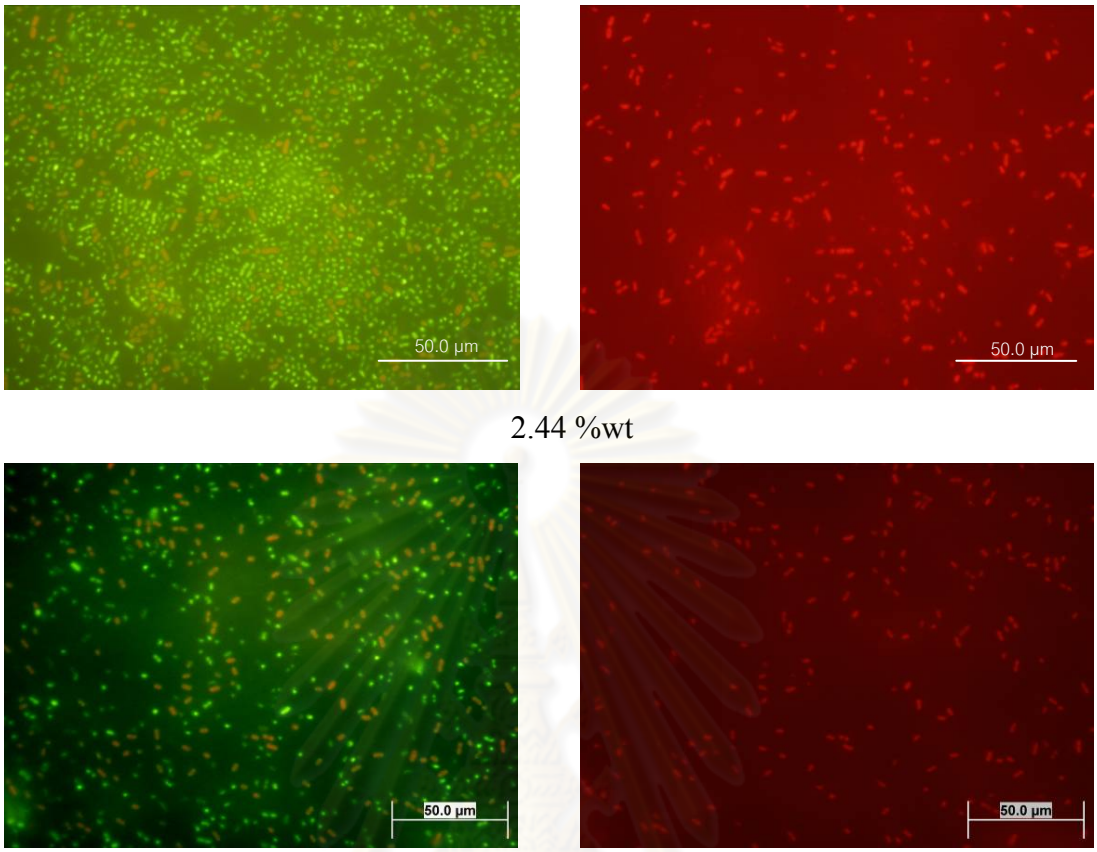

Figure 4.86 Florescence micrograph of Gram-negative *A. Baylyi* strain GFJ2 attaching on electrospun chitosan/PVA fibers that were prepared with various chitosan contents, after 24 h of incubation time.

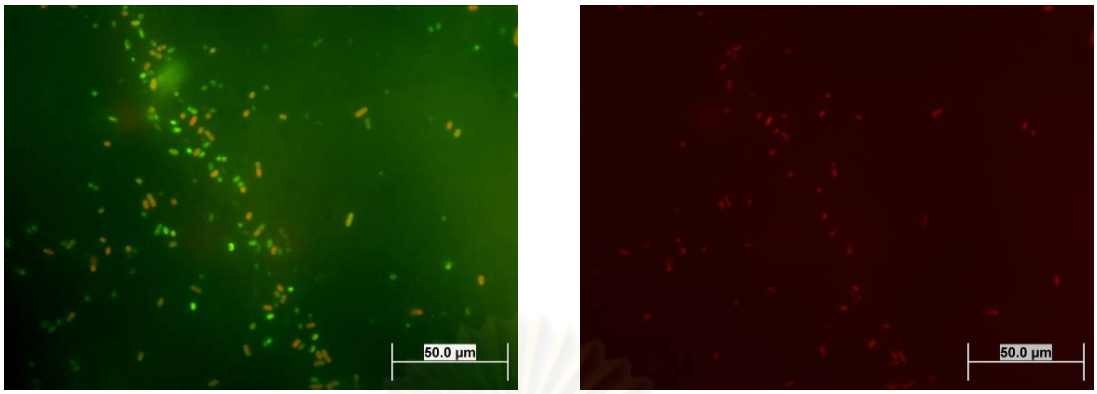

13.04 %wt

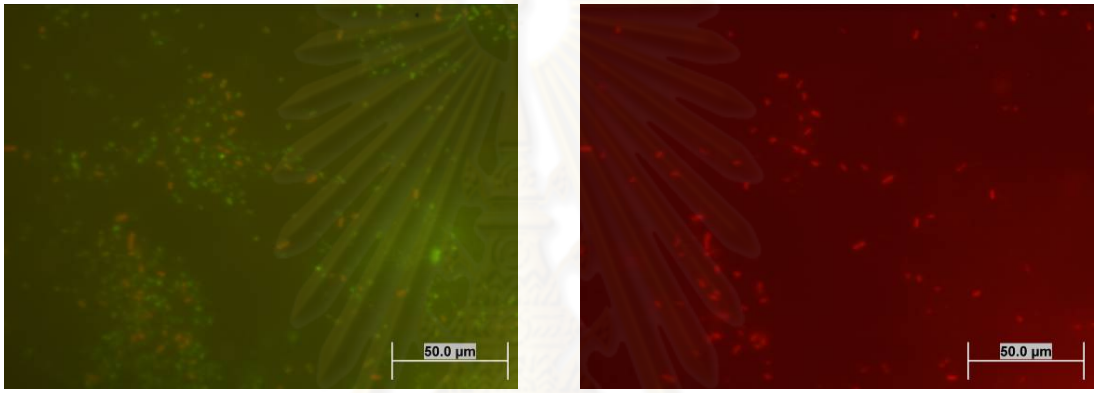

28.57 %wt

Figure 4.86 (continued).

Furthermore, to investigate the effect of molecular weight on chitosan/PVA nanofibers fabricated by electrospinning, the chitosan with molecular weight 100 kDa, 400 kDa and 760 kDa were used. The nanofibers were tested with Gram-negative *Acinetobacter baylyi* strain GFJ2 bacteria using the incubation time of 24 h. The results are shown in Figure 4.87

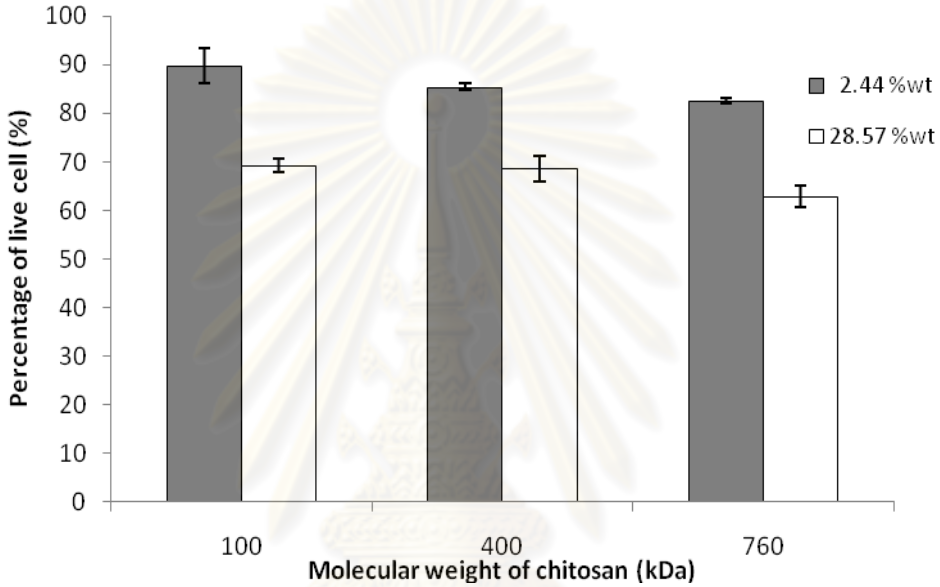

Figure 4.87 Percentage of live cells for Gram-negative *Acinetobacter baylyi* strain GFJ2 attaching on chitosan/PVA nanofibers formed with various chitosan contents (%wt) and various chitosan molecular weights, after the incubation time of 24 h.

These results confirmed that molecular weight of chitosan affected viability of cells. Molecular weight of chitosan directly related to cationic the behavior of chitosan such as chain conformation, solubility and degree of substitution. High molecular weight chitosan could have block arrangement of acetylated and deacetylated units and would increase the number of amino groups (NH_3^+) per molecule. However, the maximum soluble amount of chitosan decreased with the molecular weight of chitosan, leading to the reduced number of free amino groups that are available for bacterial attachment [33]. The results regarding the micrograph of live cells and dead cells attaching on chitosan/PVA fibers are shown in Figure 4.88 -4.90.

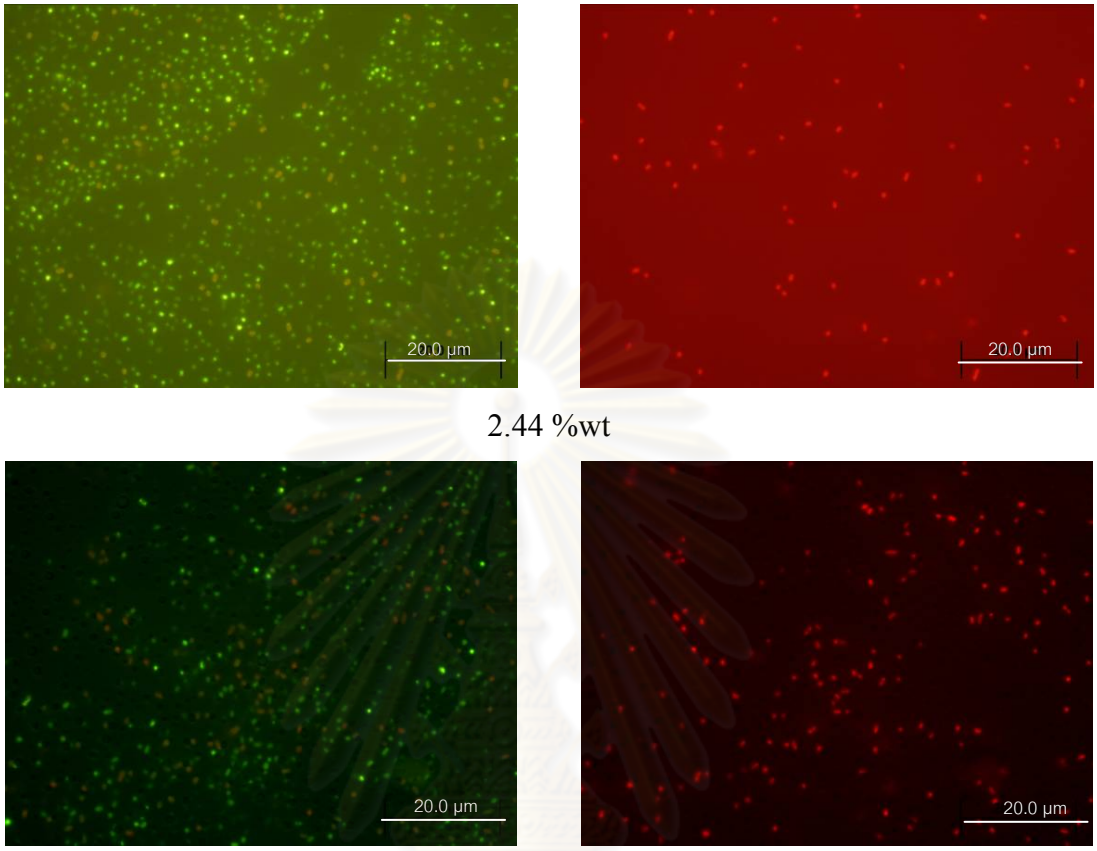

Figure 4.88 Fluorescence micrograph of Gram-negative *A. baylyi* strain GFJ2 attaching on chitosan/PVA nanofibers that were formed from chitosan with molecular weight of 100 kDa in various chitosan contents (%wt), after 24 h of incubation.

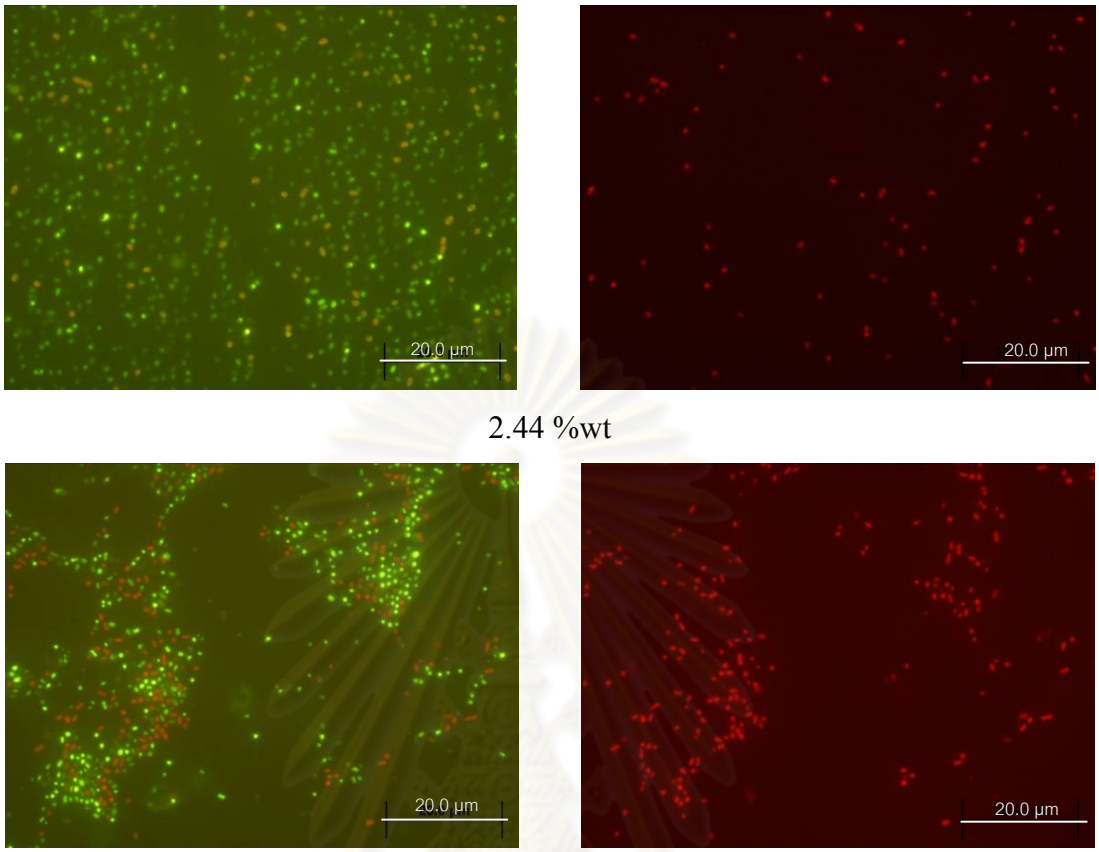

Figure 4.89 Fluorescence micrograph of Gram-negative *A. baylyi* strain GFJ2 attaching on chitosan/PVA nanofibers that were formed from chitosan with molecular weight of 400 kDa in various chitosan contents (%wt), after 24 h of incubation.

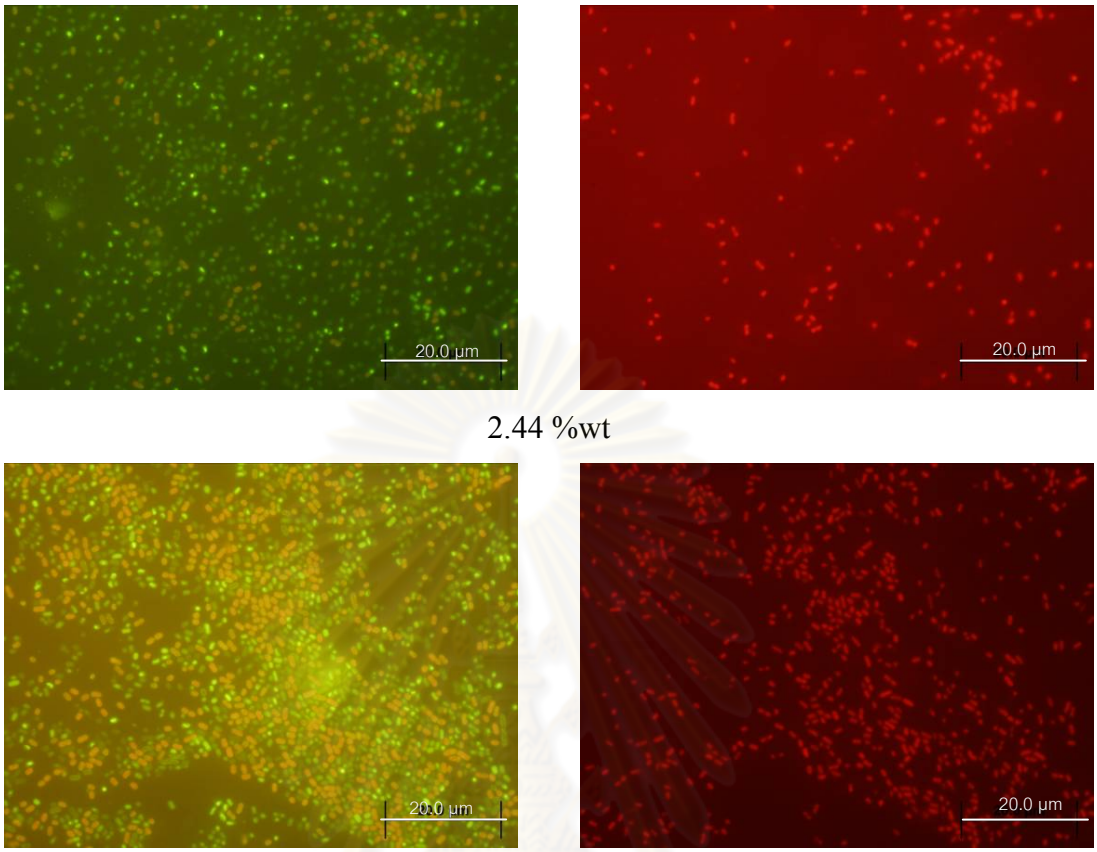

Figure 4.90 Fluorescence micrograph of Gram-negative *A. baylyi* strain GFJ2 attaching on chitosan/PVA nanofibers that were formed from chitosan with molecular weight of 760 kDa in various chitosan contents (%wt), after 24 h of incubation.

CHAPTER V

CONCLUSIONS AND RECOMMENDATIONS

The conclusions of this research are as follows,

1.) The electrospinning of the solution containing pure chitosan could not produce nanofibers within the experimental range investigated. Only sprayed droplets were obtained.

2.) The chitosan nanofibers could be fabricated via electrospinning technique only when chitosan was previously hydrolyzed or with the addition of polymer to the solution as the spinning aid.

3.) The chitosan in different form as a support material is an important factor affecting the bacterial attachment and cells viability.

4.) The relationship between the nature of bacteria cells and the physicochemical properties of chitosan is an important factor affecting the bacterial attachment and cells viability.

The recommendations for further experiments are as follows,

1.) The analyses of mechanical and thermal properties of chitosan would give more understanding in the process to fabrication of the nanofibers structure.

2.) The temperature and air moisture on the electrospinning parameters would provide more knowledge of their effects on fiber morphology.

3.) The measurement of electric charge distribution on the chitosan solution would give more insight on the mechanism of cells attachment.

4.) The measurement of the outer and inner cell membranes permeability would be helpful for the explaination of the absorption of bacterial cells on chitosan.

REFERENCES

[1] Chandy T., Sharma CP. Chitosan-as biomaterial. Biomaterials Artif Cells Artif Organ 18 (December 1999): 1-24.

[2] Min, B.M., Lee, S.W., Lim, J.N., You,Y., Lee, T.S., Kang, P.H., and Park, W.H. Chitin and chitosan nanofibers: electrospinning of chitin and deacetylation of chitin nanofibers. Polymer 45 (2004): 7137-7142.

[3] Don, T.M., King, C.F., Chiu, W.Y., and Peng C.A. Preparation and characterization of chitosan-g poly(vinyl alcohol)/poly(vinyl alcohol) blends used for the evaluation of blood-contacting compatibility. Carbohydrate Polymers 63 (2006):331-339.

[4] Koski, A., Yim, K., and Shivkumar, S. Effect of molecular weight on fibrous PVA produced by electrospinning. Material Letters 58 (2004): 493-497.

[5] Zong, XH., Kim, KS., Fang, DF., Ran, SF., Hsiao, BS., and Chu, B. Structure and process relationship of electrospun bioabsorbable nanofiber membrances. Polymer 43 (2002): 4403-4412.

[6] Huang ZM, Zhang YZ, Kotaki M, and Ramakrishna S. A review on polymer nanofibers by electrospinning and their application in nanocomposites. Composite Science Technology 63 (2003): 2223-2253.

[7] Hohman, MM., Shin, M., Rutledge, G., and Brenner, MP. Electrospinning and electrically forced jets. Applications Physics Fluids 13 (2001): 2221-2236.

[8] Georgiou, G., and Francisco, J.A. Practical applications of engineering Gram-negative bacterial cell surfaces. Biology Technology 11 (1993): 6-10.

[9] Hui, L., Xiao, H. W., and Li, P. S. Chitosan kills bacteria through cell membrane damage. International Journal of Food Microbiology 95 (2004): 147– 155.

[10] Milena, I., Nadya, M., and Nevena M. Electrospun nano-fibre mats with antibacterial properties from quaternised chitosan and poly(vinyl alcohol). Carbohydrate Research 341 (2006): 2098–2107.

[11] Bhattarai, N., Omid, V., Frederick, A., and Zhang, M. Electrospun chitosan-based nanofibers and their cellular compatibility. Biomaterials 26 (2006): 6176–6184.

[12] Milena, I., Kirilka, S., Nadya, M., Nevena, M., and Iliya R. Electrospun nano-fibre mats with antibacterial properties from quaternised chitosan and poly(vinyl alcohol). Carbohydrate Research 341 (2006): 2098–2107.

[13] Dzenis, YA. Hierarchical nano-/micromaterials based on electrospun polymer fibers: predictive models for thermomechanical behavior. Journal Computer-Aided Materials Design 3 (1996): 403–408.

[14] Doshi, J., and Reneker, DH. Electrospinning process and applications of electrospun fibers. Electrostatics 35 (1995): 151–160.

[15] Ohkawa, K., Cha, DI., Kim, H., Nishida, A., and Yamamoto, H. Electrospinning of chitosan. Macromolecule Rapid Communication 25 (2004): 1600–1605.

[16] Homa, H., Seyed, A., Hosseini R., and Masoumeh, V. Electrospinning of chitosan nanofibers: Processing optimization. Carbohydrate Polymers 77 (2009): 656-661.

[17] Min, BM., Lee, SW., Lim, JM., Young, Y., Lee, TS., Kang, PH., and Park, WH. Chitin and chitosan nanofibers: electrospinning of chitin and deacetylation of chitin nanofibers. Polymer 45 (2004): 7137–7142.

[18] Ma, J., Wang, H., He, B., and Chen, J. A preliminary in vitro study on the fabrication and tissue engineering applications of a novel chitosan bilayer material as a scaffold of human neofetal dermal fibroblasts. Biomaterials 22 (2001): 331–336.

[19] Megelski, S., Stephens, JS., Chase, DB., and Rabolt, JF. Micro and nanostructured surface morphology on electrospun polymer fibers. Macromolecules 22 (October 2002): 8456-8466.

[20] Dutta, P.K., Shipra, T., Mehrotra, G.K., and Dutta J.D. Perspectives for chitosan based antimicrobial films in food applications. Food Chemistry 114 (2008): 1173–1182.

[21] Pakakrong, S., Artphop, N., Poonlarp, C., and Pitt, S. In vitro biocompatibility of electrospun and solvent-cast chitosan substrata towards Schwann, osteoblast, keratinocyte and fibroblast cells. European Polymer Journal 46 (2010): 428–440.

[22] Hong, K. N., Shin, H. L., Samuel, P., and Meyers. Antibacterial activity of chitosans and chitosan oligomers with different molecular weights. International Journal of Food Microbiology 74 (2002): 65– 72.

[23] Byung, M. M., Jung, N. L., Young, Y., Taek, S. L., and Won H. P. Chitin and chitosan nanofibers: electrospinning of chitin and deacetylation of chitin nanofibers. Polymer 45 (2004): 7137–7142.

[24] Pillai, W. P., Chandra, P., and Sharma Chitin and chitosan polymers: Chemistry, solubility and fiber formation. Polymer Science 34 (2009): 641–678.

[25] Dongwen, R., Huaan, Z., Weiyang, X., Wei, W., and Xiao, M. A preliminary study on fabrication of nanoscale fibrous chitosan membranes in situ by biospecific degradation. Journal of Membrane Science 280 (2006): 99–107.

[26] Eugene K. Implantable applications of chitin and chitosan. Biomaterials 24(January 2003): 2339–2349.

[27] Hsieh, L. Chitosan bicomponent nanofibers and nanoporous fibers. Carbohydrate Research 341 (2006): 374–381.

[28] Helander, I.M., Ahvenainen, J., and Rhoades S. Chitosan disrupts the barrier properties of the outer membrane of Gram-negative bacteria. International Journal of Food Microbiology 7 (2001): 235–244.

[29] Inmaculada, A., Ruth, H., Inés Paños, Beatriz, M., and Niuris A. Functional Characterization of Chitin and Chitosan. Current Chemical Biology 3 (2009): 203-230.

[30] Jen, M. Y., Te, L. L., Ming, C. Y. Evaluation of chitosan/PVA blended hydrogel membranes. Journal of Membrane Science 236 (2004): 39-51.

[31] Ki, M. Y., Yasuko, M., Masaaki, K., and Ferry I. Nanoparticle filtration by electrospun polymer fibers." Chemical Engineering Science 62 (2007): 4751 – 4759.

[32] Doktycz M.J., Hoyt P.R., Pelletier D.A., Wud S., Allison D. P. AFM imaging of bacteria in liquid media immobilized on gelatin coated mica surfaces. Ultramicroscopy 97 (2003): 209–216.

[33] Zhiyong, S., Recep, A., Xinghong Y., and David W. P. Efficient Immobilization and Patterning of Live Bacterial Cells. Langmuir NIH Public Access 24, 8 (2008): 4161–4167.

[34] Cassidy, M. B., Lee, H., and Trevors, J. T. Environmental applications of immobilized microbial cells: A review. Journal of Industrial Microbiology 16 (1996): 79–101.

APPENDICES

APPENDIX A

SIZE DISTRIBUTION OF FIBER DIAMETER OF CHITOSAN/PVA COMPOSITE

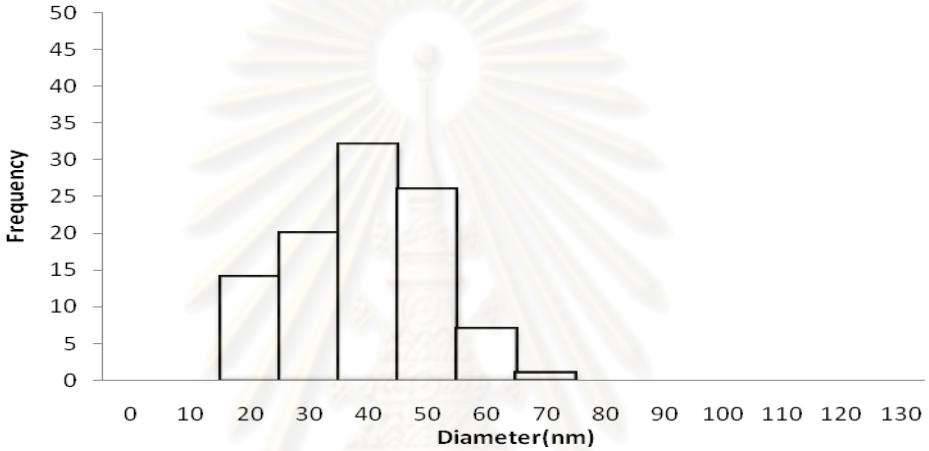

Figure A-1 Size distribution of fiber diameter of chitosan/PVA composite at 0.004 %w/v chitosan content, MW of chitosan of 100 kDa.

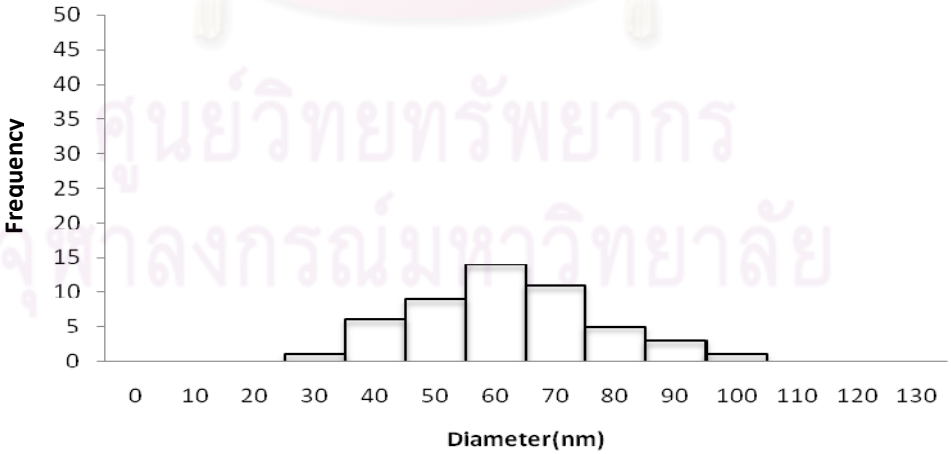

Figure A-2 Size distribution of fiber diameter of chitosan/PVA composite at 0.008 %w/v chitosan content, MW of chitosan of 100 kDa.

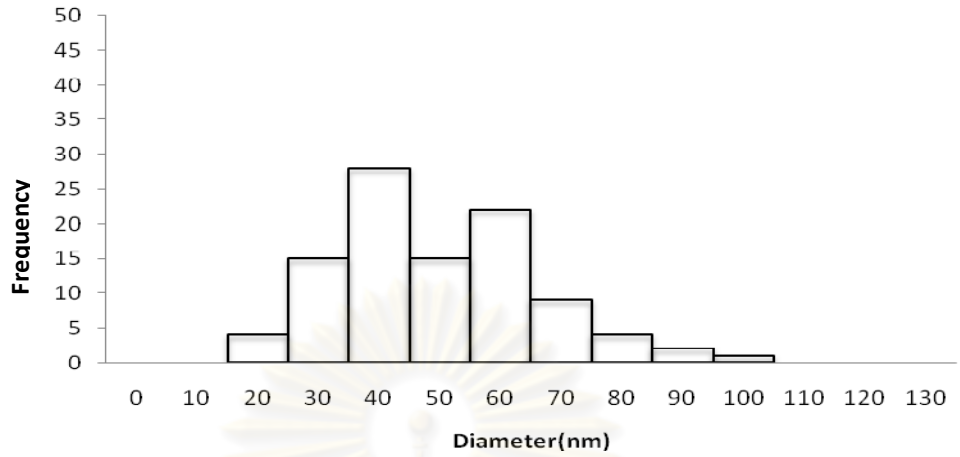

Figure A-3 Size distribution of fiber diameter of chitosan/PVA composite at 0.012 %w/v chitosan content, MW of chitosan of 100 kDa.

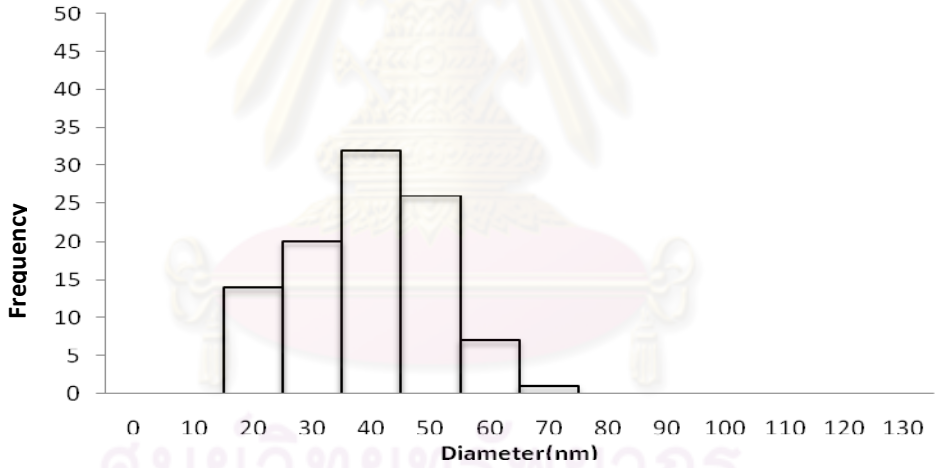

Figure A-4 Size distribution of fiber diameter of chitosan/PVA composite at 0.016 %w/v chitosan content, MW of chitosan of 100 kDa.

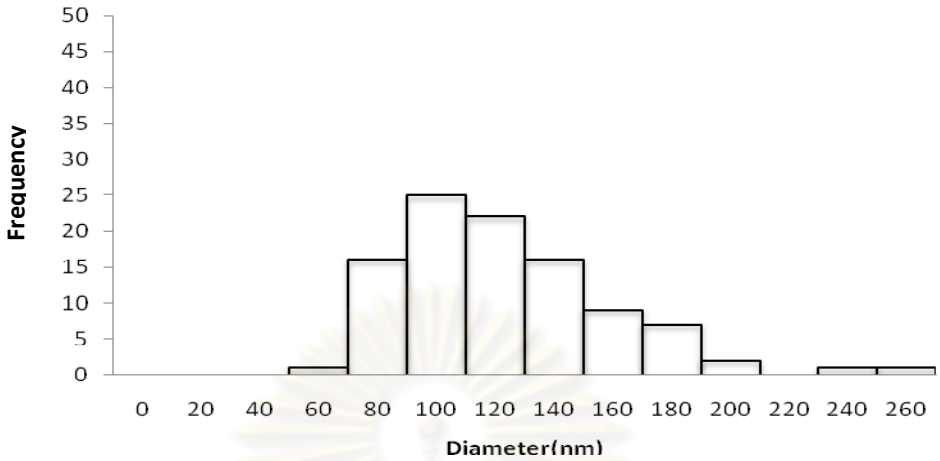

Figure A-5 Size distribution of fiber diameter of chitosan/PVA composite at 0.003 %w/v chitosan content, MW of chitosan of 400 kDa.

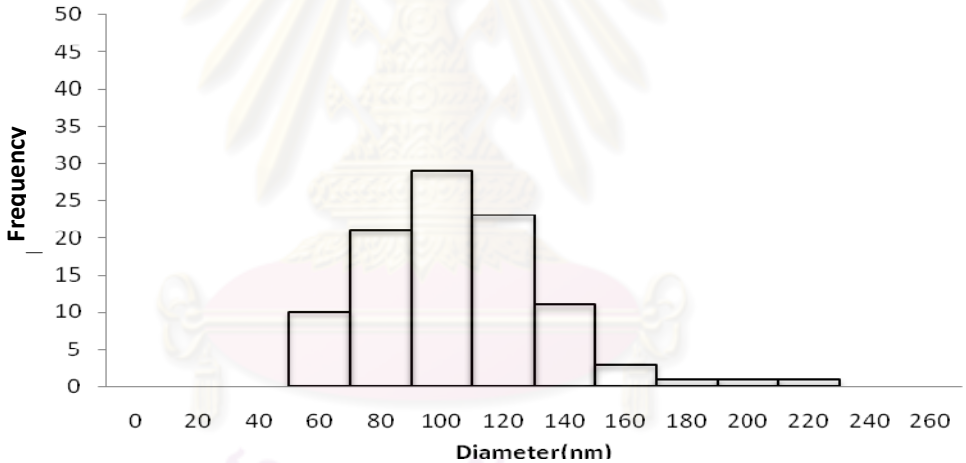

Figure A-6 Size distribution of fiber diameter of chitosan/PVA composite at 0.006%w/v chitosan content, MW of chitosan of 400 kDa.

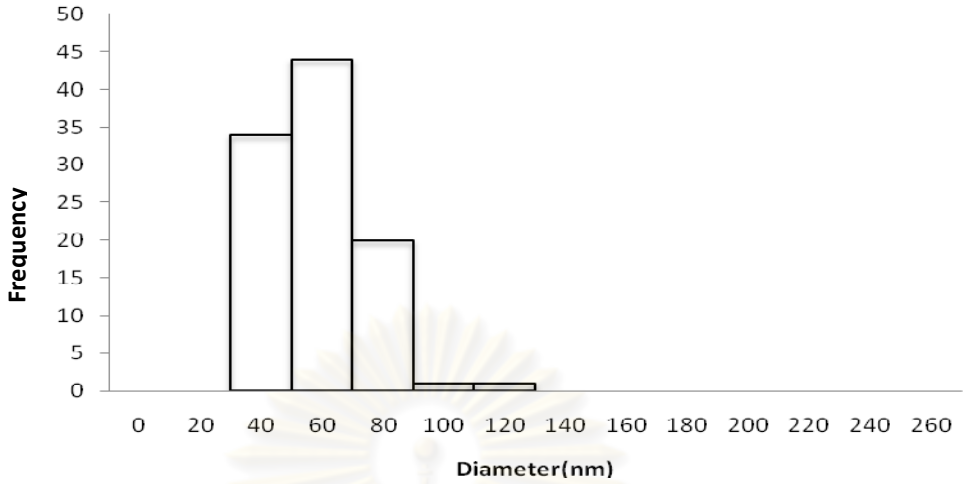

Figure A-7 Size distribution of fiber diameter of chitosan/PVA composite at 0.009%w/v chitosan content, MW of chitosan of 400 kDa.

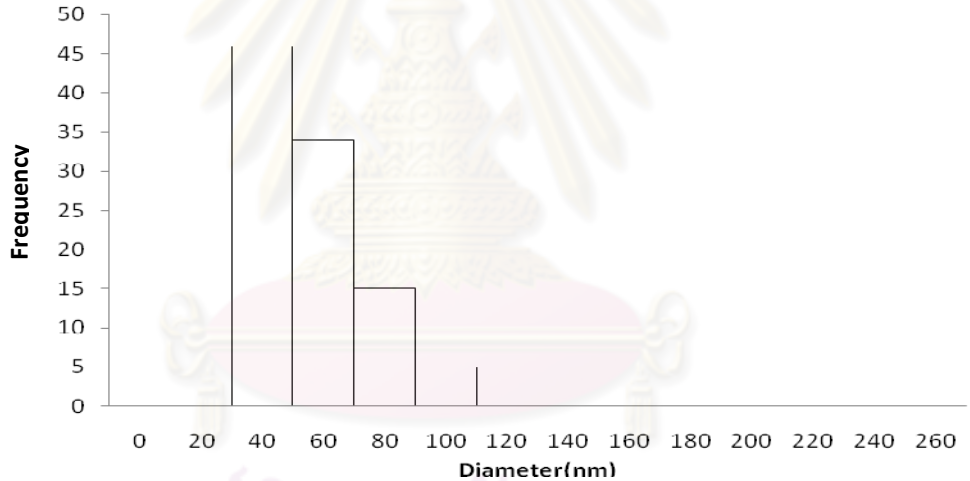

Figure A-8 Size distribution of fiber diameter of chitosan/PVA composite at 0.012%w/v chitosan content, MW of chitosan of 400 kDa.

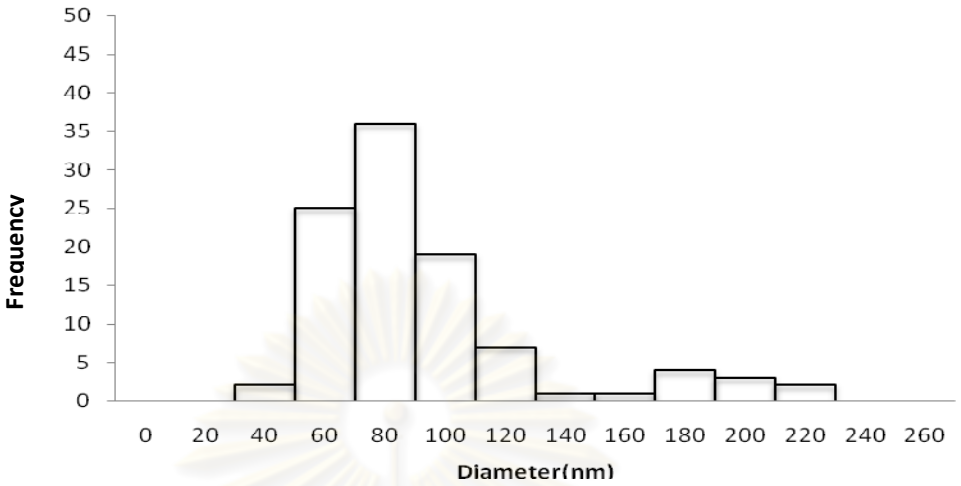

Figure A-9 Size distribution of fiber diameter of chitosan/PVA composite at 0.002 %w/v chitosan content, MW of chitosan of 760 kDa.

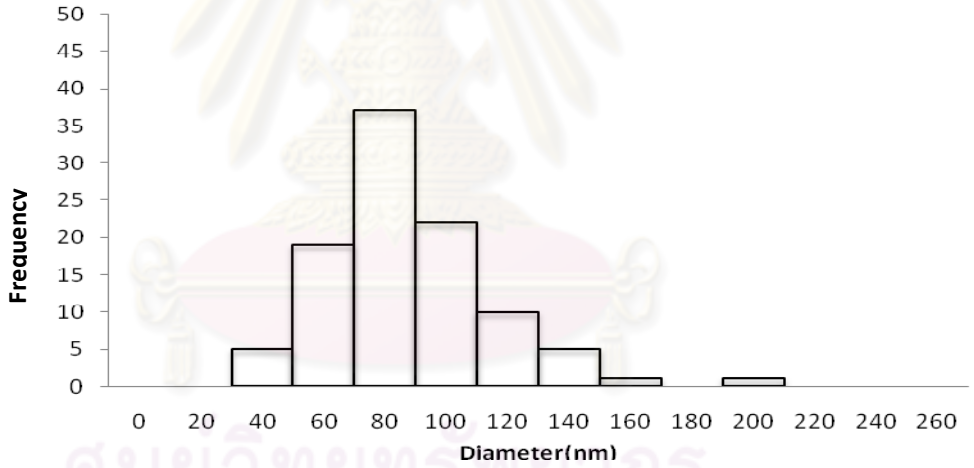

Figure A-10 Size distribution of fiber diameter of chitosan/PVA composite at 0.004 %w/v chitosan content, MW of chitosan of 760 kDa.

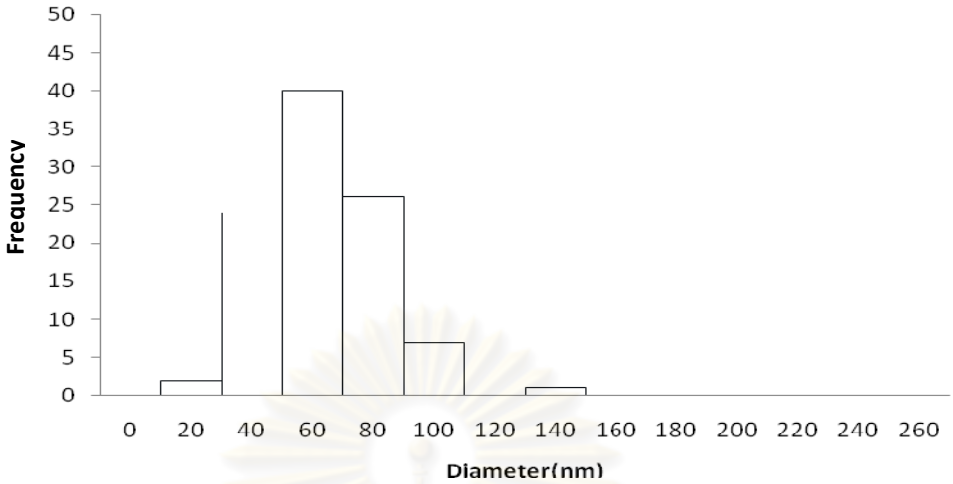

Figure A-11 Size distribution of fiber diameter of chitosan/PVA composite at 0.006 %w/v chitosan content, MW of chitosan of 760 kDa.

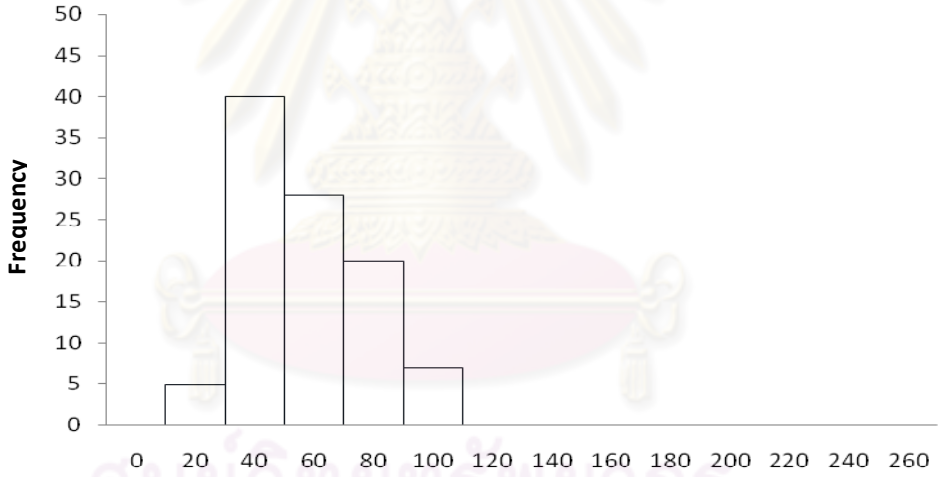

Figure A-12 Size distribution of fiber diameter of chitosan/PVA composite at 0.008 %w/v chitosan content, MW of chitosan of 760 kDa.

APPENDIX B

STANDARD CURVES FOR BACTERIAL CELLS CONCENTRATION

B.1 Preparation of Standard Curve for Bacterial Cells Concentration

In order to prepare the standard curve for bacterial cells concentration measurement, the following procedure is followed.

5 ml from broth medium

⇩ Incubated for 20h

100 ml of medium (1% inoculum)

(Shaked at 250 rpm at 45°C for *Brevibacillus agri* strain 13 and at room temperature for *Acinetobacter baylyi* strain GFJ2)

⇩ Centrifuge at 5000 rpm, 15 minutes

The high density cells were placed into 20 ml of bacterial solution

⇩

Measured optical density by spectrophotometer at 600 nm (OD_{600}).

⇩

Diluted 10µl of the bacterial solution to 100µl of nutrient solution

(Serial dilutions =10^{-8} -10^{-14} from the original medium solution)

⇩

10µl of the serial solution was droped onto the agar plate and spread plate

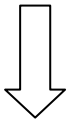

Incubated for 20h

(45°C for *Brevibacillus agri* strain 13 and at room temperature for *Acinetobacter baylyi* strain (GFJ2)

Counted the colonies forming units

B.2 Determination of Colony Forming Units per ml (CFU/ml)

For example

From the spectrophotometer, OD_{600} = 1.0

From 10µl of the serial solution was counted = 6 colonies (CFU)

Before the dilution those 6 colonies were in a volume = 10^{-12} (1/µl)

Thus the original concentration = $\frac{\text{6 colonies}}{10^{-2} \times 10^{-12}}$

Therefore, at OD_{600} is 1.0 = 6×10^{14} CFU/ml

The standard curve of bacterial cells were shown in Figure B-1 and Figure B-2 for Gram-positive *Brevibacillus agri* strain No13 and Gram-negative *Acinetobacter baylyi* strain GFJ2, respectively.

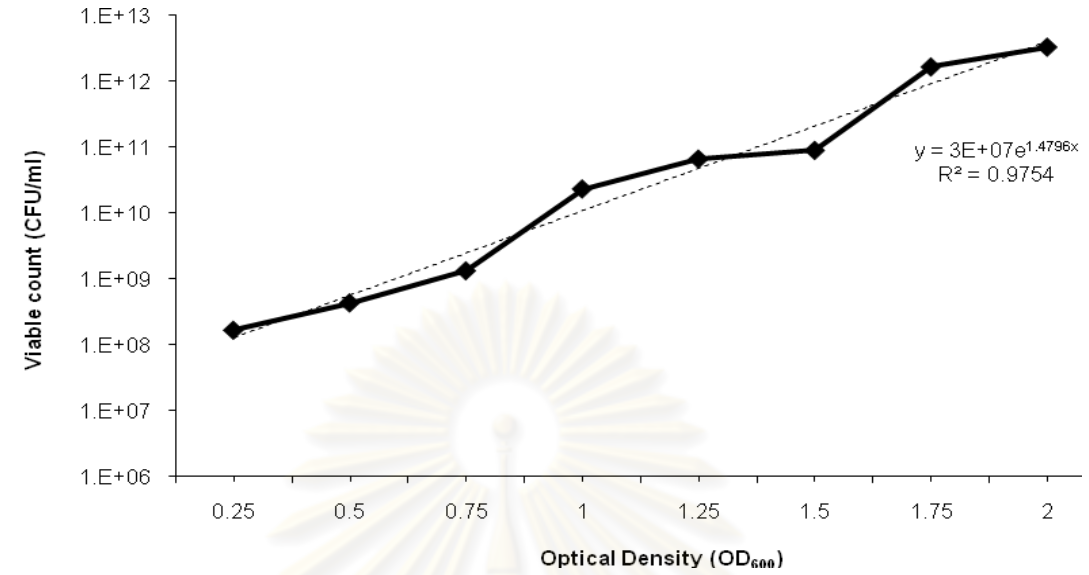

Figure B-1 The standard curve of Gram-positive *Brevibacillus agri* strain No13 between optical density (OD_{600}) and the colony forming units (CFU/mL) at 45°C, 24 hours incubated time by using the spread plate technique.

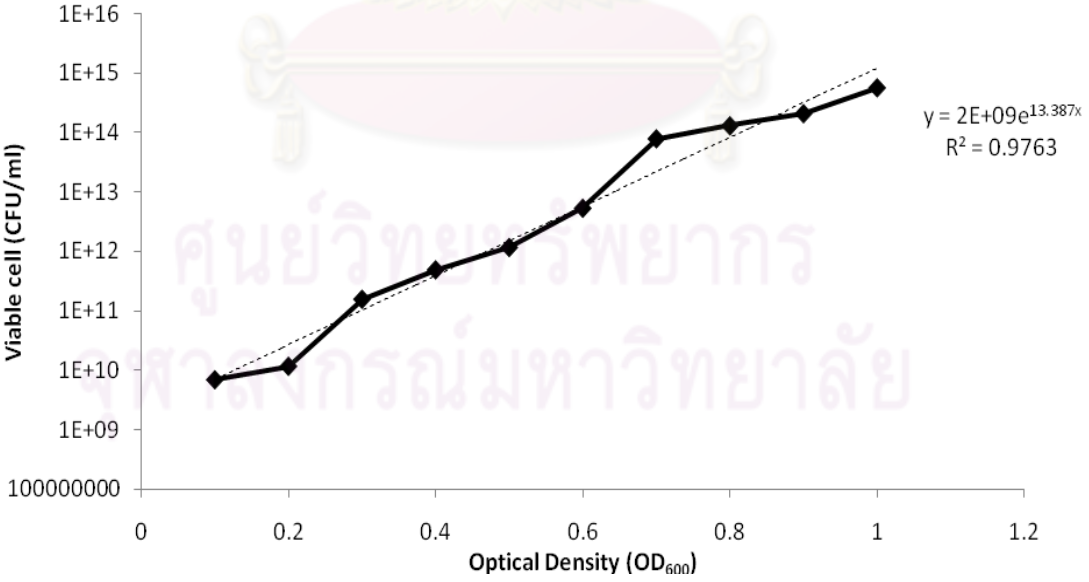

Figure B-2 The standard curve of Gram-negative *Acinetobacter baylyi* strain GFJ2 between optical density (OD_{600}) and the colony forming units (CFU/mL) at room temperature, 24 hours incubated time by using the spread plate technique.

APPENDIX C

DETERMINATION OF NUMBER OF CELLS ATTACHED ON CHITOSAN NANOFIBERS

In order to determine the bacterial cells attached on chitosan nanofibers, the optical density of the initial bacterial cell solution and that of the washed solution was measured by spectrophotometer at 600 nm (OD_{600}). The Colony Forming Unit (CFU) was calculated from a standard calibration curve for *Acinetobacter baylyi* strain GFJ2 and *Brevibacillus agri* strain 13 as followed.

For example, Gram-negative *Acinetobacter baylyi* strain GFJ2 of the hydrolyzed chitosan at 6h and 12h for incubation time.

OD_{600} of the initial bacterial cells solution is 0.88 $=2.6545 \times 10^{14}$ CFU/ml

100µl of the initial bacterial cells solution $=2.6545 \times 10^{14} \times (10^{-1})$

Thus, CFU of initial bacterial cells $=2.6545 \times 10^{13}$

OD_{600} of the first washed solution is 0.1507 $=1.5038 \times 10^{10}$ CFU/ml

500µl of the first of washed solution $=1.5038 \times 10^{10} \times (5 \times 10^{-1})$ CFU

Thus, CFU of the first washed solution $=7.519 \times 10^{9}$

OD_{600} of the second washed solution is 0.1993 $=2.8823 \times 10^{10}$ CFU/ml

500µl of the second of washed solution $=2.8823 \times 10^{10} \times (5 \times 10^{-1})$ CFU

Thus, CFU of the second washed solution $=1.4412 \times 10^{10}$

Since Total CFU attachment $= CFU_{initial} - CFU_{first\ washed} - CFU_{second\ washed}$

$= (2.6545 \times 10^{13}) - (7.519 \times 10^{9}) - (1.4412 \times 10^{10})$

$= 2.6503 \times 10^{13}$ cells

Therefore, the total bacterial cells were attached on the support = 2.6503×10^{13} cell

APPENDIX D

FT-IR SPECTRA OF CHITOSAN

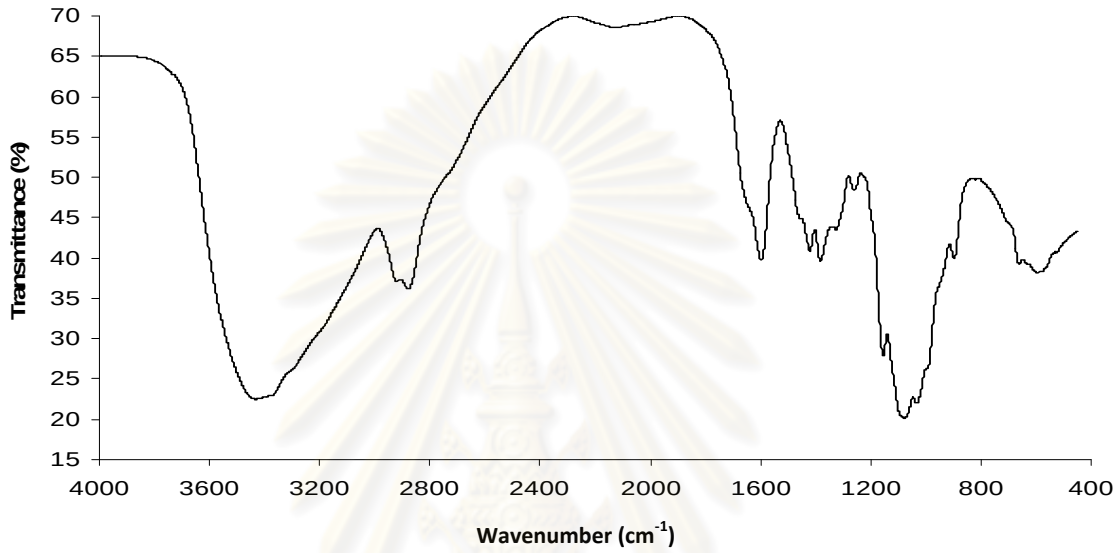

Figure D-1 FT-IR spectra of the chitosan hydrolyzed for 6 h.

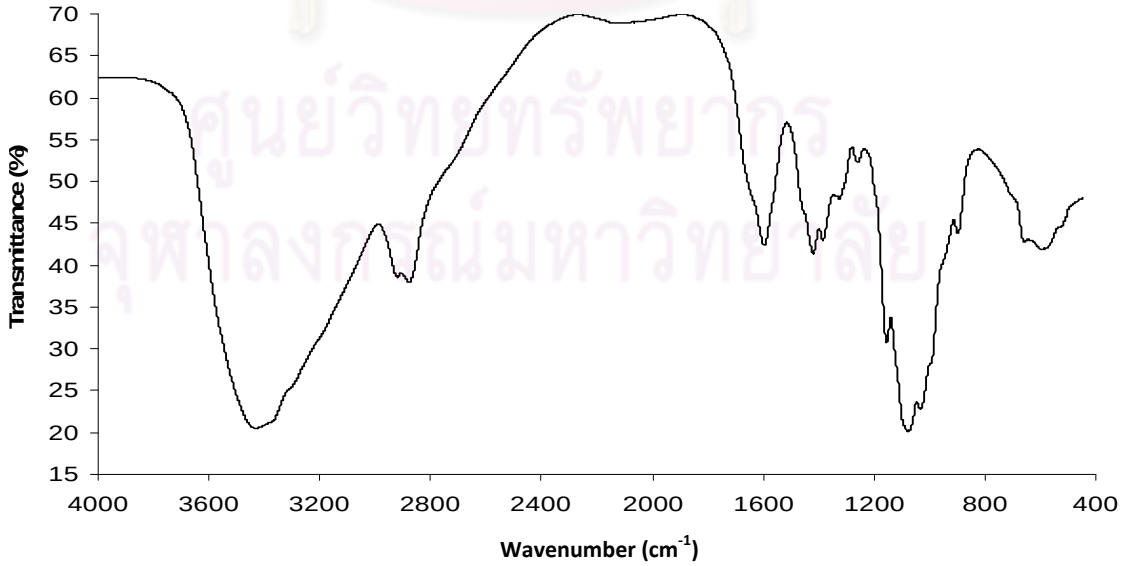

Figure D-2 FT-IR spectra of the chitosan hydrolyzed for 12 h.

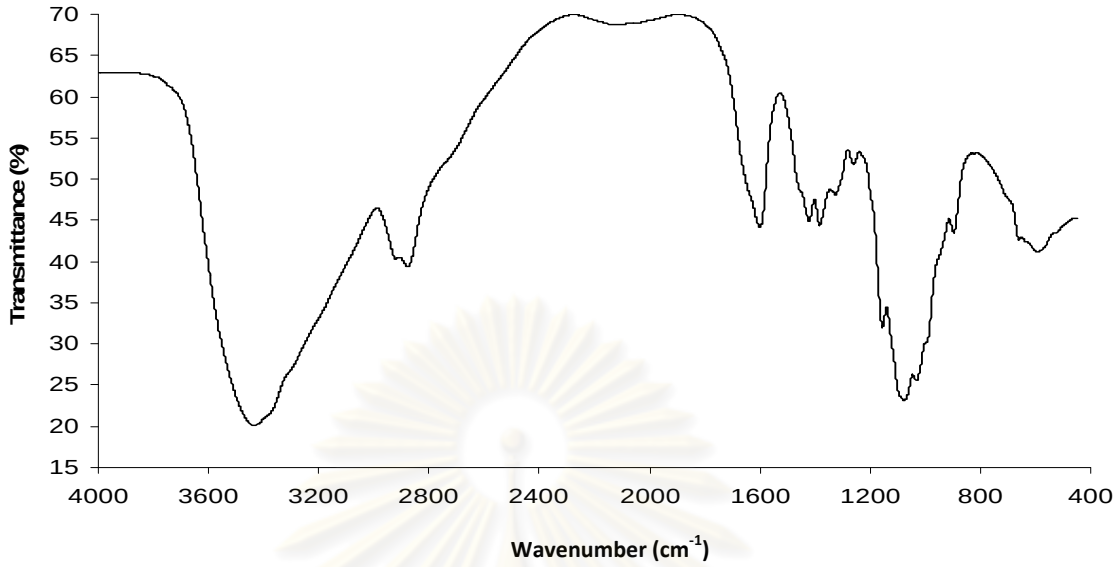

Figure D-3 FT-IR spectra of the chitosan hydrolyzed for 24 h.

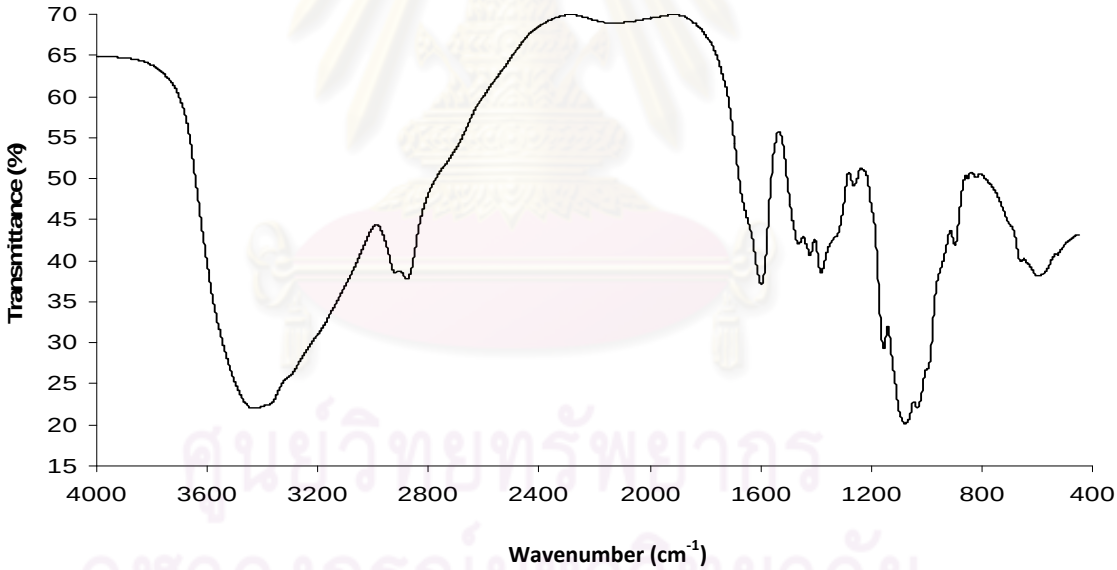

Figure D-4 FT-IR spectra of the chitosan hydrolyzed for 36 h.

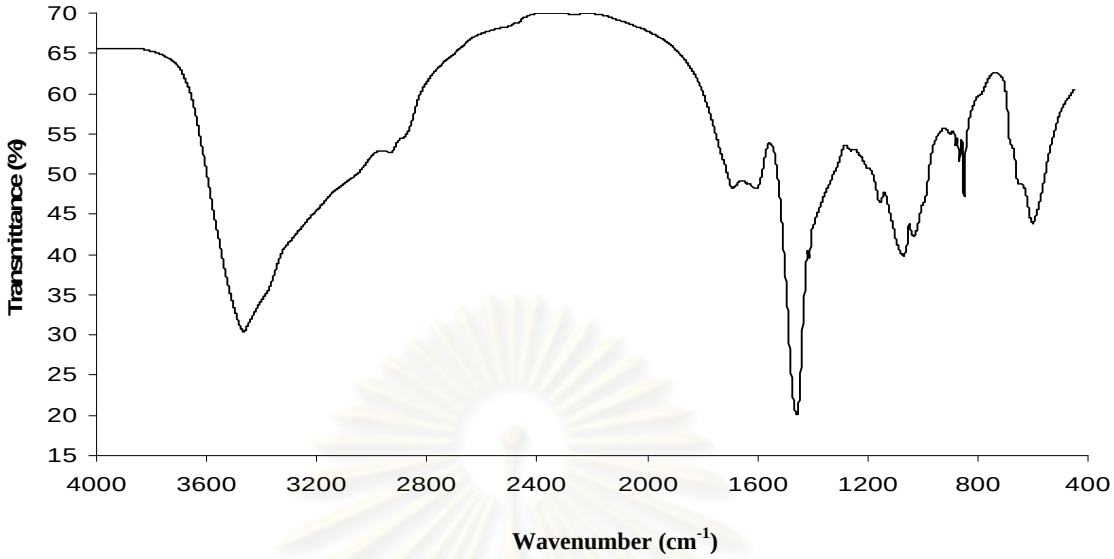

Figure D-5 FT-IR spectra of the chitosan hydrolyzed for 48 h.

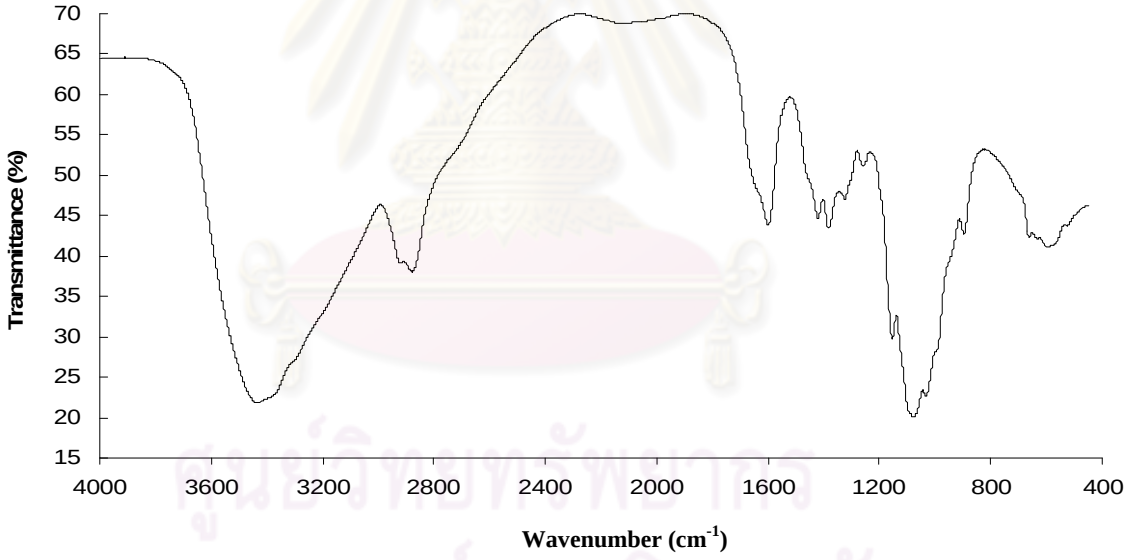

Figure D-6 FT-IR spectra of the chitosan at molecular weight 100 kDa.

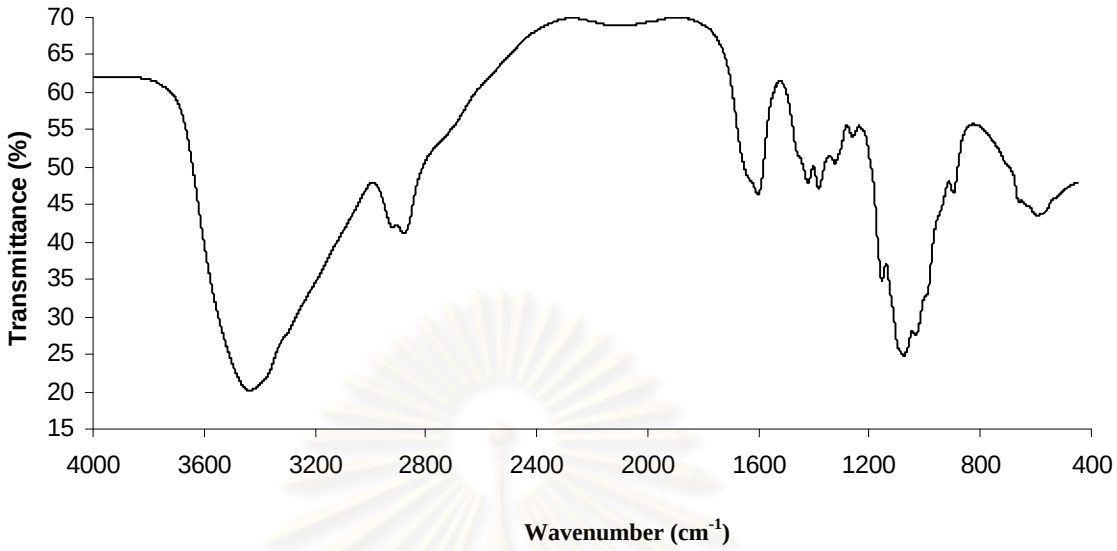

Figure D-7 FT-IR spectra of the chitosan at molecular weight 400 kDa.

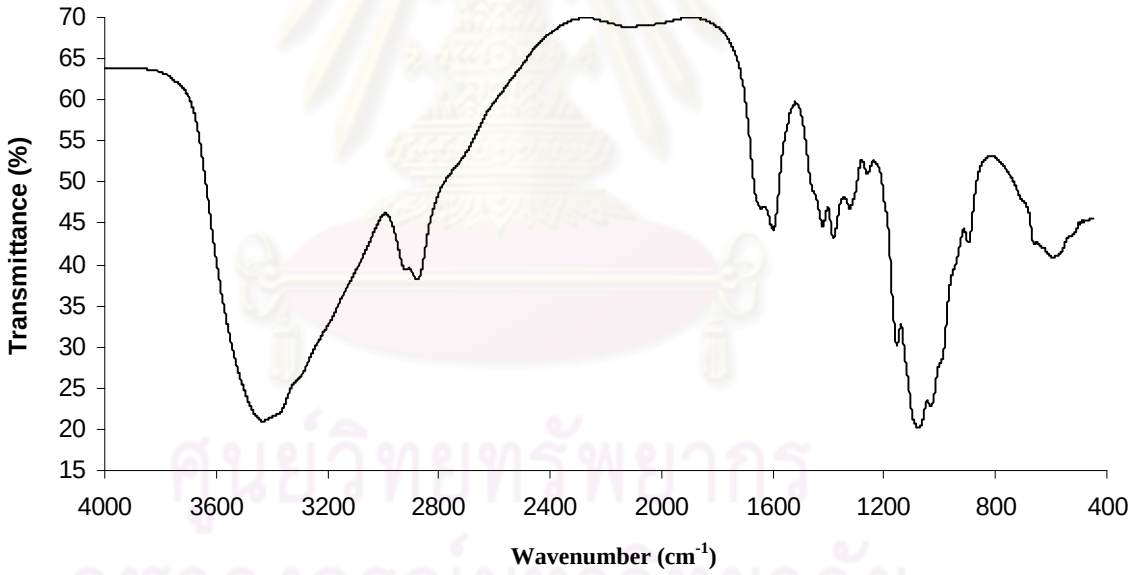

Figure D-8 FT-IR spectra of the chitosan at molecular weight 760 kDa.

APPENDIX E

DETERMINATION OF FIBER PERCENTAGE IN CHITOSAN NANOFIBERS

The percentage of the electrospun nanofibers was measured with SemAfore image analyzing program. For each experiment, were determined from the data of about the randomly selected 5 x 5 μm and 50 measurements from SEM micrograph for 5 times was followed.

For example

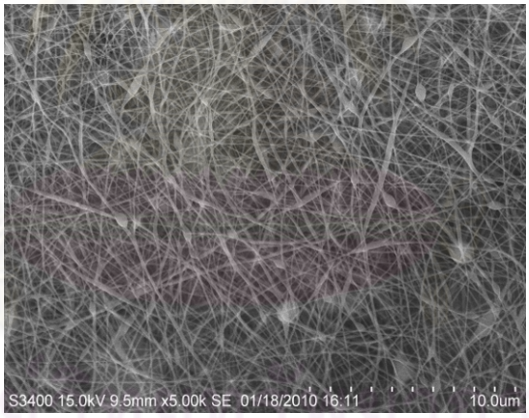

Figure E-1 Example of SEM micrographs of electrospun nanofibers.

Table E-1 Fiber percentage of electrospun fibers in Figure E-1.

Area (5 x 5 μm)	Measurement		
	Fiber	Bead	Percentage of fiber (%)
1	47	3	94
2	43	7	86
3	44	6	88
4	46	4	92
5	45	5	90
Average			90

APPENDIX F

MORPHOLOGY OF BARE FIBERS DIPPED IN WATER

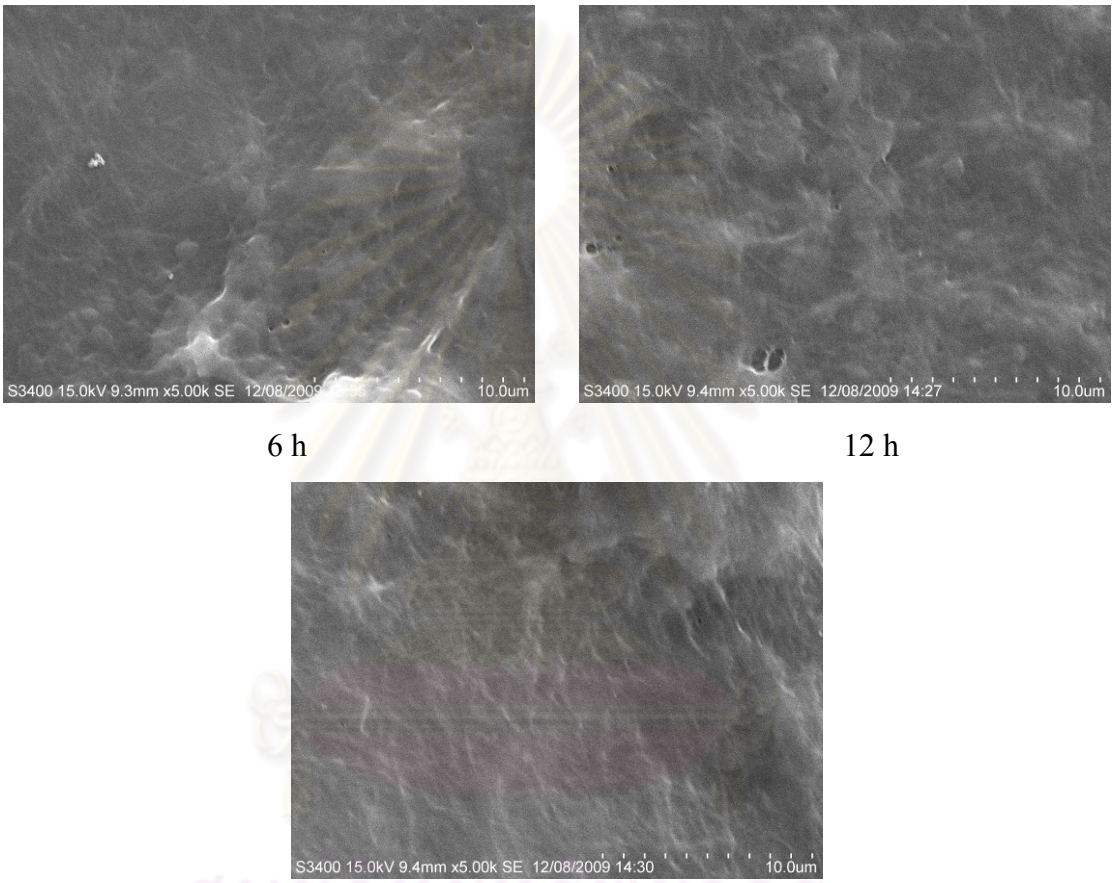

6 h 12 h

24 h

Figure F-1 SEM micrographs of electrospun chitosan/PVA composite nanofibers with 0.04 wt% PVA content, after dipping in water for various periods of time. The molecular weight of chitosan was 400 kDa.

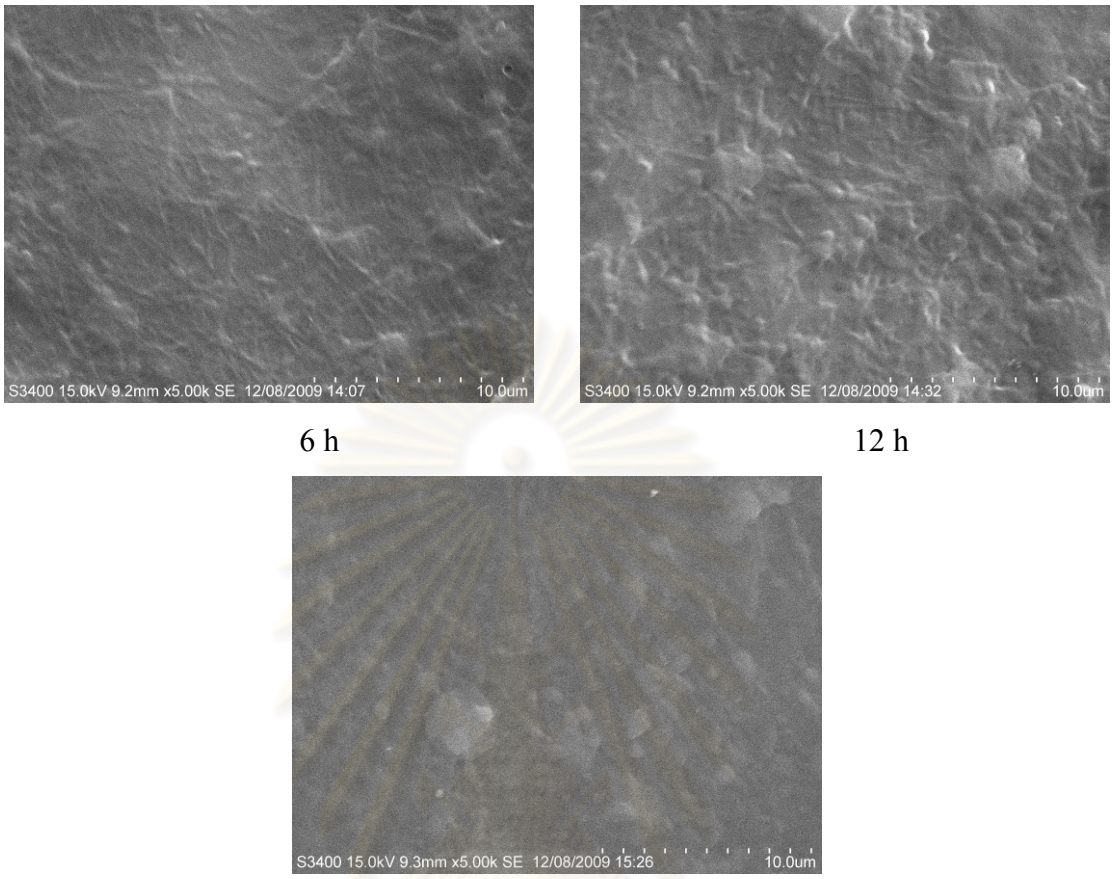

Figure F-2 SEM micrographs of electrospun from chitosan/PVA composite nanofibers with 0.06 wt% PVA content, after dipping in water for various periods of time. The molecular weight of chitosan was 400 kDa.

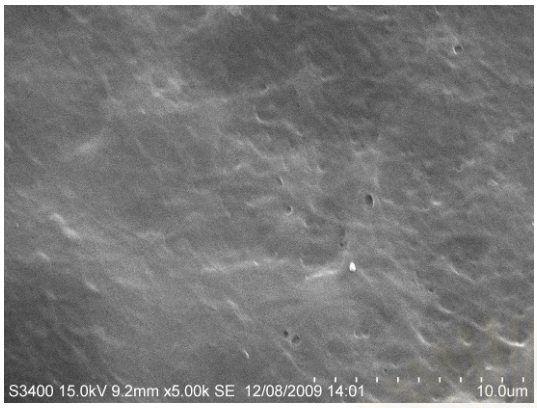

6 h

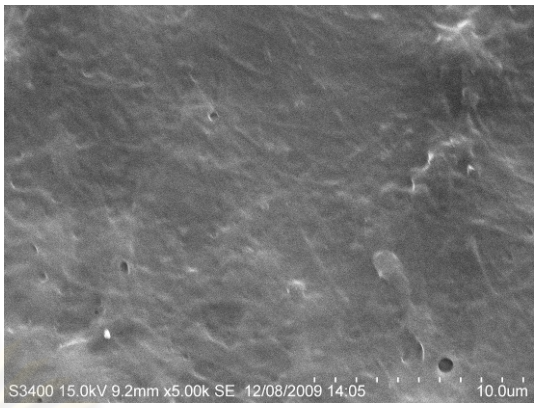

12 h

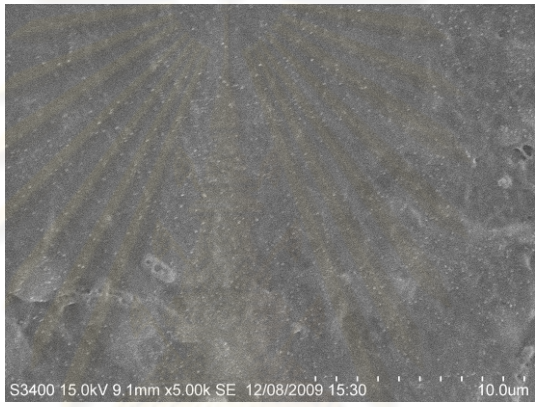

24 h

Figure F-2 SEM micrographs of electrospun from chitosan/PVA composite nanofibers with 0.08 wt% PVA content, after dipping in water for various periods of time. The molecular weight of chitosan was 400 kDa.

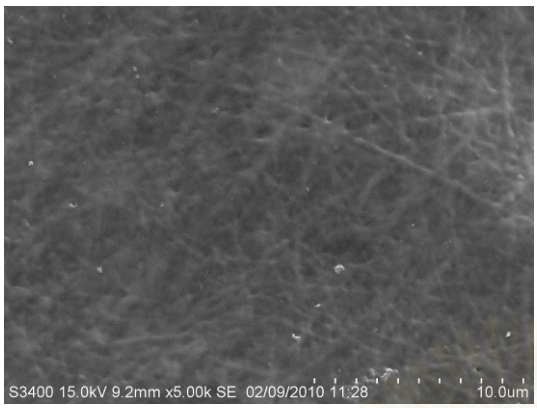

6 h

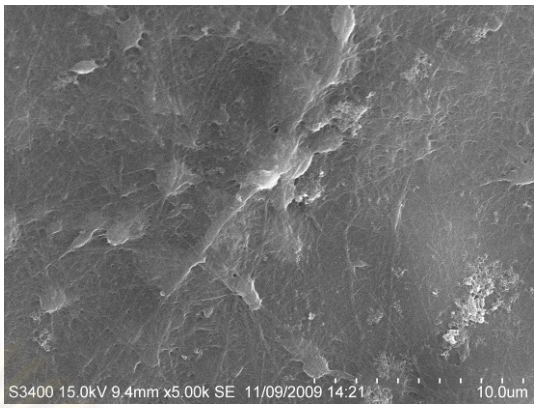

12 h

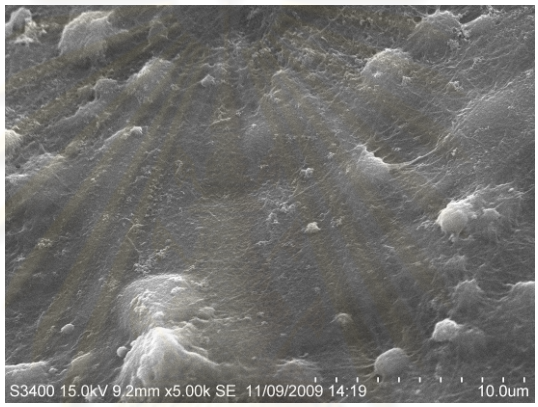

24 h

Figure F-4 SEM micrographs of electrospun from chitosan/PVA composite nanofibers with 0.04 wt% PVA content, after dipping in water for various periods of time. The molecular weight of chitosan was 760 kDa.

6 h

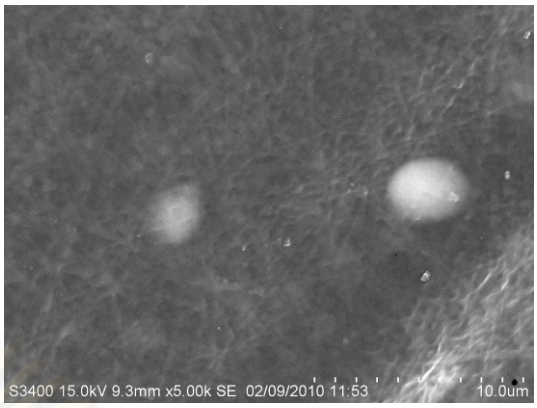

12 h

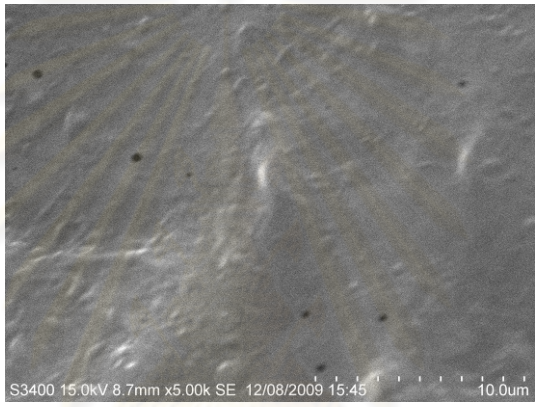

24 h

Figure F-5 SEM micrographs of electrospun from chitosan/PVA composite nanofibers with 0.06 wt% PVA content, after dipping in water for various periods of time. The molecular weight of chitosan was 760 kDa.

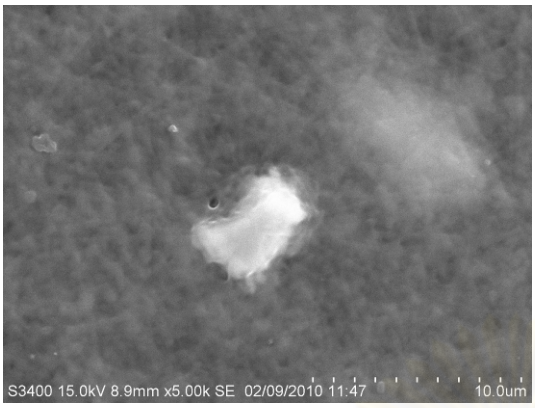

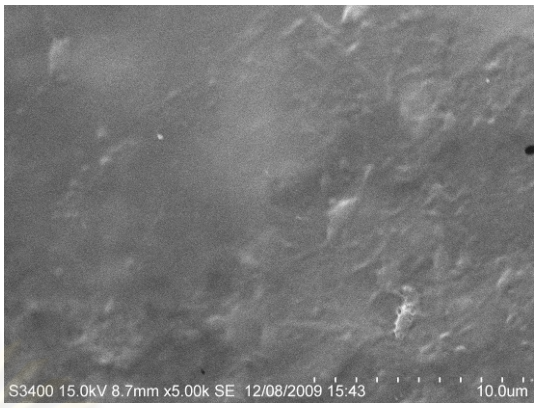

6 h 12 h

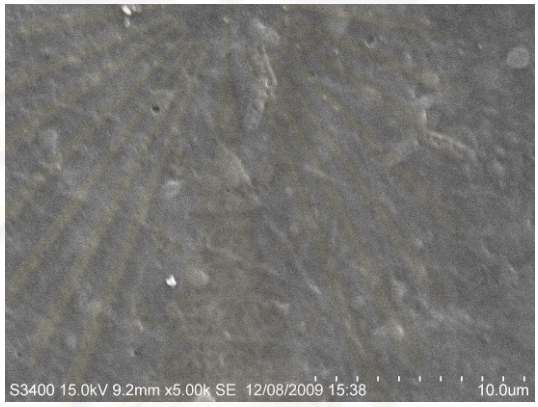

24 h

Figure F-6 SEM micrographs of electrospun from chitosan/PVA composite nanofibers with 0.08 wt% PVA content, after dipping in water for various periods of time. The molecular weight of chitosan was 760 kDa.

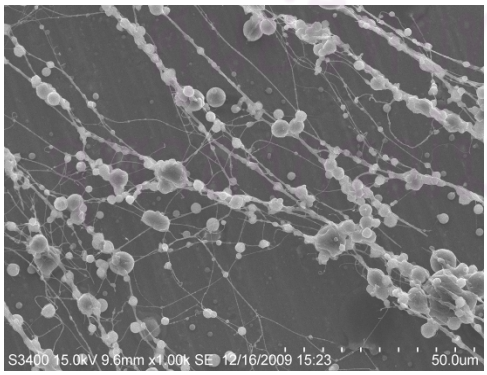

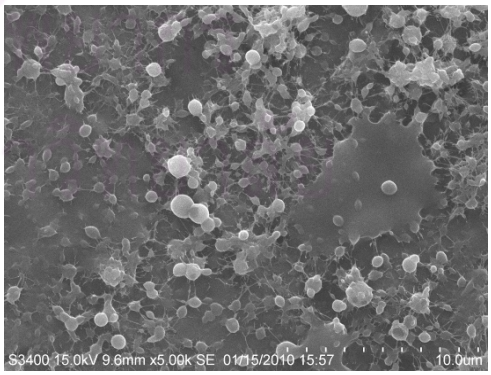

12 h 24 h

Figure F-7 SEM micrographs of electrospun from chitosan hydrolyzed for 24 h after dipping in water for various periods of time. The molecular weight of chitosan was 76

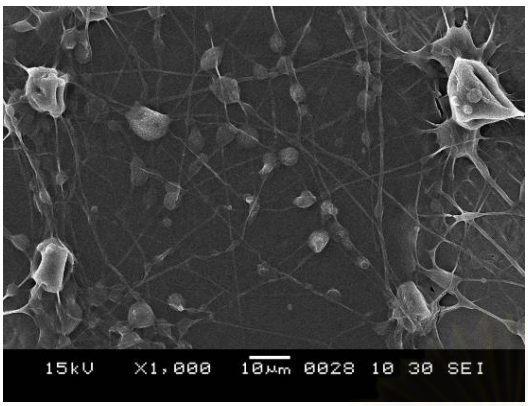

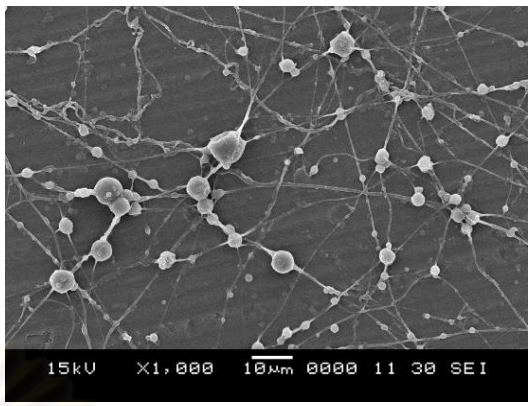

12 h 24 h

Figure F-8 SEM micrographs of electrospun from chitosan hydrolyzed for 36 h after dipping in water for various periods of time. The molecular weight of chitosan was 760 kDa.

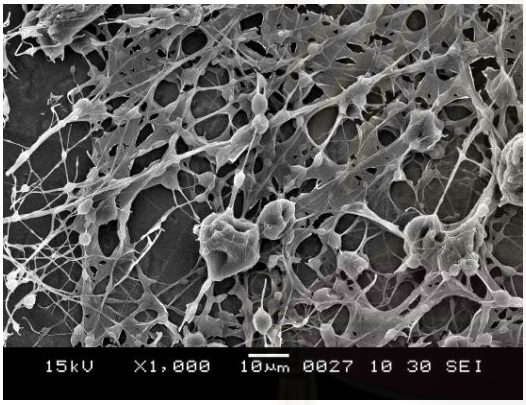

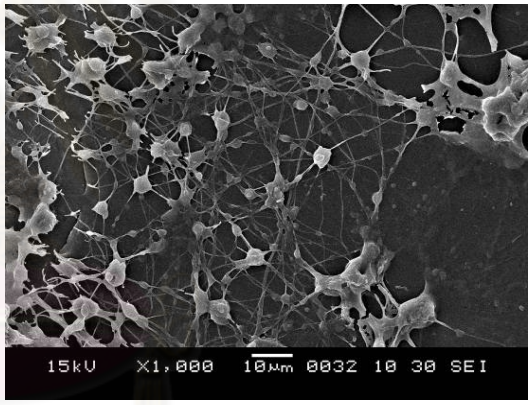

12 h 24 h

Figure F-9 SEM micrographs of electrospun from chitosan hydrolyzed for 48 h after dipping in water for various periods of time. The molecular weight of chitosan was 760 kDa.

VITAE

Miss Prissadawan Chumanee was born on December 14th, 1984 in Nakhornsithammarat, Thailand. She attended Wat Chaichumpol for primary school and Princess Chulabhorn's College, Trang for high school. She received a Bachelor Degree of Engineering, Department of Chemical Engineering from Thammasat University, in 2006. Since 2007, she has been a graduate student studying Chemical Engineering as a major course at Chulalongkorn University. During her studies towards the Master's Degree, she won awards on poster presentation at 6th Asian Aerosol Conference in 2009.